RASSF1A regulation of transcription factors in tumourigenesis and stem cell fate determination

Angelos Papaspyropoulos

St Peter's College

This thesis is submitted for the Degree of Doctor of Philosophy.

Trinity 2014

CRUK/MRC Oxford Institute for Radiation Oncology

Department of Oncology

University of Oxford







Abstract

RASSF1A regulation of transcription factors in tumourigenesis and stem cell fate determination

Submitted for the Degree of Doctor of Philosophy

Angelos Papaspyropoulos, St Peter's College, Trinity 2014

RASSF1A silencing is the most widely reported epigenetic event in sporadic human malignancies and is increasingly observed to be associated with poorer prognosis and outcome in lung, breast and bladder cancers amongst others. By performing a genetic screen in mice using Sleeping Beauty (SB) transposon-mediated insertional mutagenesis, we identified candidate genes associated with tumourigenesis in the absence of Rassf1a. A top hit in our screen was the terminal differentiation transcription factor Runx2. In this study, we describe how together loss of RASSF1A and RUNX2 exacerbate oncogenic YAP1-TEAD complexes and how RUNX2, p73 and TEAD effectively compete for YAP1 association. Interestingly, YAP1-TEAD complexes, as well as RUNX factors have been known to be important regulators of embryonic development by affecting cell fate. We show that RASSF1A is a novel regulator of stem cell pluripotency by introducing a cross link between the Hippo and Wnt signalling pathways, via TEAD and β-catenin. More specifically, we demonstrate that RASSF1A is a barrier to somatic cell reprogramming by activating differentiation circuits, but its loss results in upregulation of the core stem cell marker network (NANOG, OCT4 and SOX2) in embryonic stem cells and the pre-implantation mouse embryo. In addition, we find that deregulation of the Hippo pathway in the absence of RASSF1A also leads to increased prevalence of stem cell characteristics in cancer and higher proportion of 'cancer stem cells'. This effect is mediated through both YAP and its paralog TAZ. Finally, we show that a second isoform of RASSF1, RASSF1C, the expression of which is maintained in cancers, contributes to cancer stem cell generation through a similar mechanism. This work concentrates on establishing the biology of RASSF1A in normal tissue and answering whether the broad prognostic value in tumours from biologically distinct tissues is due to a fundamental control of stem cell pluripotency.

Acknowledgements

This thesis has been the product of hard work over the last 4 years in Oxford. The research included here was generously funded by the Medical Research Council. The completion of this DPhil, however, would have not been possible without the contribution of certain people.

First and foremost, I would like to thank my supervisor, Dr Eric O'Neill. Eric's support was indispensable throughout these years. His supervision helped me broaden my scientific thinking and progressively made me an independent scientist by also providing me with the freedom to test my own ideas. I honestly don't think I would have taken as much as I have out of this DPhil without such a good mentor.

I would also like to thank the other members of the lab with whom I had numerous fruitful conversations and shared concerns. Thank you Dafni Pefani, Aswin Abraham, Nikola Vlahov, Leanne Bradley, Delia Koennig and Anna Grawenda!

Finally, how could this have been possible without the support of friends and family? I thank all my friends here in Oxford for making this city such an enjoyable place to live and my family for their endless support!

Contents

Chapter 1 Introduction 1

1.1 Cancer 1

1.2 The RASSF1A Tumour Suppressor 2

1.3 The RASSF1C Isoform 10

1.4 The Hippo Pathway In Cancer 12

1.4.1 YAP and TAZ 15

1.4.2 TEA Domain Transcription Factor Family (TEAD) 17

1.4.3 Runt-related Transcription Factor Family (RUNX) 19

1.4.4 p73 20

1.4.5 β-catenin 21

1.5 Embryonic Stem Cells (ESCs) 23

1.5.1 The Hippo Pathway In Development 28

1.6 Cancer Stem Cells (CSCs) 34

1.7 Objectives Of The Study 37

Chapter 2 Materials and Methods 39

2.1 Cell lines And Culture 39

2.2 Cell Fractionation 40

2.3 Co-Immunoprecipitation from Whole Cell Lysates 41

2.4 Co-Immunoprecipitation from Nuclear Extracts 42

2.5 Western Blot Analysis 42

2.6 Sample Preparation for Mass Spectrometry 44

2.7 Clonogenic Survival Assay 45

2.8 Resazurin Viability Assay 45

2.9 xCELLigence Proliferation Assay 45

2.10 Reverse-Transcriptase PCR (RT-PCR) 46

2.11 Quantitative Real-Time PCR (qRT-PCR) 46

2.12 Agarose gel Production 47

2.13 Immunofluorescence 48

2.14 Transfection 49

2.14.1 siRNA/plasmid Forward Transfection 49

2.14.2 siRNA/plasmid Reverse Transfection 50

2.14.3 siRNA/plasmid Electroporation 50

2.15 Infection 52

2.15.1 shRNA Lentiviral Transduction 52

2.15.2 Plasmid Retroviral Transduction 53

2.16 Generation and Maintenance of Stable Cell Lines 54

2.17 Preparation of Replication – Deficient Feeder Cells 54

2.18 Adaptation of E14Tg2a mESCs to Feeder – Free Conditions 55

2.19 Alkaline Phosphatase Staining 57

2.20 Reprogramming of MEFs into iPSCs 57

2.21 Generation and Maintenance of iPSC Lines 58

2.22 LIF Withdrawal Assay 59

2.23 Embryoid Body (EB) Formation 59

2.24 Differentiation of iPSCs into Dendritic Cells (DCs) 59

2.25 Flow Cytometry 60

2.26 Chromatin Immunoprecipitation (ChIP) 61

2.27 Bacterial Transformations 62

2.28 Genotyping 62

2.29 Sequencing 63

2.30 Statistics 63

2.31 Tables 64

Chapter 3 Loss of Rassf1a Synergises With Deregulated Runx2 Signalling In Tumourigenesis 69

3.1 Introduction 69

3.2 RASSF1A Regulation of YAP1 Transcriptional Complexes 70

3.3 Genes Promoting Tumourigenesis in a *Rassf1a* null Background 72

3.4 Transcription Factor Competition for YAP1 Binding 73

3.5 Loss of RUNX2 In The Absence of RASSF1A Increases YAP1-TEAD1 Complex Formation 75

3.6 YAP1-TEAD1-Dependent Clonogenicity Requires Loss of RASSF1A or p73 78

3.7 RASSF1A and RUNX2 Limit YAP1-TEAD1-Dependent Cell Viability and Proliferation 80

3.8 TEAD1 is Required for Oncogenic Activity Induced by RASSF1A Loss 83

3.9 Loss of RASSF1 and RUNX2 in Human Tumours 85

3.10 Nuclear Localisation of RASSF1A 86

3.11 Discussion 87

Chapter 4 RASSF1A is a Key Regulator of Pluripotency via Novel Yap-Tead-β-catenin-Mediated Control of *Oct4* 95

4.1 Introduction 95

4.2 RASSF1A is a Barrier to Reprogramming 97

4.3 *Rassf1a* -/- iPSCs Demonstrate Elevated Stem Cell Marker Expression 103

4.4 *Rassf1a* -/- iPSCs Demonstrate Increased Resistance to Differentiation 106

4.5 Loss of Rassf1a Inhibits Differentiation of iPSCs to DCs 109

4.6 Endogenous Rassf1a Expression Increases Upon Differentiation 112

4.7 RASSF1A Downregulates Stem Cell Marker Expression by Promoting Yap-p73-Driven Differentiation in Mouse ESCs 114

4.8 Rassf1a Loss in ESCs Increases Stem Cell Markers via Yap1-Tead2 121

4.9 Tead2, Yap1 and β-catenin Together Form a Stable Complex in the Absence of Rassf1a 125

4.10 Loss of Rassf1a Causes Recruitment of Yap1-Tead2-β-catenin to the *Oct4* Promoter 131

4.11 Rassf1a Regulates Lats-Mediated Phosphorylation of Yap1 136

4.12 RASSF1A Impairs Mouse Embryonic Development via p73 143

4.13 Discussion 146

Chapter 5 RASSF1A Loss Contributes to Cancer Stem Cell Generation Through YAP/TAZ 157

5.1 Introduction 157

5.2 RASSF1A Stabilises TAZ-p73 Transcriptional Complexes 159

5.3 Loss of RASSF1A Destabilises TAZ-p73 Complexes to Favour TAZ-Dependent Oncogenic Complexes 160

5.4 RASSF1A Loss Causes Nuclear Accumulation of β-catenin and TAZ 163

5.5 RASSF1A Regulates the Downstream Effector of Notch Signalling, HES1 167

5.6 RASSF1A Loss Increases Stem Cell Markers in Cancer Cells 169

5.7 RASSF1A Limits Stem Cell Marker Expression in Cancer Cells 173

5.8 The RASSF1C Isoform of RASSF1A Has Opposite Effects on Cancer Stem Cell Generation 175

5.9 RASSF1C Functions in a Paracrine Manner 178

5.10 Discussion 180

Chapter 6 Discussion 184

Chapter 7 Appendix 194

7.1 *Sleeping Beauty* mutagenesis screen 194

7.2 RASSF1 and RUNX2 Expression in Clinical Samples 197

7.3 RASSF1A Regulates Stem Cell Fate in ESCs and iPSCs 199

7.4 RASSF1A Role in the Mouse Embryo 203

7.5 The Role of RASSF1A in Cancer Stem Cell Generation 208

Chapter 8 References 211

Figures list

Chapter 1 Introduction

Figure 1.1 Structure of the *RASSF1* gene and RASSF1 isoforms 3

Figure 1.2 Summary of the key events regulating RASSF1A function 10

Figure 1.3 YAP and TAZ protein structures 23

Figure 1.4 The Hippo signalling pathway in tumourigenesis and development 33

Chapter 2 Materials and Methods

Figure 2.1 Adaptation of feeder – dependent E14Tg2a cells to feeder – free conditions 56

Table 2.1 siRNA sequences used during this project 64

Table 2.2 shRNA sequences used during this project 65

Table 2.3 Primers used for mRNA and promoter (ChIP) qRT-PCR and transgene expression 65

Table 2.4 Antibodies used during this project 66

Chapter 3 Loss of *Rassf1a* synergises with deregulated Runx2 signalling in tumourigenesis

Figure 3.1	RASSF1A enhances YAP1-p73 and restricts YAP1-TEAD1 complexes	72
Figure 3.2	RUNX2 and TEAD1 transcription factor competition for binding to YAP1	75
Figure 3.3	Dual downregulation of RASSF1A and RUNX2 further increases YAP1-TEAD1 complexes	77
Figure 3.4	RASSF1A and RUNX2 limit YAP1-TEAD1-dependent colony formation	80
Figure 3.5	RASSF1A and RUNX2 limit YAP1-TEAD1-dependent cell viability and proliferation	82
Figure 3.6	TEAD1 silencing reverses the oncogenic phenotypes in the absence of RASSF1A/RUNX2	84
Figure 3.7	RASSF1A localises specifically in the nucleus of U2OS cells	87
Figure 3.8	Model depicting proposed YAP1 complex formation in response to RASSF1A	92

Chapter 4 RASSF1A is a key regulator of pluripotency via novel Yap-Tead-β-catenin-mediated control of *Oct4*

Figure 4.1	Experimental design of the somatic cell reprogramming procedure	98
Figure 4.2	*Rassf1a -/-* MEFs exhibit faster and more efficient reprogramming	100
Figure 4.3	*Rassf1a -/-* MEF reprogramming rates are decreased to WT rates when RASSF1A is re-introduced	102
Figure 4.4	Re-introduction of RASSF1A into *Rassf1a -/-* MEFs rescues the reprogramming efficiency	103
Figure 4.5	iPSC colony isolation and characterisation	104
Figure 4.6	*Rassf1a -/-* iPSCs express higher levels of stem cell markers	105
Figure 4.7	*Rassf1a -/-* iPSCs show increased resistance to differentiation	107
Figure 4.8	Morphological differences in iPSC colonies upon LIF withdrawal	109
Figure 4.9	Differentiation capacity of iPSCs towards dendritic cells (DCs)	111

Figure 4.10 Endogenous Rassf1a levels increase upon ESC differentiation 113

Figure 4.11 RASSF1A reduces stem cell marker levels in ESCs 115

Figure 4.12 RASSF1A increases differentiation marker mRNA levels at the expense of stem cell markers 117

Figure 4.13 RASSF1A expression fosters Yap1-p73 complex formation at the expense of Yap1-Tead2 and Yap1-β-cat in ESCs 120

Figure 4.14 Yap1-p73 complexes are required for ESC differentiation in the presence of RASSF1A 121

Figure 4.15 Rassf1a depletion increases stem cell marker protein levels in ESCs 122

Figure 4.16 Rassf1a depletion increases stem cell marker mRNA levels at the expense of differentiation markers 124

Figure 4.17 Rassf1a depletion promotes Yap1-Tead2 and Yap1-β-cat complex formation at the expense of Yap1-p73 in ESCs 125

Figure 4.18 In the absence of Rassf1a, stable Yap1-Tead2-β-cat complexes are formed and the stem cell marker upregulation is Yap-dependent 128

Figure 4.19 Stem cell marker upregulation occurring in the absence of Rassf1a is not mediated through Tead1, but via β-cat and Tead2 130

Figure 4.20 RASSF1A expression restricts *Oct4* promoter occupancy by both Yap1-Tead2 and Yap1-β-cat in ESCs 132

Figure 4.21 Elevated *Oct4* transcription in the absence of Rassf1a requires promoter occupancy by intact Yap1-Tead2-β-cat complexes 135

Figure 4.22 Lats1 is indispensable for stem cell marker upregulation in the absence of Rassf1a 137

Figure 4.23 The LATS-dependent YAP1 phosphorylation sites S127 and S109 follow a distinct pattern in response to RASSF1A 139

Figure 4.24 pS127 YAP1 associates with p73 only in the presence of RASSF1A 141

Figure 4.25 pS109 YAP1 is required for Yap1-Tead2 and Yap1-β-cat interactions, whereas pS127 YAP1 facilitates only Yap1-p73 142

Figure 4.26 Model depicting the proposed role of Rassf1a as a regulator of pluripotency via Yap1-Tead2-β-cat-mediated control of *Oct4* 155

Chapter 5 RASSF1A loss contributes to cancer stem cell generation through YAP/TAZ

Figure 5.1 RASSF1A overexpression promotes TAZ-p73 complexes at the expense of TAZ-TEAD1 and TAZ-β-CAT 160

Figure 5.2 RASSF1A loss increases TAZ-TEAD1 and TAZ-β-CAT levels at the expense of TAZ-p73 162

Figure 5.3 RASSF1A loss causes β-catenin nuclear accumulation 165

Figure 5.4 Loss of RASSF1A results in increased nuclear accumulation of both TAZ and β-catenin 166

Figure 5.5 RASSF1A overexpression decreases endogenous HES1 levels 168

Figure 5.6 RASSF1A silencing increases endogenous HES1 and NANOG mRNA levels in cancer cells. 171

Figure 5.7 RASSF1A silencing upregulates the core stem cell marker protein levels in cancer cells 172

Figure 5.8 RASSF1A overexpression restricts stem cell marker expression in cancer cells 174

Figure 5.9 RASSF1C overexpression increases stem cell markers in cancer cells 176

Figure 5.10 RASSF1C promotes TAZ-TEAD1 complexes at the expense of TAZ-p73 in MDA-MB-231 cells 177

Figure 5.11 RASSF1C expression in MDA-MB-231 cells is accompanied by paracrine effects 179

Chapter 6 Discussion

Figure 6.1 Model of RASSF1A/RASSF1C effects on YAP transcription factor partners 186

Chapter 7 Appendix

Figure 7.1 Loss of Rassf1a promotes tumourigenesis 194

Figure 7.2 Insertions in the Runx2 gene 195

Figure 7.3 Analysis of RUNX2 and RASSF1 expression across different tumor types 197

Figure 7.4 Microarray analysis of RUNX2 and RASSF1 expression in leukemias and colorectal cancers 198

Figure 7.5 Tead2 KD reduces stem cell marker levels in *Rassf1a* -/- iPSCs 199

Figure 7.6 Experimental controls 200

Figure 7.7 Controls for the generation of shRNA-expressing ESC lines 201

Figure 7.8 Additional experimental controls 202

Figure 7.9 Rassf1a depletion increases stem cell marker protein expression in the mouse embryo 203

Figure 7.10 Rassf1a depletion increases stem cell marker transcript levels in the mouse embryo 204

Figure 7.11 RASSF1A overexpression reduces stem cell markers 205

Figure 7.12 RASSF1A impairs mouse embryonic development via p73 206

Figure 7.13 Knockdown of p73 alone does not cause a developmental defect 207

Figure 7.14 Yap1 nuclear localisation in the mouse embryo from 2-8-cell stage 207

Figure 7.15 Raw experimental data from key experiments 209

Figure 7.16 Additional raw experimental data from key experiments 210

Table 7.1 The most statistically significant genes affected by transposon insertion in *Rassf1a -/- Sleeping Beauty* mice 196

Table 7.2 RASSF1A interplay with the Notch signalling pathway 208

Abbreviations

ABCP	Apicobasal Cell Polarity Protein
AKT	RAC-alpha serine/threonine-protein kinase
APC	Anaphase Promoting Complex
APC	Adenomatous Polyposis Coli Protein
APC	Antigen Presenting Cells
APS	Ammonium Persulfate
ASPP	Apoptosis-Stimulating of p53 protein
ATCC	American Type Culture Collection
ATM	Ataxia telangiectasia muatated
BAX	BCL2-associated X protein
BCL2L1	BCL2-like 1
BF	Bright-field microscopy
BIRC5	baculoviral IAP repeat containing 5
BMP4	Bone morphogenic protein 4
BS	Binding Site on the promoter
BSA	Bovine Serum Albumin
c-ABL	ABL proto-oncogene 1, non-receptor tyrosine kinase
CaCl2	Calcium Chloride
CDC	Cell division control protein (e.g. cdc42, cdc20)
CDK	Cyclin-dependent kinase
cDNA	Complementary DNA
Cdx2	Caudal type homeobox 2
ChIP	Chromatin Immunoprecipitation
CHK	Checkpoint kinase
CIS	Common Insertion Sites
cm	centimetre
co-IP	co-immunoprecipitation
CPCs	Cardiac Progenitor Cells
CpG	Dinucleotide consisting of cytosine followed by guanine
CSCs	Cancer Stem Cells
CTGF	Connective Tissue Growth Factor
DAPI	4',6-diamidino-2-phenylindole
DAXX	Death Domain-associated protein
DC	Dendritic Cell
DE	Distal Enhancer of the *Oct4* promoter
DMEM	Dulbecco's-Modified Eagles Medium
DMSO	Dimethylsulfoxide
DNA	Deoxyribonucleic acid
DNMT3B	DNA methyltransferase 3B
DOX	Doxycycline
DTT	Dithiothreitol

DVL	Disheveled protein
E8.5	Embryonic Day 8.5
EB	Embryoid Body
EDTA	Ethylene diamine tetraacetic acid
EGTA	Ethylene glycol tetraacetic acid
EMT	Epithelial-To-Mesenchymal Transition
ESCs	Embryonic Stem Cells
Ex	Exon
FBS	Fetal Bovine Serum
FLAG	An epitope tag of the sequence DYKDDDDK
FSG	Fish Skin Gelatin
GATA4	GATA binding protein 4
GFP	Green Fluorescent Protein
GM-CSF	Granulocyte-macrophage colony-stimulating factor
GSK3	Glycogen synthase kinase-3
GTP	Guanosine Triphosphate
h	hour
HA	An epitope tag of the sequence YPYDVPDYA
HAUSP	Herpes virus-associated ubiquitin-specific protease
HBS	HEPES Buffered Saline
HCl	Hydrogen Chloride
HDAC	Histone deacetylase
HES1	Hairy and enhancer of split-1
HGF	Hepatocyte growth factor
HIC1	Hypermethylated in Cancer 1
Hippo	*Drosophila* homolog of MST
HSP70	Heat Shock Protein 70
ICM	Inner Cell Mass
IGF	Insulin-like growth factor
IL-3	Interleukin 3
IP	Immunoprecipitation
iPSCs	Induced Pluripotent Stem Cells
JNK	c-Jun-NH2-kinase
kb	kilobase (DNA)
KCl	Potassium Chloride
KD	Knockdown
KH2PO4	Monopotassium Phosphate
KLF4	Krueppel-like factor 4
LATS	Large Tumour Suppressor
LB	Luria Broth
LGR-5	Leucine-rich repeat containing G protein-coupled receptor 5
LIF	Leukemia Inhibitory Factor
LOH	Loss of Heterozygosity
LPS	Lipopolysaccharides

MAP1B	Microtubule-associated protein 1B
MDM2	Mouse double minute 2 protein
mg	milligram
min	minute
ml	millilitre
MOAP-1	modulator of apoptosis-1
mRNA	Messenger RNA
MS	Mass Spectrometry
MSCs	Mesenchymal Stem Cells
MST	Mammalian Sterile 20-like Protein
Myod1	Myogenic differentiation 1
Na2HPO4	Sodium Phosphate Dibasic
Na3VO4	Sodium Orthovanadate
NaCl	Sodium Chloride
NaF	Sodium Fluoride
NDR	Nuclear Dbf2-related kinase 1
NF2	Neurofibromin-2 (Merlin)
nm	nanometre
nM	nanomolar
NP40	Nonidet P-40
OCT4	Octamer-binding transcription factor 4
PAGE	Polyacrylamide gel electrophoresis
PBS	Phosphate Buffered Saline
PCR	Polymerase Chain Reaction
PE	Proximal Enhancer of the *Oct4* promoter
PFA	Paraformaldehyde
PIWIL1	Piwi-like RNA-mediated gene silencing 1
PKC	Protein Kinase C
PLA	Proximity Ligation Assay
PML	Promyelocytic leukemia protein
PMSF	Phenylmethylsulfonyl fluoride
PUMA	p53 upregulated modulator of apoptosis
PVDF	polyvinylidene fluoride
qRT-PCR	quantitative Real Time PCR
RA	Ras Association Domain
RABP1	RASSF1A-binding protein 1 (or C19ORF5)
RAF-1	Raf-1 proto-oncogene, serine/threonine kinase
RASSF	Ras Association Domain Containing Family of Proteins
Rb	Retinoblastoma protein
RNA	Ribonucleic acid
RNAi	RNA interference
RNF4	Ring finger protein 4
RT	Room Temperature
RT-PCR	Reverse-transcriptase PCR

RUNX	Runt-related transcription factor
SARAH	**Sa**v, **RA**SSF, **H**ippo
SAV1	Salvador homolog 1
SCF	Skp1-Cul1-F-box
SCs	Stem Cells
SDF1	Stromal cell-derived factor 1
SDS	Sodium Dodecyl Sulphate
sec	second
shRNA	short hairpin RNA
siRNA	Small Interfering RNA molecule
SMAD	Homolog of the *Drosophila* protein MAD
SNARE	SNAP (Soluble NSF Attachment Protein) Receptor
SOX2	SRY (sex determining region Y)-box 2
SRC	Proto-oncogene tyrosine-protein kinase SRC
TAD	Transcription Activation Domain
TAE	Tris-acetate-EDTA
TAZ	Transcriptional co-activator with PDZ-binding motif
TBS	Tris Buffered Saline
TCF/LEF	T-cell factor/Lymphoid Enhancer Factor
TE	Trophectoderm
TEAD	TEA Domain Family Member
TEMED	Tetramethylethylenediamine
TET ON	Tetracycline ON Inducible Vector
TID	TEAD Interacting Domain
TNF	Tumour Necrosis Factor
U	Unit
v/v	Volume per volume
w/v	Weight per volume
WT	Wild-type
WTX	APC membrane recruitment protein 1
YAP	Yes-associated protein
µg	microgram
µl	microlitre
µM	micromolar

Chapter 1

Introduction

1.1 Cancer

Cancer has been traditionally defined as a blend of diseases leading to unregulated growth of cells. It has been argued that as normal cells evolve progressively to a neoplastic state, they acquire eight major traits which render them tumourigenic and ultimately malignant. These traits, which are collectively referred to as the 'Hallmarks of Cancer' are: sustaining proliferative signaling, evading growth suppressors, resisting cell death, enabling replicative immortality, inducing angiogenesis, activating invasion and metastasis, deregulating cellular energetics and avoiding immune destruction. Genomic instability, together with inflammation, set the grounds for the acquisition of these biological capabilities (Hanahan and Weinberg 2011).

The foundation of cancer research has been set in the identification of mutations which generate oncogenes with dominant gain of function, such as the *ras* oncogenes, which were discovered over three decades ago (Der, Krontiris et al. 1982, Parada, Tabin et al. 1982, Santos, Tronick et al. 1982). The discovery of oncogenes was accompanied by the identification of tumour suppressor genes, such as the "guardian of the genome" *p53* (Lane and Crawford 1979, Finlay, Hinds et al. 1989), which have been shown to exhibit recessive loss of function. Inactivation of tumour suppressor genes has been considered to be more crucial than the activation of oncogenes, as tumour suppressors are charged with monitoring the genomic integrity and activating

protection mechanisms, like programmed cell death and senescence in cells experiencing damage. However, tumour suppressors are not inactivated only via gene mutations. Other mechanisms involve gene deletion, loss of heterozygosity (LOH) and epigenetic alterations, including promoter hypermethylation and histone modifications.

1.2 The RASSF1A tumour suppressor

As a bona fide tumour suppressor, *RASSF1A* is found to be inactivated in the majority of human cancers, mostly via promoter hypermethylation occurring at the CpG island (reviewed in Jones and Laird 1999, Esteller, Corn et al. 2001, Donninger, Vos et al. 2007), attributed mainly to the function of DNA methyltransferase 3B (DNMT3B) (Palakurthy, Wajapeyee et al. 2009). Loss of RASSF1A is increasingly associated with poorer prognosis and outcome in a wide spectrum of cancers including lung, breast and bladder (Kawai, Sakano et al. 2010, Buhmeida, Merdad et al. 2011, Wang, Wang et al. 2011).

RASSF1A[1] belongs to the Ras association domain family of proteins and is one of the eight transcripts (A-H) encoded by the *RASSF1* gene, which is located in the 3p21.3 chromosomal region (Figure 1.1). The RASSF family consists of 10 members (RASSF1-10), each of which produces multiple splice variants, with the exception of RASSF9 and 10 (Richter, Pfeifer et al. 2009). These proteins received their name due the presence of a Ras association (RA) domain, which interacts with Ras GTPases (Richter, Pfeifer et al. 2009).

Note: *RASSF1A* and RASSF1A refer to the human gene and protein respectively, whereas *Rassf1a* and Rassf1a to the mouse gene and protein. This is also the case for YAP, TEAD, RUNX, TAZ, TCF and RASSF1C, as per the established gene and protein nomenclature.

RASSF proteins are sub-divided into classical RASSF proteins (RASSF1-6) and N-terminal RASSF proteins (RASSF7-10), depending on the location of the RA domain (Sherwood, Manbodh et al. 2008). Classical RASSF proteins contain an additional functional domain, called Salvador-RASSF-Hippo (SARAH), which has been found to facilitate protein-protein interactions and homo- and heterodimerisation of RASSF proteins (Hwang, Ryu et al. 2007). Lastly, RASSF1A and RASSF5A also contain an N-terminal domain with known homology to the C1 domain of PKC, which possesses a zinc finger, important for mediating protein-protein interactions (Newton 1995, Harjes, Harjes et al. 2006).

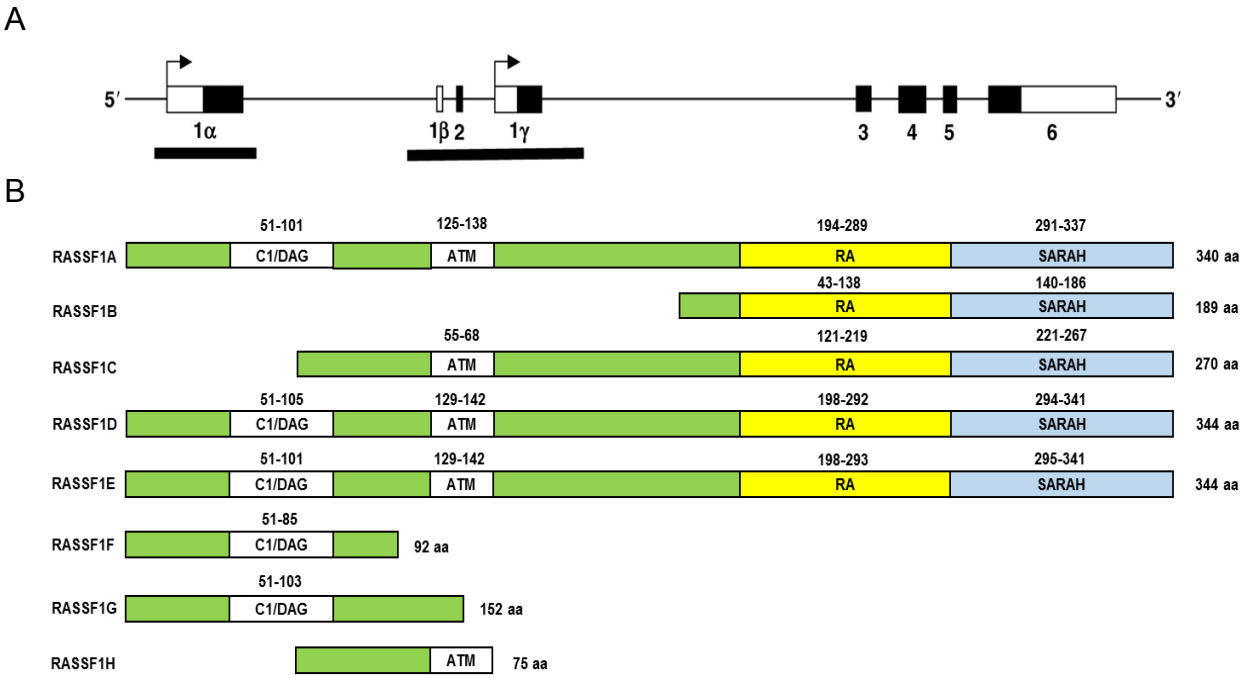


Figure 1.1. Structure of the *RASSF1* gene and RASSF1 isoforms. A. The *RASSF1* gene locus contains eight exons (boxed regions) and two different promoters (arrows) with two related CpG islands (black bars). Black boxes represent coding regions and white boxes non-coding regions. **B.** Structure of the RASSF1 isoforms. C1/DAG: conserved region 1 diacylglycerol-binding domain; ATM: ATM-kinase consensus phosphorylation sequence; RA: RalGDS/AF6 Ras association domain; SARAH: Salvador-RASSF-Hippo interaction domain. The position of each domain is indicated above the isoforms. The total number of amino acids of each protein is provided on the right (adapted from Donninger, Vos et al. 2007).

Mice lacking *Rassf1a* develop spontaneous tumours, especially in combination with *p53* loss (Tommasi, Dammann et al. 2005, van der Weyden, Tachibana et al. 2005, Tommasi, Besaratinia et al. 2011). Moreover, double *Rassf1a* and *p53* knockout mice display high incidence of aneuploidy and tetraploidy, suggesting an important role for RASSF1A in the maintenance of genomic integrity. RASSF1A is a multifunctional protein involved in a wide variety of biological processes, such as microtubule dynamics, cell cycle and mitotic progression, induction of apoptosis, as well as the DNA damage response (Figure 1.2).

RASSF1A has been found to create contacts with microtubules via its N- and C-terminals (Rong, Jin et al. 2004, El-Kalla, Onyskiw et al. 2010). Additionally, a yeast two-hybrid screen identified the microtubule-associated proteins MAP1B and C19ORF5 (RABP1) as RASSF1A binding partners (Dallol, Agathanggelou et al. 2005). The dynamic interaction of RASSF1A with the cytoskeletal structure is reflected in the fact that while during interphase it is bound to cytoplasmic microtubules, during prophase it shuttles to the centrosome, further translocating to the spindle poles during metaphase/ anaphase and localising at the midzone and midbody during telophase (Rong, Jin et al. 2004). Furthermore, RASSF1A overexpression has been found to stabilise microtubules, thereby impeding cell motility and invasiveness, whereas silencing of RASSF1A is associated with disruption of cell-cell adhesion and increased migratory effects (Liu, Tommasi et al. 2003, Rong, Jin et al. 2004, Dallol, Agathanggelou et al. 2005), which indicates that by associating with the microtubules, the protein exerts part of its tumour suppressive functions. However, phosphorylation of RASSF1A by Aurora-A

kinase on Thr 202 and Ser 203 and protein kinase C on Ser 197 and Ser 203 can weaken its microtubule association capacity, possibly by introducing inhibitory conformational changes on RASSF1A (Rong, Jin et al. 2004, Verma, Ganesan et al. 2008).

Cell cycle progression is also affected by RASSF1A signalling, as its overexpression causes G1/S arrest, accompanied by Cyclin D1 reduction, possibly by inhibition of mRNA translation (Shivakumar, Minna et al. 2002). Others have attributed the Cyclin D1 reduction in RASSF1A-mediated suppression of Ras-dependent c-Jun-NH2-kinase (JNK) phosphorylation, which inhibits JNK signalling and, consequently, the expression of target genes, such as Cyclin D1 (Whang, Kim et al. 2005). Furthermore, a yeast-two-hybrid screen identified the transcription factor $p120^{E4F}$, which is implicated in G1 cell cycle arrest, as a RASSF1A binding partner and subsequent research showed that the RASSF1A-induced G1 arrest was enhanced by $p120^{E4F}$-dependent repression of the cyclin A2 promoter. Cyclin A2 is important for CDK2 regulation and, thus, entry into S phase (Fenton, Dallol et al. 2004, Ahmed-Choudhury, Agathanggelou et al. 2005). RASSF1A is lost in the majority of human tumours, yet it is expressed in normal cells, which raises the question of how these cells are able to overcome the G1 arrest induced by RASSF1A. In answer of this question, it has been shown that RASSF1A is degraded by the Skp1-Cul1-F-box (SCF) complex to allow transition to the S phase. During G1, RASSF1A is phosphorylated by Cyclin D-CDK4 on Ser 203 and this phosphorylated form is recognized by the SCF complex, which triggers the proteasome-dependent degradation of RASSF1A.

This explains why the expression levels of RASSF1A are low during S phase (Song, Song et al. 2008).

The anaphase promoting complex (APC) is a ubiquitin ligase complex, essential for progression through the G1 and M phases of the cell cycle, which works in conjunction with Cdc20. In prometaphase, RASSF1A is encountered in the spindle poles, associated with C19ORF5 (RABP1), where it interacts with Cdc20, thereby inhibiting APC/Cdc20 activation, whose function is to degrade cyclins A and B in order to allow mitotic progression to occur (Song, Song et al. 2004, Song, Chang et al. 2005). However, Aurora A-mediated phosphorylation of RASSF1A on Ser 203 reverses the inhibitory effects of RASSF1A on the APC/Cdc20 complex, possibly by targeting RASSF1A for degradation (Song, Song et al. 2009, Chow, Wong et al. 2012). Additionally, during M phase RASSF1A is phosphorylated by Aurora B on Ser 203, promoting association with Syntaxin 16, a t-SNARE protein important for cytokinesis. This phosphorylation has been shown to be crucial for RASSF1A localisation to the midzone and midbody as well as efficient cytokinesis. Abrogation of RASSF1A expression results in mitotic defects leading to multinucleated cells (Song, Kim et al. 2009). Recently, it was also shown that CHK1-mediated phosphorylation of RASSF1A on Ser 184 is sufficient to limit RASSF1A association with the microtubules and cause M-phase arrest (Jiang, Rong et al. 2014). Moreover, Jiang et al. (2011) provided evidence that like G1/S transition, G2/M transition is also followed by proteasomal-dependent degradation of RASSF1A, via the Cul4A-DDB1-RING complex to allow normal mitotic progression to take place.

Besides its implication in cell cycle regulation, RASSF1A holds a pivotal role in eliciting apoptosis, mostly through the extrinsic pathway. It has been established that RASSF1A is able to directly interact with MST1/2 kinases via their common SARAH domains, resulting in increased histone H2B phosphorylation on Ser 14, chromatin condensation and Fas-induced apoptosis (Oh, Lee et al. 2006). In the absence of RASSF1A, MST-dependent apoptosis is drastically reduced (Oh, Lee et al. 2006). Fas-induced apoptosis through the RASSF1A-MST1 interaction also revealed the importance of NDR1/2 kinase activation in this process, as knockdown of NDR1/2 or the co-activator MOB1 inhibited RASSF1A-mediated apoptotic induction (Vichalkovski, Gresko et al. 2008, Pearce, Komander et al. 2010).

RASSF1A-driven activation of MST2 has been found to be critical for induction of p73-dependent apoptosis. In the absence of RASSF1A, the survival kinase Akt phosphorylates MST2 on its N- and C-terminals to keep it inactive in a complex with Raf1 (Romano, Matallanas et al. 2010). In the presence of RASSF1A, the MST2-Raf1 inhibitory complex is disrupted to be replaced by MST2-RASSF1A complexes, which stimulate p73-dependent transcription of apoptotic target genes, such as *PUMA,* through the Hippo pathway kinase cascade (Matallanas, Romano et al. 2007). RASSF1A has been described to promote apoptosis in an MST1/2-independent fashion too. In this context, upon death receptor stimulation, RASSF1A interacts with the modulator of apoptosis-1 (MOAP1), promoting an interaction with the pro-apoptotic protein Bax, which permeabilises the mitochondrial membrane to orchestrate apoptotic events (Baksh, Tommasi et al. 2005, Foley, Freedman et al. 2008). A role for RASSF1A in protection against inflammation-induced

injury, via restriction of NF-kB signalling, was also recently described (Gordon, El-Kalla et al. 2013).

Work in our lab has shown that in response to DNA damage, RASSF1A is phosphorylated on Ser 131 by the master sensor of double strand breaks, ATM. This results in MST2 activation and, subsequently, p73-dependent apoptotic response (Hamilton, Yee et al. 2009). The importance of the ATM activation site integrity on RASSF1A is demonstrated by the fact that a single nucleotide polymorphism in this region, leading to conversion of alanine to serine at residue 133 of RASSF1A (p.Ala133Ser) is sufficient to occlude RASSF1A-mediated MST2 activation, culminating in a defective DNA damage response (Yee, Grochola et al. 2012).

Moreover, Song et al. (2008) showed that in response to DNA damage, RASSF1A can cause disruption of the MDM2-DAXX-HAUSP complex, leading to MDM2 self-ubiquitination, p53 stabilisation and G1/S cell cycle arrest, suggesting that, apart from p73, RASSF1A is also likely to involve regulation of p53 responses. In line with this, RASSF1A-p.133Ser negatively affected the activation of p53, indicated by the poor survival and accelerated age of onset observed in soft tissue sarcoma patients carrying the allele coding for RASSF1A-p.133Ser (Yee, Grochola et al. 2012).

It was not until recently that a role for RASSF1A was provided for the first time in somatic stem cells. Teng et al. (2011) demonstrated that human bone marrow-derived mesenchymal stem cells (MSCs) harbouring targeted promoter methylations of *RASSF1A* and Hypermethylated in Cancer 1 (*HIC1*), acquired oncogenic phenotypes of contact inhibition, increased proliferation

and migration, drug resistance and pluripotency. Additionally, mice carrying targeted MSCs exhibited increased tumour formation, whilst stem cell self-renewal marker levels, such as Oct4, were maintained in tumour xenografts. Of note is also the fact that these cells were still able to respond to differentiation signals, indicating that methylation of *RASSF1A* and *HIC1* can account for the transformation of somatic stem cells to cancer stem cells.

RASSF1A promoter methylation has been reported in over 37 tumour types (Dammann, Schagdarsurengin et al. 2005, Volodko, Gordon et al. 2014) and its methylation status has been strongly linked with tumour grade and metastasis (Fendri, Masmoudi et al. 2009, Hu, Chen et al. 2010, Tommasi, Pinto et al. 2011, Kim, Chae et al. 2012, Kajabova, Smolkova et al. 2013). As anticipated, *RASSF1A* methylation has been associated with decreased responsiveness to DNA damaging therapies, leading to the implementation of DNA methyltransferase inhibitors, e.g. Zebularine, in an attempt to reverse its promoter methylation (Dote, Cerna et al. 2005, Honda, Haruta et al. 2008). The use of Zebularine was shown to indeed increase cancer cell sensitivity to irradiation treatment both *in vitro* and *in vivo*, as well as to cisplatin (Balch, Yan et al. 2005, Dote, Cerna et al. 2005), however, increased sensitivity to cisplatin was also observed following the use of another DNA methyltransferase inhibitor, 5-aza-2'-deoxycytidine (Decitabine) (Beyrouthy, Garner et al. 2009), which was found to target mainly DNMT3B, the DNA methyltransferase responsible for *RASSF1A* promoter hypermethylation (Palakurthy, Wajapeyee et al. 2009). Clinically, 5-aza-2'-deoxycytidine alone or in combination with histone deacetylase (HDAC) inhibitors has led to increased responsiveness to therapy both in myelodysplasia and leukemia

patients, as indicated by phase I and II trials (Garcia-Manero, Kantarjian et al. 2006, Ruter, Wijermans et al. 2006, Karahoca and Momparler 2013). The clinical effect of 5-aza-2'-deoxycytidine on solid tumours is still under investigation.

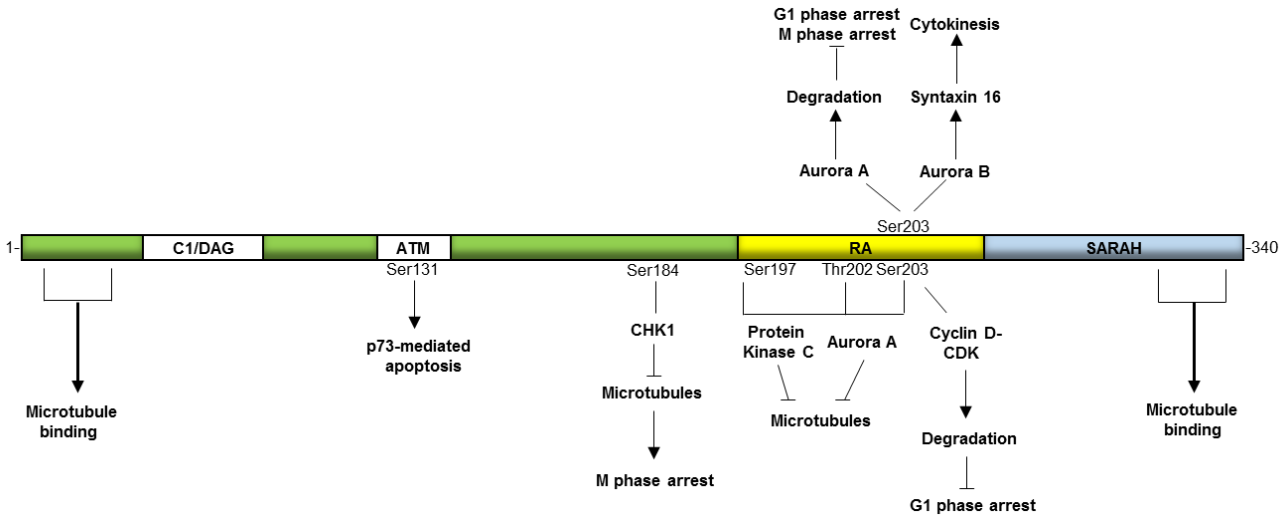


Figure 1.2. Summary of the key events regulating RASSF1A function. The N- and C-terminals of RASSSF1A are necessary for association with microtubules. The schematic depicts the key phosphorylation sites on RASSF1A leading to alterations in microtubule dynamics, cell cycle progression, DNA-damage response and RASSF1A degradation.

1.3 The RASSF1C isoform

Unlike RASSF1A, the RASSF1C isoform of the *RASSF1* gene, is not epigenetically silenced in tumours and does not display tumour suppressive functions. On the contrary, its involvement in osteoblast and lung cancer cell proliferation and breast cancer cell migration/invasion, rather renders *RASSF1C* an oncogene (Amaar, Minera et al. 2006, Reeves, Baldwin et al. 2010, Reeves, Baldwin et al. 2012). Recently, it was demonstrated that RASSF1C is a highly unstable protein, whose expression is regulated by Mule

E3 ligase-dependent polyubiquitynation (Zhou, Li et al. 2012). Furthermore, the association of RASSF1C with another ligase, $SFC^{\beta\text{-}TrCP}$, was shown to promote β-catenin accumulation by inhibiting β-catenin $SFC^{\beta\text{-}TrCP}$-mediated degradation. This effect, which was displayed upon RASSF1C overexpression or RASSF1A downregulation, suggested the existence of a dynamic equilibrium between the two isoforms, crucial for regulating β-catenin stabilisation (Estrabaud, Lassot et al. 2007). RASSF1C has also been found to form a complex with the histone modifying enzyme DAXX in the nucleus. DAXX degradation upon DNA damage releases RASSF1C in the cytoplasm, where it triggers DNA damage response through the SAPK/JNK pathway (Kitagawa, Kajiho et al. 2006). Clinically, RASSF1C expression has been correlated with adverse prognosis of a number of tumour types (Pelosi, Fumagalli et al. 2010). To date, no *Rassf1c* knockout mouse has been established.

Interestingly, RASSF1C was recently found to be implicated in the upregulation of stem cell self-renewal genes. Reeves et al. (2012) showed that RASSF1C was responsible for the elevated expression of *PIWIL1*, a stem cell self-renewal gene found to be overexpressed in several human cancers, especially lung. Moreover, RASSF1C overexpression, due to PIWIL1 stabilisation, was shown to limit the inhibitory effects of the anti-cancer agent betulinic acid on lung cancer cell proliferation (Reeves, Firek et al. 2014), thereby introducing a link between RASSF1C-mediated cancer stem cell generation and resistance to therapy.

1.4 The Hippo pathway in cancer

The Hippo signalling pathway, first discovered in *Drosophila*, is an evolutionary conserved regulator of tissue growth and organ size, whose perturbation, apart from inducing tumourigenesis in model organisms, occurs in a wide spectrum of human cancers, including lung, colorectal, ovarian and liver cancer (comprehensively reviewed in Pan 2010, Harvey, Zhang et al. 2013). The Hippo pathway exerts its tumour suppressive properties in response to cell-cell adhesion, mechanical cues stemming from changes in cellular shape, as well as growth factor signalling (Fan, Kim et al. 2013, Harvey, Zhang et al. 2013). Its deregulation, on the other hand, can occur as a result of disrupted cell polarity or gene mutations affecting its components (Figure 1.4).

The heart of the mammalian Hippo pathway consists of a core kinase cascade which initiates with the STE20-like protein kinases 1 and 2 (MST1/2) signalling to large tumour suppressor 1 and 2 (LATS1/2) NDR protein kinases (Justice, Zilian et al. 1995, Harvey, Pfleger et al. 2003, Chan, Nousiainen et al. 2005) to result in the phosphorylation of the YAP oncoprotein (Huang, Wu et al. 2005, Dong, Feldmann et al. 2007, Zhao, Wei et al. 2007) and its paralog TAZ (Lei, Zhang et al. 2008). MST1/2 and LATS1/2 activity has been shown to require the function of the Salvador homolog 1 (SAV1) and MOB kinase activator (MOB1A and MOB1B) adaptor proteins (Tapon, Harvey et al. 2002, Callus, Verhagen et al. 2006, Praskova, Xia et al. 2008). Phosphorylation of YAP on Ser 127 and TAZ on Ser 89 by LATS1/2 leads to the introduction of 14-3-3 binding sites on them. YAP and TAZ are, subsequently, accumulated in the cytoplasm to associate with 14-3-3 proteins,

where they are also subject to proteasome-dependent degradation (Dong, Feldmann et al. 2007, Zhao, Wei et al. 2007). YAP and TAZ act as transcription factor co-activators, therefore, in their active, unphosphorylated form, they can stimulate the transcription of genes involved in proliferation, cell viability and epithelial-to-mesenchymal transition (EMT) through their association with factors such as TEADs and SMADs (Ota and Sasaki 2008, Zhao, Ye et al. 2008, Chan, Lim et al. 2009, Zhang, Liu et al. 2009, Hong and Guan 2012). Of these, TEADs have been considered to be the master mediators of the tumourigenic potential of YAP and TAZ (Hong and Guan 2012).

Upstream components of the Hippo pathway are essential for transducing various signals to the core kinase cassette to repress YAP and TAZ activity. Little is known about the KIBRA-WILLIN-NF2 complex, of which NF2 is the most extensively studied component. NF2 has been identified as a tumour suppressor, as *NF2* mutations are known to give rise to tumours of the nervous system (Rouleau, Merel et al. 1993, Trofatter, MacCollin et al. 1993), as well as hepatocellular carcinomas and bile duct tumours (Benhamouche, Curto et al. 2010, Zhang, Bai et al. 2010). NF2 has been considered to possess key roles as a cell-surface receptor and in adherens junction-mediated cell contact inhibition, as loss of expression, similarly to YAP overexpression, is sufficient for cells to overcome inhibition and promote growth (Lallemand, Curto et al. 2003, Zhao, Wei et al. 2007). NF2 activation has been shown to be dependent on the cell-surface hyaluronic acid receptor CD44 (Morrison, Sherman et al. 2001).

The apicobasal cell polarity (ABCP) proteins, including mammalian Scribble (SCRIB) are also upstream components which can activate the pathway by directly associating with MST1/2 and LATS1/2 (Cordenonsi, Zanconato et al. 2011). Although the mechanism is not entirely clear, it has been postulated that mislocalisation or aberrant overexpression of ABCP proteins can lead to tissue overgrowth via YAP and TAZ activation (Humbert, Grzeschik et al. 2008). Recently, Yu et al. (2012) provided for the first time evidence that G protein-coupled receptor (GPCR) signalling was acting independent of the core Hippo pathway components and was able to circumvent MST1/2 in order to directly influence LATS1/2 activity.

The apoptosis-stimulating protein of p53 (ASPP) family holds important roles in tumourigenesis (Trigiante and Lu 2006), as its members can induce apoptosis through transcriptional regulation of p53 (Gillotin and Lu 2011, Godin-Heymann, Wang et al. 2013, Lu, Breyssens et al. 2013). Phosphorylation of ASPP1 by LATS2 promotes LATS2-ASPP1 translocation to the nucleus, where the complex associates with p53 and activates apoptosis (Aylon, Ofir-Rosenfeld et al. 2010). Interestingly, this interaction is inhibited by YAP in response to constitutively active H-RAS (Aylon, Ofir-Rosenfeld et al. 2010). However, in cell lines where ASPP1 is predominantly cytoplasmic, ASPP1 enhances YAP/TAZ activity by preventing LATS1-mediated phosphorylation of YAP, resulting in YAP nuclear accumulation. This promotes YAP-mediated repression of *BIM*, which inhibits apoptosis (Vigneron, Ludwig et al. 2010, Vigneron and Vousden 2012). TAZ has been also shown to be activated by ASPP2, which prevents its proteasomal

degradation by promoting its dephosphorylation on Ser89 (Liu, Lv et al. 2011, Schlegelmilch, Mohseni et al. 2011).

Furthermore, as mentioned above, RASSFs have also been identified as activators of the Hippo pathway (Praskova, Khoklatchev et al. 2004, Matallanas, Romano et al. 2007), with the exception of RASSF6, which appears to play an inhibitory role (Ikeda, Kawata et al. 2009). Nevertheless, apart from the upstream elements directly implicated in activating the core kinase cascade, there are other entities, such as the key junctional proteins E-cadherin (Kim, Koh et al. 2011), angiomotins (Zhao, Li et al. 2011), Crumbs (Varelas, Samavarchi-Tehrani et al. 2010) and α-catenin (Schlegelmilch, Mohseni et al. 2011), which bind to and inactivate YAP and TAZ by causing their cytoplasmic accumulation to cell-cell junctions, independently of the core pathway components (Schroeder and Halder 2012).

1.4.1 YAP and TAZ

Yes-associated protein (YAP), which was first characterised twenty years ago (Sudol 1994), is one of the founding members of the Hippo pathway. YAP1 was also the first protein found to contain a WW domain, important for mediating protein-protein interactions with ligands possessing PPxY consensus motifs (Chen and Sudol 1995, Sudol, Bork et al. 1995, Macias, Hyvonen et al. 1996). Apart from the WW domain, which is located within the N- terminal half, YAP also contains a proline-rich region (PR) at the N-terminus, followed by a TID (TEAD Interacting Domain) region, the latter encoding the crucial regulatory S127 phosphorylation site (reviewed by Sudol and Harvey 2010). Next to the WW domain, towards the C-terminus, there is

an SH3 binding motif (SH3-BM) (Ren, Mayer et al. 1993) and a TAD (transcription activation domain) region containing a coiled-coil (C) domain and a PDZ binding motif (PDZ-BM) (Figure 1.2). The TAD region encodes another important phosphorylation site, Y357, involved in Src/Yes kinase-dependent YAP regulation, as well as c-ABL-dependent YAP-p73 complex stabilisation (Zaidi, Sullivan et al. 2004, Levy, Adamovich et al. 2008). The two main isoforms of human YAP1, YAP1-1 and YAP1-2, which contain one WW and two WW domains respectively, are products of alternative mRNA splicing (Sudol, Bork et al. 1995). The YAP paralog TAZ (transcriptional co-activator with PDZ-binding motif), which appears to be the other effector of the Hippo signalling pathway, differs from YAP structurally in that it lacks a PR domain, an SH3-binding motif, a C domain and a PDZ-binding motif (Hong and Yaffe 2006, Mauviel, Nallet-Staub et al. 2012) (Figure 1.3).

YAP has emerged as a highly potent oncogene based on the initial observation that its overexpression in the liver induces hyperplasia, while prolonged elevated expression results in oncogenesis (Camargo, Gokhale et al. 2007, Dong, Feldmann et al. 2007). In line with this, the *YAP* gene locus is amplified at varying frequencies in many human and murine tumours, such as hepatocellular carcinomas and mammary tumours (Overholtzer, Zhang et al. 2006, Zender, Spector et al. 2006, Pan 2010), thus establishing YAP as an independent prognostic marker for disease-free and overall survival in hepatocellular carcinoma patients (Xu, Yao et al. 2009, Pan 2010). On the other hand, increased TAZ expression was detected in 21% of primary breast tumours and evidence was provided that TAZ can drive the invasiveness of breast cancer cells (Chan, Lim et al. 2008). Consistently, it has been shown

that YAP/TAZ overexpression can trigger anchorage-independent growth and EMT in immortalised mammary and pancreatic epithelial cells (Overholtzer, Zhang et al. 2006, Dong, Feldmann et al. 2007, Zhao, Ye et al. 2008, Chan, Lim et al. 2009, Zhang, Liu et al. 2009). A recent report, however, has demonstrated that TAZ functions downstream of EMT, suggesting that it is dispensable for initiating EMT (Cordenonsi, Zanconato et al. 2011).

Moreover, although increased incidence of tumourigenesis has been linked with elevated YAP/TAZ nuclear accumulation (Zender, Spector et al. 2006, Dong, Feldmann et al. 2007, Zhao, Wei et al. 2007, Chan, Lim et al. 2008), numerous reports suggest an additional, tumour suppressive role for YAP in facilitating p73-mediated apoptosis, directed by differential upstream signalling (Strano, Munarriz et al. 2001, Basu, Totty et al. 2003, Matallanas, Romano et al. 2007, Oka, Mazack et al. 2008, Yuan, Tomlinson et al. 2008, Pan 2010). As mentioned above, YAP and TAZ are both transcription factor co-activators, and therefore, they interact with a wide spectrum of transcription factors, including TEAD, RUNX and p73 to exert the previously described and other functions (Figure 1.3).

1.4.2 TEA domain transcription factor family (TEAD)

The majority of YAP/TAZ biological functions has been attributed to their transcriptional pairing with TEAD proteins (Vassilev, Kaneko et al. 2001). TEAD protein family consists of four members (TEAD1-4), all of which act as transcription factors, but are engaged in unique physiological roles. TEAD1 is required for cardiac muscle gene expression (Chen, Friedrich et al. 1994),

TEAD2 is expressed immediately after fertilisation and only during the first seven days of development (Kaneko, Cullinan et al. 1997), TEAD3 expression takes place in the placenta and cardiac muscle (Azakie, Larkin et al. 1996, Jacquemin, Hwang et al. 1996) and TEAD4 is important in skeletal muscle gene activation (Jacquemin, Hwang et al. 1996). TEAD1/2 knockout mice display limited cell proliferation and increased apoptosis (Sawada, Kiyonari et al. 2008), resembling the phenotype of YAP knockout mice (Zhang, Bai et al. 2010). Disruption of YAP-TEAD1 complex formation by resolving the hydrogen bond between the Ser 94 residue on YAP and the Tyr 406 residue on TEAD1 (Chen, Chan et al. 2010, Li, Zhao et al. 2010), results in downregulation of YAP target genes and, consequently, impairs the ability of YAP to foster cell proliferation, transformation and EMT (Ota and Sasaki 2008, Zhao, Ye et al. 2008, Lian, Kim et al. 2010, Schlegelmilch, Mohseni et al. 2011).

TAZ is also capable of interacting with TEAD1, causing similar effects as YAP-TEAD1 complexes with regards to cell growth, EMT and migration. Like YAP-TEAD1, TAZ-TEAD1 complexes lead to enhanced transcription of the *CTGF* target gene, a key regulator of cell adhesion, proliferation and migration (Mahoney, Hong et al. 2005, Zhang, Liu et al. 2009). Due to the above, pharmacological disruption of YAP/TAZ-TEAD complexes has been a matter of intense study, culminating in the discovery of small inhibitory molecules, such as verteporfin, to be implemented in new therapeutic strategies against cancer (Liu-Chittenden, Huang et al. 2012).

1.4.3 Runt-related transcription factor family (RUNX)

The RUNX family of transcription factors consists of three members, RUNX1-3, which all hold crucial roles in development and cancer (reviewed by Blyth, Cameron et al. 2005). Like TEAD proteins, each RUNX family member possesses distinct roles; RUNX1 is involved in definitive hematopoiesis (Okuda, van Deursen et al. 1996) , RUNX2 plays a pivotal role in osteoblast and chondrocyte differentiation (Komori, Yagi et al. 1997, Otto, Thornell et al. 1997) and RUNX3 is implicated in gastrointestinal and neuronal development (Levanon, Bettoun et al. 2002, Li, Ito et al. 2002). However, aside from their physiological roles, *RUNX* genes can act either as tumour suppressors or oncogenes, depending on the context. For example, in the presence of estrogen signalling, RUNX2 becomes oncogenic and is, thus, recognised as a prometastatic marker for several types of breast cancer. While it is also a marker of metastasis in prostate cancer, in other cancers, like osteosarcomas, RUNX2 exhibits tumour suppressive activity (Akech, Wixted et al. 2010, Martin, Zielenska et al. 2011, Chimge, Baniwal et al. 2012, Chimge and Frenkel 2013).

Residues 374-440 of RUNX2 contain a conserved PPxY motif, via which it binds to YAP/TAZ WW domains to form active transcriptional complexes (Yagi, Chen et al. 1999). Zaidi et al. (2004) showed that in osteoblast cells, inhibition of Src/Yes kinase activity blocks YAP phosphorylation on Tyr 357, resulting in disruption of endogenous YAP-RUNX2 complexes, which act to repress skeletal gene transcription. In addition to this report, which presents YAP as an inhibitor of RUNX2 activity in driving osteoblast gene differentiation, others have found that TAZ regulates RUNX2 in the exactly

opposite way, as it strongly activates RUNX2-driven genes during terminal osteoblast differentiation (Hong, Hwang et al. 2005, Byun, Sung et al. 2014). Given that RUNX proteins act as tumour suppressors in the majority of cancers, where YAP/TAZ are mostly nuclear, an overall tumour suppressive function could be inferred for YAP/TAZ-RUNX2 complexes.

1.4.4 p73

p73 is a tumour suppressor belonging in the p53 transcription factor family and, to date, is the best characterised pro-apoptotic YAP effector. In a complex with YAP, the p73α and β isoforms have been shown to elicit apoptosis in response to stimuli such as ionising radiation and chemically induced DNA damage, through interaction of their PPxY-containing motif with the WW domain of YAP (Basu, Totty et al. 2003, Strano, Monti et al. 2005, Matallanas, Romano et al. 2007, Hamilton, Yee et al. 2009). Following treatment with DNA damaging agents, YAP-p73 complexes drive the induction of the pro-apoptotic genes *PUMA*, *Bax*, *p53AIP1*, *Killer/DR5*, *PDCD5* and *PIG3*, and are abrogated upon silencing of YAP (Basu, Totty et al. 2003, Strano, Monti et al. 2005, Matallanas, Romano et al. 2007, Levy, Adamovich et al. 2008, Hamilton, Yee et al. 2009). p73 is essential for YAP translocation to the nucleus and, conversely, YAP is required for acetylation of p73 by p300, which allows the initiation of p73-mediated transcription of target genes, implying a mutual requirement for YAP and p73 towards the induction of apoptosis (Costanzo, Merlo et al. 2002, Strano, Monti et al. 2005). Furthermore, in response to DNA damage, c-ABL-mediated phosphorylation

of YAP on Tyr 357 has appeared to increase YAP stability and subsequent interaction with p73 to drive apoptosis (Levy, Adamovich et al. 2008).

Besides c-ABL, additional proteins are also able to promote YAP-p73-mediated apoptosis. Promyelocytic leukemia protein (PML), apart from being a target of YAP-p73 regulation itself, is also part of a feedback loop triggering YAP-p73-induced apoptosis (Lapi, Di Agostino et al. 2008). Moreover, as it was also previously mentioned, the tumour suppressor RASSF1A is a key regulator of YAP-p73 complex formation through the Hippo pathway, as it activates MST1/2 by disrupting an inhibitory association with RAF-1 (O'Neill, Rushworth et al. 2004, Matallanas, Romano et al. 2007, Romano, Matallanas et al. 2010, Guo, Zhang et al. 2011). To date, there has been no documented evidence of a potential TAZ-p73 interaction.

1.4.5 β-catenin

β-catenin, which constitutes the primary downstream effector of Wnt signalling pathway, regulates key processes in development and cancer by functioning as a transcriptional co-activator. Upon active Wnt signalling, β-catenin translocates to the nucleus, where in conjunction with TCF/LEF family transcription factors, it induces gene transcription (Behrens, von Kries et al. 1996, Molenaar, van de Wetering et al. 1996). In the absence of Wnt signals, however, β-catenin is phosphorylated by a protein network consisting of GSK-3, axin, WTX and adenomatous polyposis coli (APC), collectively referred to as the “β-catenin destruction complex”. Following its phosphorylation, β-catenin is targeted for proteolytic degradation (Aberle, Bauer et al. 1997, Major, Camp et al. 2007, Rivera, Kim et al. 2007, Clevers and Nusse 2012).

Interestingly, YAP/TAZ and β-catenin are targeted for ubiquitination and degradation by the same E3 ubiquitin ligase, $SCF^{\beta\text{-}TRCP}$ (Aberle, Bauer et al. 1997, Dong, Feldmann et al. 2007, Zhao, Wei et al. 2007, Azzolin, Zanconato et al. 2012), implying the existence of a common regulatory pattern. In support of this, YAP/TAZ and β-catenin have been shown to interact. The generation of several YAP mutants harbouring various point mutations revealed that the E66 residue on YAP, which is highly conserved between YAP and TAZ, is responsible for the interaction of YAP with β-catenin (Imajo, Miyatake et al. 2012). Functionally, dissection of the mechanisms underlying colorectal and other β-catenin driven cancers, highlighted the requirement of YAP/TAZ transcriptional complexes, such as β-catenin-YAP1-TBX5, in promoting malignant transformation and survival via transcription of the anti-apoptotic genes *BCL2L1* and *BIRC5* (Rosenbluh, Nijhawan et al. 2012).

An additional link between the Hippo pathway and β-catenin was provided by Varelas et al. (2010), who showed that cytoplasmic TAZ could bind to the Wnt signalling protein Disheveled (Dvl) to promote β-catenin degradation. Another report suggested that YAP/TAZ interaction with β-catenin in the cytoplasm could prevent nuclear localisation of β-catenin (Imajo, Miyatake et al. 2012). In both cases, deregulation of the Hippo pathway led to the transcriptional activation of β-catenin and YAP/TAZ. Heallen et al. (2011) also provided evidence that β-catenin stabilisation was required for increased cardiomyocyte proliferation and cardiomegaly in Hippo mutants. Furthermore, a recent report demonstrated for the first time that upon retardation of Wnt signalling, YAP/TAZ can actually incorporate in the β-catenin destruction

complex to attract the E3 ubiquitin ligase SCF$^{\beta\text{-TRCP}}$, culminating in β-catenin degradation (Azzolin, Panciera et al. 2014).

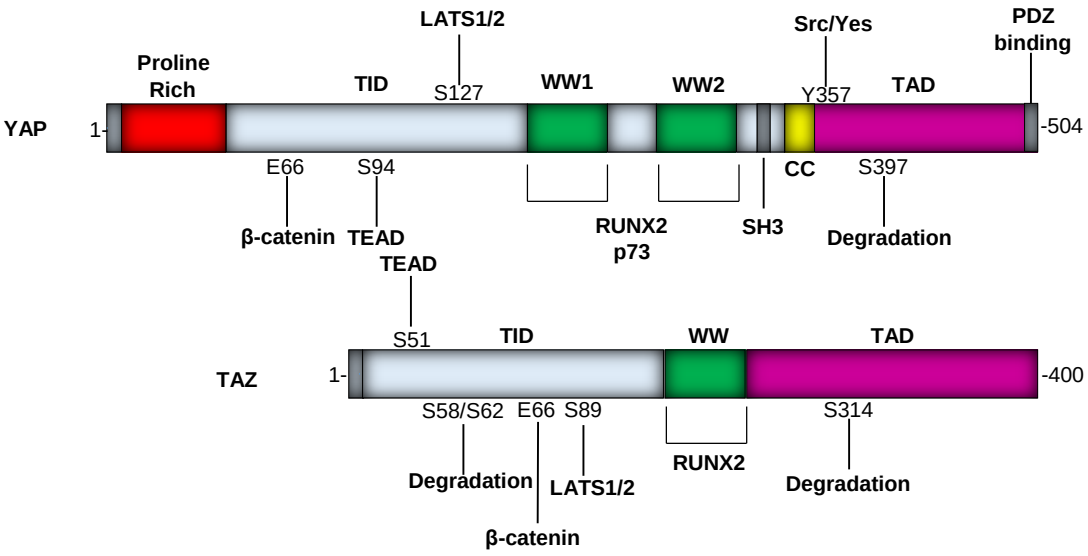


Figure 1.3. YAP and TAZ protein structures. Schematic illustrating the domains contained in YAP and TAZ as well as key sites for binding to important regulatory factors and degradation. TID: TEAD-Interaction domain; CC: coiled-coil domain; TAD: Transcription activation domain.

1.5 Embryonic stem cells (ESCs)

The investigation of the set of properties shared between cancer and stem cells, such as the increased proliferative potential and the ability to migrate, has long been the aim of several studies. In this scope, stem cells have been frequently used as a suitable biological system to ask key questions pertaining to tumourigenesis.

Embryonic development initiates with the fertilised oocyte, which after several rounds of mitotic divisions gives rise to the embryo and extra-embryonic tissues. From the zygote until the early blastocyst stage, cells maintain a totipotent state, which is gradually lost as they undergo functional specialisation, a process collectively defined as differentiation (reviewed by

Surani, Hayashi et al. 2007, Cockburn and Rossant 2010). Embryonic stem cells (ESCs) are isolated from embryos at the blastocyst stage. Thirty years after the establishment of the first mouse ESC cultures (Evans and Kaufman 1981), it is being stated that pluripotent ESCs comprise an *in vitro* system of cell differentiation, equivalent to that in the early embryo (Evans 2011).

One of the fundamental properties of ESCs is their ability to self-renew indefinitely. Cell cycle regulation in ESCs is characterised by the presence of an unusually short G1 phase and lack of a G1/S checkpoint, which have been attributed to the absence of cyclin D proteins, the presence of hyperphosphorylated retinoblastoma (Rb) protein and unresponsiveness to CDK4 activity. However, upon induction of differentiation, cyclin D proteins begin to be expressed and responsiveness to CDK4 activity is restored (Savatier, Lapillonne et al. 1996, Pauklin, Pedersen et al. 2011).

Pluripotency constitutes the most important feature distinguishing ESCs from all the other cell types, given that ESCs have the unique capacity to differentiate *in vitro* into tissues belonging to any of the three embryonic germ layers (endoderm, mesoderm, ectoderm) (Villa-Diaz, Ross et al. 2013). In contrast, tissue-specific stem cells reside in adult tissues, such as the epidermis and the intestine and their role is to generate only the differentiated cell types of those tissues, thereby contributing to their repair and maintenance (Barker, Bartfeld et al. 2010). *In vivo*, injection of ESCs into immune-compromised mice causes the formation of teratomas containing tissues deriving from all three germ layers (Jaenisch and Young 2008, Pauklin, Pedersen et al. 2011). In order to accomplish the contradictory tasks of self-renewal and production of differentiating cells, stem cells implement

two different types of cell division: asymmetric and symmetric. Through asymmetric cell division, each stem cell divides to generate one daughter which maintains stem cell traits and one daughter which differentiates, thereby serving both purposes (self-renewal and differentiation) in one round. The disadvantage of asymmetric cell division, however, is that it does not allow stem cell populations to expand in number, which is achieved via symmetric divisions, the latter resulting exclusively in the production of self-renewing daughters. It has been argued that SCs have the ability to either only divide symmetrically, like ESCs do in the beginning of development, or use a combination of symmetric and asymmetric divisions, like neural and epidermal progenitors, which switch from dividing symmetrically in the beginning of development to dividing asymmetrically at later stages (Betschinger and Knoblich 2004, Clevers 2005, Lechler and Fuchs 2005, Morrison and Kimble 2006).

The existence of an autoregulatory network of three transcription factors - Nanog, Oct4 and Sox2 - has been shown to be crucial for the maintenance of pluripotency. The primary function of this network is to limit the expression of lineage-specific genes, while maintaining pluripotency-related gene expression at high levels (Boyer, Lee et al. 2005, Loh, Wu et al. 2006, Pauklin, Pedersen et al. 2011). In the absence of these factors, mouse ESCs are forced to differentiate towards extra-embryonic lineages. Nanog constitutes the only exception, as *Nanog* null mouse ESCs are able to maintain a completely undifferentiated state (Chambers, Silva et al. 2007). Although the exact role of *Nanog in vivo* remains elusive, targeted disruption of *Oct4* and *Sox2* in pre-implantation mouse embryos leads to extended

differentiation of the pluripotent inner cell mass (ICM) into extra-embryonic tissue, implying that both *Oct4* and *Sox2* are required for maintaining pluripotency (Nichols, Zevnik et al. 1998, Chambers, Colby et al. 2003). Surprisingly, however, Masui et al. (2007) found that the expression of several pluripotency-related genes was not influenced by the absence of Sox2. Furthermore, the observation that enforced expression of Oct4 rescues ESC differentiation even in the absence of Sox2 underlines the indispensable role of Oct4 in the maintenance of pluripotency (Masui, Nakatake et al. 2007). In line with this, Oct4 was identified as the master regulator of the balance between pluripotency and differentiation, as critical changes in its expression pattern are sufficient to affect ESC fate (Niwa, Miyazaki et al. 2000).

In 2006 it was demonstrated for the first time that combined overexpression of the core stem cell markers Oct4 and Sox2 with the transcription factors Klf4 and c-Myc could reprogramme mouse embryonic fibroblasts to stem cells displaying equivalent developmental potential to ESCs, thereby eliminating the requirement for an embryo (Takahashi and Yamanaka 2006). The reprogrammed cells, which were named “induced pluripotent stem cells - iPSCs”, could also derive from human somatic cells (Takahashi, Tanabe et al. 2007, Park, Zhao et al. 2008). However, iPSCs exhibit a number of important differences when compared to ESCs. One such difference is their increased genomic instability, attributed to the lack of genome-protecting mechanisms during the additional phases of somatic differentiation and reprogramming. The resulting genomic abnormalities include mutations linked to known tumourigenic loci (Mayshar, Ben-David et al. 2010, Hussein, Batada et al. 2011, Laurent, Ulitsky et al. 2011).

Additionally, genomic analyses of early passage iPSCs have shown that they might retain somatic cell-specific DNA methylation at regions close to CpG islands, implying that they carry an “epigenetic memory” related to their previous fate. Consequently, this leads to variations in gene expression which might affect iPSC usage as an alternative to ESCs (Doi, Park et al. 2009, Kim, Doi et al. 2010, Polo, Liu et al. 2010, Bar-Nur, Russ et al. 2011, Puri and Nagy 2012).

Due to their unique properties, ESCs hold great promise as a system for deciphering normal development and disease, as well as tools for the treatment of currently incurable disorders, such as spinal cord injury, Parkinson’s disease and certain types of blindness. To that end, intensive research efforts have focused on ESC differentiation towards various cell lineages, since successful transplantation of the derived tissues would contribute enormously to future regenerative medicine (Bjorklund, Sanchez-Pernaute et al. 2002, Murry and Keller 2008, Puri and Nagy 2012). Furthermore, the generation of iPSCs has brought the field a step closer to *in vitro* disease modeling and even individualised regenerative approaches, as transplantation of tissue grafts derived from patient-specific iPSCs would eliminate histocompatibility issues. However, the use of ESCs and iPSCs *in vivo* has so far been accompanied by increased incidence of tumourigenesis and teratoma formation, attributed to their enormous proliferation potential, as well as the remaining pool of undifferentiated cells within the resulting differentiated tissue (Bjorklund, Sanchez-Pernaute et al. 2002, Miura, Okada et al. 2009, Puri and Nagy 2012). It is essential that these problems are

rectified before the wide spectrum of ESC and iPSC applications can be brought to the clinic.

1.5.1 The Hippo pathway in development

Emerging data suggest that one of the ways through which the Hippo pathway controls organ size is direct regulation of stem cell proliferation and maintenance. Stem cell number is a key determining factor of the final size of an organ (Depaepe, Suarez-Gonzalez et al. 2005, Stanger, Tanaka et al. 2007). Along these lines, several findings highlight the importance of the pathway in modulating the activity of stem cells in tissue regeneration and development (Figure 1.4).

Perturbation of the Hippo pathway has been linked with the maintenance of pluripotency. In ESCs, loss of Mst1/2 leads to upregulation of stem cell markers and rapid proliferation, accompanied by limited differentiation potential (Li, Chen et al. 2013). Similarly, loss of Lats2 renders ESCs less responsive to differentiation signals, whereas its expression is upregulated during differentiation (Aylon, Sarver et al. 2014). This is in keeping with the observation that silencing of LATS2 enhances the generation of human iPSCs, implying that lack of LATS2 can increase the pluripotent pontential of cells (Qin, Blaschke et al. 2012).

The impact of the terminal effectors of Hippo signalling, Yap/Taz on ESC and iPSC pluripotency has drawn a great amount of attention over the last years. In the majority of cases, Yap and Taz appear to resonate their functions to elicit similar effects. In human ESCs, TAZ was found to be responsible for the shuttling of SMAD2/3 complexes in and out of the nucleus

in a TGFβ-dependent manner. Loss of TAZ resulted in disruption of TGFβ signalling and, consequently, loss of pluripotency (Varelas, Sakuma et al. 2008). On the other hand, in response to BMP signalling, YAP was found to bind to SMAD1 to trigger gene transcription necessary for human ESC maintenance (Alarcon, Zaromytidou et al. 2009). Furthermore, YAP-TEAD complexes, which in tumourigenesis were shown to drive proliferation and metastasis, were found to be necessary in promoting self-renewal in ESCs and iPSCs. More specifically, Yap-Tead2 complex formation was shown to be essential for the transcription of *Oct4* in mouse ESCs (Tamm, Bower et al. 2011). Similar findings were reported in mouse iPSCs (Lian, Kim et al. 2010).

A number of studies have provided evidence that the Hippo pathway regulates self-renewal and repair of tissues, such as the intestinal epithelium (reviewed by Li and Clevers 2013). YAP overexpression in the intestine leads to expansion of undifferentiated progenitor cells (Camargo, Gokhale et al. 2007), although loss of YAP in the normal tissue causes no detectable defects (Cai, Zhang et al. 2010).

YAP appears to be involved in an interplay with the Notch signalling effector Hes1, which acts as a differentiation repressor, since YAP overexpression culminates in the expansion of Hes1-positive progenitor cells in the intestine. This phenotype can be reversed either with the use of Notch signalling inhibitors, such as γ-secretase inhibitors (Camargo, Gokhale et al. 2007) or YAP depletion (Zhou, Zhang et al. 2011). Recently, it was suggested that Notch signalling acts downstream of YAP in hepatocytes and inactivation of Hippo signalling results in adult hepatocytes acquiring progenitor-like characteristics, implying that YAP and Notch synergise to induce

dedifferentiation processes in the liver (Yimlamai, Christodoulou et al. 2014). Interestingly, cross talk between YAP and Notch signalling was observed in neural stem cells as well, where YAP overexpression diminished the effect of Notch inhibition, thus leading to an increased number of progenitor cells (Li, Hibbs et al. 2012). Additionally, apart from YAP overexpression, it was shown that inhibition of MST2 and LATS1/2 also led to an increase in the neural progenitor pool, accompanied by enhanced self-renewal and limited differentiation potential. These phenotypes could be reversed upon disruption of YAP-TEAD complexes, implying that YAP activity is mediated through TEAD factors in neural stem cells as well (Cao, Pfaff et al. 2008).

As with other tissues, skin regeneration is also dependent on progenitor cells, which differentiate to produce epidermis, sebaceous glands and hair follicles (Owens and Watt 2003, Fuchs 2007). The proliferation rate of these epidermal progenitors increases upon YAP nuclear localisation, but it progressively declines when YAP is silenced, resulting in several defects, such as thinning of the skin and lack of epidermal tissue (Schlegelmilch, Mohseni et al. 2011, Zhang, Pasolli et al. 2011). Depletion of Sav1 in mouse embryos is accompanied by the same effects as Yap nuclear accumulation on skin generation, however, this is not the case for Mst1/2 and Lats1/2 knockdowns, indicating that in this context Yap is not regulated by the canonical Hippo pathway. Indeed, in human keratinocytes YAP was shown to be regulated mostly by α-catenin, a component of the adherens junctions, which in response to cell density, detains YAP in the cytoplasm (Lee, Kim et al. 2008, Schlegelmilch, Mohseni et al. 2011). Cardiomyocyte proliferation was also found to be affected by the Hippo pathway, since depletion of Sav1

led to cardiomegaly in mice. Furthermore, β-catenin, an established promoter of heart growth, was identified for the first time as a binding partner of Yap and this interaction was held responsible for intensifying Wnt-dependent cardiomyocyte proliferation (Heallen, Zhang et al. 2011). Parallel studies (Xin, Kim et al. 2011, von Gise, Lin et al. 2012) revealed that apart from YAP-β-catenin, YAP-TEAD complexes also display an active role in cardiomyocyte proliferation. Additionally, it was suggested that YAP coupling with the insulin-like growth factor (IGF) inhibited β-catenin degradation, thereby resulting in enhanced heart growth (Shiojima and Walsh 2006, Matsui, Nakano et al. 2008, Heallen, Zhang et al. 2011, Xin, Kim et al. 2011, von Gise, Lin et al. 2012).

Like in cancer, functions of YAP and TAZ overlap in development, but are not entirely redundant, indicated by the fact that despite *Yap* null mice die at E8.5 (Morin-Kensicki, Boone et al. 2006), *Taz* null mice are viable (Hossain, Ali et al. 2007). Yap/Taz double knockout, however, leads to lethality even before the morula stage (16-32 cells). An example illustrating that YAP and TAZ occasionally do have separable functions is provided in myoblasts and skeletal muscle progenitor cells, where although YAP overexpression blocks differentiation (Watt, Judson et al. 2010, Judson, Tremblay et al. 2012), TAZ induces it by stabilising Myod1, a myoblast-specific differentiation factor (Jeong, Bae et al. 2010).

Expectedly, the Hippo pathway exerts important functions early in embryogenesis as well. Nishioka et al. (2009) proposed a model according to which Yap localises in the nucleus of outside cells of the pre-implantation mouse embryo, where in association with Tead4 it promotes differentiation

into trophectoderm, via upregulation of trophoblast genes such as Cdx2. Due to Lats-dependent phosphorylation and increased mechanical stress, Yap is sequestered in the cytoplasm of inner embryonic cells, where it cannot support differentiation and, hence, cells of the inner cell mass remain pluripotent. According to another report (Leung and Zernicka-Goetz 2013), Angiomotin, along with Angiomotin-like 2 are the key determinants of the balance between pluripotency and differentiation in the pre-implantation mouse embryo, as loss of these proteins causes differentiation of the inner cell mass.

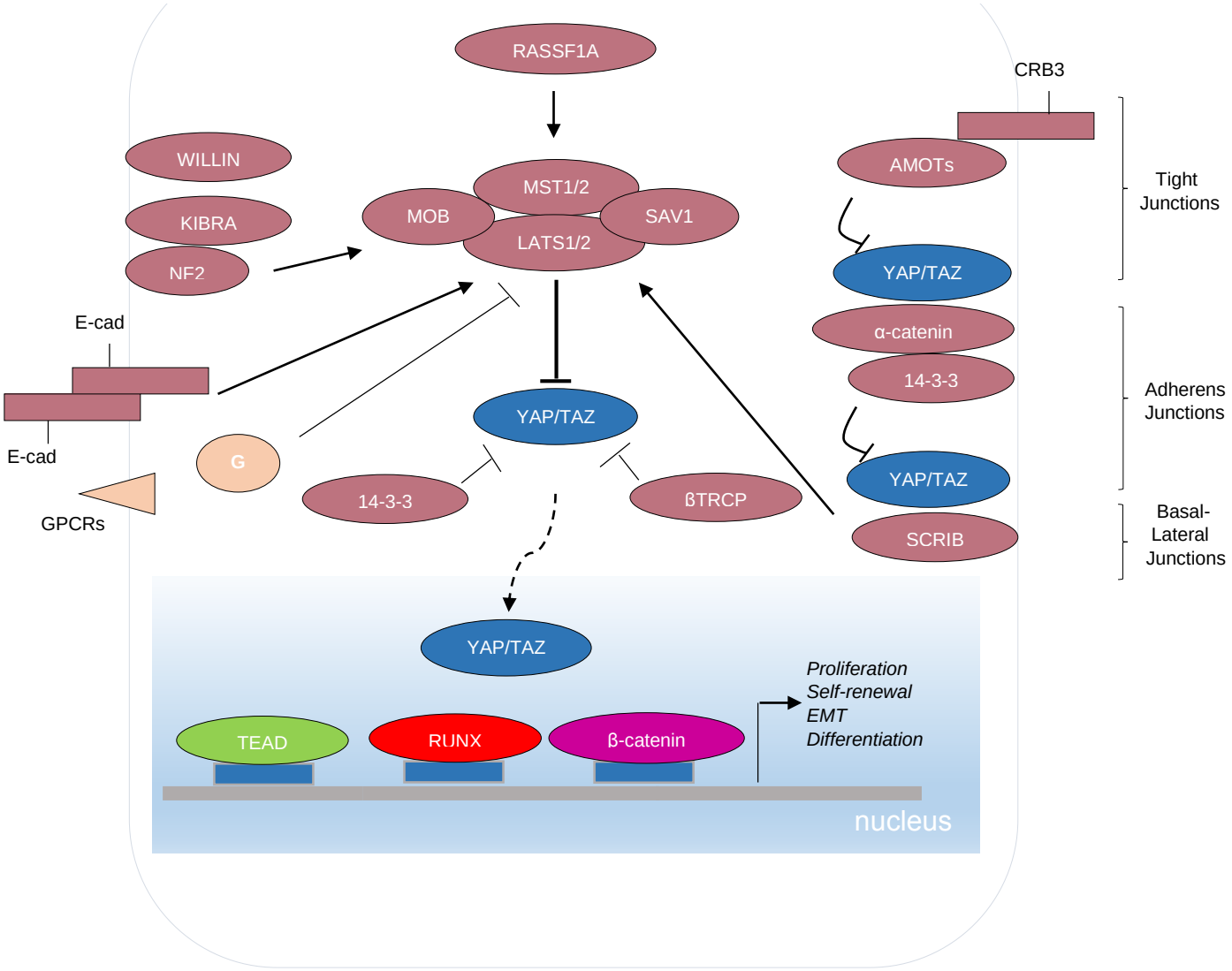


Figure 1.4. The Hippo signalling pathway in tumourigenesis and development. The core kinase cascade, consisting of MST1/2, LATS1/2, MOB and SAV1 is activated upon stimulation by various signals, resulting in YAP/TAZ inactivation. Deregulation of the Hippo pathway results in YAP/TAZ translocation to the nucleus, where in association with transcription factors and other transcriptional co-activators, they promote the expression of target genes involved in proliferation and metastasis, as well as stem cell self-renewal. YAP/TAZ can also be detained in the cytoplasm by Hippo pathway-independent mechanisms, involving junctional components.

1.6 Cancer stem cells (CSCs)

The observation that all cells within a tumour are not identical and some cancers, like teratocarcinomas, contain cell populations which are more differentiated than others, led to the suggestion that the undifferentiated cell populations are stem-like cancer cells, referred to as cancer stem cells (CSCs) (reviewed by Beck and Blanpain 2013). For many cancers, CSCs constitute a distinct population which can be prospectively isolated from the remainder of the tumour cells and can demonstrate clonal long-term repopulation and self-renewal capacity (Clarke, Dick et al. 2006, Nguyen, Vanner et al. 2012, Kreso and Dick 2014). Along these lines, two models have been proposed to explain tumour growth. According to the stochastic model, tumour cells self-renew or differentiate randomly, whereas the CSC model suggests that only a proportion of cancer cells has by default the capacity to self-renew or differentiate. Both models result in tumour heterogeneity, which can be further enhanced by the presence of new somatic mutations, some of which also confer survival advantages (Greaves and Maley 2012). Like normal stem cells, which exhibit increased resistance to programmed cell death in response to DNA damaging agents compared to their committed progeny and are more susceptible to genetic mutations, CSCs are expected to display similar phenotypes, accounting for tumour lapse following therapy (Mohrin, Bourke et al. 2010, Sotiropoulou, Candi et al. 2010, Beck and Blanpain 2013).

Various assays are being employed to identify CSCs and evaluate their self-renewal potential, such as *in vitro* serial passaging of colonies and spheres, as well as serial transplantation of tumour cells. Recently, serious

efforts have been made to track CSCs in tumours of the brain (Chen, Li et al. 2012), the gut (Schepers, Snippert et al. 2012) and the skin (Driessens, Beck et al. 2012). In the intestine, by assessing the clonogenic potential of LGR5-expressing cells, it was extrapolated that CSCs are, in fact, normal SCs which are able to initiate tumourigenesis and can, subsequently, exacerbate tumour growth (Schepers, Snippert et al. 2012). However, identification of CSCs is considered to be challenging, due to the lack of universal markers, even though several cell surface markers, such as CD133 have been related with the existence of CSCs in various types of tumours (Grosse-Gehling, Fargeas et al. 2013). Factors, such as the tumour microenvironment, which contribute to tumour plasticity, render the use of these markers often unreliable. For instance, although $CD44^{high}/CD24^{low}$ cell surface marker expression pattern is thought to underline the existence of CSCs in human breast cancers, CSC-free populations can also give rise to $CD44^{high}/CD24^{low}$ cells, implying that these markers cannot always be used as reliable readouts for identifying CSC lesions (Al-Hajj, Wicha et al. 2003, Fillmore and Kuperwasser 2008, Gupta, Fillmore et al. 2011).

Reports have suggested that tumourigenesis and somatic cell reprogramming are governed by similar mechanisms, as tumour progression is, in fact, the outcome of dedifferentiation processes (Bennett 1983, Gabbert, Wagner et al. 1985). In accordance with this, CSCs exhibit dedifferentiated phenotypes. One such example are CD271-positive melanoma CSCs, which have lost expression of common melanocytic markers, as part of reversing to a more immature state (Boiko, Razorenova et al. 2010). Furthermore, CSC generation has been linked with upregulation of stem cell markers, such as

OCT4, NANOG and SOX2 and their target genes, which are normally enriched in ESCs, highlighting the common mechanisms underlying pluripotency and tumourigenesis (Hochedlinger, Yamada et al. 2005, Ben-Porath, Thomson et al. 2008, Chen, Shi et al. 2008, Viswanathan, Powers et al. 2009). The observation that forced expression of OCT4 alone can induce dedifferentiation of melanoma and other cancer cell types (Hochedlinger, Yamada et al. 2005, Ben-Porath, Thomson et al. 2008, Chen, Shi et al. 2008, Viswanathan, Powers et al. 2009, Kumar, Liu et al. 2012), together with the numerous reports linking its upregulation with poor clinical outcome in various tumour types (Magnifico, Albano et al. 2009, Saigusa, Tanaka et al. 2009, Zhang, Han et al. 2010), have established OCT4 as a biomarker of CSC manifestation.

A screen performed in 993 primary breast tumours identified the Hippo pathway gene signature in high-grade (G3) tumours. YAP/TAZ activation, observed in tumours containing $CD44^{high}/CD24^{low}$ cell populations, implied their involvement in CSC generation. Indeed, TAZ downregulation in these cell populations led to limited self-renewal capacity, whereas its overexpression caused higher cell proliferation rates with enhanced CSC properties, such as increased resistance to chemotherapeutic agents (Cordenonsi, Zanconato et al. 2011). In keeping with these data, TAZ/YAP were shown to be endogenously upregulated in high-grade glioblastomas due to hypomethylation of their gene promoters. TAZ knockdown in these tumours resulted in impaired self-renewal, invasion and tumour-initiation ability (Bhat, Salazar et al. 2011).

Killing CSCs directly, impairing their self-renewal properties or forcing them to differentiate, comprise different strategies towards restricting tumour growth. Today, promyelocytic leukemia patients are treated with retinoic acid and arsenic, which are leukemic cell differentiation-promoting agents. This approach, based on forcing cancer cells to differentiate, results in cure (de The and Chen 2010). Similarly, bone morphogenic protein 4 (BMP4), which promotes differentiation of brain CSCs is a promising therapeutic target, as it has appeared to inhibit tumour growth *in vivo*, following transplantation of BMP4-coated beads together with brain CSCs into immunodeficient mice (Piccirillo, Reynolds et al. 2006). Currently, research has been focusing on the discovery of pharmacological compounds which are capable of targeting exclusively CSCs to stimulate their differentiation, without affecting normal SC pools (Sachlos, Risueno et al. 2012).

1.7 Objectives of the study

This study aims to unravel the molecular mechanism by which RASSF1A suppresses tumourigenesis and discover additional factors contributing to its tumour suppressive function. The project also aims to elucidate the cellular consequences that result from RASSF1A loss in cancers, contributing to the emergence of CSC phenotypes.

The attempt to develop a model describing the role of RASSF1A in tumourigenesis would be incomplete, without investigating its function in normal tissue. Given its involvement with one of the master regulators of tissue growth and organ size, the Hippo pathway, we aim to study the

potential role of RASSF1A in development, using ESCs and the pre-implantation embryo as tools.

Dissecting the physiological role of RASSF1A to provide better insight in tumourigenesis might prove to be of great importance towards the design of therapeutic approaches, given that RASSF1A loss, apart from deregulating the clinically relevant Hippo pathway, is itself one of the most frequent events in cancer.

CHAPTER 2

Materials and Methods

2.1 Cell lines and culture

U2OS, U2OS tet-on inducible cells expressing control vector or FLAG-RASSF1A, HCT116, HeLa, MDA-MB-231, MCF7, HEK293T, SNL76/7 and MEF (wild type, Rassf1a -/- or constitutively expressing HA-RASSF1A) cell lines were maintained in DMEM (High Glucose, Sodium Pyruvate) supplemented with 10 % fetal bovine serum (FBS), 1 % glutamine and 1 % penicillin/streptomycin at 37 ^{o}C in 5 % CO_2 and 20 % O_2, with the exception of MEFs that were kept in a 3 % O_2 incubator. All media and supplements were purchased from Gibco (Life Technologies). U2OS, HCT116, HeLa, MDA-MB-231, MCF7, HEK293T, SNL76/7 cell lines were obtained from ATCC. MEFs (wild type and Rassf1a -/-) were provided to us by Dr Louise van der Weyden, Sanger Institute, Cambridge, UK.

In the inducible cell lines, RASSF1A expression was stimulated with the addition of doxycycline (Sigma) in the medium at appropriate concentrations for the cell line and/or level of expression as indicated.

E14Tg2a mouse embryonic stem cells (obtained from ATCC), iPSCs and the subsequently derived stable lines (shGFP, shRassf1a, shTead2, shRassf1a/shTead2 expressing cell lines) were maintained in medium that consists of DMEM (High Glucose, Sodium Pyruvate, Gibco) supplemented with 0.01 % LIF (ESGRO, Millipore), 10 % Knockout Serum Replacement (Invitrogen), 2 % ES-grade Fetal Calf Serum (Invitrogen), 1 % L-glutamine (Gibco), 1 % non-essential amino acids (Gibco) and 0.0008 % β-mercaptoethanol (Sigma). The cells were kept at 37 ^{o}C in 5 % CO_2 and 20 % O_2.

The cells were passaged upon reaching confluency by rinsing with sterile Phosphate Buffered Saline (PBS; 137 mM NaCl, 2.7 mM KCl, 10 mM Na_2HPO_4, 1.76 mM KH_2PO_4, pH 7.4) before trypsinising with 0.25 % Trypsin-EDTA solution (Gibco). The stem cells were collected by centrifugation (500 x g, 5 min), after which the supernatant was removed and the cell pellet was resuspended thoroughly in medium to ensure single-cell suspensions. Stem cells were cultured in gelatin coated dishes or flasks (0.1 % gelatin, Sigma). All the other cell lines were collected after trypsinisation, spun down, resuspended in medium, split and kept in T175 flasks (Sarstedt).

Cell freezing was carried out by trypsinising, resuspending in media, centrifuging at 500 x g for 5 min, aspirating the supernatant and resuspending in freezing media (90 % FBS, 10 % Dimethyl Sulfoxide (DMSO) for non-stem cells, 90 % ESC media, 10 % DMSO for stem cells). Cryovials containing cells were aliquoted and placed in liquid Nitrogen.

Cell thawing was carried out by placing the cryovials in a 37 ^{o}C waterbath after removal from liquid Nitrogen. Thawed cells were resuspended in cell culturing medium, centrifuged and then placed into gelatin coated dishes (stem cells) or T25 flasks (non-stem cells) to expand. After 24 hours, confluent cells were moved to larger flasks. Stem cells were split and maintained in the original expansion dishes.

2.2 Cell fractionation

Cell fractionation was performed using the NE-PER Nuclear and Cytoplasmic Extraction Reagents Kit (Thermo Scientific). Briefly, 5 x 10^6 cells were harvested with trypsin-EDTA and centrifuged at 500 x g for 5 min in a 1.5 ml microcentrifuge tube. The cells were then rinsed with PBS and centrifuged at 500 x g for 3 min. The

supernatant was carefully removed and the cell pellet was resuspended in ~100 µl ice-cold CER I reagent (depending on the size of the cell pellet), vortexed and incubated on ice for 10 min. Following that, ~5 µl ice cold CER II reagent was added to the tube, which was vortexed and incubated on ice for 1 min. After vortexing again, the tube was centrifuged for 5 min at maximum speed and the supernatant (cytoplasmic extract) was immediately transferred to a pre-chilled tube, which could be stored at -20 ^{o}C. The insoluble fraction (pellet) was then suspended in ~50 µl ice-cold NER reagent and was vortexed for 15 sec every 10 min for 40 min in total. Lastly, the tube was centrifuged at maximum speed for 10 min and the supernatant (nuclear extract) could be stored at -80 ^{o}C in a microcentrifuge tube.

2.3 Co-immunoprecipitation from whole cell lysates

Cells were washed with PBS, trypsinised and pelleted via centrifugation in a tube or scraped off the dish using a rubber policeman prior to co-immunoprecipitation. For lysate preparation, cells were lysed in ice-cold 1 % (v/v) Nonidet P40 lysis buffer (20 mM Hepes pH 7.5, 1 % NP40 (Roche), 150 mM NaCl, 0.5 mM EDTA, 50 mM NaF, 10 mM β-glycerophosphate, 0.5 mM Na_3VO_4 and 1 x EDTA free protease inhibitors (Roche)). Lysates were cleared by centrifugation at 4 ^{o}C at 10000 x g for 10 min and then were subject to sonication for 15 sec at 20% amplitude. Samples were normalized with Bradford protein assay (see 2.5) and equal volumes of protein (1 - 2 mg) were used per reaction per experiment. Immunocomplexes were precipitated with Protein G sepharose (Sigma) or Dynabeads Protein G (Life Technologies). A list of the antibodies used can be found on Table 2.4. IP incubations lasted for 3 hours at 4 ^{o}C, rotating at 30 rpm. Afterwards, the beads were washed three times with NP40 wash buffer (lysis buffer without phosphatase and protease inhibitors). IP

samples were resuspended in 50 µl 1 x Laemmli sample buffer (12.5 % glycerol (v/v), 2 % SDS (w/v), 78 mM Tris pH 6.8, 720 mM β-mercaptoethanol, bromophenol blue) and boiled (100 ^{o}C; 5 min).

2.4 Co-immunoprecipitation from nuclear extracts

Nuclear lysates were prepared as described previously (Schreiber et al., 1989) with the addition of modifications. Briefly, 3-5 million cells were trypsinised and harvested by centrifuging at 1500 x g for 5 min. The pellet was resuspended in TBS (Tris buffered saline). The cells were again pelleted by centrifugation and the pellet, after aspirating TBS, was resuspended in 1-2 ml cold buffer A (10 mM HEPES pH 7.9, 10 mM KCl, 0.1 mM EDTA, 0.1 mM EGTA, 1 mM DTT, 0.5 mM PMSF) by gently pipetting in a tip. The cells were left on ice for 15 min to swell, after which 75-125 µl of 10 % Nonidet P40 was added. The tube was then vigorously vortexed for 10 sec and centrifuged for 5 min. The supernatant, which constitutes the cytoplasmic fraction was removed (it can be stored at -20 ^{o}C). The nuclear pellet was resuspended in 150 µl ice-cold lysis buffer (150 mM NaCl, 20 mM Hepes pH 7.5, 0.5 mM EDTA, 1 % NP40, protease and phosphatase inhibitors) and the sample was subject to sonication for 15 sec at 20% amplitude. The nuclear extract was centrifuged for 5 min in a microfuge at 4 ^{o}C and the supernatant was normalised and used to perform the immunoprecipitation as described above.

2.5 Western blot analysis

All the protein samples were quantified before being run on a western blot. As mentioned above, samples designated to be used for IPs were lysed in 1 % NP40

lysis buffer and normalised through Bradford protein assay, whereas extract samples were lysed in Laemmli Lysis Buffer (50 mM Tris-HCl pH 6.8, 2 % SDS, 50 mM NaF, 10 mM β-glycerophosphate, 0.5 mM Na_3VO_4 and 1 x EDTA free protease inhibitors (Roche)) and normalised by NanoDrop (Thermo Scientific). For Bradford assays, a standard Bovine Serum Albumin (BSA) curve was generated, ranging from 0 – 2000 mg/ml. All the samples were diluted 1/10 in PBS and the absorbance at 595 nm was determined in a plate reader (BMG POLARstar Omega). In immunoprecipitates the appropriate volume of 1 x Laemmli sample buffer was used, while in extracts 4 x Laemmli sample buffer was used.

Immunoprecipitates and cell lysates were resolved on 10 % or gradient 4-12 % Bis-Tris Nu-PAGE gels (Invitrogen) or self-cast gels (10 % resolving gel – 30 % acrylamide: 0.8 % Bis solution, 375 mM Tris pH 8.8, 0.1 % SDS, 0.1 % APS, 0.01 % TEMED) at 120 Volts. Novex MOPS running buffer was used for pre-cast gels, whereas SDS-PAGE running buffer (25 mM Tris, 190 mM Glycine, 0.1 % SDS) was used for self-cast gels. Pre-cast gels were run into Novex mini cell tanks and self-cast gels into BioRad Mini Protean TetraCell tanks.

After the electrophoresis was complete the gels were placed onto PVDF (polyvinylidene fluoride) membranes (Millipore) for the protein transfer process to take place. PVDF membranes needed to be activated in 100 % methanol before use. The transfer was done into BioRad Mini Protean TetraCell tanks filled with transfer buffer (25 mM Tris, 190 mM Glycine, 20 % Methanol) at 100 Volts.

After the transfer, membranes were blocked with 5 % non-fat milk (Fluka) in PBS 0.1% Tween or 5 % BSA (Fisher) in PBS 0.1 % Tween for 30 min. The primary antibody (Table 2.4) incubation was at 4 ^{o}C overnight in milk or BSA. Following the primary antibody incubation the membranes were washed four times with PBS 0.1%

Tween before incubation with secondary antibody (Table 2.4) (1 h), were further washed at least six times before the application of standard enhanced chemiluminescence substrate (Pierce) or high sensitivity substrate (Millipore), exposed to X-ray film (Kodak) and developed in a XoGraph processor. For quantification purposes, the intensity of the Western blot bands on the film was determined using the ImageJ densitometry software.

Stripping buffer (2% SDS, 62.5 mM Tris pH 6.8) was occasionally used on membranes, with the addition of β-mercaptoethanol (0.7% of the final solution). Following incubation for 30 min at 50 ^{o}C, the membranes were washed three times in PBS 0.1 % Tween and blocked into 5 % milk.

2.6 Sample preparation for Mass Spectrometry

Samples were prepared according to the protocol for co-immunoprecipitations from whole cell lysates (2.3) with a few modifications. Specifically, only Dynabeads Protein G were used to precipitate the proteins of interest. Moreover, after the 3 h incubation on the end-to-end rotator, the immunoprecipitates were washed four times, the two first being with NP40 lysis buffer and the last two only with filtered PBS to avoid the use of detergent. Finally, the tubes were left uncapped to air-dry for approximately 15 min and no Laemmli sample buffer was added to the immunoprecipitates. The samples were subject to mass spectrometry analysis for post-translational modifications using an Orbitrap mass spectrometer. The mass spectrometry analysis was performed by Dr David Gomez, Systems Biology Ireland.

2.7 Clonogenic Survival Assay

Cells were transfected with the indicated siRNAs and 24 hours later trypsinised and replated in 6-cm dishes (Corning) at a density of 350 cells per dish. They were then incubated at 37 ^{o}C in 5 % CO_2 and 20 % O_2 for 11 days to allow colonies to form. On the 11th day cells were fixed and stained with crystal violet solution (0.5 % (w/v) crystal violet, 50 % (v/v) methanol, 10 % (v/v) ethanol). Lastly, the amount of stained colonies was counted.

2.8 Resazurin Viability Assay

Cells were transfected with the indicated siRNAs and 24 hours later trypsinised and replated in wells of 6-well dishes at a density of 7.5 x 10^3 cells /well. They were incubated at 37 ^{o}C in 5 % CO_2 and 20 % O_2 for a day until they became attached. The cell culturing medium was then aspirated and 1 ml of resazurin (10 mg/ml, Sigma) was added into each well and the dishes were kept in the incubator for 2h, after which 200 μl were removed from each well and placed into a well of a 96-well plate (Costar). Immediately following that, resazurin reduction was measured in a plate reader at excitation wavelength 530 nm and emission wavelength 590 nm. 3 days later a second measurement was made by aspirating the previous resazurin and adding new, depending on the confluency of the cells.

2.9 xCELLigence Proliferation Assay

For this purpose an xCELLigence system (Roche) that assesses cell growth in real-time by conductivity reduction was used. 50 μl of complete DMEM were added

to the bottom of each well of an E-plate and the plate was loaded into the xCELLigence analyser and placed in a 37 ^{o}C, 5 % CO_2, 20 % O_2 incubator for half an hour. Afterwards, 100 µl of complete DMEM containing 5 x 10^3 cells were added to each well and measurements were taken every 30 min for 5-7 days.

2.10 Reverse-Transcriptase PCR (RT-PCR)

Reverse-Transcriptase PCR was done according to the Power SYBR Green Cells-to-Ct Kit protocol. Briefly, cells growing in flasks or plates were washed once with PBS, trypsinised and counted, after trypsin was neutralised by the addition of cell culturing medium. 5 x 10^4 cells were centrifuged at 500 x g for 5 min, washed once with ice-cold PBS and the pellet was lysed in the presence of DNase I. For that, 25 µl of lysis solution were added to the pellet and the lysis reaction was mixed by thoroughly pipetting up and down. Following a 5 min incubation of the lysis reactions at room temperature, 2.5 µl of Stop Solution were added and the reaction was mixed again by thorough pipetting. After a 2 min incubation at room temperature the RT Master Mix was prepared by placing in a tube 25 µl of 2 x SYBR RT Buffer, 2.5 µl of 20X RT Enzyme Mix and 17.5 µl of Nuclease-free water per sample. The Master Mix for each reaction was placed in a PCR tube and 5 µl of the previously made lysate were added to it, after which the reactions were transferred to a thermal cycler (BIO-RAD, My cycler) where they were incubated at 37 ^{o}C for 60 min, 95 ^{o}C for 5 min to inactivate the RT enzyme. The samples could then be stored at -20 ^{o}C.

2.11 Quantitative Real-Time PCR (qRT-PCR)

Quantitative Real-Time PCR was done according to the Power SYBR Green Cells-to-Ct kit protocol. After the production of cDNA from the RT reactions, the

cDNA was diluted down 2-4 times (depending on the abundance of the mRNA each time) in Nuclease-free water. The PCR Cocktail was then assembled by placing in a tube 5 μl of Power SYBR Green PCR Master Mix, 0.2 μl of Forward and Reverse PCR Primer mix (10 μM stock concentration) and 0.8 μl of Nuclease-free water for each sample. The PCR cocktail for each sample was placed in a well of a 96-well plate (Life Technologies), and the qRT-PCR reaction was assembled with the addition of 4 μl of the diluted cDNA for a total reaction volume of 10 μl. Subsequently, the plates were covered by sealing film (VWR) and placed in the real-time PCR instrument (Applied Biosystems), which was programmed as follows: Stage 1. Enzyme Activation (Hold), Repeats 1, Temperature 95 ^{o}C, Time 10 min, Stage 2. PCR (cycle), Repeats 40, Step 1. Temperature 95 ^{o}C, Time 15 sec, Step 2. Temperature 60 ^{o}C, Time 1 min, Stage 3. Dissociation Curve, Step 1. Temperature 95 ^{o}C, Time 15 sec, Step 2. Temperature 60 ^{o}C, Time 1 min, Step 3. Temperature 95 ^{o}C, Time 30 sec, Step 4. Temperature 60 ^{o}C, Time 15 sec. The further analysis of the results was done using the machine software.

For qRT-PCR following ChIP and ChIP seq, the PCR Cocktail per sample consisted of: 10 μl of Power SYBR Green PCR Master Mix, 4 μl of Forward and Reverse PCR Primer mix (5 μM stock concentration), 1 μl sterile Nuclease-free water and 5 μl DNA sample (ChIP or Input), in order to acquire a total reaction volume of 20 μl. The Input samples were at a 2.5 ng/μl concentration.

2.12 Agarose gel production

1 – 1.5 % agarose gels were used to determine the size of sonicated chromatin before performing ChIP and ChIP seq as well as for the genotyping of cell lines (MEFs). 1 – 1.5 g of agarose was dissolved in 100 ml 1 x TAE (40 mM Tris, 18 mM

Glacial acetic acid, 1 mM EDTA pH 8) buffer by microwaving for 3 min. After the addition of 0.003% ethidium bromide solution (10 mg/ml, Sigma), the mixture was poured into a BioRad tank and left to solidify for approximately 30 min. The gel was then covered with 1 x TAE buffer and the samples supplemented with 4 x DNA loading buffer (50 % glycerol, 1 x TAE, Orange G) and along with 1 Kb Plus Ladder (Invitrogen) were loaded into the wells and the gel was run at 100 Volts for approximately 45 min. The gel was then read in UV light for the detection of bands or smears and pictures were taken and analysed with the use of a camera (Canon) and the Quantity One software respectively.

2.13 Immunofluorescence

Cells plated onto normal or gelatin coated glass coverslips (Fisher) were washed twice with PBS before fixation in 4 % Paraformaldehyde solution (PFA, 16 % (w/v) Paraformaldehyde diluted in PBS) for 15 min. The cells were then washed three times with PBS, permeabilised with 0.2 % Triton X solution (in PBS) for 10 min and washed again with PBS before 0.2 % Fish Skin Gelatin (FSG, made in PBS) blocking solution was used for 1 hour at RT. Following that, the cells were incubated in primary antibody (Table 2.4) overnight at 4 ^{o}C and then washed three times with PBS before secondary antibody (Table 2.4) incubation for 1 h at RT. The cells were washed one last time with PBS, left to dry and the coverslips with the cells were mounted onto microscope slides using Prolong Gold antifade reagent with DAPI (Life Technologies). The coverslips were sealed with nail varnish and pictures of the cells were acquired using a Nikon 90i microscope with the NIS elements software, a Leica DM IRBE microscope with Simple PCI6 software or a confocal Zeiss LSM710 microscope with the Zeiss ZEN software.

2.14 Transfection

2.14.1 siRNA/plasmid Forward Transfection

This applies for all cell lines with the exception of ESCs and MEFs. Cells were transfected with siRNAs the following day after having been plated in antibiotic-free medium (DMEM supplemented with 10% FBS and 1% glutamine), when they were approximately 50% confluent. The transfection reagent used was DharmaFect 1 (Thermo Scientific) or Lipofectamine 2000 (Life Technologies). The siRNA:DharmaFect or siRNA:Lipofectamine 2000 ratio was indicated by the respective protocols for RNA interference (approximately 1:1). OPTI-MEM serum-reduced medium (Invitrogen) was used for the dilution of the transfection reagent and the siRNAs. The concentration of the siRNAs in the transfection medium was 50 - 100 nM from a 10 - 20 μM stock. A list of all the siRNAs used is provided on Table 2.1.Briefly, for every transfection the desired amount of siRNAs was diluted into the appropriate amount of OPTI-MEM (depending on the final transfection volume, as indicated by the protocol) in a 1.5 ml microcentrifuge tube (Sarstedt). The transfection reagent was also diluted into the same amount of OPTI-MEM in a separate 1.5 ml microcentrifuge tube. 5 min later the components of the two tubes were mixed and the mixture was incubated for 20 min at RT to allow the siRNA:liposome complexes to form. Following that, the mixture was added in a dropwise fashion to the cells. 6 h later, the cell growing medium was changed into antibiotic-supplemented DMEM. The cells were harvested 48 h after transfection and the knockdowns were assessed by western blotting or qRT-PCR.

In order to transfect the same cell lines with plasmid vectors, the cells were plated in the same medium as above. The transfection reagent used was Lipofectamine

2000. 5 - 10 μg of plasmid were used per transfection at a DNA:Lipofectamine 2000 ratio of approximately 1:1. The transfection process was identical to the one described above.

2.14.2 siRNA/plasmid Reverse Transfection

Reverse Transfection was used in ESC lines. The transfection reagent was Lipofectamine 2000 and the siRNA:Lipofectamine 2000 ratio was approximately 1:1. OPTI-MEM was used for the dilution of the transfection reagent and the siRNAs. The concentration of the siRNAs in the transfection medium was 100 nM from a 10 - 20 μM stock. Briefly, for every transfection the desired amount of siRNAs was diluted into the appropriate amount of OPTI-MEM (depending on the final transfection volume, as indicated by the protocol) in a 1.5 ml microcentrifuge tube. Lipofectamine 2000 was also diluted into the same amount of OPTI-MEM in a separate 1.5 ml microcentrifuge tube. 5 min later the components of the two tubes were mixed in a gelatin coated dish and the mixture was incubated for 15 - 20 min at RT. 2 - 2.5 x 10^6 cells resuspended into 1 ml of LIF-supplemented ESC medium were then added to the mixture before additional LIF-supplemented ESC medium was added to make it up to the desired transfection volume. The cells were harvested 48 h after transfection and the knockdowns were assessed by western blotting or qRT-PCR.

Plasmid transfections were done identically. Normally 5 - 10 μg of plasmid were used in a DNA:Lipofectamine 2000 ratio of 1:1.

2.14.3 siRNA/plasmid Electroporation

In ESCs RNA interference was also achieved via electroporation. Fresh medium was added to the cells 4 h prior to transfection and the cells were subsequently

rinsed with PBS and detached from the gelatin coated plates by trypsinisation. Trypsin was quenched with the addition of ESC medium and 2.5 x 10^6 cells per transfection were spun at 500 x g for 5 min before the pellet was resuspended in PBS and spun down as before. The cells were subsequently resuspended in 90 µl of Mouse ES Cell Nucleofector Solution (Lonza). The concentration of siRNA used for the transfection was 150 nM from 10 - 20 µM stock. The appropriate amount of siRNA was placed in a 1.5 ml microcentrifuge tube to which 10 µl of Mouse ES Cell Nucleofector Solution was added. The contents of the two tubes were mixed and the mixture was transferred into an electroporation cuvette. The programme used for Nucleofection was A-013 on a Nucleofector II device (Lonza). After the electroporation was complete, 500 µl of pre-warmed ESC culture medium were placed to the cuvette and by using a plastic pipette the cells from the cuvette were plated on gelatin coated dishes containing ESC medium and cultured for 48 h in a 37 ^oC, 5 % CO_2, 20 % O_2 incubator. 48 h later the cells were harvested and the knockdown was assessed via western blotting or qRT-PCR.

Plasmid transfection via electroporation in ESCs was done in exactly the same way as above. Generally, 10 µg of plasmid were used per transfection and the expression was assessed via immunofluorescence or western blotting 24 – 48 h post transfection.

Plasmid transfection was only done via electroporation in MEFs. In this case, cell culturing medium was aspirated from the plates and the cells were washed once with PBS and trypsinised. 1-2 x 10^6 cells were centrifuged at 500 x g for 5 min. The supernatant was aspirated and the pellet resuspended in OPTI-MEM at a concentration of 1 - 2 x 10^6 cells/200 µl. 5 – 10 µg of plasmid were added to a 1.5 microcentrifuge tube to which the previous 200 µl suspension was subsequently

added. Following that, the DNA/cell mixture was placed into an electroporation cuvette, which was in turn loaded on the Nucleofector II device and the A-023 programme was run. Immediately after the electroporation, 500 µl of pre-warmed medium were added to the cuvette and with the use of a plastic pipette the content of the cuvette was transferred into a dish containing normal MEF culturing medium (complete DMEM). The expression was assessed via WB or qRT-PCR 24 – 48 h post transfection.

2.15 Infection

2.15.1 shRNA Lentiviral Transduction

ESCs were infected with lentiviruses for the producton of stable cell lines. For this purpose, 3 days prior to infection HEK293T cells were seeded into T75 flasks at a concentration of 4 x 10^6 cells/flask. One day later, 293T cells were transfected as follows: in a 30 ml container (Universal) were placed 10 µg of the shRNA plasmid of interest (appropriate shRNA sequence cloned into pLKO.1 puro vector), 10 µg pMDLg/pRRE construct, 5 µg pRSV-Rev construct and 6 µg pMD2.G construct (all three of them code for the packaging components of the virus), 100 µl 2.5 M $CaCl_2$ and sterile water was added up to 1 ml. While bubbling, 1 ml of 2 x HBS (HEPES Buffered Saline; 280 mM NaCl, 55 mM HEPES, 1.5 mM NaH_2PO_4) buffer of pH 7.08 was added to the DNA/Ca mix and the mixture was let stand for 1 min before it was placed dropwise to the 293T cells. The following day, the medium was aspirated and 5 ml of fresh complete DMEM medium were placed on 293T cells. On the same day, 1.5 x 10^6 ESCs were plated onto gelatinised flasks in LIF-supplemented medium. The day after, ESCs were infected by removing the viral particle-containing

supernatant from the attached 293T cells and placing it to the ESCs with the use of 10 ml syringes (Terumo) and 0.45 μm filters (Millipore) in order to discard leftover 293T cells. Polybrene (Sigma, 8 mg/ml, 1:1000) was added to the supernatant prior to filtering. 24 h following the infection, the viral supernatant was removed and the ESCs were washed 10 times in PBS, after which fresh compete ESC medium was added. The cells were washed in PBS for at least 4 days (10 washes each day) before they could be used outside the tissue culture. A list of the shRNAs used in this study is provided on Table 2.2.

2.15.2 Plasmid Retroviral Transduction

MEFs were infected with retroviruses for the generation of stable cell lines. To that end, 4 days prior to infection HEK293T cells were seeded into 10 cm dishes at a concentration of 5 x 10^6 cells/dish. At least 7 h later, 293T cells were transfected as follows: in a 30 ml container (Universal) 10 μg of the plasmid of interest (appropriate sequence cloned into pBabe puro vector), 10 μg of the packaging plasmid pCL-Eco and 100 μl 2.5 M $CaCl_2$ were placed and sterile water was added up to 1 ml. While bubbling, 1 ml of 2 x HBS buffer of pH 7.08 was added to the DNA/Ca mix and the mixture was let stand for 1 min before it was placed dropwise to the 293T cells. The following day, the medium was aspirated and 10 ml of fresh complete DMEM medium were added to 293T cells. On the same day, 2 x 10^5 MEFs were plated onto 10 cm dishes in complete DMEM medium. The following day, MEFs were infected by removing the viral particle-containing supernatant from the attached 293T cells and placing it to the former with the use of 10 ml syringes (Terumo) and 0.45 μm filters (Millipore) in order to discard leftover 293T cells. Polybrene (Sigma, 8 mg/ml,

1:1000) was added to the supernatant prior to filtering. 24 and 31 h later a second and third infection respectively were performed exactly as described above.

2.16 Generation and maintenance of stable cell lines

Following the infections of MEFs and ESCs with the desired vectors, the cells were cultured in the presence of selection agent, the appropriate concentration of which was determined by performing a kill curve with a wide range of concentrations. The minimum amount of agent which was sufficient to kill all the cells in culture in a certain amount of time was used for the same period to select for the mutants.

MEFs transfected with pBabe puro HA-RASSF1A or empty vector were cultured in the presence of 1 – 2 μg/ml of puromycin for 2 – 3 days. The selection started a day after the last infection, when the medium was replaced with fresh one containing puromycin. The incorporation of the plasmid into the genome was validated via western blot.

ESCs transfected with pLKO.1 puro shGFP, shRassf1a #1, shRassf1a #2 and shTead2 were cultured in the presence of 1.75 μg/ml of puromycin for 2 days. The selection started on the day of the last wash with PBS, when fresh medium containing the aforementioned amount of puromycin was added. The stable incorporation of the plasmid into the genome was validated via western blot (for Tead2) or qRT-PCR (for Rassf1a).

2.17 Preparation of replication – deficient feeder cells

Feeder cells were used in part for culturing E14Tg2a cells as well as for reprogramming MEFs into iPSCs. On Day 1, a vial of frozen SNL76/7 cells was thawed to two gelatin coated 15 cm dishes containing 20 ml of complete DMEM

medium. On Day 5, thirty two 15 cm dishes were gelatinised and 20 ml of complete DMEM were added to each. The cells in the plates prepared on Day 1 were passaged to the new thirty two plates (1:16 passaging) and on Day 10, provided that the cells would reach confluency, Mitomycin C (Sigma) solution was prepared by adding 4 ml of PBS into each of the three Mitomycin C (2 mg/each) vials which were required for the treatment of all the cells. The vials were shaken for Mitomycin C to completely dissolve before the solution was transferred to a 50 ml tube to which PBS was added up to a final volume of 12.5 ml. Following that, 370 µl of Mitomycin C solution were added to each plate and the cells were incubated at 37 ^{o}C for 2.5 h. The media was aspirated from the plates and they were washed once with PBS before 4 ml of trypsin were added to each. After 5 min incubation time, 4 ml of complete DMEM were added to each plate and cells were dissociated, harvested and centrifuged at 500 x g for 5 min in one tube. The pellet was resuspended in 25 ml of complete DMEM medium, after which the cells were counted and frozen down in aliquots of 21 x 10^6 cells/cryovial. Each vial could be thereby used to provide an adequate feeder layer for 5 – 6 10 cm dishes (at a concentration of 4.2 x 10^6 cells/dish). Cells were thawed as described above (2.1).

2.18 Adaptation of E14Tg2a mESCs to feeder – free conditions

A vial of E14Tg2a stem cells acquired from ATCC, adapted to feeder – dependent conditions was thawed in a 37 ^{o}C waterbath. Thawed cells were resuspended in cell culturing medium and centrifuged. The supernatant was aspirated and the pellet was resuspended in 3 ml of complete ESC medium containing LIF. The 3 ml were equally aliquoted into three gelatin coated 10 cm dishes, which contained 10 ml of complete ESC medium and no feeder cells. During

the first 2 passages the cells exhibited a differentiated phenotype (Figure 2.1A), but renewing the medium and passaging the cells every 2 days steadily resulted in the formation of distinctive stem cell colonies that retained their round shape (Figure 2.1B). After passage 5, all the colonies in the dish were round, fitting the morphological criteria for pluripotent stem cell colonies in culture (Evans, Kaufman et al., 1981) and stained positive for alkaline phosphatase (2.19).

Alternatively, cells were thawed as described above and seeded into gelatinised feeder - containing 3 cm dishes with complete ESC medium. 2 days later, they were trypsinised and seeded into feeder – free gelatin coated 6 cm dishes, where they were passaged twice. At passage 3, they were transferred into feeder – free 10 cm dishes. The feeder cells used were replication deficient MEFs, as they were pre - treated with Mitomycin C (see 2.17). Passaging the cells, consequently, in the 10 cm dishes 2 – 3 times resulted in a complete depletion of the feeder layer and by that point, the stem cells, fully adjusted to the feeder – free culture retained the morphological features of pluripotent stem cells in culture.

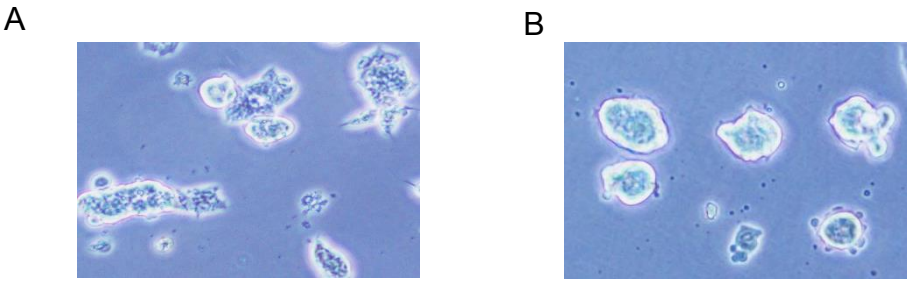


Figure 2.1 Adaptation of feeder – dependent E14Tg2a cells to feeder – free conditions. A. E14Tg2a cell colonies cultured in complete ESC medium in the absence of feeders exhibit irregular shape at passage 2. **B.** E14Tg2a cell colonies cultured in complete ESC medium in the absence of feeders are round at passage 5.

2.19 Alkaline Phosphatase Staining

For the purpose of staining stem cell or iPSC colonies for alkaline phosphatase expression, the Vector Black Alkaline Phosphatase Substrate Kit II was used. Briefly, cells cultured in 10 cm dishes were washed with PBS before the assay buffer was used. For every dish, 5 ml of 100 mM Tris – HCl, pH 9.5 were placed in a 15 ml Falcon tube and supplemented with 2 drops of Reagent 1, 2 and 3. Before the addition of each Reagent, the solution was mixed well. PBS was then aspirated off the plates and the assay buffer was added to the cells, after which the cells were kept in the dark for approximately 20 – 30 min. The buffer was subsequently removed and the cells were washed again with PBS. Colonies expressing alkaline phosphatase were stained brown/black.

2.20 Reprogramming of MEFs into iPSCs

Reprogramming was performed by utilising the established "Yamanaka cocktail" of transcription factors (Sox2, Klf4, Oct4, c-Myc, referred to as SKOM) (Takahashi et al., 2006). Briefly, feeder cell - containing 10 cm dishes were prepared as described above (2.17) at least one day before initiating reprogramming. In order to induce reprogramming of MEFs into iPSCs the piggyBac transposition system (Woltjen et al., 2009) was used**.** In a 1.5 ml microcentrifuge tube 10 µg of SKOM transposon were mixed with 2 µg of PBase transposase per transfection. The plasmids were acquired from Dr Pentao Liu, Wellcome Trust Sanger Institute, Cambridge, UK. The complete DMEM medium was aspirated from the feeder plates and 10 ml of complete ESC media were added instead. Media was aspirated from MEF plates, which were washed with PBS, trypsinised, counted and subject to electroporation as described above (2.14.3). Immediately after the transfection, the electroporated

MEFs were transferred to the feeder dishes and left in culture for approximately 11 days before they were stained for alkaline phosphatase expression (2.19). The medium in the plates was renewed every 2 days. The cells which were not used for the alkaline phosphatase assay, were left to produce bigger iPSC colonies which were isolated and expanded to generate iPSC lines (see 2.21).

2.21 Generation and maintenance of iPSC lines

Isolation and expansion of iPSCs was achieved after iPSC colonies had been growing for 15 – 20 days since reprogramming was initiated. More specifically, 50 μl of trypsin per well were added to a gelatin coated 96 – well plate, depending on the number of colonies to be picked. The original dish containing the iPSC colonies (along with the feeder cells and the non – reprogrammed MEFs) was prepared by removing the medium and washing once with PBS. Subsequently, individual colonies were picked using a P – 10 pipette (Eppendorf) set to 4 μl. Each colony was transferred into a well of the 96 – well plate, which was placed in a 37 ^{o}C incubator for 10 min for the cells to dissociate. Afterwards, 50 μl of complete ESC medium were added to each well and the colonies were further dissociated by vigorously pipetting up and down 10 – 12 times. The cells were allowed to attach to the plate and assessed every day for stem cell colony formation. When colonies approached confluency, they were trypsinised and transferred to a gelatinised 24 – well plate. The same process was repeated several times until the cells were seeded to gelatinised 12-, 6- well plates, 3-, 6- and eventually 10 cm dishes. iPSCs were frozen down as described above (2.1). iPSC lines were not kept in culture for longer than 10 passages.

2.22 LIF withdrawal assay

ESCs and iPSCs originally cultured in complete ESC medium (ESC medium supplemented with LIF as described in 2.1) were subject to LIF – free culture (ESC medium without the addition of LIF) for 4 – 20 days and assessed periodically for morphological features, stem cell expression markers and differentiation capacity via microscopy, western blotting, qRT-PCR and *in vitro* differentiation assays (see 2.24).

2.23 Embryoid body (EB) formation

iPSCs originally cultured in complete ESC medium were trypsinised, counted and replated to 90 mm non – gelatinised Petri dishes (Sterilin) at a concentration of 4 x 10^5 cells/dish in a total volume of 20 ml ESC medium in the absence of LIF to promote differentiation. The cells were cultured for 8 days, observing periodically to ensure that the medium did not become exhausted. Proliferation of stem cells under these conditions resulted in the formation of large aggregates that comprise embryoid bodies (EBs), the latter being macroscopic at approximately day 4 – 5 of culture.

2.24 Differentiation of iPSCs into dendritic cells (DCs)

After embryoid body formation had taken place (see 2.23) or on Day 8 of iPSC culture under the conditions described in 2.23, all EBs were transferred to a 50 ml Falcon tube and allowed for 10 – 20 min to sediment under unit gravity. Following that, the medium was replaced with fresh ESC medium prior to transferring to new Petri dishes. On Day 14 of iPSC culture, the EBs were harvested by sedimentation and washed gently twice in complete DMEM medium. The EBs were subsequently seeded at low density (approximately 10 – 30 EBs per plate) into non – gelatinised

10 cm tissue culture plates in ESC medium supplemented with 2 % GM – CSF – conditioned medium (Life Technologies) and 1000 U/ml of recombinant IL – 3 (rIL – 3;R & D systems). Following overnight culture, a proportion of the EBs attached to the dishes and began to develop colonies in a radial fashion which continued to grow until they eventually formed a stromal layer. DCs were observed around the perimeter of the colonies approximately 4 days later and continued to expand. It was essential that the medium into which DCs grew was replaced well before it started to change colour. The success of the process was validated via microscopic observation of the morphology of the cells, as well as flow cytometric analysis of the expression of the dendritic cell surface markers cd54 (icam – 1) and cd11c (Table 2.4).

2.25 Flow Cytometry

Following the differentiation assay in 2.24, cells were subject to flow cytometric analysis for expression of markers cd54 and cd11c (Table 2.4). Fixation and immunostaining of cells were done according to the Cell Signaling Technology protocol for Flow Cytometry. Briefly, the medium was aspirated from the plates, the cells were washed with PBS, trypsinised, counted (10^6 cells/condition), centrifuged at 500 x g, 5 min in a 15 ml Falcon tube, washed in 1 ml PBS and fixed for 10 min at 37 ^oC in 2 % (v/v) formaldehyde. The tubes were then chilled on ice for 1 min, after which immunostaining took place (without permeabilisation). For immunostaining, 3 ml Incubation buffer (0.5 % BSA in PBS) were added to each tube and rinsed by centrifugation two times. The pellet was afterwards blocked in 100 µl Incubation buffer for 10 min at RT before the primary antibody was added. After 1 h incubation at RT, the cells were rinsed with Incubation buffer by centrifugation and finally left in

incubation buffer containing secondary antibody for 30 min at RT. The buffer was removed by centrifugation and the pellet was resuspended in 0.5 ml of PBS and analysed on the flow cytometer (BD FACSCalibur).

2.26 Chromatin Immunoprecipitation (ChIP)

ChIP from stem cells was done according to the ChIP-IT High Sensitivity kit (Active Motif). Briefly, cell fixation was performed using 1/10 growth medium volume of Fixative Solution which was added to the medium and quenched by the addition of 1/20 medium volume of Stop Solution. After fixation, the cells were pelleted and washed twice with ice-cold PBS before they were resuspended in Chromatin Prep Buffer and homogenised in a chilled dounce homogeniser for 30 strokes. The cells were pelleted again and subject to sonication (Bioruptor Plus, Diagenode; low amplitude, pulse for 30 sec on and 30 sec off for 20 min) in ChIP buffer. At that point, 1/20 of the chromatin preparation was extracted to generate the Input from which the chromatin concentration per condition was determined and adequate amount was run on an agarose gel (2.12) to analyse chromatin size. The next step involved the making up of the immunoprecipitation reactions using 15 – 30 µg of chromatin and 4 µg of antibody (Table 2.4) per ChIP reaction. After the reactions were set up, the chromatin/antibody mixture was incubated on an end-to-end rotator at 4 ^{o}C overnight. 30 µl Protein G agarose were used per ChIP to which the reactions were added and the new mixture was incubated on an end-to-end rotator at 4 ^{o}C for 3 h. Following that, the whole ChIP reactions with the beads were washed thoroughly and transferred to DNA elution columns via which the ChIP DNA was isolated with the use of Elution Buffer. The final step (DNA purification) included the flow of the precipitated DNA through DNA purification columns that resulted in the elution of 200

μl of purified DNA (in Purification Elution Buffer). This volume was used to perform qRT - PCR analysis (2.11).

2.27 Bacterial transformations

DH5α chemically competent *E.coli* acquired from Invitrogen were incubated with the appropriate amount of plasmid on ice for 30 min in a 15 ml Falcon tube. Heat shock was then induced for 30 sec by placing the tube into a 42 ^{o}C water bath to allow the bacteria to intake the plasmids. LB broth was added and the tube was placed in a shaking incubator for 1h at 37 ^{o}C. 1/10 of the transfected bacteria were transferred into a solid LB plate containing the antibiotic to which the plasmid was resistant and the plate was subsequently placed into the incubator overnight. The following day, a bacterial colony from the plate was isolated and placed into a tube containing LB broth and antibiotic at a concentration of 1/1000 and the tube was then incubated at 37 ^{o}C for approximately 8h. 1/15 of that mini culture was placed into a 200 ml flask containing antibiotic and LB broth, which was kept in the incubator overnight. The day after, the whole culture in the flask was aliquoted into Falcon tubes, which were centrifuged at 1600 x g for 10 min at 4 ^{o}C in order to collect the pellet (transfected bacteria). Plasmid isolation and purification were performed using QIAfilter Plasmid Maxi Kit and QIAprep Spin Miniprep Kit (Qiagen).

2.28 Genotyping

MEFs were genotyped following the protocol for isolation of DNA from 1 – 2 x 10^6 cultured cells provided by the Qiagen FlexiGene DNA kit. Briefly, 10^6 cells were harvested in a 1.5 ml microcentrifuge tube as pellet before the addition of lysis buffer (FG1). After the addition of proteases (FG2) and incubation at 65 ^{o}C for 10 min, isopropanol was added to the mixture and the pellet was collected by centrifugation.

70 % ethanol was added to the pellet, which, after centrifugation and removal of the supernatant was left to air-dry. Finally, DNA was resuspended in FG3 buffer. The extracted DNA was then run on an agarose gel (2.12) to test the presence of the *Rassf1a* gene.

2.29 Sequencing

Sequencing of plasmids was performed by Sanger (Source Biosciences) and the preparation of samples was carried out following the company's guidelines. More specifically, in order to sequence short hairpin (sh) containing vectors, the DNA samples contained 1.5 µg DNA, 9 µl betaine (Sigma) and sterile water up to 15 µl. Short hairpin vectors were sequenced using the LKO.1 5' promoter primer. Sequencing of all the other plasmids in this study was carried out by preparing DNA samples containing 1.5 µg DNA and using the T7 promoter and SP6 promoter primers.

2.30 Statistics

Each experiment was performed at least three times to be statistically significant. For reprogramming experiments, in particular, different pools of MEFs deriving from two individual *Rassf1a*^{WT} and $^{-/-}$ embryos were used. All the data were analysed using Excel formulae for the extraction of the mean, standard deviation and error bars. The p-values were determined using Student's p-test and were interpreted according to Prism's guidelines (http://www.graphpad.com/guides/prism/6/statistics/index.htm?extremely_significant_results.htm).

2.31 Tables

Table 2.1. siRNA sequences used during this project.

siRNA	Sequences (sense)	Supplier
Non-targeting sequence 2	Not available	Thermo Scientific
siGENOME SMARTpool Human RASSF1	ACGCACAAGGGCACGUGAA CAAGGACGGUUCUUACACA GCAAGAAGCCACCCUCCUU CUACAUAACUUCCUACGUA	Thermo Scientific
GeneSolution Human RUNX2	CAGCACGCTATTAAATCCAAA CAGCAGCACTCCATATCTCTA CACCTTGACCATAACCGTCTT CAGAAGCTTGATGACTCTAAA	Qiagen
GeneSolution Human TEAD1	ATGGCCGATTTGTATACCGAA CCCGTAAGCAGTGCCTTAGTA CACATTGGGCATGCCAACCAT CGCCGCTTCATTGCACATTCA	Qiagen
siGENOME Human TP73	GCAAGCAGCCCAUCAAGGA	Thermo Scientific
Human RASSF1A	GACCUCUGUGGCGACUUCA	Eurofins MWG OPERON
Human YAP1	GACAUCUUCUGGUCAGAGA	Eurofins MWG OPERON
Stealth siRNA Mouse Rassf1a	CAGAACTCATTGAACTACGCGAGCT	Invitrogen
GeneSolution Mouse Tead2	CTCGAAGGAAATCGAGAGAAA ATGGTTTATGTTTGAAGGAGA TAGGGATGTAATCTTATCTCA ATGGAATGTTCCAGACGTGAA	Qiagen
GeneSolution Mouse Yap1	CTGGTCAAAGATACTTCTTAA ATGGAGAAGTTTACTACATAA ACCCTTGAACATATACATTTA AACATCCTATTTAAATCTTAA	Qiagen
GeneSolution Mouse Catnb	CAGGGTGCTATTCCACGACTA CAGATAGAAATGGTCCGATTA CTCACTTGCAATAATTACAAA CAGATGGTGTCTGCCATTGTA	Qiagen
GeneSolution Mouse Trp73	CTGAATGAAAGTACCACCAAA TGAGATCTTGATGAAAGTCAA CCCACTCTTGAAGAAGTTGTA AGGGAAGTCGCTCATGAACTA	Qiagen
GeneSolution Mouse Lats1	CAGGAAATCTGCAACATTCAA ATGGAGCTTTATAATATTAAT CCCAATTATATTGCACCTGAA TAGTGTATGTTTAATAAACTA	Qiagen

GeneSolution Mouse Tcf3	CCGAGTGTACCCTGAAGGAAA CAGCAGTGCCTTACCACTGTA CAGGCTGTCTCGGGACTCCAA AAAGGAAGCATTATTGGTCAA	Qiagen
siGENOME SMARTpool Mouse Tcf4	GAACCAAUUCCCAUCGUAA CGACAAGAAGGAUAUCAAA GUACGGAACUAGUCUUCUC GCAGGGAUCUUGGGUCACA	Thermo Scientific
GeneSolution Mouse Tead1	TAGACTTATCTTTGTAACTAA CAGGTTCTTGCCAGAAGGAAA AACATATATAGTATATTTAAA CTGGGCGGACTTAAACTGCAA	Qiagen

Table 2.2. shRNA sequences used during this project.

shRNA	Sequences (5'→3')	Supplier
Mouse Rassf1a #1	CCGG-CTGCAAGTTCACCTGCCATTA-CTCGAG-TAATGGCAGGTGAACTTGCAG-TTTTTG	Eurofins MWG OPERON
Mouse Rassf1a #2	CCGG-GCGGAGCCAGAACTCATTGAA-CTCGAG-TTCAATGAGTTCTGGCTCCGC-TTTTTG	Eurofins MWG OPERON
Mouse Tead2	CCGG-CCTCTTAGAAAGGAACCGGAA-CTCGAG-TTCCGGTTCCTTTCTAAGAGG-TTTTTG	Eurofins MWG OPERON

Table 2.3. Primers used for mRNA and promoter (ChIP) qRT-PCR and transgene expression.

Primer Name	Sequence
qRT-PCR Human NANOG	FW: GGTGTGACGCAGAAGGCCTCA REV: CCCAGTCGGGTTCACCAGGCA
qRT-PCR Human HES1	FW: ATTCCTCGTCCCCGGTGGCT REV: GCTTGGAATGCCGCGAGCTATCTTT
qRT-PCR Human 18S	FW: AGTCCCTGCCCTTTGTACACA REV: GATCCGAGGGCCTCACTAAAC
qRT-PCR Mouse Rassf1a	FW: GTGGAGACTTCATCTGGGGC REV: CAGCCTCATCCACGTTCGTA

qRT-PCR Mouse Nanog	FW: AAGGATGAAGTGCAAGCGGT REV: GGTGCTGAGCCCTTCTGAATC
qRT-PCR Mouse Oct4	FW: TGTGGACCTCAGGTTGGACT REV: TTTCATGTCCTGGGACTCCTC
qRT-PCR Mouse Sox2	FW: CAGGAGTTGTCAAGGCAGAGA REV: CTTAAGCCTCGGGCTCCAAA
qRT-PCR Mouse Bmp4	FW: ACCAATGGAGCCATTCCGTA REV: ACGACCATCAGCATTCGGTT
qRT-PCR Mouse Vimentin	FW: AGCAGTATGAAAGCGTGGCT REV: CAGGGACTCGTTAGTGCCTTT
qRT-PCR Mouse Gata4	FW: GCTCCATGTCCCAGACATTC REV: ATGCATAGCCTTGTGGGGAC
qRT-PCR Mouse Nestin	FW: GAGGCGCTGGAACAGAGATT REV: CACAGCCAGCTGGAACTTTTC
qRT-PCR Mouse Gapdh	FW: CTCCACTCACGGCAAATTCA REV: CGCTCCTGGAAGATGGTGAT
qRT-PCR Mouse Oct4-cMyc junction	FW: AAGATCAAGTATTGAGTATTCC REV: GCTGGTGATAGAAATTCTCTTCCT
Mouse Oct4 proximal enhancer (Hattori et al., 2004)	FW: GGAGGTGCAATGGCTGTCTTGTCC REV:CTGCCTTGGGTCACCTTACACCTCAC
Mouse Oct4 distal enhancer (Tead2 binding site) (Tamm et al., 2011)	FW: GCAGAAGGTCAGGTCCACTC REV: AGAACCCCACGACATCACTC
Mouse Oct4 distal enhancer (β-catenin binding site) (Yi et al., 2011)	FW: TGGGGGCAGAGAAGATGGTTG REV: AAGGCAGCGACTTGGAAGCC
Mouse β-actin promoter (Hattori et al., 2004)	FW: AAATGCTGCACTGTGCGGCG REV: AGGCAACTTTCGGAACGGCG
Mouse Nanog promoter (Rodda et al., 2005)	FW: TAAAGTGAAATGAGGTAAAGCC REV: GGAAAGATCATAGAAAGAAGAG
Mouse Sox2 upstream element (Chew et al., 2005)	FW:ATTAGTCTGCTCTTCCTCGGAATGGTTGG REV:TGATGCTTGTTAAAAACGCTTCGCTCCT

Table 2.4. Antibodies used during this project. WB: Western Blot and IF: Immunofluorescence.

Antibody	**Company**	**Clone/Catalogue Number**	**Dilution (Assay)**
RASSF1	Santa Cruz Biotechnology	3F3/Sc-58470	1/300 (WB)
β-CATENIN	Santa Cruz Biotechnology	Sc-7199	1/1000 (WB), 1/100 (IF)

FLAG M2	Agilent	200472-21	1/2000 (WB)
GAPDH	Abcam	2251-1	1/10000 (WB)
HA Tag	Millipore	05-904	1/1000 (WB)
TEAD1 (TEF-1)	BDTransduction Laboratories	610922	1/1000 (WB)
P73	Epitomics	EP436Y	1/2000 (WB)
YAP1	Santa Cruz Biotechnolgy	H-125/Sc-15407	1/1000 (WB), 1/100 (IF)
YAP1	Santa Cruz Biotechnology	63.7/Sc-101199	1/750 (WB), 1/100 (IF)
TEAD2 (TEF-4)	Santa Cruz Biotechnology	Sc-67115	1/1000 (WB)
TEAD2 (TEF-4)	GeneTex	GTX47542	1/1000 (WB)
RUNX2	Santa Cruz Biotechnology	M-70/sc-10758	1/1000 (WB)
LAMIN B1	Abcam	Ab16048	1/10000 (WB)
HSP70	Santa Cruz Biotechnology	W27/sc-24	1/1000 (WB)
NANOG	Abcam	Ab80892	1/1000 (WB), 1/100 (IF)
OCT4	Abcam	Ab19857	1/1000 (WB), 1/100 (IF)
SOX2	Millipore	10H9.1/MAB4423	1/500 (WB), 1/100 (IF)
Ki67	Millipore	AB9260	1/100 (IF)
CD54 (ICAM-1)	Novus Biologicals	NBP1-72025	1/100 (FACS)
CD11c	Abcam	3.9/ab11029	1/100 (FACS)

TCF3	Santa Cruz Biotechnology	E-2/sc-166411	1/750 (WB)
TCF4	Cell Signaling Technology	C48H11/2569	1/1000 (WB)
TAZ	Abcam	Ab118373	1/1000 (WB)
TAZ	Santa Cruz Biotechnology	H-70/sc-48805	1/1000 (WB), 1/100 (IF)
Phospho-YAP (Ser127)	Cell Signaling Technology	4911	1/1000 (WB)
LATS1	Bethyl Laboratories	A300-477A-1	1/1000 (WB)
HES1	Millipore	AB5702	1/1000 (WB)
FIBRILLARIN	Abcam	Ab5821	1/10000 (WB)
C-MYC	Millipore	9E10/CBL430	1/1000 (WB)
DYKDDDK Tag (FLAG)	Cell Signaling Technology	2368	1/2000 (WB)
HRP conjucated anti-Mouse	Jackson ImmunoResearch	315-035-048	WB (1/5000)
HRP conjucated anti-Rabbit	Jackson ImmunoResearch	711-035-152	WB (1/5000)
HRP conjucated anti-Goat	Santa Cruz Biotechnology	Sc-2020	WB (1/10000)
Alexa fluor goat anti-rabbit 488 nm	Invitrogen	A-11008	IF (1/500)
Alexa fluor goat anti-mouse 594 nm	Invitrogen	A-11005	IF (1/500)
Alexa fluor goat anti-rabbit 594 nm	Invitrogen	A-11012	IF (1/500)
Alexa fluor goat anti-mouse 488 nm	Invitrogen	A-11001	IF (1/500)
Alexa fluor goat anti-rabbit 633 nm	Invitrogen	A-31576	IF (1/500)
Alexa fluor goat anti-mouse 568 nm	Invitrogen	A-21422	IF (1/500)

Chapter 3

Loss of *Rassf1a* synergises with deregulated Runx2 signalling in tumourigenesis

3.1 Introduction

The RASSF1A tumour suppressor is inactivated through point mutation or promoter hypermethylation in the majority of human cancers. It is a multifunctional protein involved in a wide range of key biological processes that hinder cancer development, including apoptosis, cell-cycle regulation, mitosis and microtubule dynamics (Donninger, Vos et al. 2007, van der Weyden and Adams 2007). Work in our group has shown that RASSF1A activation is dependent on ATM signalling upon DNA damage, which phosphorylates RASSF1A on serine 131 (S131). RASSF1A is a component of the MST/LATS (Hippo) pathway as its phosphorylated form interacts directly with MST kinases and promotes active YAP1-p73 transcriptional complexes, resulting in the upregulation of pro-apoptotic genes, such as *PUMA* (Matallanas, Romano et al. 2007, Hamilton, Yee et al. 2009).

Apart from p73, YAP1 has been found to associate with a number of other transcription factors, including TEAD1 (Vassilev, Kaneko et al. 2001) and RUNX2 (Yagi, Chen et al. 1999), indicating that, at least in mammals, it displays a pleiotropic role. YAP1-TEAD1 complexes drive the expression of genes involved in proliferation and epithelial-to-mesenchymal transition (EMT) (Zhao, Ye et al. 2008, Chan, Lim et al. 2009). It has been well established that deregulation of the MST/LATS pathway leads to tissue overgrowth and tumourigenesis through increased formation of YAP1-TEAD1 complexes (Ota

and Sasaki 2008, Zhao, Ye et al. 2008, Chan, Lim et al. 2009, Zhang, Liu et al. 2009). On the other hand, YAP1-RUNX2 complexes are involved in regulating the expression of differentiation-related genes (Blyth, Vaillant et al. 2010).

Loss of RASSF1A in tumours prevents the formation of YAP1-p73 complexes (Matallanas,Romano et al. 2007) and, additionally, *Rassf1a* homozygous null mice exhibit faster death rates than their wild-type counterparts due to increased tumour formation (van der Weyden, Tachibana et al. 2005). Therefore, one of the aims of this study was to understand whether RASSF1A signalling determines the choice of transcription factor partner for YAP1 and if loss of RASSF1A expression in cancer switches YAP1 from a tumour suppressor into an oncogene.

Moreover, van der Weyden et al demonstrated in 2005 that the tumour incidence observed in *Rassf1a* null mice was significantly increased following exposure to mutagens. This suggested that additional genes collaborate with *Rassf1a* loss in tumourigenesis. Hence, the additional aim was to identify these genes and their function and develop a mechanism through which new insights into RASSF1A-mediated tumour suppression would be provided.

3.2 RASSF1A regulation of YAP1 transcriptional complexes

RASSF1A has been identified as an upstream component of the MST/LATS pathway, as it binds MST kinases via a shared C-terminal SARAH (SAlvador, RASSF1A, Hippo) domain (Guo, Tommasi et al. 2007). It is through this kinase cascade that RASSF1A signals to YAP1 and activates

p73 resulting in enhanced transcription of p73 target genes in response to DNA damage (Hamilton, Yee et al. 2009). However, since YAP1 is also found to associate with transcription factors other than p73 (Strano, Munarriz et al. 2001), for example TEAD1 (Vassilev, Kaneko et al. 2001) and RUNX2 (Yagi, Chen et al. 1999), and these transcriptional complexes facilitate different, often opposite, biological processes, we sought to investigate whether the presence of RASSF1A signalling is the key element to determine YAP1 transcriptional pairing. More specifically, since RASSF1A has been actively linked with tumour suppressor functions, often through p73 (Matallanas, Romano et al. 2007, Hamilton, Yee et al. 2009), we hypothesised that RASSF1A signalling might favour YAP1-p73 complex formation at the expense of YAP1-TEAD1.

Therefore, we used human osteosarcoma U2OS cells inducibly expressing FLAG-tagged RASSF1A via a Tet-on system to address our initial questions. The cells were treated with doxycycline at a concentration of 0.5 µg/mL for 24 h to allow sufficient expression of RASSF1A to take place. The cells were subsequently harvested and lysed before we performed YAP1 immunoprecipitations in order to assess YAP1-p73 and YAP1-TEAD1 complex formation. Our results demonstrated that doxycycline-induced expression of RASSF1A limited the ability of YAP1 to associate with TEAD1 and promoted association with p73 (Figure 3.1).

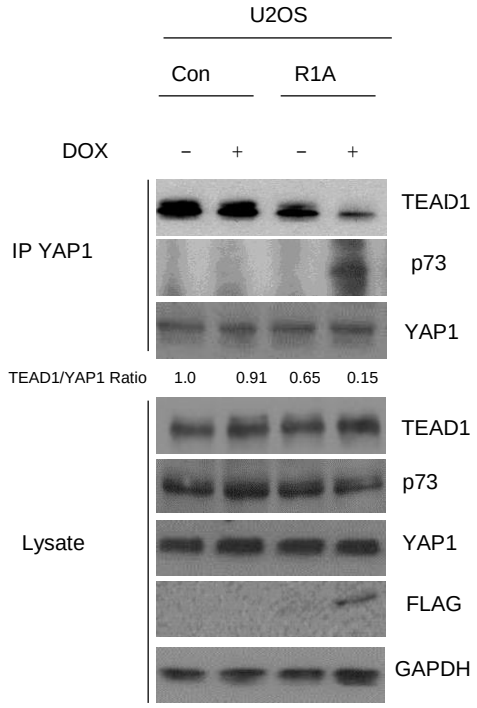


Figure 3.1. RASSF1A enhances YAP1-p73 and restricts YAP1-TEAD1 complexes. Human osteosarcoma U2OS cells tet-on inducibly expressing control vector (Con) or FLAG-RASSF1A (R1A) were treated with doxycycline (DOX) at a concentration of 0.5 µg/mL for 24 h. Top panel: YAP1 immunoprecipitates were western blotted with the indicated antibodies (right). Bottom panel: cell lysates were blotted with the indicated antibodies (right).

3.3 Genes promoting tumourigenesis in a *Rassf1a* null background

Long latency in tumour development observed in *Rassf1a -/-* mice was reduced when the mice were treated with chemical mutagens or ionising radiation (van der Weyden, Tachibana et al. 2005). This strongly suggested that additional mutations in other genes than *Rassf1a* alone exacerbate the oncogenic phenotype.

In order to identify potential factors which exacerbate tumourigenesis in the absence of RASSF1A, we performed a *Sleeping Beauty* transposon-mediated insertional mutagenesis screen in collaboration with the David Adams Laboratory in the Sanger Institute, Cambridge, UK. *Sleeping Beauty* screens

allow identification of key genes and pathways that are relevant to disease (Dupuy, Akagi et al. 2005, Keng, Yae et al. 2005, Mates, Chuah et al. 2009).

Rassf1a -/- Sleeping Beauty mice developed tumours significantly faster than their wild type *Sleeping Beauty* littermates (average life span of 35 and 44 weeks for *Rassf1a -/-* and *Rassf1a* +/+ mice respectively) (Supplementary Figure 7.1A). Additionally, all mice in both cohorts developed leukemias/lymphomas (Supplementary Figure 7.1B) and immunohistochemical analysis of a section of the leukemias/lymphomas showed that the majority of them were poorly differentiated lymphomas (van der Weyden, Papaspyropoulos et al. 2012) (Supplementary Figure 7.1C). The common insertion sites (CIS) were identified by the method described by van der Weyden and Papaspyropoulos et al. in 2012 and revealed 10 genes potentially contributing to tumourigenesis in a *Rassf1a* null background (Supplementary Table 7.1). *Runx2* was selected out of this set of genes (Supplementary Figure 7.2), not only as a known transcriptional regulator of osteogenesis (Sato, Morii et al. 1998), but mainly due to being a well-known YAP1 binding partner (Yagi, Chen et al. 1999).

3.4 Transcription factor competition for YAP1 binding

In section 3.2 it was described how RASSF1A signalling causes YAP1 to alter its preference for transcription factor binding. In the presence of RASSF1A, YAP1-p73 complexes were prominent whereas, YAP1-TEAD1 was the predominant interaction in the absence of RASSF1A signalling. To test whether RUNX2 was similarly able to compete with TEAD1 for YAP1 association, we focused on complexes within the nuclear compartment, due to

emerging alternative functions for YAP1 at cell junctions (Schlegelmilch, Mohseni et al. 2011, Zhao, Li et al. 2011).

U2OS cells were transfected with either non-targeting siRNAs or siRNAs targeted against RUNX2 and TEAD1. After 48 h cells were harvested and nuclear lysates were obtained by nuclear-cytoplasmic fractionation. YAP1 immunoprecipitations were carried out from the nuclear lysates. Reduction of RUNX2 expression resulted in elevated levels of TEAD1 in YAP1 immunoprecipitates indicating enhanced YAP1-TEAD1 interaction (Figure 3.2A). This suggested the existence of competition between transcription factors for association with YAP1. In order to test this hypothesis, we downregulated TEAD1 and, interestingly, observed an increase in YAP1-RUNX2 levels (Figure 3.2B). Western blots of nuclear lysates indicate that expression levels of RUNX2, TEAD1 and YAP1 are equivalent in all cases, ruling out the possibility that total protein variations were responsible for the differences observed in the co-immunoprecipitations. LAMIN B1 was used as a nuclear and HSP70 as a cytoplasmic marker respectively.

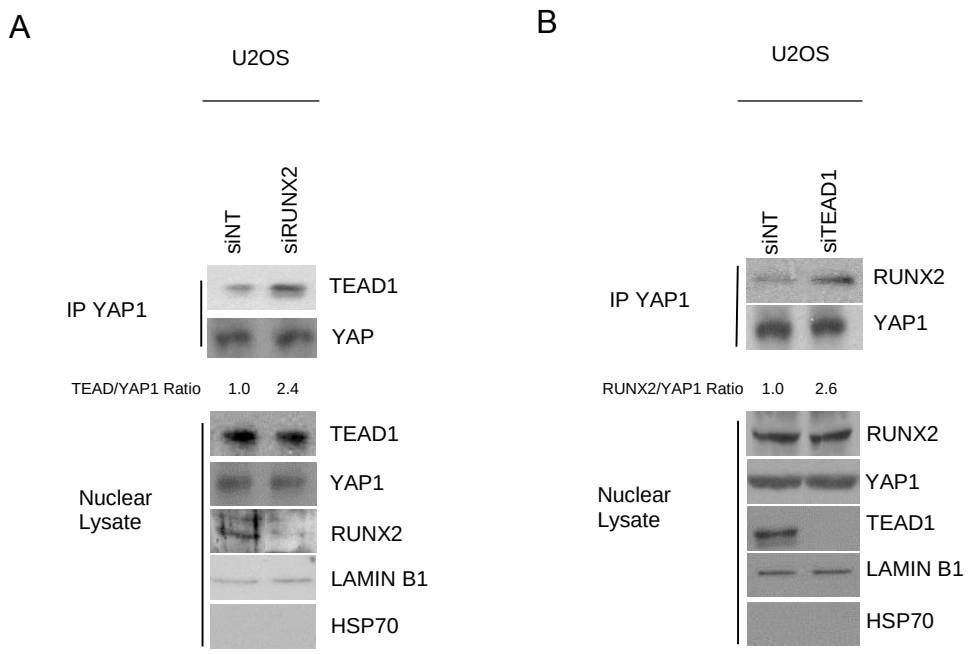


Figure 3.2. RUNX2 and TEAD1 transcription factor competition for binding to YAP1. A. U2OS cells were transfected with either non-targeting siRNA (siNT) or siRNA against RUNX2 (siRUNX2). YAP1 immunoprecipitates from nuclear lysates were western blotted with the indicated antibodies (right). **B.** U2OS cells were tranfected with either non-targetting siRNA (siNT) or siRNA against TEAD1 (siTEAD1). YAP1 immunoprecipitates from nuclear lysates were western blotted with the indicated antibodies (right).

3.5 Loss of RUNX2 in the absence of RASSF1A increases YAP1-TEAD1 complex formation

To further validate the findings of the *Sleeping Beauty* mutagenesis screen (section 3.4), according to which *Runx2* silencing in a *Rassf1a* null background led to enhanced tumourigenesis, we required an appropriate *in vitro* system. All the *in vitro* data described so far were acquired from osteosarcoma cells (U2OS), not only because they retain endogenous expression of RASSF1A, but also due to the high expression levels of RUNX2, and involvement in bone formation (Sato, Morii et al. 1998). To complement the findings in U2OS cells we also employed HCT116 colon

cancer cells which fulfil both criteria (RASSF1A and RUNX2 expression), allowing us to have confidence that our results are valid and not cell line-specific.

U2OS and HCT116 cells were transfected either with single siRNAs (targeting RASSF1A and RUNX2 individually) or dual siRNAs targeting both RASSF1A and RUNX2 to achieve single and double knockdowns respectively. 48 h later cells were harvested and subjected to fractionation to obtain the nuclear fraction, which was used to perform YAP1 co-immunoprecipitations (Figure 3.3). In both cell lines, depletion of RASSF1A or RUNX2 alone resulted in an increase in YAP1-TEAD1 complexes. The double knockdown of RASSF1A/RUNX2 resulted in elevated levels of the YAP1-TEAD1 complex in both U2OS and HCT116 cells compared to siRASSF1A alone (Figures 3.3A and 3.3B). This observation suggested that dual downregulation of RASSF1A and RUNX2 may indeed exacerbate tumourigenesis through further stabilisation of YAP1-TEAD1.

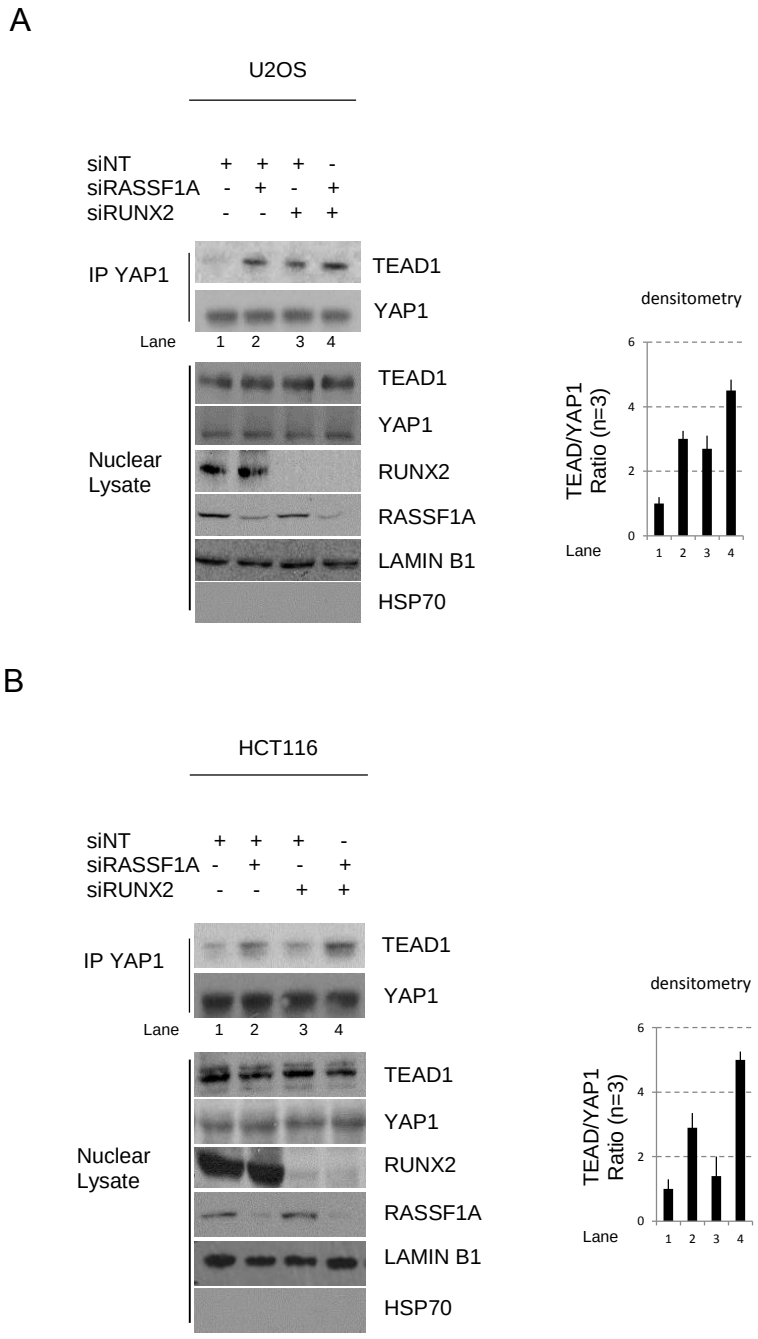


Figure 3.3. Dual downregulation of RASSF1A and RUNX2 further increases YAP1-TEAD1 complexes. A. U2OS cells transfected with either non-targeting siRNA (siNT), siRNA to RASSF1A (siRASSF1A) and/or siRNA to RUNX2 (siRUNX2). YAP1 immunoprecipitates from nuclear lysates were western blotted with the indicated antibodies (right). **B.** Human colorectal carcinoma HCT116 cells were transfected with either siNT, siRASSF1A and/or siRUNX2 and YAP1 immunoprecipitates from nuclear extracts were western blotted with the indicated antibodies (right). Densitometry for A and B is provided on the right. $P < 0.001$ (Student's t test) for the control (lane 1) against dual siRNA (lane 4).

Therefore, as these experiments demonstrate that RASSF1A and RUNX2 loss results in elevated YAP1-TEAD1 interaction, it was important to verfiy whether the cells exhibit increased tumourigenic behaviour as a result of this enhanced complex formation. To test this, we assessed their metabolic activity/viability, proliferative capacity and their ability to form colonies.

3.6 YAP1-TEAD1-dependent clonogenicity requires loss of RASSF1A or p73

To investigate whether the elevated levels of YAP1-TEAD1 had an impact on the tumourigenic potential of cells, we performed colony formation assays in osteosarcoma U2OS cells. Since RASSF1A exerts its tumour suppressive functions by promoting YAP1-p73 complexes (Matallanas, Romano et al. 2007) (Figure 3.1), we reasoned that silencing of p73 should therefore be epistatic to RASSF1A depletion. Cells were targeted with siRNAs to RASSF1, RUNX2, both RASSF1/RUNX2, both p73/RUNX2, or p73 alone (Figure 3.4). The cells were plated on 6 cm dishes and allowed to form colonies for 11 days, before they were stained with crystal violet. In line with promotion of YAP1-TEAD1 levels, the number of U2OS colonies observed in the absence of both RASSF1 and RUNX2 was higher than single knockdown of either RASSF1 or RUNX2 alone. Similarly, the combination of sip73 with siRUNX2 resulted in equivalent enhanced clonogenicity (Figure 3.4).

YAP1 is the key central component, as its binding preferences, driven by upstream signals, like RASSF1A, determine different biological processes and prescribe different cell functions. We highlighted the importance of YAP1 by

demonstrating that transcription factors actively compete for binding (Figure 3.2). Therefore, we reasoned that exogenous overexpression of YAP1 might resolve the competition and allow the formation of all three complexes. In U2OS cells, we employed the same approach as above to induce single and double knockdowns, in presence or absence of FLAG-YAP1 overexpression. Interestingly, YAP1 overexpression only increased clonogenicity when RUNX2 was depleted in conjunction with either RASSF1A or p73 (Figure 3.4). Lysates from the same pool of transfected cells were acquired 48 h after transfection to validate the efficiency of the siRNA-mediated knockdowns and plasmid overexpression (Figure 3.4).

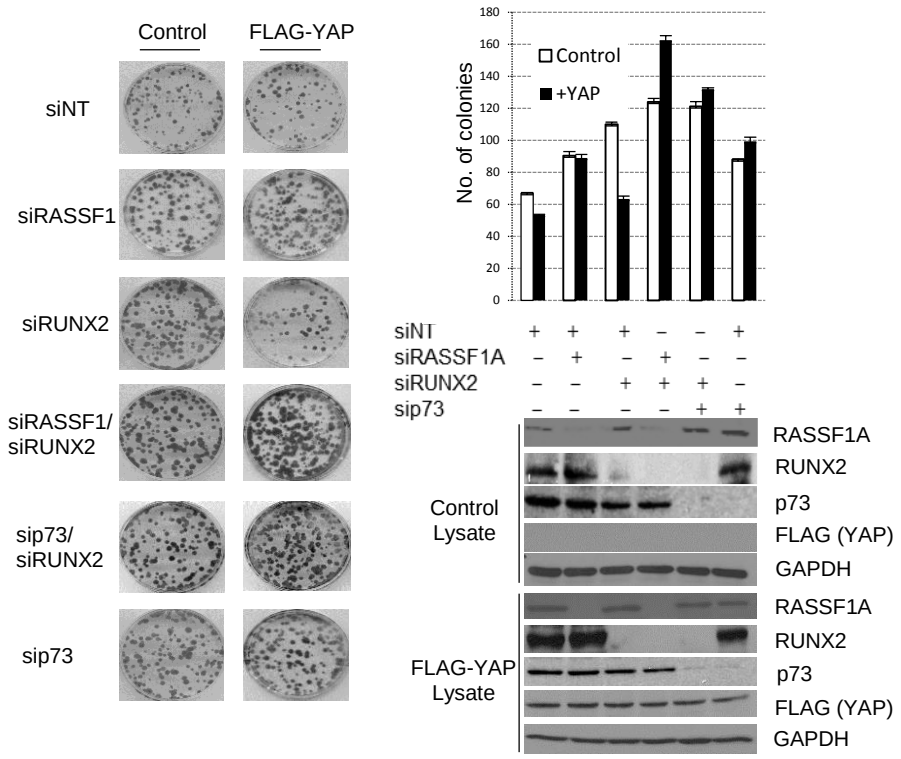


Figure 3.4. RASSF1A and RUNX2 limit YAP1-TEAD1-dependent colony formation. U2OS cells were transfected with either pCDNA (Control) or FLAG-YAP1 and indicated siRNAs (left panel) and were allowed to form colonies for 11 days before they were fixed and visualised by crystal violet staining. Top right panel: quantification of the number of colonies in each condition. Student's t test was used to derive the statistics: $P < 0.001$ for siRASSF1A versus siRASSF1A/siRUNX2; $P = 0.023$ for siRUNX2 versus siRASSF1A/siRUNX2; $P < 0.001$ for sip73 versus sip73/siRUNX2. Bottom right panel: whole cell lysates from all the conditions were western blotted with the indicated antibodies.

3.7 RASSF1A and RUNX2 limit YAP1-TEAD1-dependent cell viability and proliferation

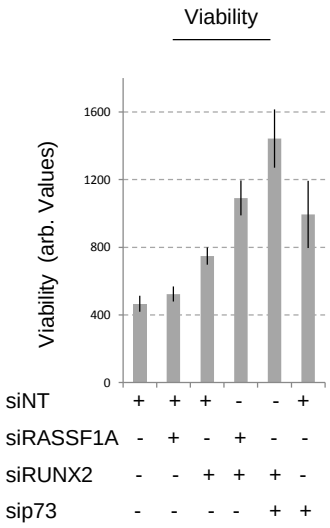
As loss of both RASSF1A and RUNX2 exacerbated the oncogenic phenotype driven by YAP1-TEAD1 complexes by leading to increased colony formation (Figure 3.4), we sought to further validate the tumourigenic potential using metabolic and real-time proliferation assays.

Resazurin reduction can be used to measure the metabolic activity of cells in culture. The observation that cancer cells demonstrate increased metabolic activity, known as the "Warburg effect" was first made back in the beginning of

the 20th century (Warburg 1925, Warburg 1956a, Warburg 1956b, reviewed by DeBerardinis, Lum et al. 2008). Thus, we used metabolic activity as a correlate for any variation in the tumourigenic potential of cells. U2OS cells transfected with the siRNAs mentioned in Section 3.6, were cultured in the presence of resazurin for 2 h before its reduction was measured. Depletion of both RASSF1A and RUNX2 resulted in a significant increase in metabolic activity in comparison to controls. In keeping with colony forming ability, RUNX2/p73 depletion similarly enhanced viability (Figure 3.5A). These measurements indicate that dual downregulation of RASSF1A or p73 together with RUNX2 result in increased viability of cancer cells.

To further support the interpretation that loss of transcription factor competition contributes to an oncogenic phenotype, we monitored proliferation in real-time. In U2OS cells we used combinations of siRNAs which should promote YAP1-TEAD1, YAP1-p73 or YAP1-RUNX2 and monitored U2OS cell growth in real-time over 7 days using an xCELLigence system. Similarly to the previous observations, silencing of RUNX2 and p73 expression (fostering YAP1-TEAD1 complexes) increased proliferation, while decrease of RUNX2 and TEAD1 (promoting YAP1-p73) suppressed cell growth. Interestingly, the dual depletion of p73 and TEAD1 (promoting YAP1-RUNX2), significantly reduced cellular proliferation (Figure 3.5B). Controls for the knockdowns are provided in Figure 3.4 (Western blots), as cells in all three assays (Figures 3.4 and 3.5) were derived from the same pool.

A



B

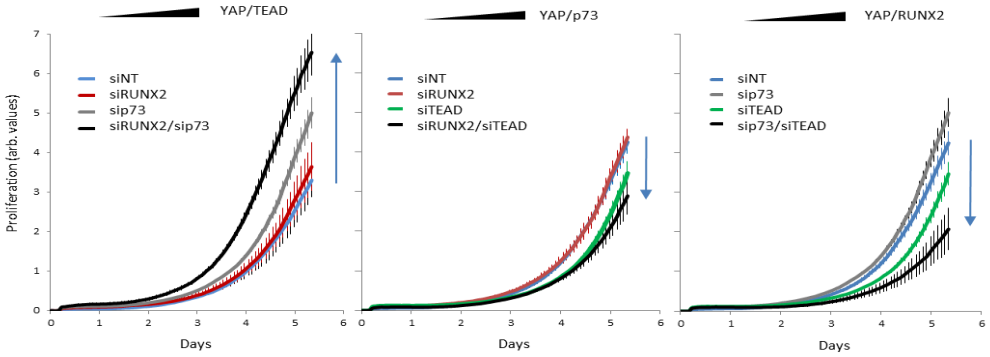


Figure 3.5. RASSF1A and RUNX2 limit YAP1-TEAD1-dependent cell viability and proliferation. A. U2OS cells were transfected with the indicated siRNAs and 48 h later cell viability was determined by the resazurin reduction assay. Student's t test was used to derive the statistics: P = 0.008 for siRASSF1A versus siRASSF1A/siRUNX2; P = 0.0101 for siRUNX2 versus siRASSF1A/siRUNX2; P = 0.0185 for sip73 versus sip73/siRUNX2. **B.** U2OS cells were transfected with the indicated siRNAs and cell proliferation was assessed in real-time via the xCELLigence system. Arrows indicate increase or decrease in proliferation caused by promoting a different transcriptional complex (black triangle) each time. P < 0.05 (Student's t test) for the controls versus the dual knockdowns.

3.8 TEAD1 is required for oncogenic activity induced by RASSF1A loss

In order to confirm that oncogenic activity stemming from RASSF1A and/or RUNX2 loss is YAP1-TEAD1-dependent, TEAD1 was co-depleted in the context of siRASSF1A and siRUNX2. We tested colony forming ability of U2OS cells and concomitantly, siTEAD1 alone or in the context of siRASSF1/siRUNX2 reduced colony formation ability (Figure 3.6A). Interestingly, knockdown of siTEAD1 and sip73 actually led to a decrease in colony numbers, suggesting that YAP1-RUNX2 complexes also prevent cells from proliferating (Figure 3.6A), correlating with observations made in Figure 3.5B.

In order to validate that TEAD1 is responsible for oncogenic behaviour in the absence of RASSF1A, we monitored viability. Knockdown of p73 resulted in a significant increase in metabolic activity as YAP1-TEAD1 and YAP1-RUNX2 complexes were promoted. Similarly, knockdown of TEAD1 brought viability levels close to the control, since YAP1-p73 and YAP1-RUNX2 complexes were then promoted due to the abrogation of YAP1-TEAD1 complexes. Surprisingly, p73 together with TEAD1 knockdown, led to significantly increased metabolic activity (Figure 3.6B). Taken together, these results suggest that the mechanism through which RASSF1A loss facilitates the appearance of oncogenic properties requires intact YAP1-TEAD1 complexes to lead the transcription of oncogenes (Zhao, Ye et al. 2008, Chan, Lim et al. 2009).

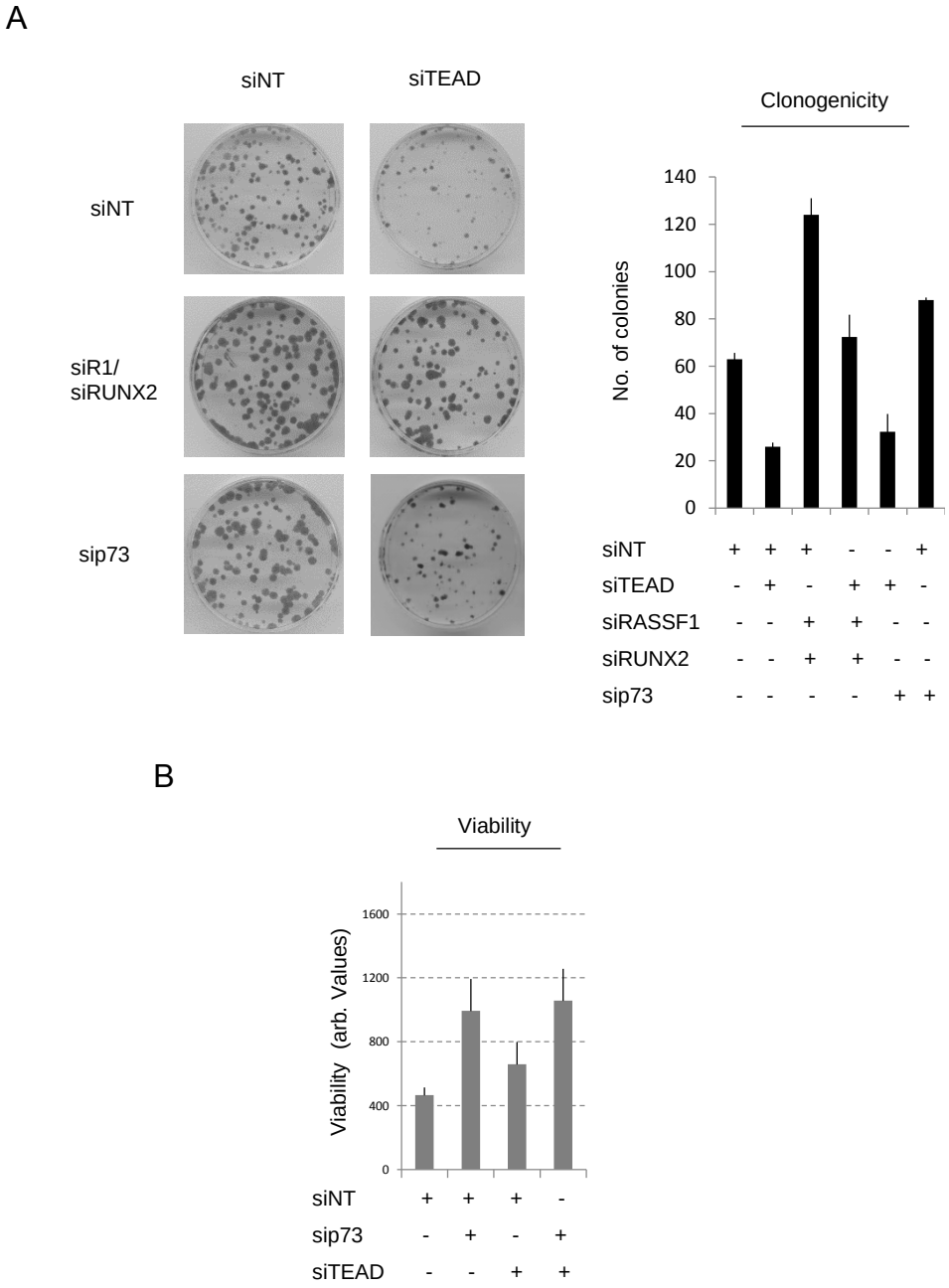


Figure 3.6. TEAD1 silencing reverses the oncogenic phenotypes in the absence of RASSF1A/RUNX2. A. U2OS cells were transfected with either non-targetting siRNA (siNT) or siRNA to TEAD1 (siTEAD1) together with the indicated siRNAs (left panel) and were allowed to form colonies for 11 days before they were fixed and visualised by crystal violet staining. The bar graph (right panel) represents quantification of the number of colonies from the respective conditions. **B.** U2OS cells were transfected with the indicated siRNAs and 72 h later their viability was assessed via resazurin reduction.

3.9 Loss of RASSF1 and RUNX2 in human tumours

In the previous sections, attention was drawn to the *in vivo* and *in vitro* observations stemming from loss of RASSF1A and RUNX2 as well as the elucidation of the mechanism through which individual or combinational silencing of these two genes contributes to oncogenesis. In an attempt to test if our results had clinical significance, we sought to determine if there was evidence of combined loss of RASSF1 and RUNX2 in human tumour cohorts.

As explained earlier, loss of RASSF1A is one of the most frequent epigenetic events and is encountered in almost all types of human cancer (reviewed in Donninger, Vos et al. 2007). Therefore, in collaboration with Dr George Poulogiannis (Harvard, USA) we aimed to explore whether *RUNX2* expression is downregulated in tumours which have lost *RASSF1A* expression.

In data sets obtained from the Oncomine repository we identified that *RUNX2* transcript levels were significantly lower in the majority of tumour types compared to their corresponding normal tissues, particularly in tumours of the brain, colon, head and neck, prostate, kidney and leukemias. (Supplementary Figure 7.3A). Furthermore, loss of *RUNX2* expression exhibited a strong association with poorer survival in patients with diffuse large B-cell or atypical Burkitt/Burkitt-like lymphomas (Supplementary Figure 7.3B). Importantly, a strong concordance in *RUNX2* and *RASSF1* expression levels was observed in precursor T-cell lymphoblastic leukemias (Supplementary Figure 7.4A). The same correlation in *RUNX2* and *RASSF1* expression was also observed in human colorectal cancers (Supplementary

Figure 7.4B). The expression microarray data for the observations in Figures 7.4A and B were obtained from ArrayExpress and Gene Expression Omnibus respectively.

These clinical observations reinforce our hypothesis that tumourigenesis is often exacerbated through concurrent downregulation of RASSF1A and RUNX2 and the mechanism which allows oncogenic phenotypes to manifest themselves involves enhanced pro-proliferative YAP1-TEAD1 interactions.

3.10 Nuclear localisation of RASSF1A

RASSF1A, along with other members of the RASSF family, has been shown to associate with and localise to microtubules upon overexpression (Sherwood, Recino et al. 2010). The microtubule localisation may play a role in the stability of tubulin, formation of the mitotic spindle and sister chromatid separation through mitosis (Gordon and Baksh 2011). It was also discovered that RASSF1A can localize in the centrosomes (Liu, Guo et al. 2008).

The fact that overexpressed RASSF1A is found in these cellular compartments strongly implies that it is actively involved in cell division and would be expected to be primarily cytoplasmic. Our findings, however, suggest that RASSF1A signalling also regulates key nuclear transcriptional processes. More specifically, RASSF1A signalling appears to act as a “switch” dictating specific YAP1 transcription factor complexes, implying close proximity and/or physical interaction with the factors involved. An *in vitro* screen for RASSF1A binding partners revealed a number of nuclear transcription factors (Supplementary Table 7.2), again suggesting that

RASSF1A may be nuclear. We, therefore, decided to check the localization of endogenous RASSF1A in U2OS cells. The available antibodies for endogenous RASSF1A were of insufficient quality to decipher localisation by immunofluorescence, however nuclear/cytoplasmic fractionation revealed exclusive localisation in the nuclear compartment (Figure 3.7).

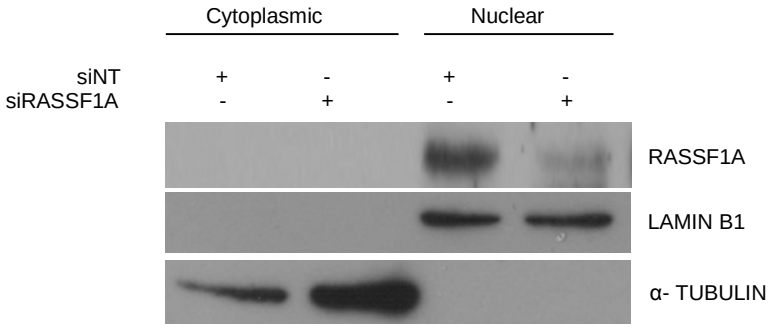


Figure 3.7. RASSF1A localises specifically in the nucleus of U2OS cells. U2OS cells, transfected with either non-targetting siRNA (siNT) or siRNA targeted against RASSF1A (siRASSF1A), were fractionated to acquire the cytoplasmic and nuclear fractions. Immunoblotting of the cytoplasmic and nuclear extracts using the indicated antibodies (right).

3.11 Discussion

Since its discovery in 2000 (Dammann, Li et al. 2000), hypermethylation of the *RASSF1A* promoter and subsequent lack of transcriptional activity of *RASSF1A* have been frequently observed in almost all tumour types (Donninger, Vos et al. 2007). It has previously been shown that *Rassf1a -/-* mice show higher death rates in comparison to their wild-type littermates due to increased incidence of tumourigenesis, predominantly lymphomas and leukemias (van der Weyden, Tachibana et al. 2005). In this study, we used *Sleeping Beauty* insertional mutagenesis to identify candidate genes that are associated with tumourigenesis in a *Rassf1a* null background. Work done in

collaboration with the Sanger Institute in Cambridge revealed that *Rassf1a -/- Sleeping Beauty* mice develop tumours significantly faster than their wild type littermates.

The isolation of the transposon insertion sites from the *Sleeping Beauty*-induced tumours resulted in the identification of a set of 10 genes, which were enriched in the *Rassf1a -/- Sleeping Beauty* tumours versus controls (Supplementary Table 7.1). Several of these genes have roles in cell cycle regulation, mitosis and mitotic progression, with reported loss of expression being found in tumours, similarly to RASSF1A, including *Foxn3* (Busygina, Kottemann et al. 2006, Chen, Liao et al. 2011), *Ppp2r2a* (Clarke, Hoffmann et al. 1993, Liu, Sempere et al. 2010), *Stag2* (Hauf, Roitinger et al. 2005, Rocquain, Gelsi-Boyer et al. 2010) and *Runx2* (Dickey-Sims, Robertson et al. 2005). Moreover, some of these genes have been shown to be interacting with the Ras signaling pathway and mutations in them are linked with tumourigenesis, including *Crebbp* (Foulds, Nelson et al. 2004, Mullighan, Zhang et al. 2011) and *Fgfr3* (Kompier, Lurkin et al. 2010, Al-Ahmadie, Iyer et al. 2011).

The mammalian Runx family of transcription factors consists of three members, RUNX1, RUNX2 and RUNX3, which are related to *Runt*, the *Drosophila* pair rule gene (Gergen and Butler 1988) and share a highly conserved DNA-binding domain and a DNA-binding cofactor. The *RUNX2* gene differs from the rest of the genes in the family because it produces the largest protein product, which possesses 2 domains that are distinct from its homologs. These are a short stretch of glutamine-alanine (QA) repeats at the N-terminus and a proline/serine/threonine (PST)-rich tract at the C-terminus

and they are both necessary for transactivation activity (Thirunavukkarasu, Mahajan et al. 1998; Supplementary Figure 7.2). The RUNX proteins participate in the regulation of cell fate decisions as well as the determination of the tumourigenic potential of cells by acting as oncogenes or tumour suppressors depending on the cell context (Blyth, Vaillant et al. 2010). Specifically, *Runx2 -/-* mouse embryonic fibroblasts (MEFs) are susceptible to spontaneous immortalisation and acquire an early growth advantage, which is resistant to stress-induced growth arrest (Kilbey, Blyth et al. 2007). Therefore, *RUNX2* can function as a tumour suppressor gene and loss of its expression constitutes an important step in oncogenic transformation. In this study, however, we were intrigued by the fact that *Sleeping Beauty* transposon insertions in the *Runx2* gene were significantly associated with tumourigenesis only in the *Rassf1a -/-* mice and not the wild type littermates, suggesting that loss of *RUNX2* alone may not be sufficient for oncogenesis.

YAP1 is a master regulator of organ size during development and has been identified as an oncogene due to its expression upregulation in human cancers (Zhao, Ye et al. 2008). In agreement with others, we found that overexpression of YAP1 enhances oncogenic behavior and the mechanism through which this is allowed to occur involves the stabilisation of YAP1-TEAD1 complexes. However, high YAP levels, in the absence of RUNX2, promoted a p73-dependent suppression of clonogenicity (Figure 3.4), thus implying that YAP1 upregulation or RUNX2 loss alone are insufficient to promote tumourigenesis and require inactivation of either RASSF1A or p73. Interestingly, both RASSF1A and p73 are frequently inactivated by epigenetic DNA methylation (Roman-Gomez, Jimenez-Velasco et al. 2004, Donninger,

Vos et al. 2007). Additionally, correlations of clinical outcome and YAP1 expression levels may benefit from further stratification of tumours displaying reduced RASSF1A or p73 (Zhang, George et al. 2011). Given that RASSF1A exerts its function through p73 and dual downregulation of p73 and RUNX2 produced identical phenotypes to RASSF1A/RUNX2 depletion (Figures 3.4 and 3.5), this indicated that RASSF1A and p73 function in an epistatic way.

The role of RUNX2 as a tumour suppressor can be also implied by the observations in Figures 3.5 and 3.6. Specifically, in Figure 3.5B, silencing of both p73 and TEAD1 resulted in a significant decrease in proliferation in comparison to siRUNX2/sip73, as assessed in real-time by the xCELLigence system. Moreover, while in Figure 3.6A, depletion of both p73 and TEAD1 led to a strong decrease in clonogenicity, in Figure 3.6B, sip73/siTEAD1 resulted in increased viability. In all these cases, YAP1-RUNX2 complexes were promoted, which were tumour suppressive, since the cells appeared to have lost their proliferative capacity, however, the increase in viability suggested that YAP1-RUNX2 might be also involved in biological processes which render the cells more metabolically active. Given the important roles of RUNX2 in terminal differentiation (Sato, Morii et al. 1998, Hong, Hwang et al. 2005), these observations are consistent with a potential switch to a RUNX2 differentiation programme.

Hypermethylation of the *RASSF1A* promoter is a frequent occurrence in the vast majority of tumours, and along with the fact that point mutations have also been found in up to 15% of primary tumours, RASSF1A becomes one of the most frequently inactivated proteins in human cancer (Donninger, Vos et al. 2007). In this chapter, we also found that *RUNX2* transcript levels were

significantly lower in a wide range of tumour types than their corresponding normal tissues (Supplementary Figure 7.3A) and absence of *RUNX2* expression exhibited a strong association with poorer survival in some tumour types (Supplementary Figure 7.3B). The most important finding, however, was the strong concordance in expression levels of RUNX2 and RASSF1 in both T-cell lymphoblastic leukemias (Supplementary Figure 7.4A) and human colorectal cancers (Supplementary Figure 7.4B). Of note is also the fact that *RASSF1A* is often found to be methylated in tumours of the gastrointestinal tract (Donninger, Vos et al. 2007) and loss of *Rassf1a* synergises with loss of *Apc* to accelerate intestinal tumourigenesis (van der Weyden, Arends et al. 2008). Taken together, these observations suggest that, at least in T-cell lymphoblastic leukemias and colorectal cancers, RUNX2 and RASSF1 expression levels can be duly used as prognostic biomarkers, with a reasonable potential of expanding their use in other types of cancer too.

In summary, the data in this chapter demonstrate that loss of *RASSF1A* switches YAP1 from a tumour suppressor to an oncogene via modulating its interaction with the transcription factors p73 and TEAD1. Additionally, the terminal differentiation factor RUNX2 also competes with TEAD1 for YAP1 association, regardless of RASSF1A and p73, and dual downregulation of RASSF1A and RUNX2 exacerbates YAP1-TEAD1 levels (Figure 3.8). This model, thereby, suggests a novel mechanism for RASSF1A-mediated tumour suppression.

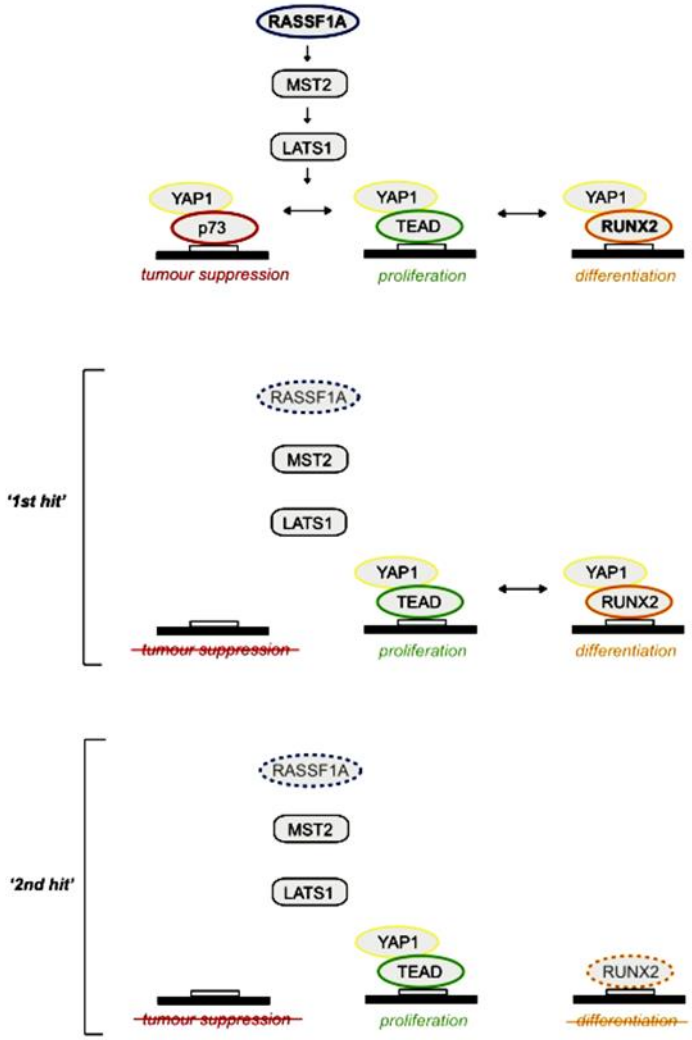


Figure 3.8. Model depicting proposed YAP1 complex formation in response to RASSF1A. YAP1 exists in a dynamic equilibrium with a number of transcriptional partners, p73, TEAD1 and RUNX2, and these interactions are regulated by upstream signals. Reduction of RASSF1A (1st hit), either genetically or via promoter methylation, ablates the formation of tumour suppressive YAP1-p73 complexes and leaves cells susceptible to changes in other tumour suppressor genes that can exacerbate tumourigenesis (Table 7.1). In the context of loss of RASSF1A, loss of RUNX2 (2nd hit) eliminates the transcription factor competition for binding to YAP1 to the advantage of TEAD1, resulting in more stable YAP1-TEAD1 complexes actively fostering proliferation.

The presence of RASSF1A exclusively in the nuclear compartment of human osteosarcoma U2OS cells implied that RASSF1A is more directly involved in nuclear functions, such as transcription factor regulation. Previous reports have shown that overexpressed RASSF1A is found on the

microtubules, centromeres and centrosomes regulating mitotic processes (reviewed by Gordon and Baksh 2011). Our results, however, illustrate for the first time that endogenous RASSF1A might be confined only in the nucleus of cell lines which express it, such as U2OS. This led us to the hypothesis that RASSF1A may be scaffolding the complexes formed by YAP1, thereby being more directly involved in transcription regulation. The direct binding of RASSF1A to elements of the YAP1 complexes might cause conformational changes, which could account for the differential YAP1 binding observed in response to RASSF1A signalling. This hypothesis is being further investigated by members of our group.

The Human Protein Atlas contains information regarding subcellular localisation of RASSF1A, based on the use of two commercially available rabbit antibodies (HPA040735 and HPA042098, Sigma) targeting different epitopes of the protein. Immunofluorescence in U2OS cells using the HPA040735 antibody showed predominant localisation of RASSF1A to the plasma membrane and cytoplasm, however, the HPA042098 antibody did not detect RASSF1A in the cells. As the Atlas classifies the reliability of the staining as uncertain and our results, with the use of a different antibody and method (cellular fractionation and immunoblotting) demonstrate nuclear localisation of endogenous RASSF1A in U2OS cells, further investigation is required to determine the exact RASSF1A localisation pattern in this cell line.

Lastly, YAP1, as well as YAP1-mediated TEAD and RUNX2 transcriptional activity have been documented to regulate stem cell self-renewal and terminal differentiation (Hong, Hwang et al. 2005, Camargo, Gokhale et al. 2007, Lian, Kim et al. 2010). p73 has been also implicated in stem cell differentiation

processes (De Laurenzi, Raschella et al. 2000, Agostini, Tucci et al. 2011). Interestingly, quite recently it was reported that *RASSF1A* hypermethylation in stem cells drives their oncogenic transformation (Teng, Hou et al. 2011). Moreover, an *in vitro* screen for RASSF1A binding partners (Supplementary Table 7.2) identified the Notch target gene, Hairy Enhancer of Split (HES1), also implicated in the determination of stem cell fate (Artavanis-Tsakonas, Rand et al. 1999, Ohtsuka, Ishibashi et al. 1999, Kageyama, Ohtsuka et al. 2007). Intrigued by these observations, we set out to discover a potential underlying role for RASSF1A in stem cell fate determination. We speculated that by studying RASSF1A signalling in a tumour-free system, such as embryonic stem cells, we would be in a better position to elucidate the physiological RASSF1A mechanism of action and subsequently apply the new knowledge back to cancer treatment.

Chapter 4

RASSF1A is a key regulator of pluripotency via novel Yap-Tead-β-catenin-mediated control of *Oct4*

4.1 Introduction

In Chapter 3 we attempted to explain the mechanism through which RASSF1A signalling regulates transcription factor usage by the major downstream effector of the Hippo pathway, YAP1. We proposed that by acting as a "switch", RASSF1A determines whether YAP1 acquires tumour suppressive (YAP1-p73), oncogenic (YAP1-TEAD1) or other –potentially differentiation-related– (YAP1-RUNX2) activity. This later point together with the fact that the proteins responsive to RASSF1A action (YAP1, p73, TEAD1, RUNX2) have been reported to hold important roles in stem cell fate regulation (De Laurenzi, Raschella et al. 2000, Hong, Hwang et al. 2005, Camargo, Gokhale et al. 2007, Lian, Kim et al. 2010, Agostini, Tucci et al. 2011), prompted us to investigate cell fate control.

Furthermore, both RASSF1A and YAP1 are well-established components of the Hippo pathway (reviewed by Pan 2010). The Hippo pathway is a critical regulator of organ size and regeneration (Camargo, Gokhale et al. 2007, Dong, Feldmann et al. 2007), governs self-renewal of intestinal stem cells in mammals (Camargo, Gokhale et al. 2007) and regulates neural, epidermal, cardiac and skeletal muscle progenitor cells in vertebrates (Shiojima and Walsh 2006, Cao, Pfaff et al. 2008, Matsui, Nakano et al. 2008, Watt, Judson et al. 2010, Heallen, Zhang et al. 2011, Schlegelmilch, Mohseni et al. 2011, Xin, Kim et al. 2011, Zhang, Pasolli et al. 2011, Judson, Tremblay et al. 2012,

Li, Hibbs et al. 2012, von Gise, Lin et al. 2012). Additionally, it was reported by Tamm et al. in 2011 that Yap1-Tead2 complexes could stimulate the expression of the core pluripotency marker Oct4 in mouse embryonic stem cells (ESCs) and inhibition of Tead2 resulted in cells undergoing differentiation.

It was not until recently that a link was provided between loss of *RASSF1A* in somatic stem cells and oncogenesis. Teng et al. (2011) demonstrated that human bone marrow-derived mesenchymal stem cells (MSCs) harbouring targeted promoter methylations of *RASSF1A* and Hypermethylated in Cancer 1 (*HIC1*), acquired oncogenic phenotypes of contact inhibition, increased proliferation and migration, drug resistance and pluripotency. Moreover, mice carrying targeted MSCs exhibited increased tumour formation, whilst stem cell self-renewal markers, such as Oct4, were maintained in tumour xenografts. In addition, an *in vitro* screen for RASSF1A binding partners identified HES1, an important factor in the maintenance of pluripotency (Artavanis-Tsakonas, Rand et al. 1999, Ohtsuka, Ishibashi et al. 1999, Kageyama, Ohtsuka et al. 2007), as part of the RASSF1A interactome (Supplementary Table 7.2).

Taken together, this body of evidence suggested that RASSF1A signalling might be implicated in stem cell fate determination. Thus, the primary aim of this study was to determine if this is the case and to elucidate the mechanism through which this may occur. The investigation of the innate functions of RASSF1A in a non-tumourigenic system, such as ESCs, would also contribute to shedding more light upon the regulatory circuits pertaining to RASSF1A-mediated tumour suppression.

4.2 RASSF1A is a barrier to reprogramming

Takahashi et al. described in 2006 the process by which terminally differentiated mouse embryonic and adult fibroblasts could be reprogrammed to a completely pluripotent state via overexpression of four transcription factors (Sox2, Oct3/4, c-Myc and Klf4), called the “Yamanaka cocktail” or SKOM (Sox2, Klf4, Oct4, c-Myc). These induced pluripotent stem cells (iPSCs) could then be differentiated into the three germ layers (mesoderm, endoderm, ectoderm) *in vitro* and grow as teratomas *in vivo* (Takahashi, Tanabe et al. 2007). Interestingly, YAP1 was found to be activated during reprogramming of human embryonic fibroblasts to iPSCs and replacement of c-Myc with YAP1 in the “Yamanaka cocktail” of transcription factors resulted in increased reprogramming efficiency (Lian, Kim et al. 2010). This was a strong indication that YAP1 constitutes a pivotal factor for the maintenance of pluripotency in both ESCs and iPSCs and this property was attributed to its association with TEAD transcription factors (Lian, Kim et al. 2010).

Given that RASSF1A loss led to increased YAP1-TEAD1 complex formation in cancer cells (Figure 3.3), we hypothesised that *Rassf1a*-null mouse embryonic fibroblasts (MEFs) may be reprogrammed to iPSCs more efficiently than their wild type counterparts. Therefore, we isolated and genotyped *Rassf1a* -/- and +/+ MEFs from mice bred at the Sanger Institute, Cambridge, UK (Supplementary Figure 7.5A) and induced reprogramming by using the piggyBac transposition system. By using this method, MEFs were transfected with a transposon carrying the four defined transcription factors (SKOM), along with a plasmid coding for transposase, to allow integration of the transposon into the genome and, thus, constitutive expression of the

Yamanaka factors (Woltjen, Michael et al. 2009). 3 days post transfection the first iPSC colonies began to emerge. A schematic explaining the procedure is presented in Figure 4.1.

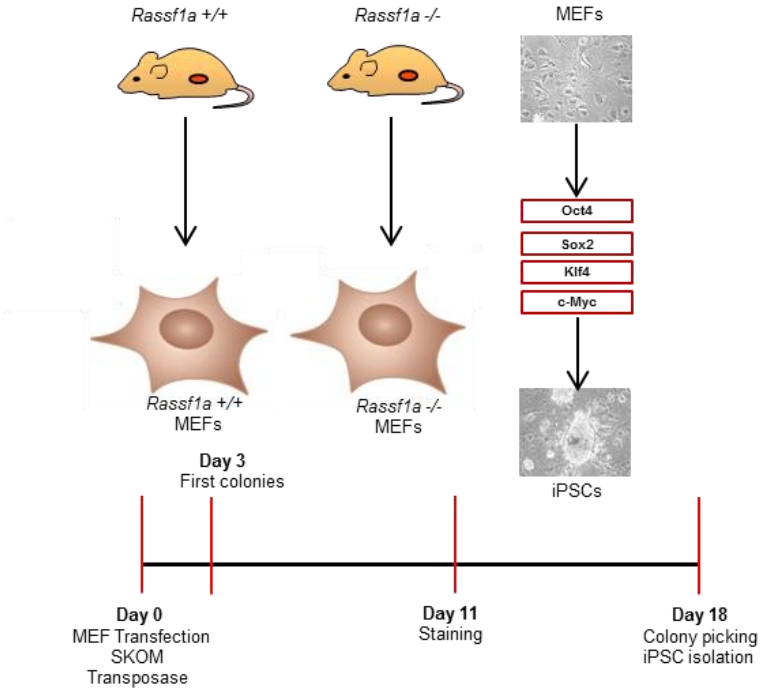


Figure 4.1. Experimental design of the somatic cell reprogramming procedure. Mouse embryonic fibroblasts (MEFs) were isolated from *Rassf1a* +/+ and -/- mice. With the "Yamanaka cocktail" of transcription factors (Sox2, Klf4, Oct4, c-Myc, SKOM), MEFs were reprogrammed to become induced pluripotent stem cells (iPSCs) using the piggyBac transposition system. The illustrated timeline describes the procedure in more detail. On Day 0 MEFs were transfected with the SKOM construct, along with a construct coding for transposase; on Day 3 the first iPSCs began to emerge; on Day 11 the colonies were stained for alkaline phosphatase; on Day 18 the iPSC colonies were isolated.

11 days after the initiation of reprogramming, colonies from both conditions were stained for alkaline phosphatase. Although alkaline phosphatase is not a marker of pluripotency itself, it has been used in conjuction with other ES cell surface-specific antigens, such as the glycolipid antigen SSEA-1 in mouse (Takahashi and Yamanaka 2006) and SSEA-3, SSEA-4, tumour-related antigen (TRA)-1-60 and TRA-1-81 in humans

(International Stem Cell, Adewumi et al. 2007, Takahashi, Tanabe et al. 2007) to characterise embryonic stem cell lines. This is usually accompanied by immunofluorescence or quantitative PCR for core stem cell marker expression, such as NANOG and OCT4 (Takahashi and Yamanaka 2006, International Stem Cell, Adewumi et al. 2007, Takahashi, Tanabe et al. 2007). Interestingly, the number of stained colonies indicated that *Rassf1a -/-* MEFs were reprogrammed more efficiently to iPSCs in comparison to *Rassf1a +/+* MEFs (Figure 4.2A).

Surprisingly, the derivative iPSC colonies from the two conditions demonstrated significant differences in shape, therefore we classified them into three categories according to their morphology: round, partially round and non-round colonies. Our observations, expressed in percentage over the total number of colonies, showed that *Rassf1a -/-* MEFs produced significantly more round colonies than the wild-type MEFs, whereas the latter produced more partially round and non-round colonies (Figure 4.2B). In the literature, clonal classification (holoclones, meroclones and paraclones) has been used to identify clonal types of primary cells with different capacities for multiplication (Barrandon and Green 1987, Pellegrini, Golisano et al. 1999) as well as cancer cells which exhibit stem-like properties and form colonies, such as prostate (Beaver, Ahmed et al. 2014) and breast (McClements, Yakkundi et al. 2013). Only holoclones (round colonies) can proliferate extensively and self-renew, whereas meroclones (noncanonical shape) exhibit limited proliferative and self-renewal capacity. Paraclones (diffused shape) are incapable of further proliferation and self-renewal (Barrandon and Green 1987, Pellegrini, Golisano et al. 1999). Clonal classification into holoclones,

meroclones and paraclones, however, does not constitute an assay to test the stemness of iPSCs induced from MEFs.

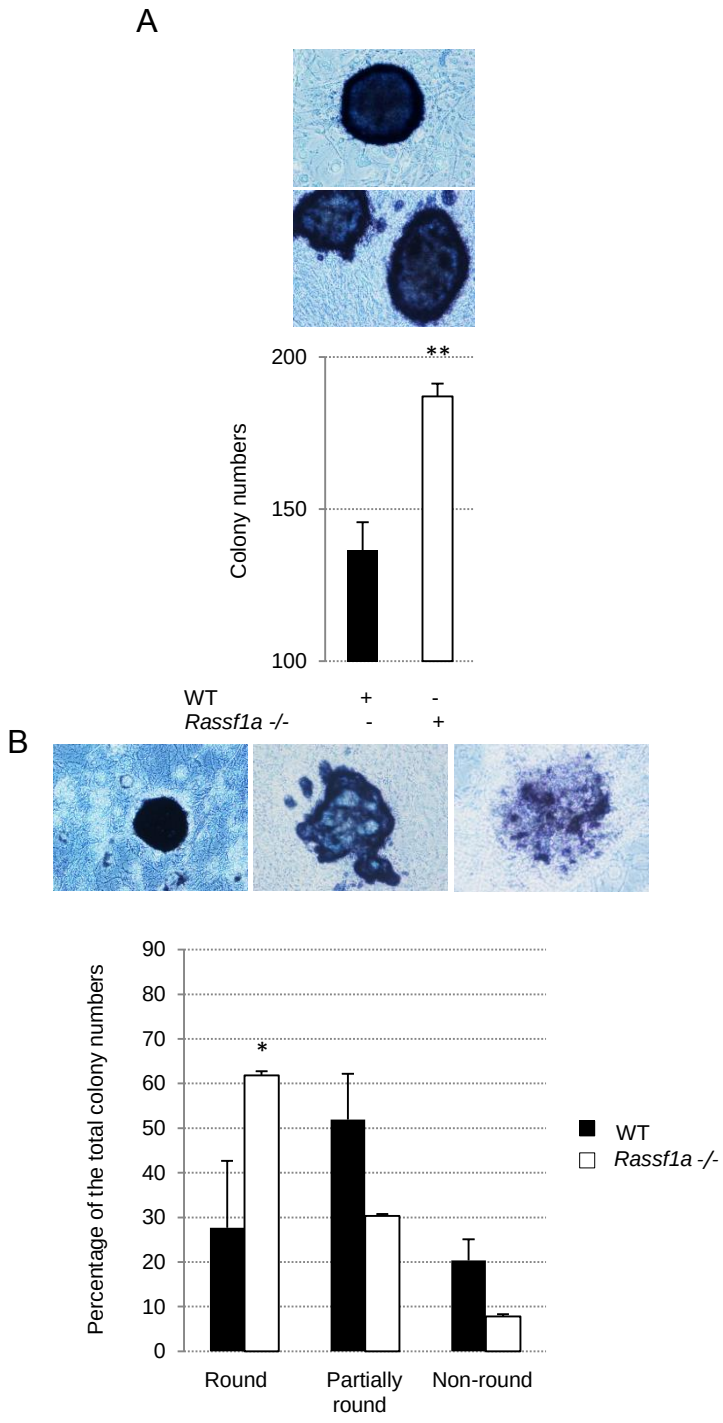


Figure 4.2. *Rassf1a* -/- MEFs exhibit faster and more efficient reprogramming. A. *Rassf1a* +/+ (WT) and -/- MEFs were stained for alkaline phosphatase 11 days after the initiation of reprogramming. Bar graph illustrating the total iPSC colony numbers from each condition. P = 0.01 (Student's t test) **B.** Alkaline phosphatase-stained iPSC colonies were classified into three categories (round, partially round, non-round) according to their morphology, as a means of assessing how pluripotent they were. Bar graphs showing the percentage of *Rassf1a* +/+ vs -/- colonies belonging to each one of the three categories. For round colonies: P = 0.05 (Student's t test).

In order to determine whether the enhanced reprogramming efficiency was indeed due to lack of *Rassf1a*, we re-introduced RASSF1A into *Rassf1a -/-* MEFs using a mouse retrovirus expressing a human HA-tagged RASSF1A (Figure 4.3A). Next, we attempted reprogramming of *Rassf1a +/+*, *Rassf1a -/-* and *Rassf1a -/- + HA-RASSF1A* MEFs following the method described above (Figure 4.1) and subsequently compared the number and morphology of the derived iPSC colonies. Introduction of HA-RASSF1A significantly reduced the number of colonies generated by *Rassf1a -/-* MEFs (Figure 4.3B) to levels comparable to controls, suggesting that restoration of RASSF1A expression in *Rassf1a -/-* MEFs was sufficient to change the reprogramming potential to that of the wild-type (Figure 4.3B).

Clonal classification of the *Rassf1a -/-* and *Rassf1a -/- + HA-RASSF1A* iPSCs demonstrated strikingly reduced round colony formation in the *Rassf1a -/- +HA-RASSF1A* condition, accompanied by an equivalent increase in the number of non-round colonies (Figure 4.4).

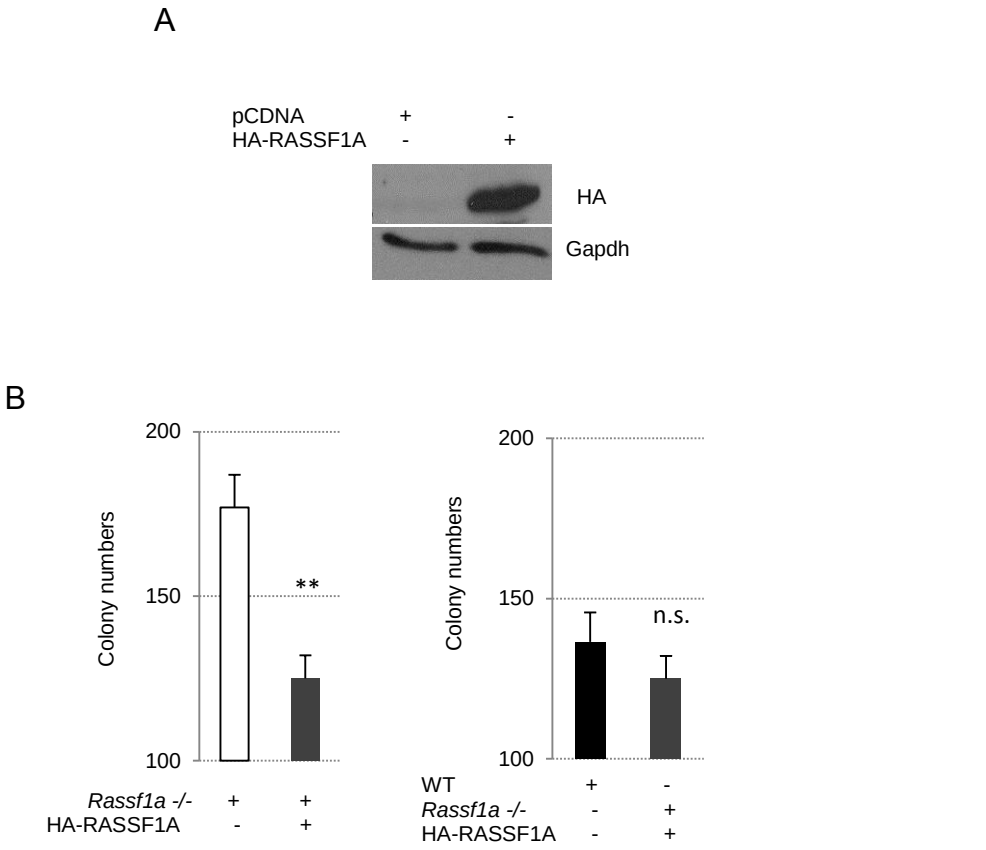


Figure 4.3. *Rassf1a -/-* MEF reprogramming rates are decreased to WT rates when RASSF1A is re-introduced. A. *Rassf1a -/-* MEFs were retrovirally infected with HA-RASSF1A. Western blot showing the expression of HA-RASSF1A in the MEFs. **B.** Left: bar graph illustrating the total iPSC colony numbers derived from *Rassf1a -/-* vs *Rassf1a -/- + HA-RASSF1A* MEFs 11 days after initiation of reprogramming. $P < 0.05$ (Student's t test). Right: bar graph showing the total iPSC colony numbers derived from *Rassf1a* +/+ (WT) vs *Rassf1a -/- + HA-RASSF1A* MEFs 11 days after initiation of reprogramming. $P = 0.14$ (Student's t test).

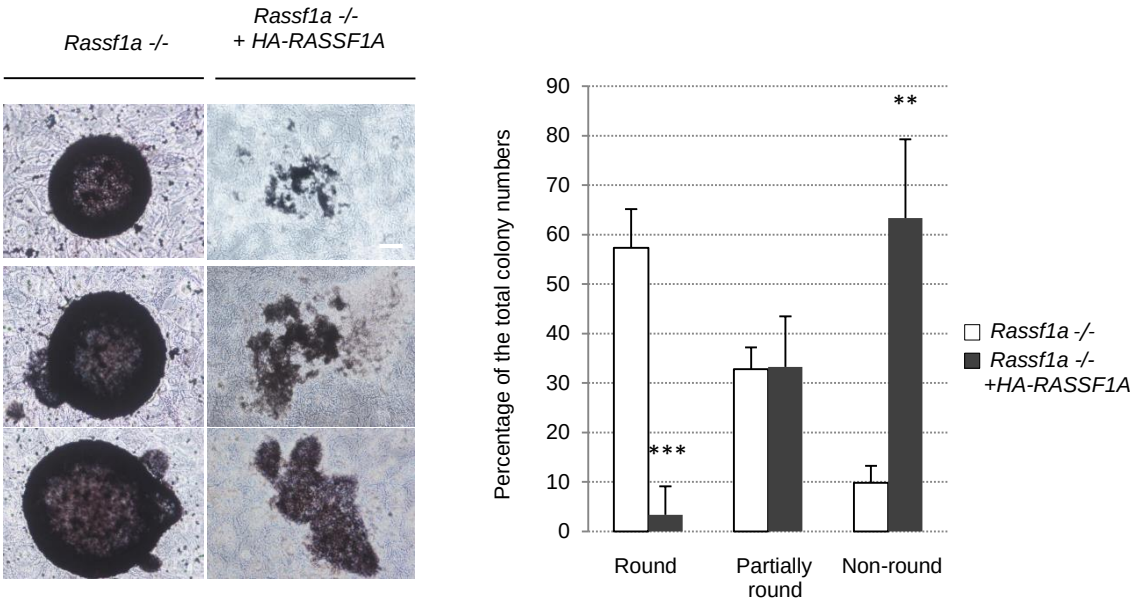


Figure 4.4. Re-introduction of RASSF1A into *Rassf1a -/-* MEFs rescues the reprogramming efficiency. Example images of iPSC colonies derived from either *Rassf1a -/-* or *Rassf1a -/- + HA-RASSF1A* MEFs (left panel). Bar graphs demonstrating the percentage differences of *Rassf1a -/-* vs *Rassf1a -/- + HA-RASSF1A* iPSC colony numbers classified into round, partially round and non-round colonies (right panel). $P < 0.001$ for round and $P = 0.004$ for non-round colonies (Student's t test).

4.3. *Rassf1a -/-* iPSCs demonstrate elevated stem cell marker expression

18 days post initiation of reprogramming, iPSC colonies from all three conditions (*Rassf1a +/+*, *-/-* and *-/- + HA-RASSF1A*) were isolated to be further expanded and characterised for stem cell marker expression and differentiation capacity (Figure 4.5A). Only colonies which up to this stage would be classified as round colonies were isolated for further examination.

To exclude the possibility that the observed reprogramming efficiency differences (Figures 4.2-4.4) were due to unequal expression levels of the SKOM constructs transfected into the MEFs, we performed quantitative Real Time PCR (qRT-PCR) for parts of the constructs described as "junctions", following the instructions of the Wellcome Trust Sanger Institute in Cambridge, UK, from which the constructs were obtained. More specifically,

we performed qRT-PCR for the Oct4-cMyc junctions and included non-transfected MEFs in the analysis as negative controls. The analysis showed that in all tested samples, the constructs were expressed at an equal level (Figure 4.5B).

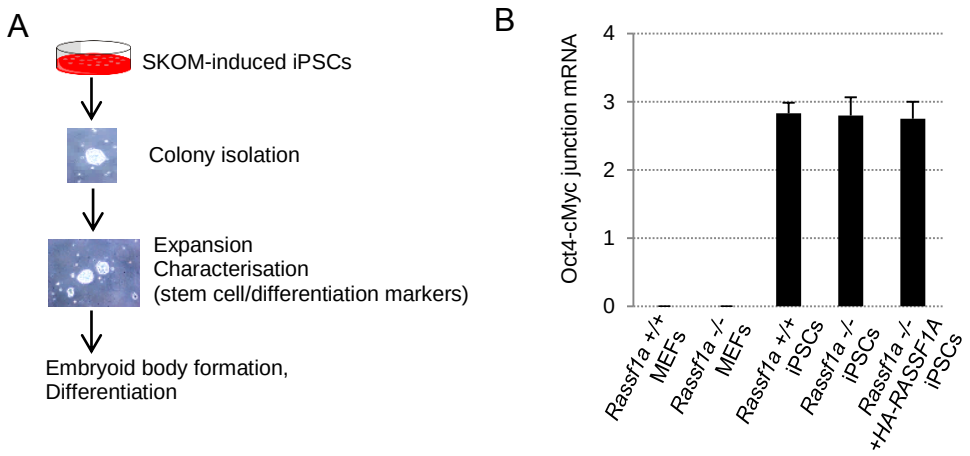


Figure 4.5. iPSC colony isolation and characterisation. A. Schematic of the steps taken to isolate and characterise iPSCs. 18 days after the beginning of reprogramming, colonies were isolated in order to be expanded and further characterised to generate iPSC lines. The iPSCs were subject to embryoid body formation and differentiation assays. **B.** qRT-PCR of *Rassf1a* +/+, -/- and -/- +*HA-RASSF1A* MEFs and iPSCs to assess mRNA expression levels of the SKOM construct in all the conditions.

In order to characterise the iPSCs, we performed qRT-PCR to assess the mRNA levels of stem cell markers. We observed that in *Rassf1a* -/- iPSCs, mRNA levels of both Oct4 and Sox2 were significantly elevated in comparison to *Rassf1a* +/+ (approximately three and half-fold and two and half-fold increase respectively) and *Rassf1a* -/- +*HA-RASSF1A* iPSCs. In our analysis, we also included *Rassf1a* +/+ and -/- MEFs as negative controls in which stem cell marker expression should be limited, as they are terminally differentiated cells (Figure 4.6A). We also assessed stem cell marker protein expression levels. For this purpose, we performed immunofluorescence for Nanog and Sox2 expression and observed a clear increase in both markers in

the *Rassf1a -/-* iPSCs in comparison to *Rassf1a +/+* (Figure 4.6B). Taken together, these data indicated that the reason for the enhanced reprogramming efficiency in the *Rassf1a -/-* condition (Figures 4.2-4.4) was the upregulation of stem cell markers, triggered by the absence of Rassf1a.

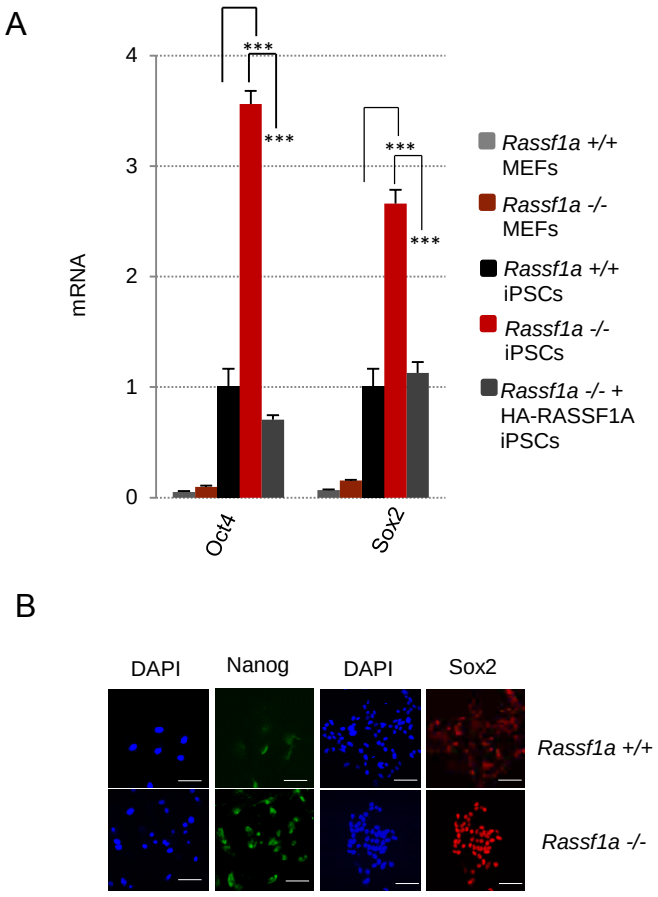


Figure 4.6*. Rassf1a -/-* iPSCs express higher levels of stem cell markers. A. qRT-PCR of *Rassf1a* +/+, -/- and -/- +*HA-RASSF1A* MEFs and iPSCs for Oct4 and Sox2. $P < 0.001$ for *Rassf1a* +/+ vs -/- and -/- vs -/- + *HA-RASSF1A* iPSCs for Oct4 and $P < 0.001$ for the respective conditions for Sox2 (Student's t test). **B.** Immunofluorescence of the protein levels of Nanog and Sox2 in *Rassf1a* +/+ vs -/- iPSCs.

4.4 *Rassf1a -/-* iPSCs demonstrate increased resistance to differentiation

For the purpose of further characterising the derived iPSC*s*, we also challenged their capacity to differentiate. Therefore, we subjected iPSCs from all three conditions to LIF withdrawal for 48 h to activate differentiation programmes and then performed qRT-PCR to test the mRNA expression levels of the mesodermal-endodermal germ layer differentiation marker Vimentin (Page 1989, Rius and Aller 1992) and the ectodermal marker Nestin (Lendahl, Zimmerman et al. 1990, Park, Xiang et al. 2010) (Figures 4.7A and B). The results demonstrated a significant downregulation of both Vimentin and Nestin in *Rassf1a -/-* iPSCs in comparison to the wild-type (Figure 4.7A). Intriguingly, *Rassf1a -/- +HA-RASSF1A* iPSCs exhibited significantly increased Nestin mRNA levels when compared to the *Rassf1a -/-* (Figure 4.7B).

The route towards terminal differentiation is usually coupled with a permanent exit from cell cycle and constitutes the most common cellular state in adult animals (reviewed by Buttitta and Edgar 2007). Therefore, cells in which a differentiation programme has been activated will transition through cell cycle less actively than a population of undifferentiated cells. To further confirm the finding that *Rassf1a -/-* iPSCs exhibit a more differentiation-resistant phenotype, we tested the expression of the proliferation marker Ki67 in cells from all three conditions via immunofluorescence (Figure 4.7C). *Rassf1a -/-* iPSCs were indeed found to express Ki67 at much higher levels than the wild-type. Interestingly, *Rassf1a -/- +HA-RASSF1A* iPSCs showed the lowest expression of Ki67 among the three conditions, indicating that they

were in the least proliferative state, most likely due to the expression of RASSF1A at even higher levels than the wild-type.

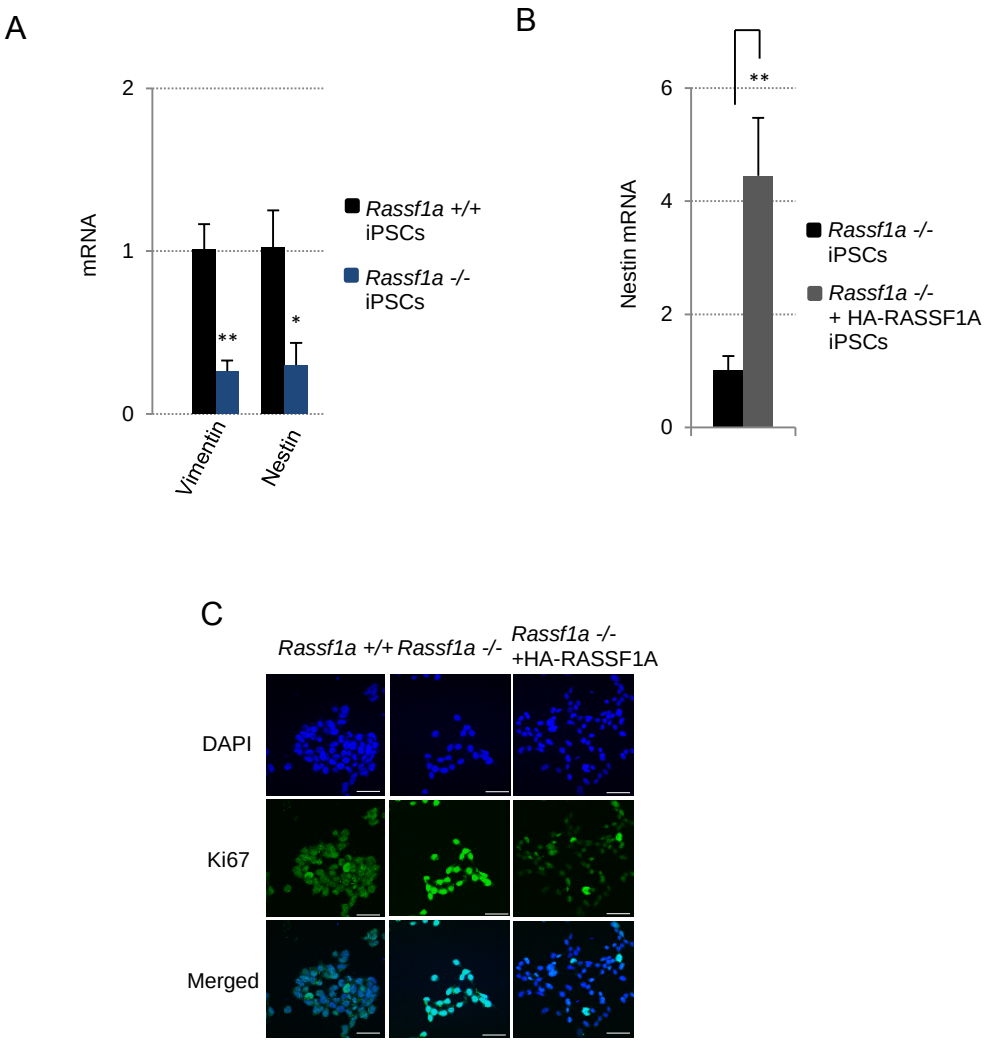


Figure 4.7. *Rassf1a -/-* iPSCs show increased resistance to differentiation. A. *Rassf1a* +/+ and -/- iPSCs were grown in the absence of LIF for 48 h to activate differentiation programmes. qRT-PCR for differentiation markers Nestin (ectoderm) and Vimentin (mesoderm-endoderm) from *Rassf1a* +/+ and -/- iPSCs. $P < 0.01$ for Nestin and $P = 0.032$ for Vimentin (Student's t test). **B.** *Rassf1a* -/- and -/- + *HA-RASSF1A* iPSCs were grown in the absence of LIF for 48 h. qRT-PCR for the differentiation marker Nestin. $P = 0.002$ (Student's t test). **C.** Immunofluorescence for the levels of proliferation marker Ki67 in *Rassf1a* +/+, -/- and -/- + *HA-RASSF1A* iPSCs.

As explained earlier, undifferentiated ESCs and iPSCs are characterised by their property to form round colonies in culture, consisting of small, compacted, self-renewing cells. Progressively differentiating colonies will

appear less round over time until cells become terminally differentiated, at which point they no longer form colonies. Along these lines, we subjected iPSCs from all three conditions (*Rassf1a* +/+, -/- and -/- +*HA-RASSF1A*) to a LIF withdrawal assay. More specifically, the LIF-containing medium in which cells grew was replaced with LIF-free medium and the cells were cultured for a further 4 days, before morphological observations were made. Surprisingly, while the majority (almost 80%) of *Rassf1a* +/+ colonies were starting to collapse 4 days after LIF withdrawal, almost 45% of *Rassf1a* -/- colonies still kept their round shape marking the maintenance of a pluripotent state, almost equivalent to that prior to LIF removal (Day 0). Additionally, at the same day, RASSF1A overexpressing iPSCs (*Rassf1a -/- +HA-RASSF1A*) had almost completely lost the ability to form colonies as the iPSCs started to resemble terminally differentiated cells and less than 5% of the colonies remained round-shaped (Figure 4.8).

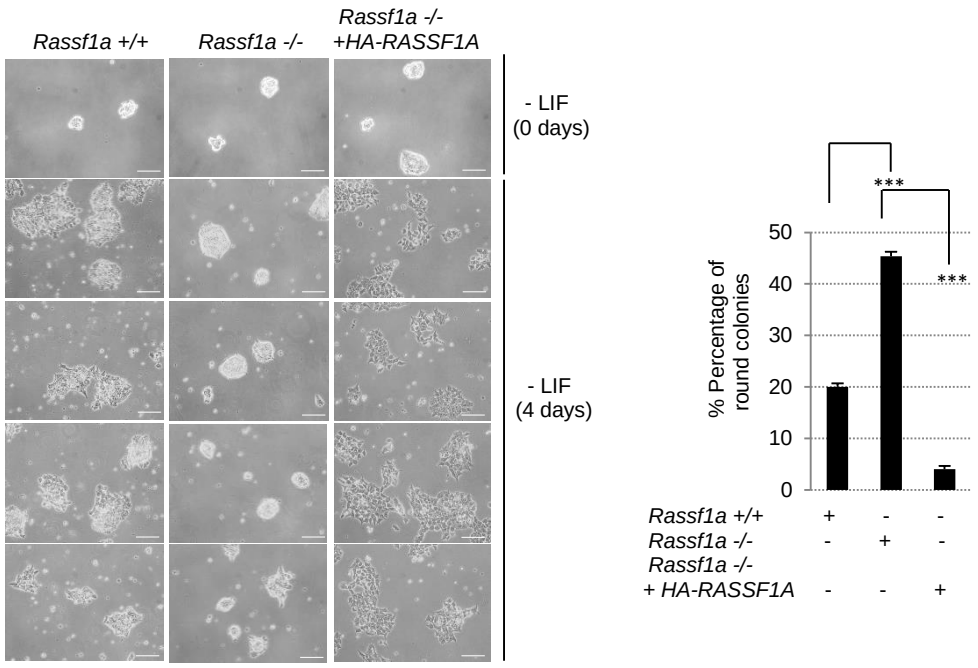


Figure 4.8. Morphological differences in iPSC colonies upon LIF withdrawal. *Rassf1a* +/+, -/- and -/- +*HA-RASSF1A* round iPSC colonies were allowed to grow in the absence of LIF for 4 days. Left panel: examples of iPSC colonies to observe the changes in shape. Right panel: quantification of the percentage of round colonies in each condition. $P < 0.001$ for *Rassf1a* +/+ vs -/- and $P < 0.001$ for *Rassf1a* -/- vs -/- + *HA-RASSF1A* (Student's t test).

4.5 Loss of Rassf1a inhibits differentiation of iPSCs to DCs

To further investigate the differentiation potential of Rassf1a-expressing versus non-expressing iPSCs, we induced targeted differentiation of *Rassf1a* +/+ and -/- iPSCs towards the dendritic cell (DC) lineage, following the protocol described by Fairchild et al. in 2000. Dendritic cells (DCs) are antigen-presenting cells (APC) of the immune system, which play a fundamental role in facilitating both the innate and adaptive immune response (reviewed by Banchereau and Steinman 1998). Briefly, iPSCs were allowed to differentiate, in the absence of LIF, until they formed three-dimensional aggregates of cells named embryoid bodies (EBs) (Doetschman, Eistetter et al. 1985, Burkert, von Ruden et al. 1991, Murry and Keller 2008). EBs were then allowed to grow in culture in the presence of recombinant interleukin-3

(rIL-3) and granulocyte-macrophage colony-stimulating factor (GM-CSF), both of which are factors inducing differentiation to DCs. A portion of the emerging DCs was lipopolysaccharide (LPS)-stimulated to verify the presence of fully differentiated and functional DCs (Winzler, Rovere et al. 1997). A schematic of the process is illustrated in Figure 4.9A, where images of *Rassf1a* +/+ and -/- EBs as well as of derived DCs are provided. Notably, while *Rassf1a* +/+ EBs completely responded, as expected, to the differentiation cues triggered by LIF withdrawal, implied by their noncanonical shape, *Rassf1a* -/- EBs maintained, at least partially, the *Rassf1a* -/- iPSC colony round shape (Figure 4.9A).

During differentiation, DCs acquire or increase the expression of the co-stimulatory adhesion molecule CD54 (ICAM-1) (Real, Kaiser et al. 2004). Hence, we sought to unveil potential differences in the ability of *Rassf1a* +/+ and -/- iPSCs to differentiate to DCs using cd54 expression as a readout. After DCs were allowed to form, equal numbers of cells from both conditions were analysed for cd54 expression versus control (unstained cells) by FACS. The results demonstrated that *Rassf1a* +/+ iPSCs were significantly more efficient at differentiating to DCs compared to *Rassf1a* -/- (Figure 4.9B).

Since LPS-mediated stimulation of DCs would lead to artificially high expression of cd54 and would not allow us to observe the natural phenotype, we implemented LPS-mediated stimulation only as a positive control for cd54 expression (Figure 4.9C).

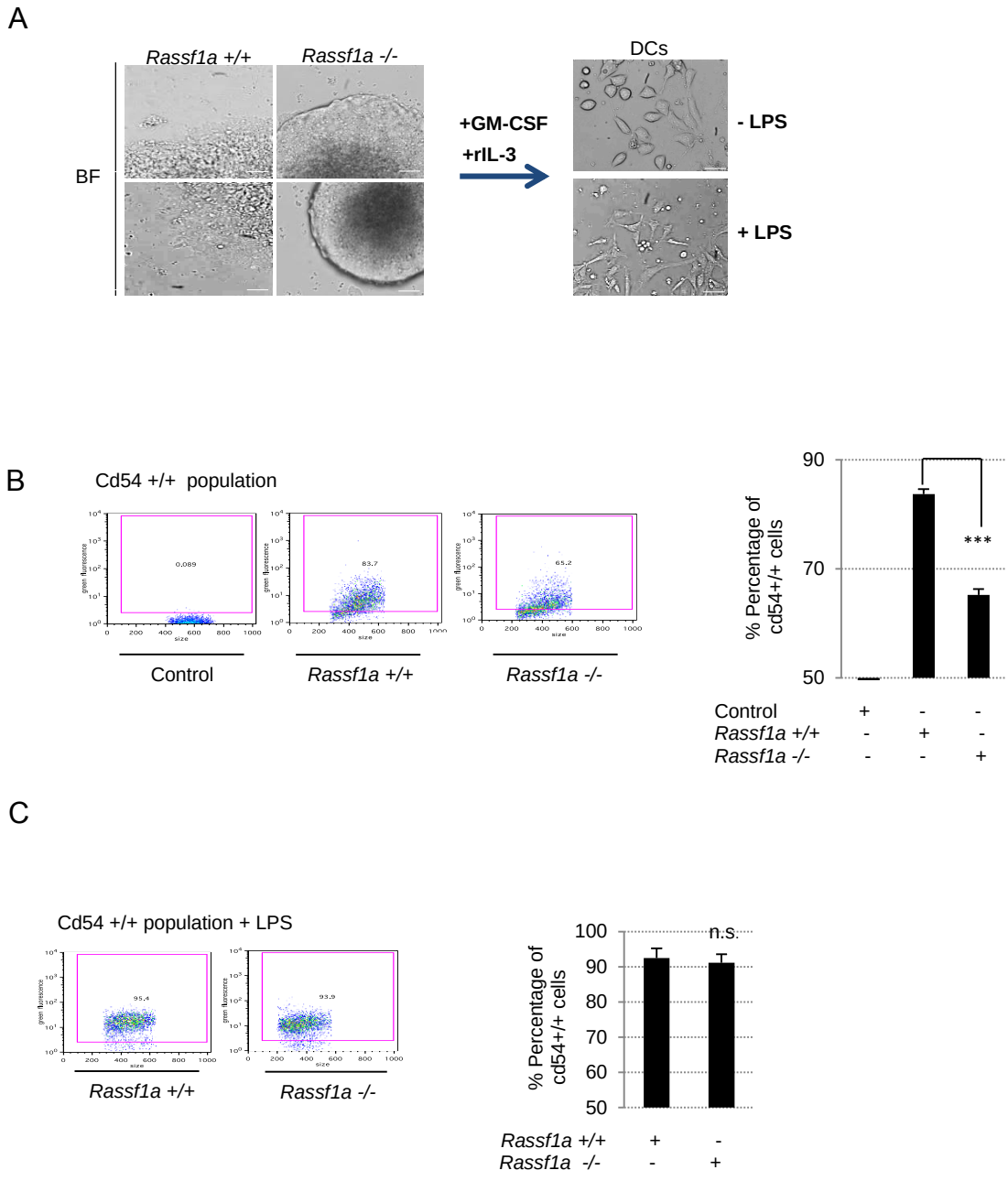


Figure 4.9. Differentiation capacity of iPSCs towards dendritic cells (DCs). A. Images showing *Rassf1a* +/+ and -/- EBs which were forced to form dendritic cells (DCs) upon GM-CSF and rIL-3 treatment. Dendritic cells were grown in the presence or absence of LPS. **B.** Left: FACS plots illustrating the cd54 +/+ cell population (iPSCs from A that became DCs) in the indicated conditions in the absence of LPS. Right: bar graphs showing the percentage of cd54 +/+ cells in each condition. P < 0.001 for *Rassf1a* +/+ vs -/- cells (Student's t test). **C.** Left: FACS plots illustrating the cd54 +/+ population (iPSCs from A that became DCs) in the indicated conditions in the presence of LPS. Right: bar graphs showing the percentage of cd54 +/+ cells in each condition. P = 0.56 (Student's t test).

By making use of this differentiation assay, we confirmed that Rassf1a-lacking iPSCs are resistant to differentiation triggers, not only via quantification of differentiation marker expression or morphological changes, but also by assessing their ability to give rise to differentiated tissue.

4.6 Endogenous Rassf1a expression increases upon differentiation

Next, we set out to investigate whether there were differences in the endogenous expression of Rassf1a during the transition from pluripotency to terminal differentiation. In order to achieve that, we turned to mouse embryonic stem cell (ESC) cultures. A pool of undifferentiated E14Tg2a ESCs, as indicated by the elevated expression of Nanog and Oct4 (Figure 4.10B), originally cultured in the presence of LIF, was allowed to continue growing for a period of 15 days in the absence of LIF, in order to permit transition to differentiation. At the end of this period, cells were clearly differentiated, as shown by the low, this time, expression of the same stem cell markers (Figure 4.10B) and, also, by the appearance of differentiated tissue within the culture, such as beating cardiac progenitor cells (CPCs) (Figure 4.10).

Equal amounts of cells from both conditions (+LIF and –LIF) were subsequently isolated to determine endogenous Rassf1a expression at the transcript as well as the protein level via qRT-PCR and Western blot respectively. Intriguingly, both Rassf1a mRNA and protein were significantly increased in the –LIF condition (Figure 4.10A). Therefore, we concluded that Rassf1a is likely to be physiologically implicated in the determination of stem

cell fate, as endogenous levels appeared to increase upon differentiation stimuli.

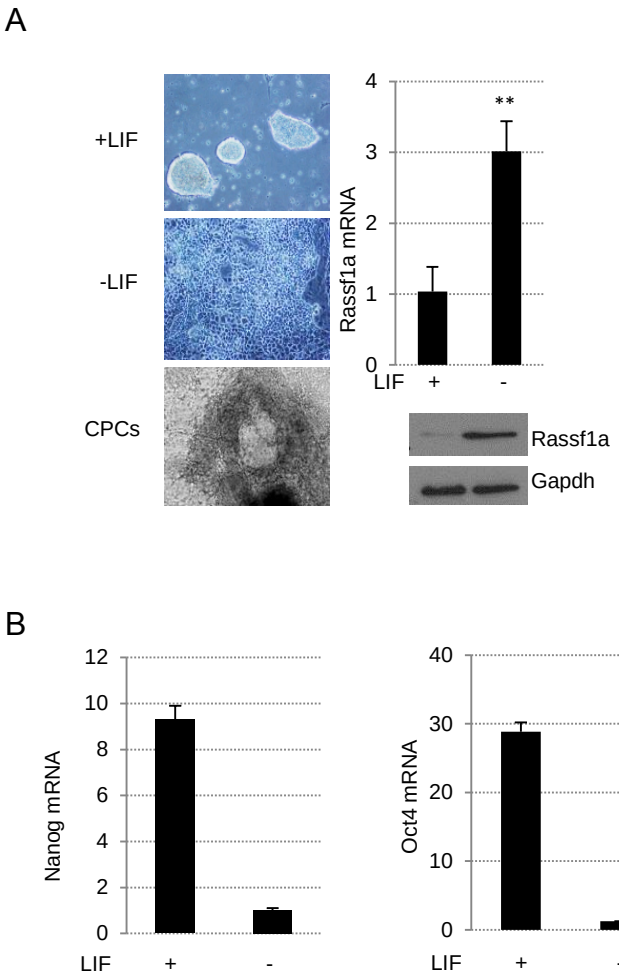


Figure 4.10. Endogenous Rassf1a levels increase upon ESC differentiation. ESCs were either grown in the presence of LIF to maintain pluripotency markers elevated or in the absence of LIF to stimulate differentiation. **A.** Left panel (top to bottom): ESCs cultured in the presence of LIF, ESCs cultured for 15 days in the absence of LIF, ESCs forming beating cardiac progenitor cells (CPCs) after 15 days without LIF. Right panel: qRT-PCR for endogenous Rassf1a mRNA levels from cells grown in the presence or absence of LIF (15 days; P = 0.0017 (Student's t test)) and Western blot showing the respective endogenous protein levels. **B.** qRT-PCR for endogenous Nanog and Oct4 mRNA levels from the conditions described in A.

4.7 RASSF1A downregulates stem cell marker expression by promoting Yap-p73-driven differentiation in mouse ESCs

Since elevated Rassf1a expression substantially restrained reprogramming of somatic cells to iPSCs (Figures 4.2-4.4) and rendered the derivative iPSCs less capable of maintaining a fully pluripotent state (Figures 4.6-4.9), we first sought to recapitulate the phenotypes observed in iPSCs in an independent system. Therefore, we implemented ESCs to address these questions and to clarify the mechanism through which RASSF1A appeared to regulate stem cell fate.

To these ends, we transfected ESCs with either zsGrCtrl empty vector (Control) or a fluorescently labelled RASSF1A, zsGrRASSF1A (R1A), and cultured both populations in the presence of LIF for up to 48 h post transfection. Control cells were more proliferative than RASSF1A overexpressing cells (Figure 4.11A), suggesting that RASSF1A delayed ESC proliferation, potentially to favour cell cycle exit towards differentiation.

We next performed immunofluorescence for stem cell markers Nanog and Oct4 and found clear downregulation in cells overexpressing RASSF1A, whereas levels were maintained in control cells (Figure 4.11). Interestingly, ESC colonies that were allowed to form from zsGrRASSF1A-expressing cells did not remain uniform for RASSF1A expression and displayed inverse staining for Nanog (Figure 4.11C).

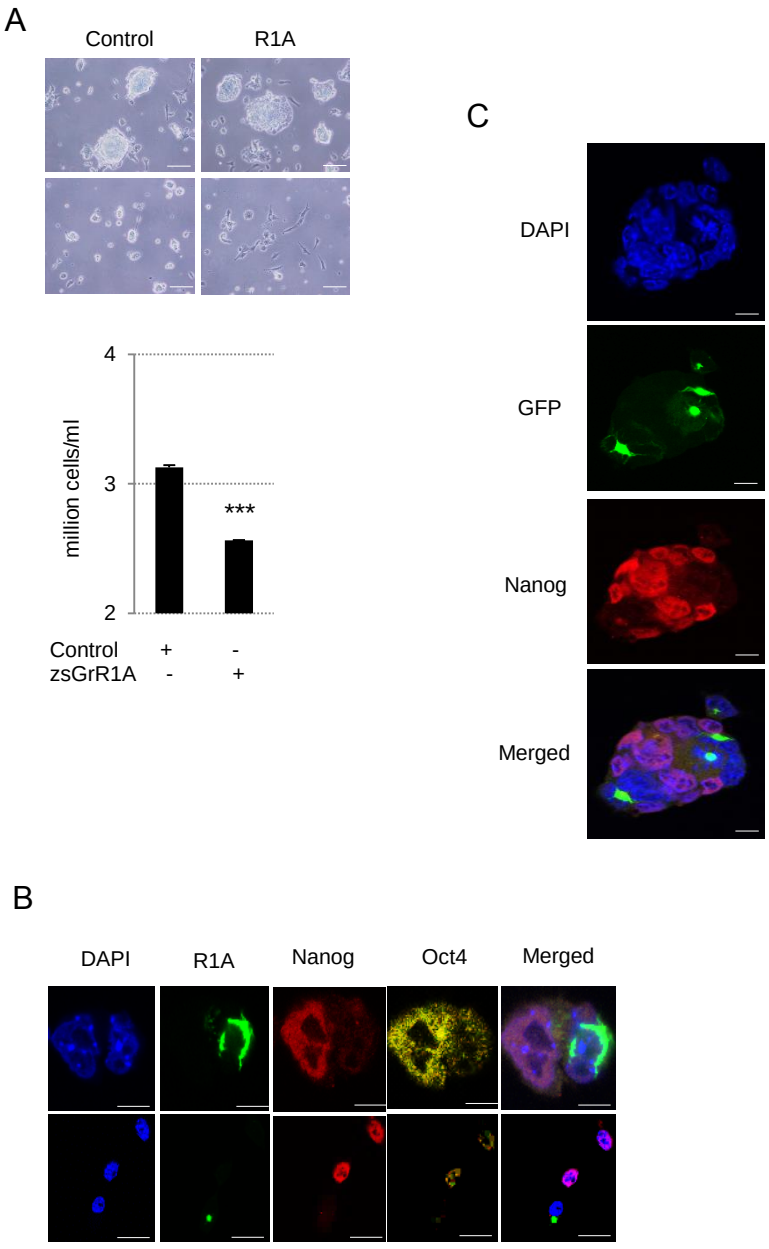


Figure 4.11. RASSF1A reduces stem cell marker levels in ESCs. A. ESCs expressing either zsGrCtrl (Control) or zsGrRASSF1A (R1A). Initially, the same number of cells was seeded for each condition (2 x 10^6 cells). Bar graphs comparing the total number of cells per condition 24 h past transfection. $P < 0.001$ (Student's t test). **B.** Immunofluorescence for Nanog and Oct4 in zsGrRASSF1A-expressing versus non-expressing ESCs. **C.** Immunofluorescence for Nanog in colonies containing zsGrRASSF1A-expressing ESCs.

In order to relate RASSF1A expression to the activation of differentiation programmes in ESCs, we tested the expression of a panel of germ layer-specific differentiation markers. The panel included Bmp4, a crucial factor for mesoderm formation in the mouse embryo (Winnier, Blessing et al. 1995),

Gata4, another mesoderm-specific differentiation factor acting downstream of Bmp4 in embryogenesis (Molkentin, Lin et al. 1997, Rojas, De Val et al. 2005), the mesoendodermal marker Vimentin (Page 1989, Rius and Aller 1992), as well as the ectoderm-specific marker Nestin (Lendahl, Zimmerman et al. 1990, Park, Xiang et al. 2010).

Extracts were obtained from the same zsGrCtrl and zsGrRASSF1A-transfected ESCs described in Figure 4.11 to carry out qRT-PCRs for the transcript levels of the differentiation markers mentioned above. While the mRNA levels of all the stem cell markers tested in parallel (Nanog, Oct4, Sox2; Figure 4.12A) significantly dropped upon RASSF1A overexpression (approximately 75% decrease of all tested), differentiation markers increased (Figure 4.12B). More specifically, Bmp4, Vimentin and Nestin were significantly upregulated upon RASSF1A overexpression in comparison to Control (almost three-fold increase for Bmp4 and five-fold for Vimentin and Nestin). This observation implied that RASSF1A expression can increase the differentiation potential of ESCs towards all three germ lineages (mesoderm, endoderm, ectoderm) by also inducing a concurrent decrease in the core stem cell marker expression.

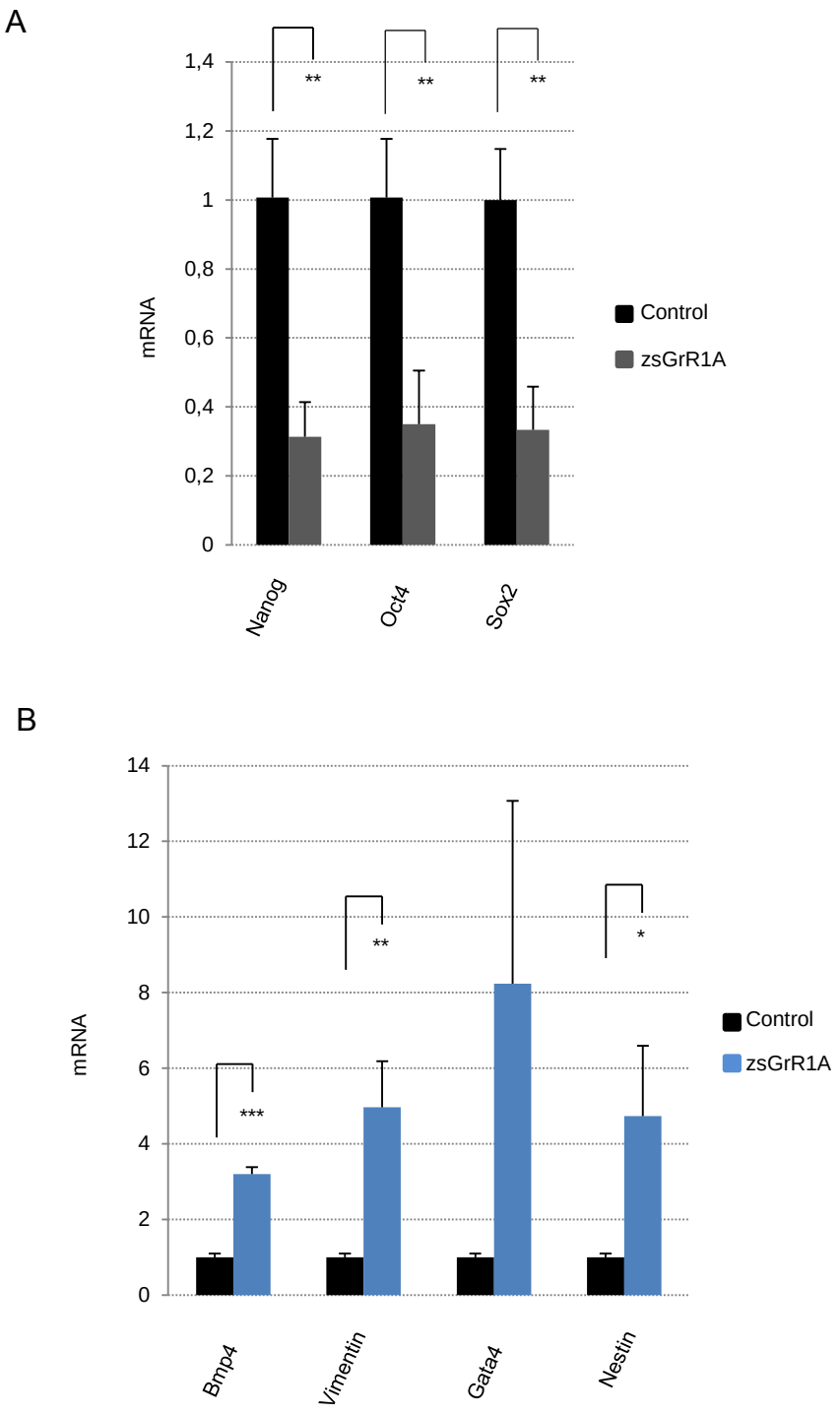


Figure 4.12. RASSF1A increases differentiation marker mRNA levels at the expense of stem cell markers. ESCs were transiently transfected with either zsGrCtrl (Control) or zsGrRASSF1A (zsGrR1A) vector. **A.** qRT-PCR for the indicated stem cell markers from Control or zsGrR1A-expressing cells harvested 48 h past transfection. P = 0.0019 for Nanog; P = 0.0083 for Oct4; P = 0.0034 for Sox2 (Control vs zsGrR1A, Student's t test). **B.** qRT-PCR for the indicated differentiation markers from Control or zsGrR1A-expressing cells harvested 48 h past transfection. P < 0.001 for Bmp4; P = 0.0025 for Vimentin; P = 0.06 for Gata4; P = 0.026 for Nestin (Control vs zsGrR1A, Student's t test).

As mentioned previously, one of the primary aims of this study was to elucidate the mechanism allowing RASSF1A to exert stem cell fate-regulating functions. In Chapter 3, we concluded that RASSF1A exerts its tumour-suppressive functions through the formation of pro-apoptotic YAP1-p73 complexes at the expense of pro-proliferative YAP1-TEAD1 (Figure 3.1). Therefore, we aimed to test for a potential role for YAP1-p73 interactions in stem cell fate determination and, particularly, differentiation in response to RASSF1A. We speculated that YAP1-p73 complex formation would be possibly occurring at the expense of YAP1-TEAD1 complexes, the latter being responsible for maintaining stem cell self-renewal (Lian, Kim et al. 2010). A recent publication (Tamm, Bower et al. 2011), however, highlighted the importance of Tead2, instead of Tead1, in stem cell self-renewal, reporting that Yap1 and Tead2 are highly expressed in undifferentiated mouse ESCs, but are downregulated upon differentiation signals. Additionally, Tead1 was found to be expressed at very low levels in undifferentiated ESCs and its endogenous expression was increased upon differentiation. The other isoforms of the TEA domain protein family, Tead3 and Tead4 show limited expression in pluripotent ESCs. Furthermore, Tamm et al. (2011) showed that Yes-Yap1-Tead2 complexes could drive the transcription of *Oct4* in response to LIF. Hence, of all four members of the family, we initially decided to focus our attention on Tead2.

β-catenin, a protein which was initially found to be implicated in human disease through its interaction with Adenomatus Polyposis Coli (APC) (Rubinfeld, Souza et al. 1993, Su, Vogelstein et al. 1993, reviewed by Clevers and Nusse 2012) and whose first link to Wnt signalling was provided in

Drosophila (Noordermeer, Klingensmith et al. 1994), became of interest to us when Heallen et al. (2011) demonstrated that YAP was able to form nuclear complexes with β-catenin, which promoted the expression of stem cell markers and contributed to cardiomyocyte proliferation and heart size control. They also showed that YAP-β-catenin interactions were abrogated in differentiating cardiomyocytes. These observations, which introduced β-catenin as a YAP binding partner, together with the extensively discussed role of β-catenin in maintaining ESC self-renewal (Sato, Meijer et al. 2004, Ying, Wray et al. 2008, Kelly, Ng et al. 2011, ten Berge, Kurek et al. 2011) urged us to explore whether there was a role for β-catenin in the RASSF1A-mediated regulation of stem cell fate.

For these purposes, ESCs expressing either zsGrCtrl (Control) or zsGrRASSF1A (R1A) were harvested 48 h post transfection, lysed and subject to Yap1 co-immunoprecipitations. We observed that Yap1-Tead2 complexes were decreased upon RASSF1A overexpression compared to the Control, whereas, at the same time, Yap1-p73 interactions were augmented. We also confirmed the interaction of Yap1 with β-catenin and, moreover, were able to show that forced RASSF1A expression restricted Yap1-β-catenin complexes, following a pattern similar to Yap1-Tead2 regulation (Figure 4.13). Total cell extracts were probed with the same antibodies to ensure that the endogenous expression levels were unchanged.

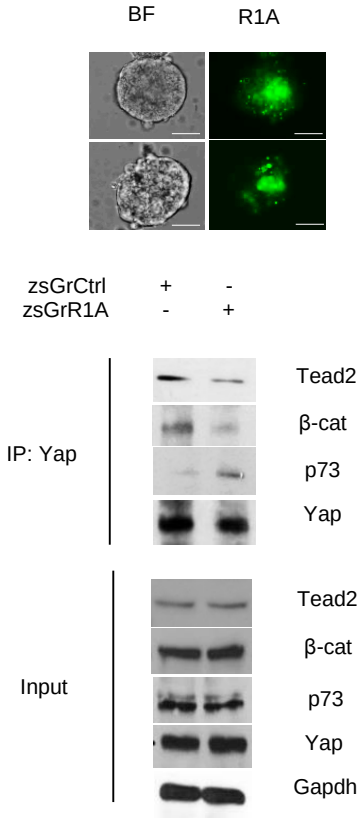


Figure 4.13. RASSF1A expression fosters Yap1-p73 complex formation at the expense of Yap1-Tead2 and Yap1-β-cat in ESCs. ESCs were transiently transfected with either zsGrCtrl or zsGrRASSF1A (zsGrR1A, R1A) expressing vectors. Top panel: indicative pictures of ESC colonies expressing R1A, assessed by immunofluorescence. Bottom panel: Yap1 co-IP from the same cells. The immunoprecipitates were blotted with the indicated antibodies.

In order to determine that Yap1-p73 is responsible for RASSF1A-driven differentiation, we depleted p73 in the presence of RASSF1A and assessed the differentiation capacity of ESCs. The results demonstrate clearly that silencing of p73 abolished the expression of differentiation markers (Bmp4, Vimentin, Gata4, Nestin) pertaining to all three germ layers (Figure 4.14). Under both conditions (Control and RASSF1A overexpression), knockdown of p73 reduced differentiation markers to an equally low expression level.

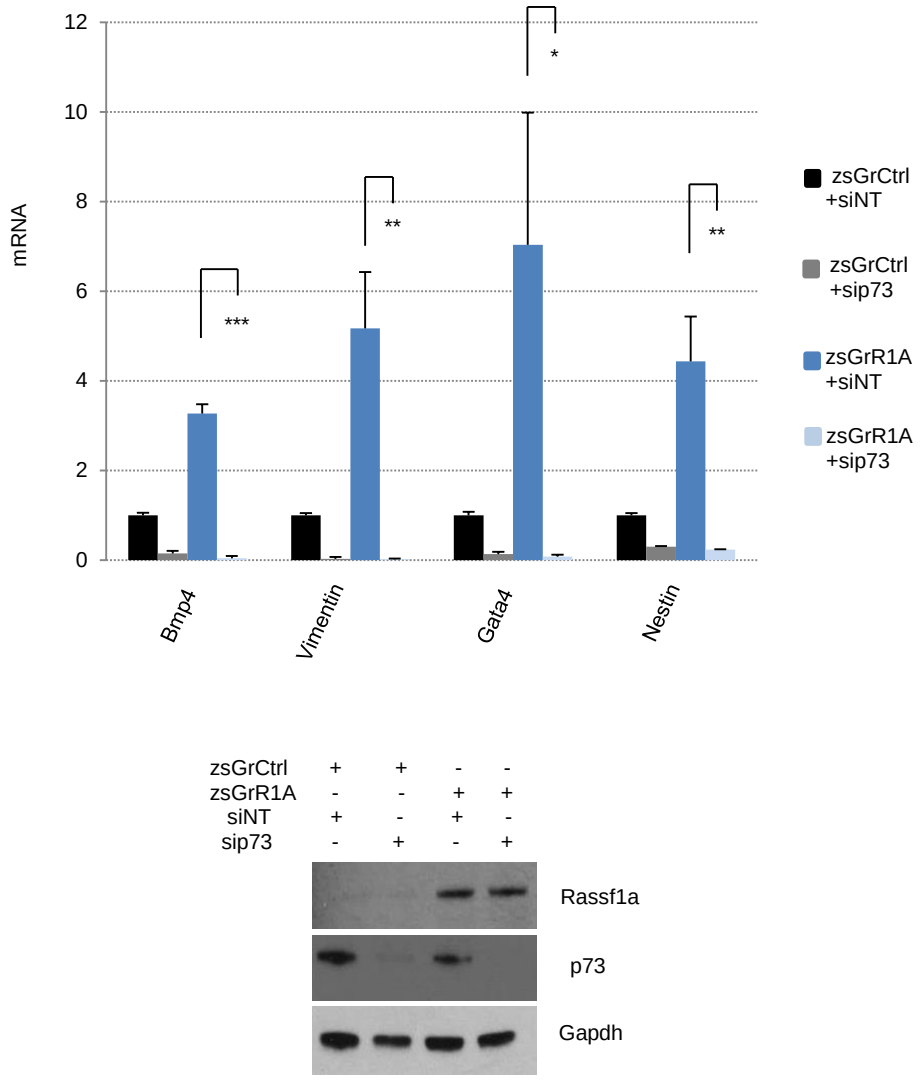


Figure 4.14. Yap1-p73 complexes are required for ESC differentiation in the presence of RASSF1A. ESCs were transiently transfected with either empty (zsGrCtrl) or RASSF1A-expressing (zsGrR1A) vectors, together with non-targeting (siNT) or p73-targeting (sip73) siRNAs. Top panel: qRT-PCR for the indicated differentiation markers from each condition 48 h past transfection. P < 0.001 for Bmp4; P = 0.0021 for Vimentin; P = 0.01 for Gata4; P = 0.0019 for Nestin (zsGrR1A+siNT versus zsGrR1A+sip73, Student's t test). Bottom panel: Western blot of the cell lysates probed with the indicated antibodies.

4.8 Rassf1a loss in ESCs increases stem cell markers via Yap1-Tead2

To further confirm the implication that RASSF1A promotes an exit from pluripotency, we transfected ESCs either with non-targeting siRNA (siNT) or Rassf1a-targeting siRNA (siRassf1a). A qRT-PCR showing the effective knockdown of Rassf1a is provided in Supplementary Figure 7.6A. As anticipated, Rassf1a depletion led to an increased proliferation rate of ESC,

as indicated by the total cell numbers 24 h post transfection (Figure 4.15A), in keeping with data above (Figure 4.11A), where RASSF1A overexpression led to decreased proliferation of ESCs. Immunostaining for Nanog expression indicates a clear increase in protein levels in ESCs lacking Rassf1a versus Control (siNT) (Figure 4.15B). Consistent with these findings, Nanog, Oct4 and Sox2 mRNA levels were similarly increased (almost three and half-fold increase for Nanog, four and half-fold increase for Oct4 and four-fold increase for Sox2; Figure 4.16A).

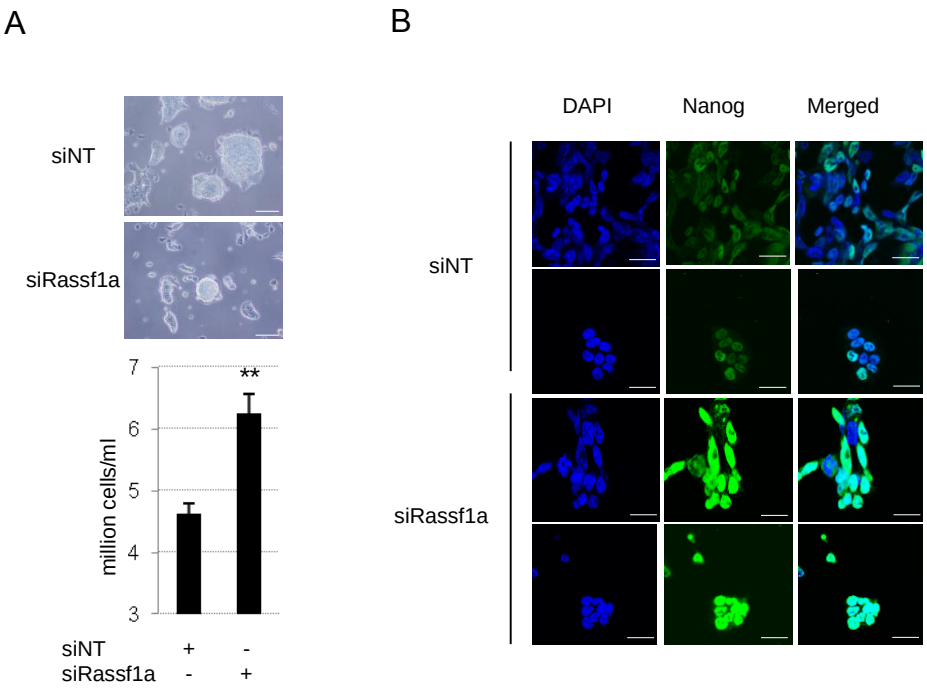
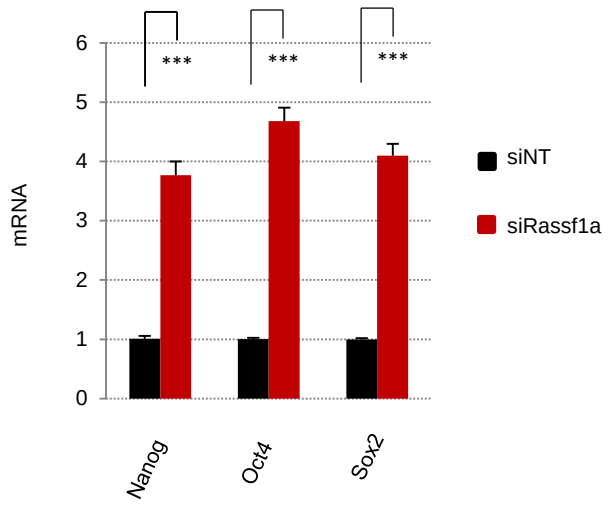


Figure 4.15. Rassf1a depletion increases stem cell marker protein levels in ESCs. A. ESCs transfected with either non-targeting (siNT) or Rassf1a-targeting (siRassf1a) siRNA. Initially, the same number of cells was seeded for each condition (2.5 x 10^6 cells). Bar graphs showing the number of counted cells per condition 24 h past transfection. P = 0.0037 (Student's t test). **B.** Immunofluorescence for Nanog in siNT versus siRassf1a-transfected ESCs.

To test whether the pluripotent phenotype emerging from Rassf1a loss is accompanied by increased resistance to differentiation, as in iPSCs (Figures 4.7-4.9), siNT and siRassf1a-transfected ESCs were switched to a LIF-free culture to induce spontaneous differentiation. The transcript levels of differentiation markers (Bmp4, Vimentin, Gata4, Nestin) were significantly downregulated in the Rassf1a knockdown condition versus Control (siNT)(Figure 4.16B). We interpreted this ubiquitous drop in differentiation marker expression as a means of global resistance to differentiation signals.

In order to establish a molecular link between Rassf1a loss and upregulation of stem cell markers, we examined Yap1 association with transcription factors in the absence of Rassf1a. Yap1 was immunoprecipitated from extracts of siNT or siRassf1a-transfected ESCs and subsequent analysis of co-immunoprecipitates by western blots indicated that Yap1-Tead2 complexes were significantly elevated upon Rassf1a depletion. This was correlated with increased Yap1-β-catenin complexes, whereas Yap1-p73 interactions diminished (Figure 4.17). Thus it became clear that Rassf1a loss fostered the formation of self-renewal-promoting Yap1-Tead2 (Lian, Kim et al. 2010, Tamm, Bower et al. 2011) and Yap1-β-catenin (Heallen, Zhang et al. 2011) complexes at the expense of Yap1-p73 complexes. Interestingly, it also appeared that RASSF1A promotes differentiation in a p73-dependent manner.

A



B

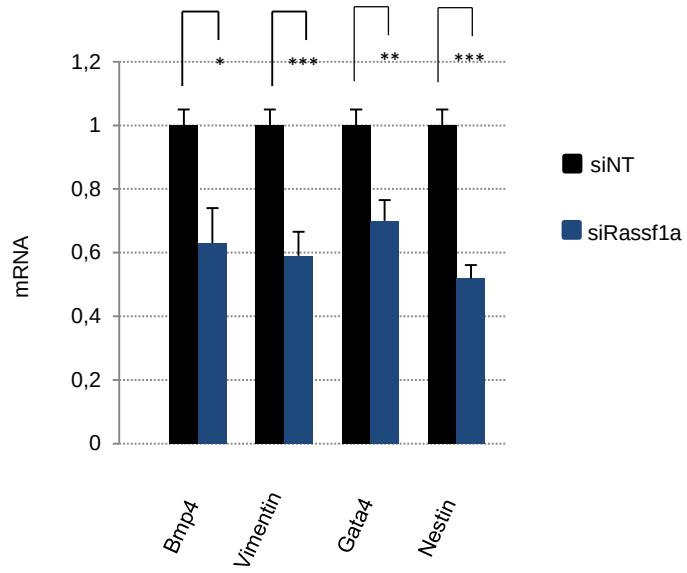


Figure 4.16. Rassf1a depletion increases stem cell marker mRNA levels at the expense of differentiation markers. ESCs were transfected with either non-targetting (siNT) or Rassf1a-targeting (siRassf1a) siRNA **A.** qRT-PCR for the indicated stem cell markers from siNT or siRassf1a-transfected cells, harvested 48 h past transfection. $P < 0.001$ for Nanog, Oct4 and Sox2 (siNT vs siRassf1a, Student's t test). **B.** ESCs were grown in the absence of LIF for 48 h past transfection to stimulate differentiation programmes. qRT-PCR for the indicated differentiation markers from siNT or siRassf1a-transfected cells, harvested 48 h past transfection. $P = 0.046$ for Bmp4; $P < 0.001$ for Vimentin; $P = 0.0016$ for Gata4; $P < 0.001$ for Nestin (siNT vs siRassf1a, Student's t test).

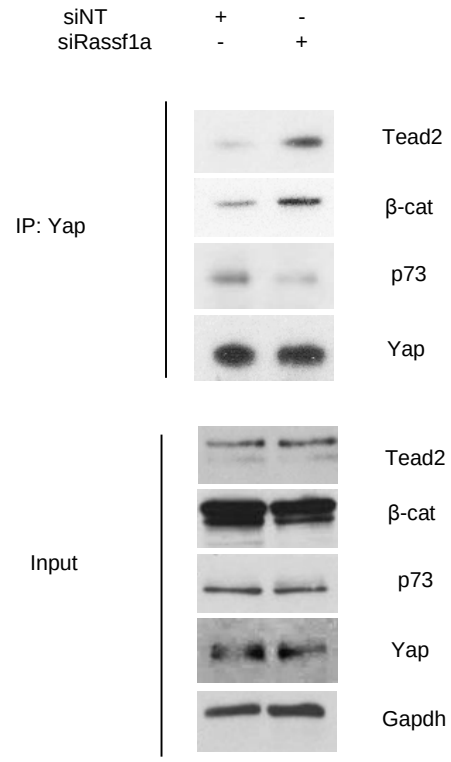


Figure 4.17. Rassf1a depletion promotes Yap1-Tead2 and Yap1-β-cat complex formation at the expense of Yap1-p73 in ESCs. ESCs were transfected with either non-targetting siRNA (siNT) or Rassf1a-targeted siRNA and harvested 48 h past transfection. Yap1 immunoprecipitates were blotted with the indicated antibodies.

4.9 Tead2, Yap1 and β-catenin together form a stable complex in the absence of Rassf1a

To further investigate Yap complexes, we utilised lentiviruses to generate mouse ESC lines stably expressing either shGFP, as a control, or shRassf1a. This ensures more efficient silencing of Rassf1a. Rassf1a mRNA levels in shRassf1a-expressing ESCs were measured via qRT-PCR against Control (shGFP) cells and indicate almost 100% knockdown efficiency, as illustrated in Supplementary Figure 7.7.

We were intrigued by the finding that Rassf1a loss exerts similar regulation on Yap1-Tead2 and Yap1-β-catenin (Figure 4.17) and sought to test the

hypothesis that Tead2 and β-catenin form a single complex. We immunoprecipitated Tead2 from shGFP and shRassf1a-expressing ESCs and identified β-catenin stabilised association specifically upon loss of Rassf1a (shRassf1a) (Figure 4.18A). Yap1 binding to Tead2, as expected (Figure 4.17) was also increased in the absence of Rassf1a (Figure 4.18A). This indicated the existence of a Yap1-Tead2-β-catenin trimeric complex, strongly stabilised upon Rassf1a loss.

Based on the recent report (Tamm, Bower et al. 2011) that Yap1-Tead2 complexes drove the transcription of *Oct4* by directly binding to promoter elements in mouse ESCs and urged by our findings, we postulated that there might be a so far unknown role for β-catenin in this process, suggesting that instead of simply Yap1-Tead2, it may be Yap1-Tead2-β-catenin complexes which contribute to the maintenance of self-renewal, under the control of RASSF1A. The recruitment of β-catenin, however, to elements of the *Oct4* promoter would most likely require a DNA-binding Tcf/Lef factor, as β-catenin has been shown to associate with such factors to facilitate transcription activation (Behrens, von Kries et al. 1996, Molenaar, van de Wetering et al. 1996, van de Wetering, Cavallo et al. 1997). Of the members of the Tcf/Lef family of transcription factors, Tcf3 has stood out as a binding factor of regulatory regions of the core stem cell factor genes in ESCs, in particular Nanog, Oct4 and Sox2 (Pereira, Yi et al. 2006, Tam, Lim et al. 2008, Yi, Pereira et al. 2008). Tcf4 has also been identified as a component of Wnt-mediated activation of genes in embryonic (Wallmen, Schrempp et al. 2012) as well as adult (Lu, Qu et al. 2012) stem cells. Interestingly, Tcf3 was detected in Tead2 immunoprecipitates (Figure 4.18A), indicating that the

identified Yap1-Tead2-β-catenin complex may include at least one additional component.

To clarify whether Tead2 and β-catenin directly interacted and to determine if the self-renewal-regulation by Rassf1a required Yap1, we targeted shRassf1a-expressing ESCs with Yap1 siRNA (siYap). The results demonstrated that although Tead2-β-catenin interaction is sustained in shRassf1a-expressing cells, this requires the presence of Yap1 (Figure 4.18B). This observation highlighted the importance of Yap1 in the Yap1-Tead2-β-catenin complex, as it indicated that Yap1 acts as a link between Tead2 and β-catenin.

To ensure that the role of Yap1 in pluripotent phenotypes conveyed by Rassf1a loss was not just a phenotype of shRassf1a-selected ESCs, we repeated Yap1 silencing in cells transiently depleted for Rassf1a (siRassf1a). Oct4 and Sox2 transcript levels were again upregulated in the absence of Rassf1a (siRassf1a), and rescued upon depletion of Yap1 (Figure 4.18C, Supplementary Figure 7.6B).

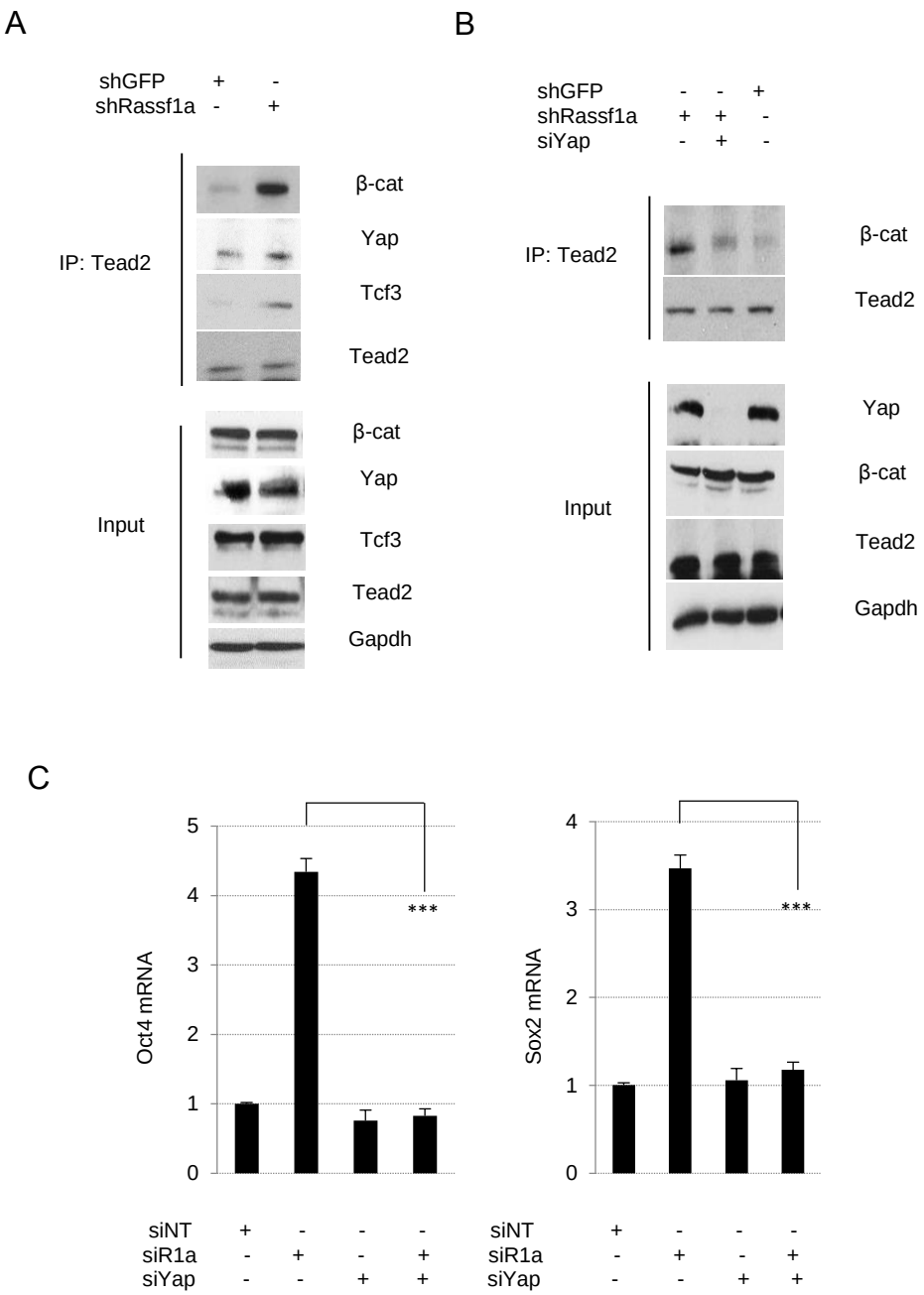


Figure 4.18. In the absence of Rassf1a, stable Yap1-Tead2-β-cat complexes are formed and the stem cell marker upregulation is Yap-dependent. ESCs were lentivirally infected with either non-targetting (shGFP) or Rassf1a-targeting (shRassf1a) shRNAs and/or transfected with the indicated siRNAs. **A,B.** Tead2 immunoprecipitates were blotted with the indicated antibodies 48 h past transfection (for the siRNAs). **C.** qRT-PCR for Oct4 and Sox2 mRNA levels from ESCs treated with the indicated siRNAs. $P < 0.001$ for both Oct4 and Sox2 (siR1A vs siR1A/siYap, Student's t test).

Tead2 is the main TEA domain protein family member that contributes to an ESC undifferentiated state (Tamm, Bower et al. 2011), however, as Tead1 is necessary for proliferation of RASSF1A-null cancer cells (Figure 3.6) we tested whether Tead1 might also complex with Yap1 and β-catenin. By using siRNA targeting Tead1 (siTead1), we concluded that Tead1 depletion had no impact on Oct4 and Sox2 levels (Figure 4.19A). Notably, however, Tead1 depletion alone led to a significant increase in both Oct4 and Sox2 mRNA (Figure 4.19A), suggesting that Tead1 may restict ESC self-renewal. This observation is also supported by reports in the literature stating that Tead1 might be important during differentiation processes (Tamm, Bower et al. 2011, Wang, Wang et al. 2013). However, unlike Tead1, both β-catenin (Figure 4.19B) and Tead2 (Figure 4.19C) are required for the increased Oct4 levels observed upon Rassf1a depletion. In ESCs, Tead2 appears to be required for Nanog and Oct4 expression (Figure 4.19C) and, in line with this, the elevated Nanog expression in *Rassf1a -/-* iPSCs is also Tead2-dependent (Supplementary Figure 7.5B).

Taken together, these data suggest that both β-catenin and Tead2 facilitate Oct4 and Nanog expression and are negatively regulated by RASSF1A. Most importantly, the observation that ablation of either Yap1, β-catenin or Tead2 alone was sufficient to inhibit the effects of Rassf1a loss on pluripotency, implied the requirement for an intact Yap1-Tead2-β-catenin complex to elicit these effects.

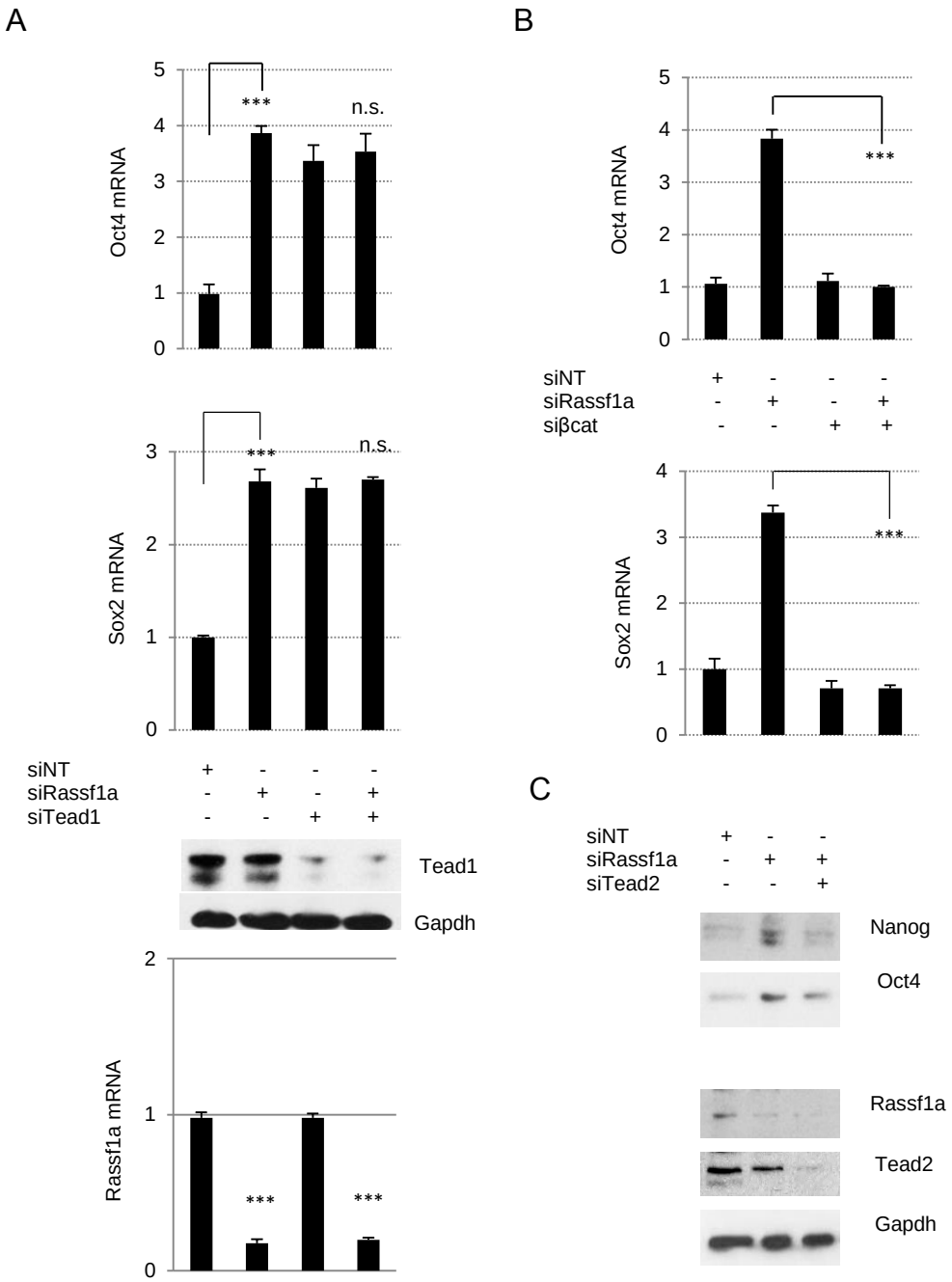


Figure 4.19. Stem cell marker upregulation occuring in the absence of Rassf1a is not mediated through Tead1, but via β-cat and Tead2. ESCs were transfected with the indicated siRNAs and the cells were harvested 48 h past transfection. **A.** Top panel: qRT-PCR for Oct4 and Sox2 mRNA levels from ESCs treated with the respective siRNAs. $P < 0.001$ (siNT against siRassf1a), $P = 0.17$ (siRassf1a against siRassf1a/siTead1) for Oct4; $P < 0.001$ (siNT against siRassf1a), $P = 0.8$ (siRassf1a against siRassf1a/siTead1) for Sox2 (Student's t test). Bottom panel: Westen blotting of the cell lysates probed with the indicated antibodies. **B.** qRT-PCR for Oct4 and Sox2 mRNA levels from ESCs treated with the respective siRNAs. $P < 0.001$ for both Oct4 and Sox2 (siNT versus siRassf1a and siRassf1a versus siRassf1a/siβ-cat, Student's t test). **C.** Western blotting of ESC lysates probed with the stated antibodies.

4.10 Loss of Rassf1a causes recruitment of Yap1-Tead2-β-catenin to the *Oct4* promoter

Based on the previous report that Yap1-Tead2 complexes were bound to elements of the *Oct4* promoter to stimulate ESC self-renewal (Tamm, Bower et al. 2011), we speculated that a similar regulatory mechanism might be driven by the Yap1-Tead2-β-catenin complex. Moreover, our data would suggest that it is likely that β-catenin, potentially through Tcf3 (Figure 4.18A), may contribute to gene transcription.

RASSF1A-expressing (zsGrRASSF1A) or control (zsGrCtrl) ESCs (Figure 4.13) were used for Yap1 chromatin immunoprecipitations (ChIP) to detect differences in the binding affinity of Yap1-Tead2-β-catenin complexes to the *Oct4* promoter upon RASSF1A overexpression, by using specific sets of primers identifying either Tead2 (Tamm, Bower et al. 2011) or β-catenin (Yi, Pereira et al. 2011) binding sites on the *Oct4* promoter. The results demonstrated a clear reduction in *Oct4* promoter occupancy by Yap1 complexes, indicating that both Tead2 and β-catenin-dependent *Oct4* binding was significantly decreased upon RASSF1A overexpression (Figure 4.20).

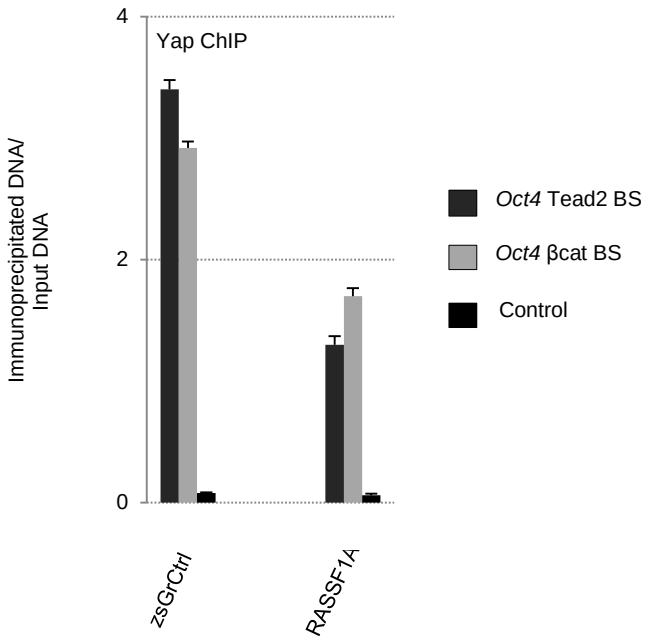


Figure 4.20. RASSF1A expression restricts *Oct4* promoter occupancy by both Yap1-Tead2 and Yap1-β-cat in ESCs. ESCs were transfected with either empty (zsGrCtrl) or RASSF1A (zsGrRASSF1A) expressing vector and subject to Yap1 ChIP 48 h post-transfection. The bar graph represents quantification (qRT-PCR) of the immunoprecipitated DNA over the Input DNA (sonicated chromatin) from each condition. BS: Binding Sites, Control: B-actin. $P < 0.001$ for both Tead2 and β-cat *Oct4* binding sites (zsGrCtrl vs RASSF1A, Student's t test).

Oct4 gene transcription is dependent on the regulatory elements lying upstream of the *Oct4* promoter. These elements, namely proximal enhancer (PE) and distal enhancer (DE) contain the binding sites for several transcription factors (Ben-Shushan, Pikarsky et al. 1993, Ovitt and Scholer 1998, Pan, Chang et al. 2002, Hattori, Nishino et al. 2004). Based on the already existing literature regarding *Oct4* gene structure (Okazawa, Okamoto et al. 1991, Yeom, Fuhrmann et al. 1996, Nordhoff, Hubner et al. 2001) and taking into account the sequences of the primers used to detect *Oct4* occupancy by Tead2 and β-catenin (Tamm, Bower et al. 2011, Yi, Pereira et

al. 2011), we created a map depicting the exact binding sites of the two transcription factors on upstream elements of the *Oct4* promoter, as well as the distance between them (Figure 4.21A). As illustrated on the map, both Tead2 (app. -4500 bp) and β-catenin (app. -1900 bp) binding sites are located in the distal enhancer (DE) region, however, they are found at opposite ends, separated by approximately 2600 bp.

Since overexpression of RASSF1A reduced *Oct4* promoter occupancy by both Tead2 and β-catenin decreased binding (Figure 4.20), we reasoned that loss of Rassf1a should increase promoter occupancy. We next employed stable shGFP, shRassf1a, shTead2 and shRassf1a/shTead2 ESC lines transfected with siRNAs to either β-catenin, Tcf3 and Tcf4, as well as with non-targeting controls (siNT). The use of stable cell lines substantially minimised the toxic effects and knockdown inefficiencies produced by multiple simultaneous transfections. Western blots showing the effective silencing of β-catenin, Tcf3 and Tcf4 in this experiment are provided in Supplementary Figures 7.7 and 7.8A. Yap1 chromatin immunoprecipitations (ChIP) were performed using the previously mentioned primers to Tead2 and β-catenin binding sites on *Oct4* promoter. Knockdown of Rassf1a (shRassf1a) led to a significant increase in *Oct4* occupancy at both sites (approximately three-fold increase in comparison to shGFP) and the additional knockdown of Tead2 (shRassf1a/shTead2) diminished *Oct4* occupancy not only by Tead2, but surprisingly also β-catenin. This implies that β-catenin localisation to the *Oct4* promoter is Tead2-dependent and suggests that the Yap1-Tead2-β-catenin-Tcf3 complex acts as a transcription-promoting unit on *Oct4*. In support of this finding, silencing of β-catenin together with Rassf1a (shRassf1a/siβcat),

reduced Tead2 promoter binding to the same extent as β-catenin (Figure 4.21B).

Intrigued by this observation, we further explored the phenomenon by assessing whether removal of Tcf3 has a similar effect. Depletion of Tcf3 in the absence of Rassf1a (shRassf1a/siTcf3) indeed decreased the affinity of both β-catenin and Tead2 to the promoter, however, to a lesser extent than knockdown of β-catenin alone (Figure 4.21B). We, therefore, reasoned that another Tcf factor, such as Tcf4, which has been reported to play a role in β-catenin-mediated transcription activation in stem cells (Lu, Qu et al. 2012, Wallmen, Schrempp et al. 2012) might be compensating for Tcf3 loss. Indeed, depletion of Tcf4 (shRassf1a/siTcf4) reduced *Oct4* occupancy at both sites (Figure 4.21B). This was surprising, because Tcf4 was not originally identified as an additional component of the Yap1-Tead2-β-catenin complex (Figure 4.18A).

Nanog and *Sox2* promoter occupancy by Yap1-Tead2-β-catenin complexes was also assessed, however, we were unable to detect an interaction of any of the complex components with elements of the promoters (data not shown). This is consistent with previous reports, stating that only Yap-Tead2 complexes were found to directly interact with elements of the *Oct4* promoter (Tamm, Bower et al. 2011).

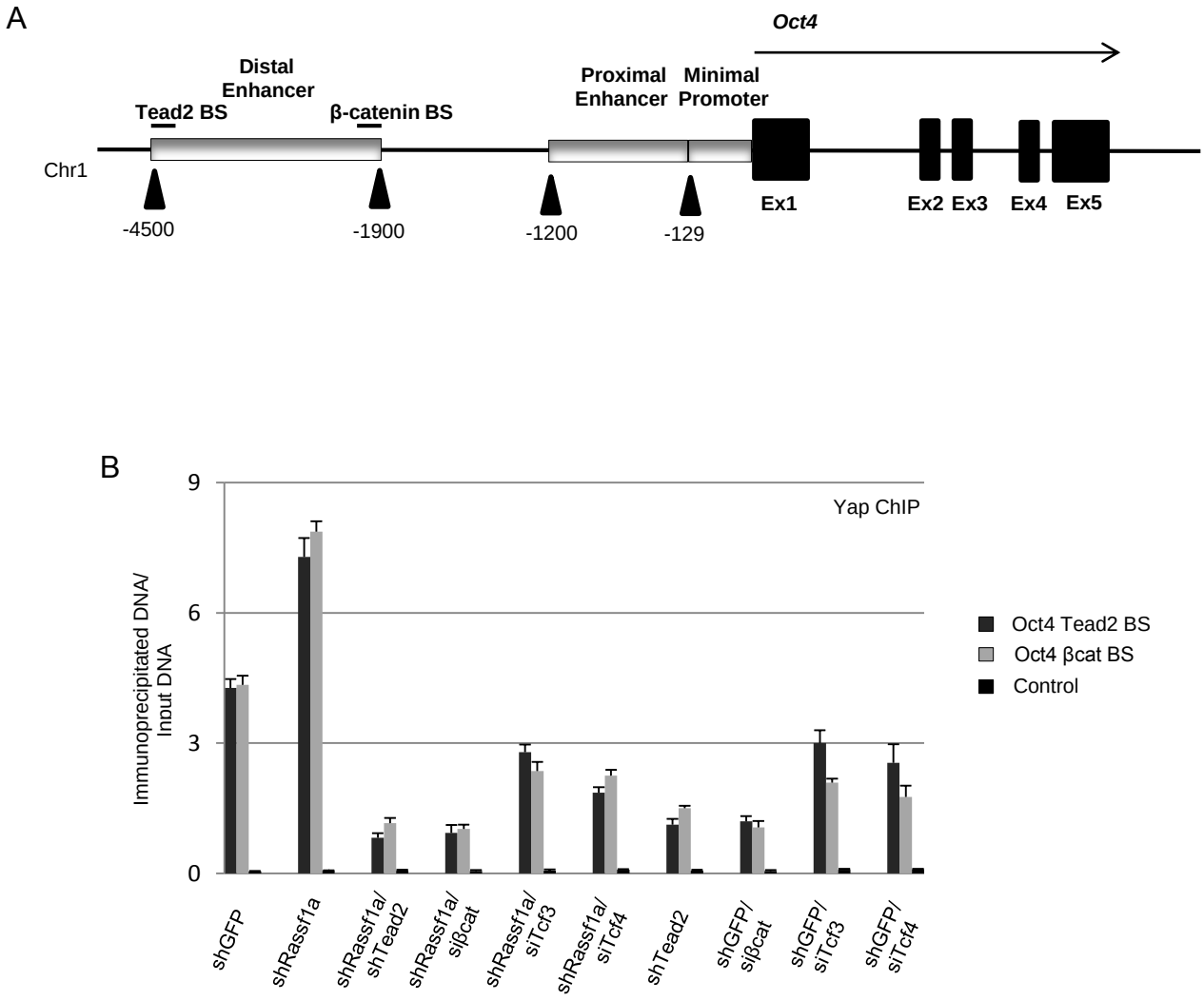


Figure 4.21. Elevated *Oct4* transcription in the absence of Rassf1a requires promoter occupancy by intact Yap1-Tead2-β-cat complexes. A. Molecular structure of *Oct4* as described by Okazawa et al., 1991, Yeom et al., 1996 and Verena Nordhoff et al., 2001. The *Oct4* gene lies in chromosome 17 and contains 5 exons (represented by black boxes Ex1-5). Upstream the minimal promoter lies a transcriptional proximal enhancer and further upstream a distal enhancer represented by grey boxes. Both Tead2 and β-cat binding sites are located at different regions of the distal enhancer, as the alignment of the primer sequences with the upstream sequence of *Oct4* (available on PubMed) revealed. **B.** ESCs were lentivirally transfected with the indicated shRNAs and/or transfected with the respective siRNAs and subject to Yap1 ChIP 48 h post-transfection. The bar graph represents quantification (qRT-PCR) of the immunoprecipitated DNA over the Input DNA (sonicated chromatin) from each condition. BS: Binding sites, Control: B-actin. $P < 0.001$ for shGFP versus shRassf1a, shRassf1a versus shRassf1a/shTead2, shRassf1a versus shRassf1a/siβ-cat, shRassf1a versus shRassf1a/siTcf3, shRassf1a versus shRassf1a/siTcf4 for both Tead2 and β-cat *Oct4* binding sites (Student's t test).

4.11 Rassf1a regulates Lats-mediated phosphorylation of Yap1

As RASSF1A is a component of the Hippo pathway resulting in MST/LATS-mediated tumour suppressive signalling to YAP (Huang, Wu et al. 2005, Dong, Feldmann et al. 2007, Matallanas, Romano et al. 2007, Zhao, Wei et al. 2007, Zhao, Li et al. 2010), we first sought to determine whether Rassf1a-mediated regulation of Yap1 in ESCs was Hippo pathway-dependent. To that end, we disrupted Hippo signalling to Yap1 by silencing Lats1, which is responsible for the inactivation of Yap-Tead complexes. Thus, we transfected ESCs with either non-targeting (siNT) siRNA or siRNAs targeting Rassf1a (siRassf1a) and Lats1 (siLats1) alone and in combination. The elevation of Oct4 and Sox2 mRNA upon silencing of Rassf1a (siRassf1a) was ablated by restricting Lats1 expression with siLats1 (Figure 4.22; Supplementary Figure 7.6D). This demonstrates that Rassf1a signalling to Yap1 is indeed conducted through the Hippo pathway kinase cascade.

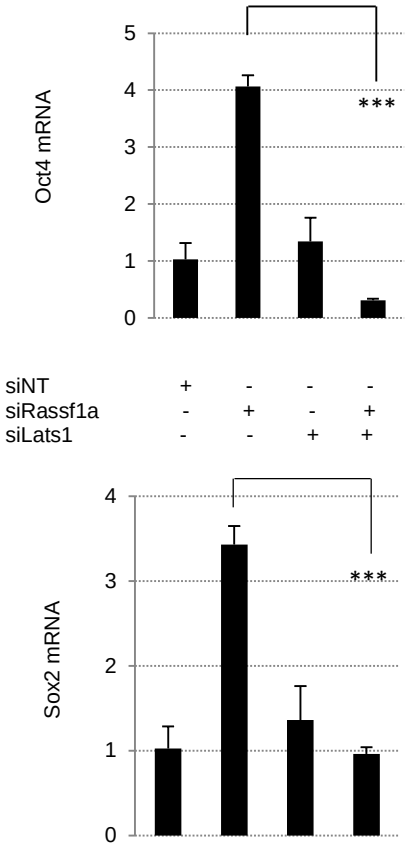


Figure 4.22. Lats1 is indispensable for stem cell marker upregulation in the absence of Rassf1a. ESCs were transfected with the stated siRNAs (siNT, siRassf1a and siLats1) and the cells were harvested 48 h post-transfection. qRT-PCR for Oct4 and Sox2. $P < 0.001$ for siNT vs siR1a and siR1a vs siR1a/siLats1 for both Oct4 and Sox2 (Student's t test).

In cancer cells, LATS-dependent phosphorylation of YAP1 occurs at HXRXXS consensus motifs and has been found to directly regulate YAP1 activity in response to various signals such as cell density (Zhao, Wei et al. 2007, Zhao, Li et al. 2010). Therefore, Yap1 phosphorylation by Lats could differ in the presence and absence of Rassf1a in ESCs, thereby affecting Yap1 function. Thus, we employed mass spectrometry (MS) to identify changes in Yap1 phosphorylation sites in the presence and absence of Rassf1a. We used ESCs transfected with either non-targeting (siNT) siRNA or siRNA to Rassf1a (siRassf1a), as well as *Rassf1a* +/+ (clone 77.5) and -/- (clone 77.3) iPSCs to address this question in two independent systems. As

there are five Lats-dependent consensus phosphorylation sites identified on human YAP1 (Zhao, Wei et al. 2007), all the cells were additionally transfected with a human FLAG-YAP1 and immunoprecipitation was performed using an anti-FLAG antibody. The subsequent analysis showed that of the five Lats-dependent phosphorylation sites, only two (S127 and S109) appeared to be phosphorylated differentially in response to Rassf1a. pS127, in particular, was significantly decreased in the absence of Rassf1a (Figure 4.23A), in both siRassf1a and *Rassf1a -/-* (clone 77.3) conditions. Surprisingly, pS109 appeared to follow the opposite pattern, displaying an increase in the absence of Rassf1a (Figure 4.23A).

In order to confirm this finding, ESCs from the MS experiment (siNT and siRassf1a-transfected; Figure 4.23A), as well as cells transfected with either empty (zsGrCtrl) or RASSF1A-expressing (zsGrR1A) vector, along with FLAG-YAP1, were lysed, western blotted and probed for pS127 YAP1 levels with a commercially available antibody. The results confirmed the MS finding that phosphorylation of YAP1 at S127 was decreased upon Rassf1a depletion (siRassf1a). Concomitantly, when RASSF1A was overexpressed, pS127 YAP1 was substantially increased, in keeping with activation of the hippo pathway and increased Lats1 activity (Figure 4.23B).

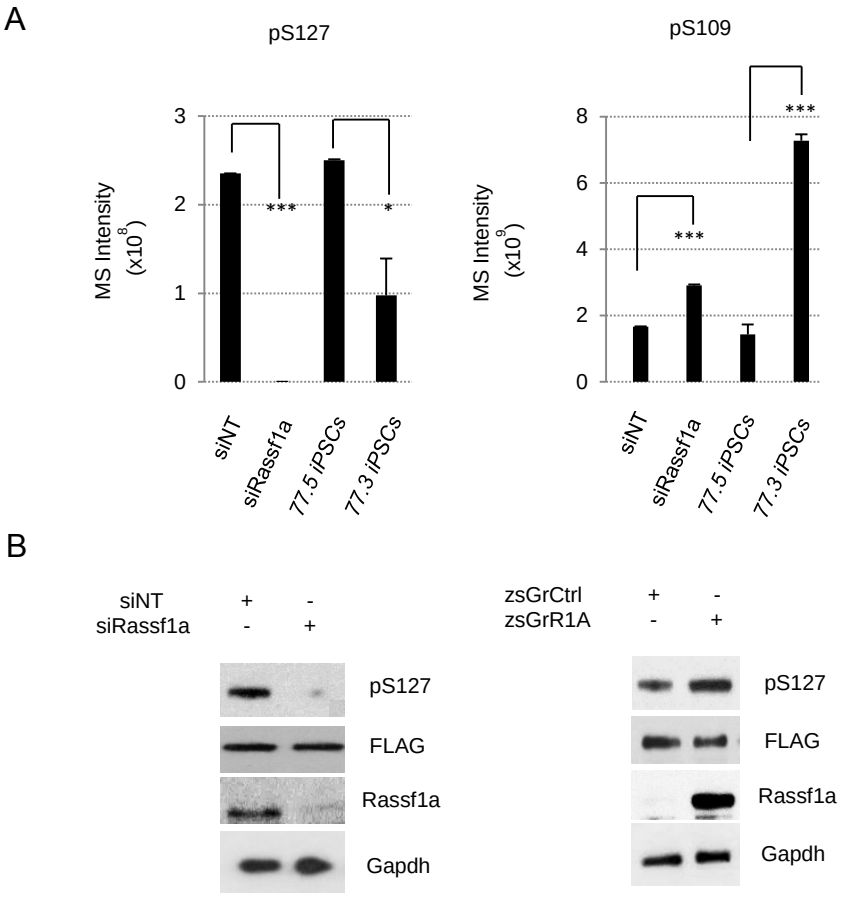


Figure 4.23. The LATS-dependent YAP1 phosphorylation sites S127 and S109 follow a distinct pattern in response to RASSF1A. A. Mass Spectrometry (MS) analysis in ESCs and iPSCs that were transfected with the indicated siRNAs (ESCs) or derived from WT MEFs (iPSC clone 77.5) or *Rassf1a -/-* MEFs (iPSC clone 77.3). Both ESCs and iPSCs were transfected with a FLAG-YAP1 construct. The cells were harvested 48 h post-transfection and the bar graphs illustrate the phosphorylation analysis results for the only sites that exhibited differences. P < 0.001 for siNT vs siRassf1a and 77.5 vs 77.3 for both pS127 and pS109. **B.** Left panel: Western blot of the ESC extracts in A using the indicated antibodies. Right panel: ESCs were transiently transfected with FLAG-YAP1 and either Control (zsGrCtrl) or RASSF1A- expressing (zsGrR1A) vector and 48 h later the cells were harvested. Western blot of the cell extracts probed with the stated antibodies.

Previous results in this chapter demonstrated that RASSF1A overexpression resulted in stable Yap1-p73 complexes (Figure 4.13). Based on the data deriving from the MS analysis, RASSF1A overexpression also resulted in elevated YAP1 phosphorylation on S127 (Figure 4.23B). Taken

together, this body of evidence suggested that the formation of YAP1-p73 complexes might be dependent on phosphorylation of YAP1 on S127. To test this hypothesis, we transfected ESCs with FLAG-YAP1, as well as a RASSF1A-expressing (zsGrR1A, R1A) construct and performed a Proximity Ligation Assay (PLA), which provides evidence of protein-protein interactions through formation of a fluorescent signal. Interestingly, confocal microscopy analysis revealed that pS127 YAP1 and p73 indeed interacted and, moreover, pS127 YAP1-p73 complexes could only be detected in RASSF1A overexpressing cells. Of note, although a proportion of these complexes appeared to be formed in the cytoplasmic compartment, their presence was also detected in the nuclear compartment of RASSF1A overexpressing ESCs (Figure 4.24; Supplementary Figures 7.8B and C).

The MS data showed that the Lats-dependent S109 YAP1 phosphorylation site was elevated in the absence of Rassf1a. Due to the lack of an available antibody to pS109 YAP1, we are currently not able to directly confirm this. However, as pS109 was elevated in the context of a Yap1-Tead2-β-catenin complex, we reasoned that making use of an S109A YAP1 mutant construct would clarify whether pS109 played a role in the Yap1-Tead2-β-catenin interaction. shRassf1a-expressing ESCs were transiently transfected with either wild type FLAG-YAP1 or ^{3}FLAG-YAP1 S109A and co-immunoprecipitation of YAP1 binding partners was assessed by western blot. Figure 4.25A demonstrates a clear increase in both YAP1-Tead2 and YAP1-β-catenin upon Rassf1a loss, when cells were transfected with the wild-type construct, but this was almost completely reversed upon expression of the mutant ^{3}FLAG-YAP S109A construct (Figure 4.25A).

Following these observations, we wished to investigate the significance of pS109 and pS127, upon RASSF1A overexpression when Yap1-Tead2-β-catenin is lost and YAP-p73 is promoted. In line with our previous data, RASSF1A overexpression limited YAP1-Tead2 and YAP1-β-catenin complexes by promoting YAP1-p73, whereas in the presence of the S127A mutant, YAP1-Tead2 and YAP1-β-catenin levels remained unchanged and YAP1-p73 interactions were abolished (Figure 4.25B). By using, however, the ^{3}FLAG-YAP1 S109A construct, we observed no differences (Figure 4.25B).

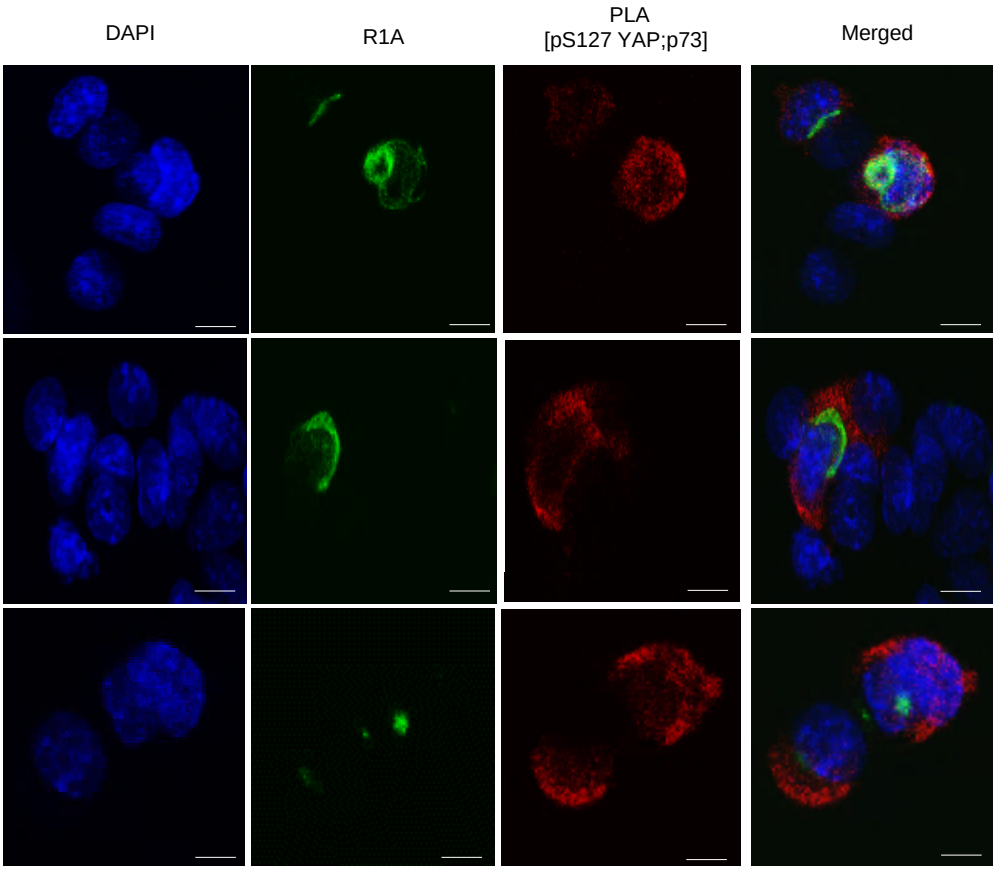


Figure 4.24. pS127 YAP1 associates with p73 only in the presence of RASSF1A. ESCs were transfected with FLAG-YAP1 and zsGrRASSF1A (R1A) and subject to Proximity Ligation Assay (PLA). Immunofluorescence for the expression of RASSF1A as well as the pS127 YAP1-p73 interaction, which is demonstrated by the red dots (PLA). Experiment done under my supervision by Konstantinos Toskas, a visiting Master's student in the lab.

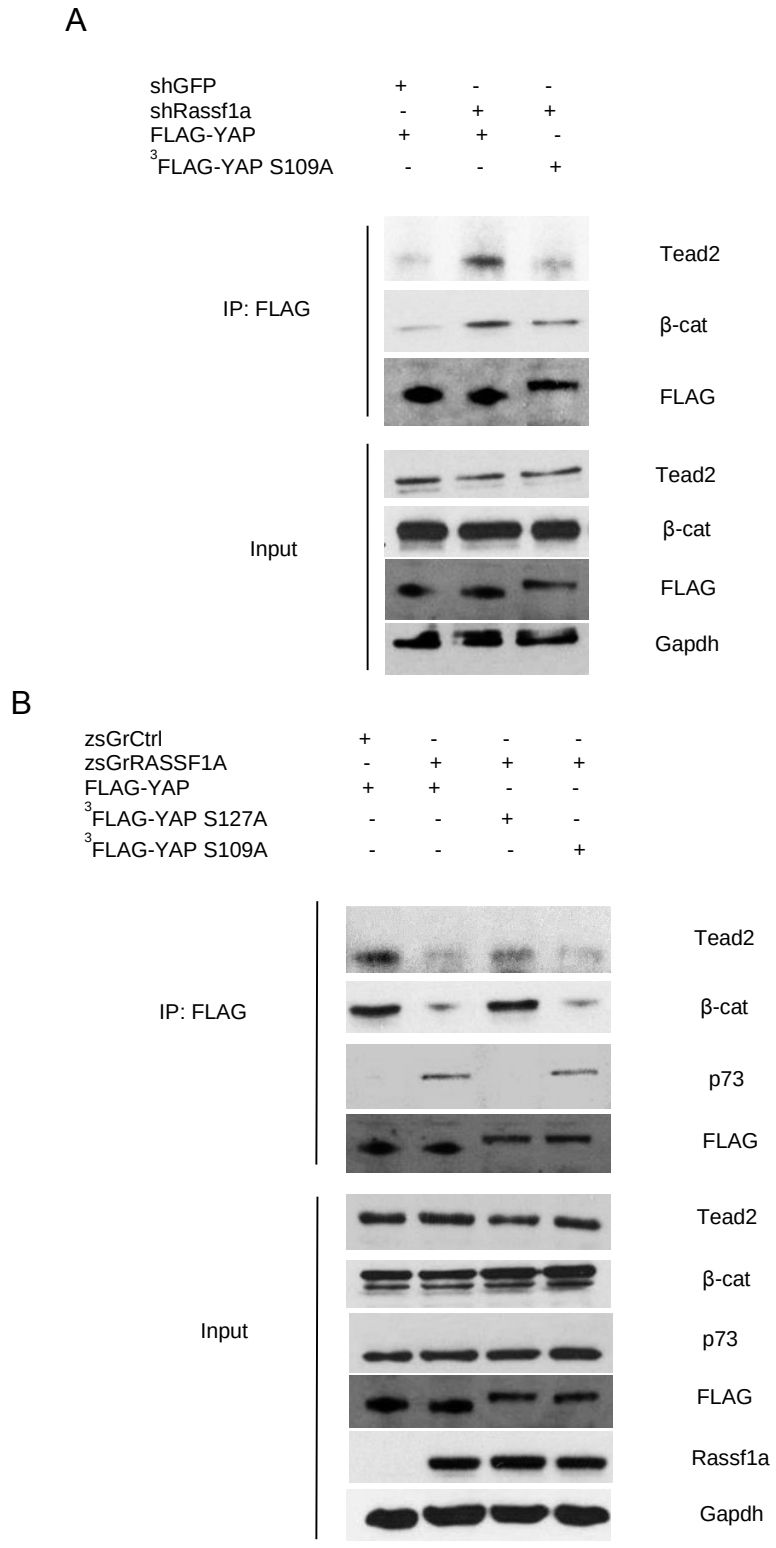


Figure 4.25. pS109 YAP1 is required for Yap1-Tead2 and Yap1-β-cat interactions, whereas pS127 YAP1 facilitates only Yap1-p73. A. ESCs stably expressing either non-targeting (shGFP) or Rassf1a-targeting (shRassf1a) shRNAs were transfected with FLAG-YAP1 or ^{3}FLAG-YAP1 S109A as indicated. FLAG immunoprecipitates were blotted with the stated antibodies. **B.** ESCs were transiently transfected either with empty (zsGrCtrl) or RASSF1A-expressing (zsGrRASSF1A) vector, together with FLAG-YAP1 or ^{3}FLAG-YAP1 S127A or ^{3}FLAG-YAP1 S109A as indicated. FLAG immunoprecipitates were blotted with the stated antibodies.

4.12 RASSF1A impairs mouse embryonic development via p73

Given that Rassf1a appeared to have an impact on fundamental aspects of stem cell biology, we became much interested in exploring the role of Rassf1a signalling during embryonic development. Thus, we set out to test our hypothesis in the pre-implantation mouse embryo, which would serve as an *in vivo* model for validating our stem cell-related observations. For this purpose, we collaborated with the Magdalena Zernicka-Goetz lab, based in the Gurdon Institute, Cambridge, UK. I designed and coordinated all the *in vivo* experiments presented in this section with the aim of elucidating the physiological role of Rassf1a signalling in embryogenesis.

Mouse embryos were microinjected with the appropriate reagents (siRNA, mRNA or DNA) at the single-cell stage and allowed to grow up to the blastocyst or earlier developmental stages depending on the requirements of each experiment. A schematic is provided in Supplementary Figure 7.9A. In order to explore the effect of Rassf1a knockdown in embryogenesis, blastomeres were microinjected with either non-targeting (siNT) siRNA or siRNA to Rassf1a (siRassf1a) and allowed to grow. Embryos at different cell stages (2-, 4-, 8-,16- and 32-cell stage) were fixed and analysed for stem cell marker expression. At all developmental stages examined, Rassf1a loss led to increased Nanog protein expression in comparison to controls, as assessed by immunofluorescence (Supplementary Figure 7.9B). Furthermore, a quantitative PCR from lysates of the same pool of embryos revealed that in line with the previous observation, both Nanog and Oct4 mRNA levels were significantly increased upon Rassf1a silencing (Supplementary Figure 7.10).

A qRT-PCR verifying Rassf1a knockdown efficiency in the embryos is provided in Supp. Figure 7.10.

In order to test for the impact of RASSF1A overexpression on pluripotency *in vivo*, embryos were transfected with either zsGrCtrl (Control) or zsGrRASSF1A (RASSF1A) mRNAs and allowed to grow. Embryos at the blastocyst stage (E3.5) were fixed and analysed for Nanog and Oct4 protein expression via immunofluorescence. As displayed in Supplementary Figure 7.11, RASSF1A overexpression drastically limited Nanog and Oct4 levels. Moreover, quantification of Oct4 intensity (normalised against DAPI nuclear staining) across all confocal stacks in all RASSF1A overexpressing embryos versus Control, demonstrated an overall decrease of approximately 40% in Oct4 protein levels (Supplementary Figure 7.11B).

Interestingly, injecting RASSF1A mRNA into the embryos at concentrations ranging between 500-1000 ng/μL prevented the embryos from further dividing and led to significantly increased lethality. Even at low concentrations of 200 ng/μL, only 70% of the embryos were able to proceed in forming blastocysts (Supplementary Figure 7.12A). A “kill curve” to determine which RASSF1A mRNA concentration is critical for embryonic lethality revealed that at concentrations higher than 300 ng/μL, embryos exhibit 100% lethality (0 out of 15 embryos survived) (Supplementary Figure 7.12A). This was surprising, because mRNA concentrations of a similar scale have been conventionally used to induce expression of various vectors in the mouse embryo. Given that the Control transfections did not lead to increased arrest or lethality, together with the observation that RASSF1A restricted stem cell marker expression (Supplementary Figure 7.11A and B), we reasoned that

this was an additional indication of RASSF1A acting as a cell fate determinant.

Our *in vitro* experiments illustrated that RASSF1A exerts its fate-determining functions through p73. Thus, we postulated that silencing of p73 would occlude RASSF1A signalling in the mouse embryo. To test this hypothesis, we transfected mouse embryos with unusually high RASSF1A mRNA concentrations, together with siRNA to p73. The concentration of RASSF1A mRNA on this occasion was 1000 ng/μL, which was exceeding by far the lethality threshold (300 ng/μL), at which all the embryos died. The same number of embryos (n=15) were also transfected with the same concentration of control vector. The majority of the control embryos (10 out of 15) were able to form blastocysts, in complete contrast to the RASSF1A-transfected ones, which all arrested and died, resulting, as previously (Supp. Figure 7.12A), in 0 out of 15 embryos surviving to the blastocyst stage. Strikingly, in embryos microinjected with both RASSF1A mRNA and sip73, the lethal phenotype was completely rescued and, additionally, the number of embryos reaching the blastocyst stage was equivalent to that of the Control (11 out of 15 embryos) (Supplementary Figure 7.12B). This dramatic phenotype strongly suggested that the key effector of Rassf1a signalling in development is indeed p73. Silencing of p73 under Control conditions (zsGrCtrl) yielded equivalent numbers to siNT-transfected embryos (Supplementary Figure 7.13).

4.13 Discussion

In this study, we aimed to explore the potential role of RASSF1A signalling in stem cell biology and embryonic development, guided by the initial observation that by acting as a tumour suppressor, RASSF1A influenced the transcription partner selection of YAP1 (TEAD, p73, RUNX2; Chapter 3) which in addition to their roles in cancer, are established stem cell fate determinants (De Laurenzi, Raschella et al. 2000, Hong, Hwang et al. 2005, Camargo, Gokhale et al. 2007, Lian, Kim et al. 2010, Agostini, Tucci et al. 2011).

Somatic reprogramming of wild-type Rassf1a MEFs led to proficient iPSCs, which were capable of forming embryoid bodies and differentiating into specified cell lineages, such as dendritic cells (DCs) (Figure 4.9). Rassf1a-null iPSCs demonstrated increased resistance to multiple differentiation stimuli (Figures 4.7A, 4.8 and 4.9). Furthermore, they appeared to be more proliferative as Ki67 staining revealed (Figure 4.7C), which was in keeping with reports in the literature providing strong correlations between high proliferation rates and elevated stem cell marker expression in ESCs (Cartwright, McLean et al. 2005) and the pre-implantation embryo (DeVeale, Brokhman et al. 2013, Lee, Bonneau et al. 2013).

Re-expression of RASSF1A restored differentiation capacity (Figures 4.3, 4.4, 4.6A, 4.7B and 4.8), and provided confirmation that the effects described in iPSCs were indeed RASSF1A-dependent. Similarly, ESCs were in complete support of this, as similar effects to iPSCs occurred upon both Rassf1a depletion (Figures 4.15 and 4.16) and overexpression (Figures 4.11

and 4.12). Most importantly, however, Rassf1a appeared to be substantially involved in the natural transition of pluripotent ESCs to a differentiated state such as the one represented by cardiac progenitor cells (CPCs), as this process was accompanied by a significant increase in its endogenous levels (Figure 4.10). Together, these observations were sufficient to verify an impactful role for Rassf1a in fate decision.

Until recently, little was known about the role of YAP1 complexes in stem cell pluripotency, with the exception of YAP1-TEAD (Lian, Kim et al. 2010, Tamm, Bower et al. 2011) and YAP1-β-catenin (Heallen, Zhang et al. 2011), both of which were shown to be positive regulators of self-renewal. We attempted to further decipher the function of YAP1 complexes, particularly from a RASSF1A perspective. Interestingly, we found that Rassf1a signalling in ESCs was conveying similar changes to Yap1 complexes to those occurring in cancer cells. In ESCs, however, these complexes were charged with completely different, developmental functions. Specifically, in response to RASSF1A, stabilised Yap1-p73 complexes resulted in increased expression of mesoderm, endoderm and ectoderm-specific differentiation markers (Bmp4, Vimentin, Gata4, Nestin), all of which were suppressed in the absence of p73 (Figures 4.12B, 4.13 and 4.14). Thus, through p73, RASSF1A elicited global differentiation of ESCs towards all cell lineages. Of note, knockdown of p73 limited differentiation markers even in the Control conditions (Figure 4.14A), potentially because endogenous Rassf1a is responsible for maintaining these markers at a baseline level in undifferentiated cells.

On the other hand, loss of Rassf1a increased the affinity of Yap1 to Tead2 and β-catenin at the expense of p73 (Figure 4.17), conferring resistance to

differentiation signals (Figure 4.16B) due to the highly upregulated core stem cell marker network (Nanog, Oct4, Sox2; Figures 4.15B and 4.16A). Intriguingly, Rassf1a loss did not stabilise Yap1-Tead2 and Yap1-β-catenin complexes independently, but we showed that Yap1, together with Tead2 and β-catenin came in one complex (Figure 4.18A). The complex, however, collapsed upon Yap1 depletion, even in the absence of Rassf1a.

Further investigation of the function of Yap1-Tead2-β-catenin complexes revealed that upon Rassf1a knockdown, these stabilised complexes were recruited specifically to the *Oct4* promoter to initiate transcription. Subsequently, both Tead2 and β-catenin created binding sites with one of the upstream elements of the promoter, the distal enhancer (DE), separated from each other by 2600 bp (Figure 4.21A). Although the binding sites were located at remote regions of the DE, intact Yap1-Tead2-β-catenin complexes were shown to be required for *Oct4* occupancy at either site (Figure 4.21B). This could be explained by the potential formation of a DNA loop bringing the two binding sites at close proximity, so as to enable the same Yap1-Tead2-β-catenin transcriptional complex to create contacts with both of them. DNA looping is a common event in gene expression regulation (Lieberman-Aiden, van Berkum et al. 2009, Sanyal, Lajoie et al. 2012, Jin, Li et al. 2013), also taking place during lineage commitment (Phillips-Cremins, Sauria et al. 2013). Alternatively, the elevated Oct4 expression in the absence of Rassf1a could be due to a bigger number of Yap1-Tead2-β-catenin enhancer complexes occupying the *Oct4* promoter independently at both sites of the DE, hence increasing the recruitment of RNA polymerase to launch transcription (Koch, Fenouil et al. 2011).

Despite the initial identification of Tcf3 as the only additional component of the complex to facilitate binding of β-catenin to DNA (Figure 4.18A), depletion of either Tcf3 or Tcf4 decreased *Oct4* promoter occupancy by the Yap1-Tead2-β-catenin complexes, suggesting that β-catenin can potentially implement both factors to execute its transcriptional functions in this context (Figure 4.21B).

Notably, even in control conditions, depletion of any of the components of the Yap1-Tead2-β-catenin complex, resulted in a significant decrease in *Oct4* promoter occupancy (Figure 4.21B), highlighting the importance of the complex even when Rassf1a was endogenously expressed and the complex less stable. Substantial restriction on Yap1-Tead2-β-catenin recruitment to the *Oct4* promoter was also achieved via exogenous expression of RASSF1A (Figure 4.20), leading to Yap1-Tead2-β-catenin complexes being replaced by Yap1-p73.

Even though loss of Rassf1a fostered the recruitment of Yap1-Tead2-β-catenin complexes specifically to the *Oct4* promoter and no binding to the *Nanog* and *Sox2* promoters was observed, the expression level of all core stem cell markers was significantly increased (Figures 4.6, 4.15B and 4.16A). Numerous reports in the literature have stated that regulation of most pluripotency-related genes, such as *Fgf4*, *Fbxo15*, *Nanog* and *Sox2*, is achieved by enhancers containing Oct4 and Sox2 binding motifs, named Oct-Sox enhancers, which are highly active in undifferentiated, but not differentiating ESCs. These enhancers are located in the upstream region of each of the regulated genes and require binding of both Oct4 and Sox2 to be activated (Yuan, Corbi et al. 1995, Nishimoto, Fukushima et al. 1999,

Tokuzawa, Kaiho et al. 2003, Kuroda, Tada et al. 2005, Rodda, Chew et al. 2005, Nakatake, Fukui et al. 2006). Sox2 itself, however, was found to be dispensable for the activation of these enhancers, as other factors, such as Sox15, unnecessary for ESC self-renewal were able to do it instead (Masui, Nakatake et al. 2007). Oct4 is, thus, the most important stem cell marker in maintaining ESC pluripotency and can regulate both Nanog and Sox2 expression via the Oct-Sox elements (Masui, Nakatake et al. 2007). ChIP-sequencing for the identification of Yap target genes and RNA sequencing for genome-wide expression profiling in response to Rassf1a are already being performed to elucidate the regulatory functions of Rassf1a.

Depletion of Lats1 in the absence of Rassf1a, rescued the elevated stem cell marker expression (Figure 4.22). This indicated that Rassf1a signalling to Yap1 was carried out through the Hippo pathway cascade. MS analysis for YAP1 phosphorylation sites in response to Rassf1a demonstrated differences in two Lats-dependent serine-phosphorylation sites (S127 and S109). We found pS127 to be downregulated in the absence of Rassf1a and elevated upon RASSF1A overexpression (Figure 4.23). Consistent with our results, Zhao et al. (2007) reported that differentiation of ESCs was accompanied by an increase in pS127 YAP1. Abrogation of this phosphorylation, disrupts the Yap1-p73 complex formation (Figure 4.25B). On the other hand, pS109 which was elevated only upon Rassf1a loss (Figure 4.23), was found to be indispensable for Yap1-Tead2-β-catenin complex formation (Figure 4.25A), but its inactivation caused no effect on Yap1-p73 (Figure 4.25B).

Similarly to ESCs, knockdown of Rassf1a in the pre-implantation mouse embryo increased stem cell markers (Supp. Figures 7.9 and 7.10), whereas

RASSF1A overexpression caused opposite effects (Supp. Figure 7.11). Most importantly, however, even at low amounts of microinjected RASSF1A mRNA (200 ng/μL), a significant proportion of the embryos failed to progress to the blastocyst stage (Supp. Figure 7.12A), but this phenotype was strikingly rescued upon depletion of p73 (Supp. Figure 7.12B). This rescue was observed even though RASSF1A expression exceeded by far the limit considered to cause arrest and lethality to 100% of the embryos, which instead, developed equivalently well to the Control (Figure 7.12B). Given the effects of Rassf1a signalling on stem cell marker regulation and taking into account reports in the literature correlating stem cell marker decrease with impaired developmental progression, and specifically early embryonic stage arrest (DeVeale, Brokhman et al. 2013, Lee, Bonneau et al. 2013), we reckoned that the reason for the extensive arrest and lethality was that embryos were forced to differentiate at a stage (before E3.5) when they were traditionally required to remain pluripotent (Figure 4.26) and that caused major disruptions to their developmental programme. In keeping with this, in a recent publication (Tan, Au et al. 2013), which complemented the previous reports by providing a gene expression screen, Rassf1 expression was shown to be increased by over two-fold following stem cell marker depletion, indicating that a possible reason for the subsequent embryonic arrest was Rassf1-driven differentiation, a process which at that stage the embryos could not afford.

A correlation of endogenous Rassf1 with Oct4 mRNA expression in the mouse embryo (Wang, Piotrowska et al. 2004) showed that maternal Rassf1 mRNA is progressively decreased until the 8/16-cell stage, where it reaches a

minimum (Figure 4.26). Oct4, as shown here (Figure 4.26) and as reported in the literature (Palmieri, Peter et al. 1994, Wang, Piotrowska et al. 2004), begins to be expressed at the 4-cell stage, reaches its maximum expression levels at the 8/16-cell stage and subsequently drops to allow differentiation signals to initiate. In support of our working hypothesis, the increase of Oct4 is always accompanied by Rassf1 decrease (4- to 8/16-cell stage), whereas Oct4 decrease is accompanied by Rassf1 increase (8/16-cell stage to late blastocyst). Moreover, the minimum expression level of Rassf1a temporally coincides with the maximum expression levels of Oct4 (8/16-cell stage) (Figure 4.26). A model highlighting the conclusions deriving from this study is provided in Figure 4.26.

With this model we also attempt to shed light on a poorly understood area of development. Nishioka et al. (2009) highlighted for the first time the crucial role of Yap1 in fine tuning the formation of trophectoderm (TE) versus inner cell mass (ICM) in the mouse embryo. TE, which surrounds the ICM, gives rise to the fetus and other extraembryonic tissues. It is, therefore, a differentiating structure. In contrast, the inside cells (ICM) comprise the pluripotent compartment and express stem cell factors at high levels. It was shown that beyond the 30-cell stage, nuclear localisation of Yap1 occurred only in the outside cells of the embryo, where it determined TE formation via Tead4, which regulated trophoblast gene transcription. On the other hand, Hippo pathway-dependent inactivation of Yap1, stimulated by increased cell contact, resulted in Yap1 retention to the cytoplasm of inside cells, thereby limiting the transcriptional activity of Tead4.

In accordance with these observations, we demonstrated nuclear localisation of Yap1 during early embryonic stages (Supp. Figure 7.14), when Rassf1 expression is low (Figure 4.26). This, according to our model allows Yap1-Tead2-β-catenin-mediated *Oct4* transcription, which causes upregulation of the other core stem cell markers as well (Nanog, Sox2) (Masui, Nakatake et al. 2007). This is facilitated by Lats, which phosphorylates Yap1 on the equivalent site of S109 in mouse (S94). It has been widely accepted by Nishioka et al. (2009) and others (Hong, Hwang et al. 2005, Dupont, Morsut et al. 2011) that localisation and activity of Yap1 are directed by the mechanical environment. Increased mechanical pressure leads to Yap1 sequestration from the nucleus to the cytoplasm. Therefore, later in development, in outside cells of the embryo (TE) which are free of mechanical pressure, we suggest that differentiation is promoted via nuclear Yap1-p73 complexes, which are formed upon naturally increasing Rassf1 expression (Figure 4.26). This is driven by Lats-dependent phosphorylation of Yap1 on the equivalent site of S127 in mouse (S112).

The increased mechanical pressure, however, to which cells of the ICM are exposed results in Yap1 relocation to the cytoplasm, where despite the increasing expression of Rassf1a, it can no longer be implicated in differentiation-related transcriptional activity. As a result, stem cell markers continue to be expressed in the ICM (Figure 4.26). Stem cells, however, deriving from the ICM, due to the absence of these mechanical signals, display nuclear Yap1, which in response to Rassf1a signalling modifies its transcriptional activity accordingly. This is likely a complementary mechanism to the one described before, especially as it can provide a potential

explanation for the difficulty Nishioka et al. (2009) encountered in explaining the dispensable role of Tead4 during differentiation.

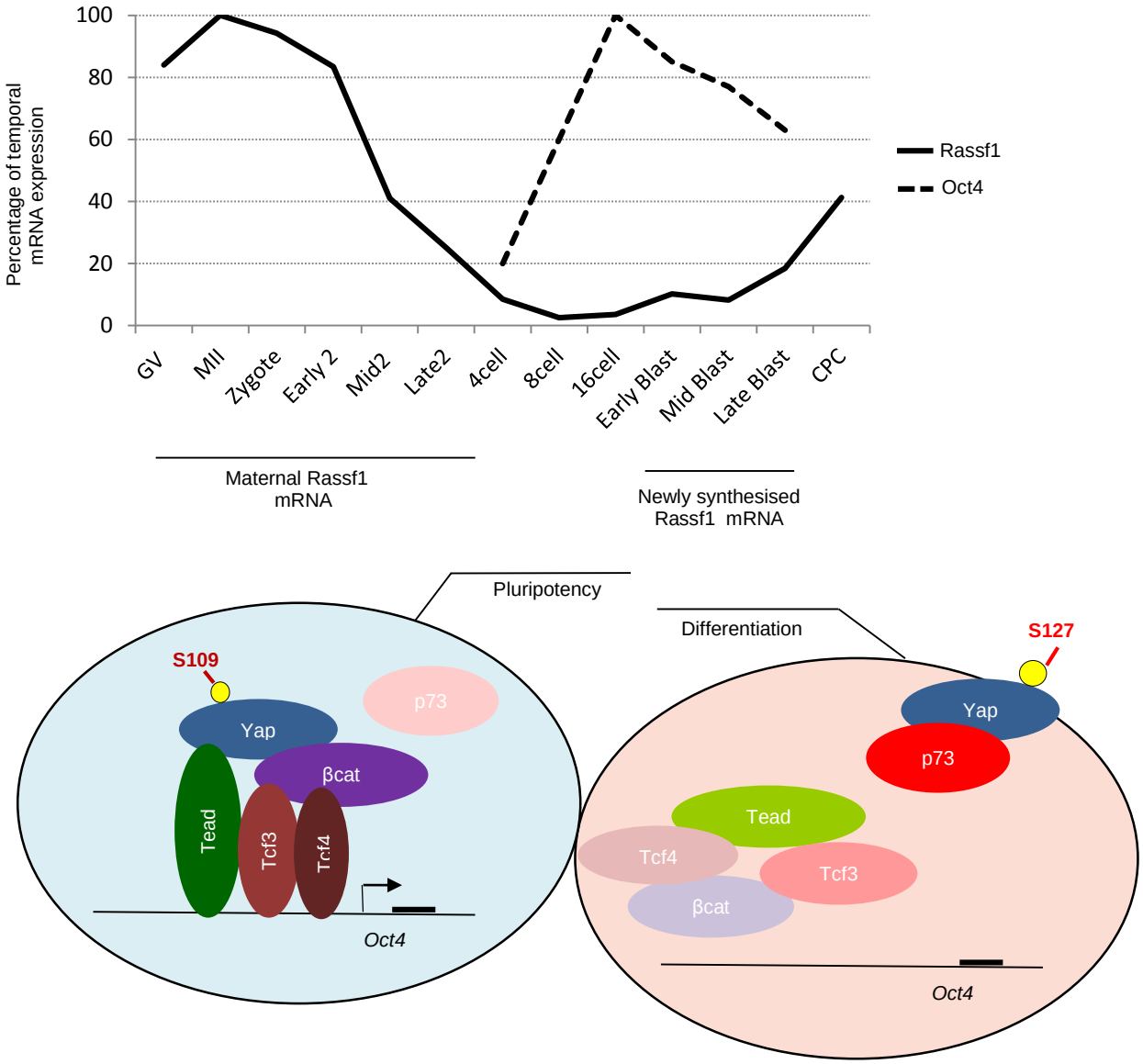


Figure 4.26. Model depicting the proposed role of Rassf1a as a regulator of pluripotency via Yap1-Tead2-β-cat-mediated control of *Oct4*. During embryogenesis, maternal Rassf1a mRNA reaches its minimum at the 8/16-cell stage, resulting in nuclear Yap1-Tead2-β-cat complexes being recruited to the *Oct4* promoter, driving its transcription to the maximum (Wang et al., 2004). New Rassf1a mRNA is subsequently synthesised to activate differentiation programmes, possibly through Yap1-p73, a process which is accompanied by decrease in Oct4 levels due to the limited Yap1-Tead2-β-cat complex formation. Yap1 differential phosphorylation pattern in response to Rassf1a signalling is the driving force of the complex formations. Similarly to the embryo, ESCs progress from pluripotency to differentiation utilising this mechanism.

As explained in the beginning of this chapter, one of the aims of investigating RASSF1A signalling in stem cell biology was to identify the normal cellular RASSF1A functions, as this would potentially highlight the significant biological processes contributing to tumourigenesis. Having developed a mechanism of action for RASSF1A-mediated regulation of pluripotency *in vitro* and *in vivo*, in combination with the data in Chapter 3 elucidating the tumour suppressive function of RASSF1A, we felt it would be highly intriguing to test whether Rassf1a loss could be a link between pluripotency and tumourigenesis.

Chapter 5

RASSF1A loss contributes to cancer stem cell generation through YAP/TAZ

5.1 Introduction

In the previous chapters, we developed a model for RASSF1A signalling in tumour suppression and stem cell fate determination. RASSF1A loss allows YAP1-TEAD1 and Yap1-Tead2-β-catenin complexes to lead oncogenic proliferation and ESC self-renewal respectively. On the other hand, RASSF1A activates apoptotic and differentiation pathways by employing YAP1-p73 complexes. The data described so far demonstrated that YAP1 is a pivotal effector of RASSF1A signalling.

The YAP paralog, TAZ, has been charged with equally important roles in cancer and development. In cancer, besides its role as an effector of the tumour suppressive Hippo pathway (Lei, Zhang et al. 2008), TAZ has been identified as a downstream target of Wnt signalling (Azzolin, Zanconato et al. 2012, Azzolin, Panciera et al. 2014), conferring cancer stem cell traits and promoting invasion and metastasis in a variety of human cancers (Chan, Lim et al. 2008, Bhat, Salazar et al. 2011, Cordenonsi, Zanconato et al. 2011, Zhou, Hao et al. 2011, Bartucci, Dattilo et al. 2014). In development, it has been linked with maintenance of stem cell pluripotency, mostly by promoting the transcription of “stemness” genes (Hong, Hwang et al. 2005, Varelas, Sakuma et al. 2008, Qin, Blaschke et al. 2012). The structural similarities between TAZ and YAP, together with the fact that TAZ interacts with TEAD factors (Mahoney, Hong et al. 2005, Zhang, Liu et al. 2009) and β-catenin

(Imajo, Miyatake et al. 2012) to accelerate cell growth, led us to investigate TAZ response to RASSF1A signalling.

Similarly to ESCs, cancer cells may proliferate indefinitely. Many reports in the literature have linked aberrant embryonic gene expression e.g. OCT4, NANOG and SOX2 with abnormal tissue growth and tumourigenesis (Monk and Holding 2001, Hochedlinger, Yamada et al. 2005, Chen, Shi et al. 2008, Viswanathan, Powers et al. 2009, Kumar, Liu et al. 2012, Leis, Eguiara et al. 2012). Tumour de-differentiation is indicative of rapid oncogenic progression and resistance to treatment, which accounts for poor prognosis (Gabbert, Wagner et al. 1985, Ben-Porath, Thomson et al. 2008). RASSF1A has been found to be implicated in this process, as transplantation of RASSF1A-methylated mesenchymal stem cells (MSCs) into mice resulted in increased tumourigenesis, accompanied by enhanced stem cell marker expression and resistance to treatment (Teng, Hou et al. 2011). The high incidence of RASSF1A promoter methylation in tumours, which suggests it is a prognostic biomarker (Kawai, Sakano et al. 2010, Buhmeida, Merdad et al. 2011, Wang, Wang et al. 2011, Xu, Shetty et al. 2012), in combination with the data described so far, urged us to explore the potential role of RASSF1A in tumour de-differentiation.

The RASSF1 gene also encodes a shorter isoform, RASSF1C. Although little is known about RASSF1C, it appears to play an opposite role to RASSF1A in cancer, as it has been found to promote proliferation and motility in breast and lung cancers (Vos, Ellis et al. 2000, Amaar, Minera et al. 2006, Reeves, Baldwin et al. 2010). Intrigued by the diametrically opposed functions of the two proteins, we wished to explore RASSF1C activity in cancer cells

with regards to YAP/TAZ regulation and the promotion of a “cancer stem cell” phenotype.

5.2 RASSF1A stabilises TAZ-p73 transcriptional complexes

Previous work has shown that Yap-p73 binding is mediated through the WW YAP1 domain and the PPxY p73 motif (Strano, Munarriz et al. 2001). Given that YAP1 and its paralog, TAZ, are 46% identical in amino acid sequence and TAZ contains WW binding domains (Webb, Upadhyay et al. 2011), we questioned whether p73 could also interact with TAZ in the presence of RASSF1A.

For this purpose, we used human osteosarcoma U2OS cells inducibly expressing a FLAG-RASSF1A construct. Cells were treated with 0.5 μg/mL of doxycycline for 24 h and subsequent TAZ co-immunoprecipitations (Figure 5.1) revealed reduced binding of both TEAD1 and β-catenin to TAZ and enhanced TAZ-p73 complex formation (Figure 5.1), indicating that TAZ was mimicking the YAP1 response to RASSF1A signalling (Figure 3.1; YAP1-p73 versus YAP1-TEAD1).

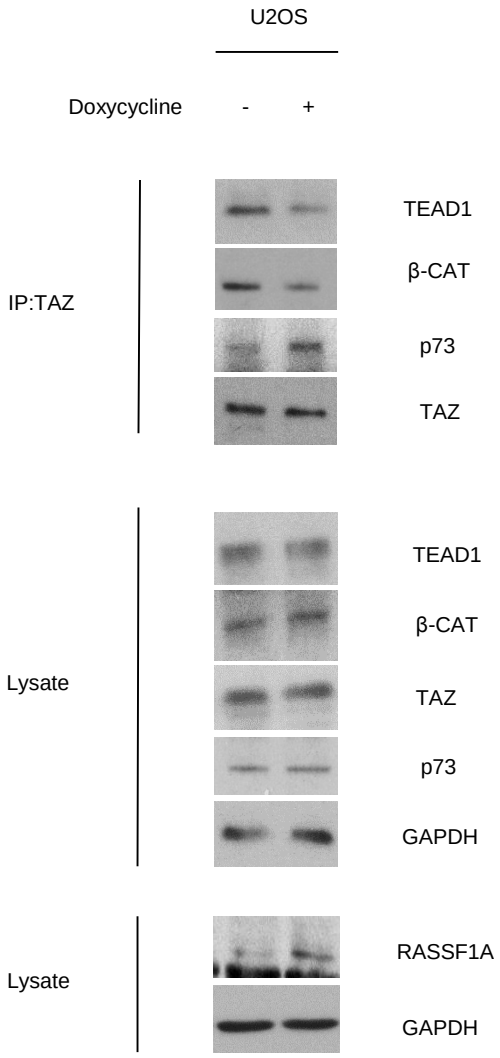


Figure 5.1. RASSF1A overexpression promotes TAZ-p73 complexes at the expense of TAZ-TEAD1 and TAZ-β-CAT. Human osteosarcoma U2OS cells Tet-On inducibly expressing FLAG-RASSF1A were treated with doxycycline at a concentration of 0.5 μg/mL for 24 h. TAZ immunoprecipitates, as well as cell lysates, were western blotted with the indicated antibodies (right).

5.3 Loss of RASSF1A destabilises TAZ-p73 complexes to favour TAZ-dependent oncogenic complexes

To confirm the above finding, we assessed TAZ transcription factor selection in response to RASSF1A loss. U2OS cells were transfected either

with non-targeting siRNA (siNT) or RASSF1A-targeting siRNA (siRASSF1A) and 48 h post transfection TAZ co-immunoprecipitations were performed (Figure 5.2A). Interestingly, in the absence of RASSF1A, TAZ-TEAD1 and TAZ-β-catenin complexes were promoted, whereas TAZ-p73 complex formation was limited (Figure 5.2A). Silencing of RASSF1A in HeLa cells influenced TAZ in a similar manner (Figure 5.2B).

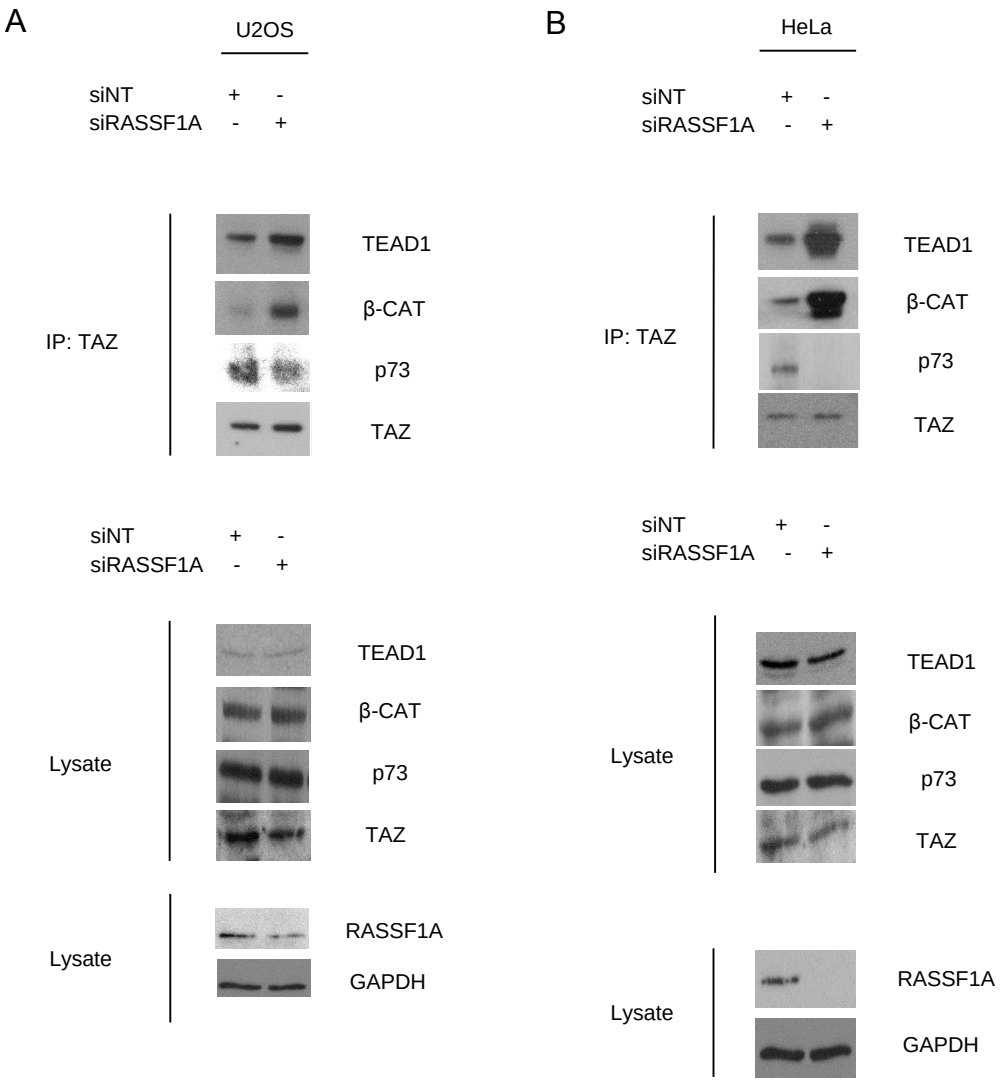


Figure 5.2. RASSF1A loss increases TAZ-TEAD1 and TAZ-β-CAT levels at the expense of TAZ-p73. A. U2OS cells were transfected with either non-targeting siRNA (siNT) or siRNA against RASSF1A (siRASSF1A). TAZ immunoprecipitates and cell lysates were western blotted with the indicated antibodies (right). **B.** HeLa cells were tranfected with either non-targeting siRNA (siNT) or siRNA against RASSF1A (siRASSF1A). TAZ immunoprecipitates were western blotted with the indicated antibodies (right).

5.4 RASSF1A loss causes nuclear accumulation of β-catenin and TAZ

TAZ-TEAD1 complexes are strictly nuclear, as TEAD transcription factors are encountered only in the nucleus (Vassilev, Kaneko et al. 2001). Additionally, it has been established that TAZ-TEAD1 complexes promote cellular growth (Mahoney, Hong et al. 2005, Zhang, Liu et al. 2009). Unlike TEAD factors, however, β-catenin shuttles between the cytoplasmic and nuclear compartment. β-catenin has been identified as an essential binding partner of various cadherins, such as E-cadherin, in adherens junctions, contributing to the establishment of cell-cell contacts (Peifer, McCrea et al. 1992, Hulsken, Birchmeier et al. 1994, Zhu and Watt 1999). Recently, an emerging role for β-catenin in microtubules and active transport was also described (Sugioka, Mizumoto et al. 2011). Moreover, β-catenin association with APC in the cytoplasm is followed by its proteasome-dependent degradation due to the activation of the "β-catenin destruction complex" (Rubinfeld, Souza et al. 1993, Su, Vogelstein et al. 1993, Aberle, Bauer et al. 1997, Li, Ng et al. 2012). TAZ also shuttles between the nuclear and cytoplasmic compartments, as in addition to its involvement in gene transcription, it is found to interact with cytoplasmic proteins, such as 14-3-3 (Lei, Zhang et al. 2008, Liu, Zha et al. 2010), respond to mechanical alterations in cell shape (Dupont, Morsut et al. 2011), hold junctional roles (Remue, Meerschaert et al. 2010, Chan, Lim et al. 2011, Zhao, Li et al. 2011) and even bind to Disheveled proteins to promote the assembly of the "β-catenin destruction complex" in the cytoplasm (Varelas, Miller et al. 2010, Azzolin, Panciera et al. 2014). Thus, we sought to investigate whether the

TAZ-β-catenin complexes promoted in the absence of RASSF1A were charged with cytoplasmic or nuclear functions.

In U2OS cells, depletion of RASSF1A promoted nuclear accumulation of β-catenin, without variation in cytoplasmic levels (Figure 5.3A). Similar results were observed in HeLa cells (Figure 5.3B). TAZ also exhibited increased nuclear localisation upon depletion of RASSF1A in U2OS (Figure 5.4A) and HeLa cells (Figure 5.4B) compared to Control (siNT). Together, these data imply that loss of RASSF1A increases TAZ-β-catenin transcriptional complexes. Recent articles have demonstrated that β-catenin–related cancers require transcriptionally active YAP/TAZ-β-catenin complexes to promote survival and tumourigenesis (Imajo, Miyatake et al. 2012, Rosenbluh, Nijhawan et al. 2012). Moreover, as mentioned above, the increase of nuclear β-catenin and TAZ appeared to occur without depletion of the cytoplasmic pools available for junctional and other activities (Figures 5.3 and 5.4).

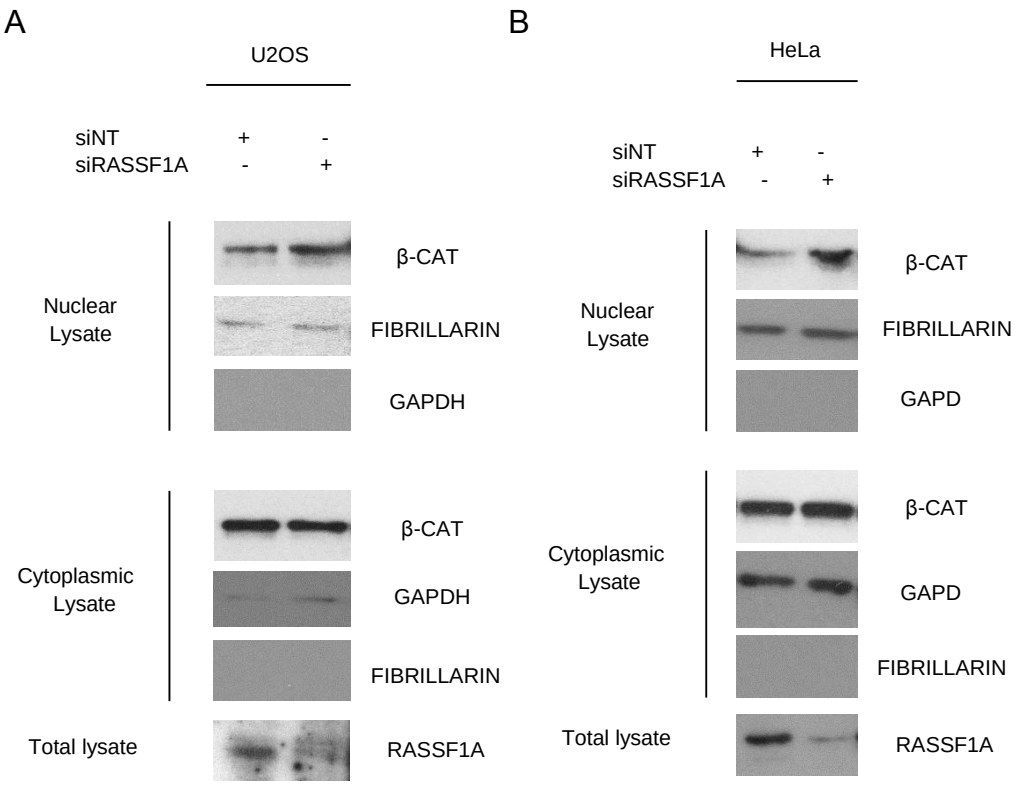


Figure 5.3. RASSF1A loss causes β-catenin nuclear accumulation. A. U2OS cells were transfected with either non-targeting (siNT) or RASSF1A-targeting (siRASSF1A) siRNA and 48 h later the cells were harvested and fractionated to acquire the nuclear and cytoplasmic lysates. Western blot of both lysates (nuclear and cytoplasmic) and totals probed with the stated antibodies (right). **B.** Same as A with HeLa cells.

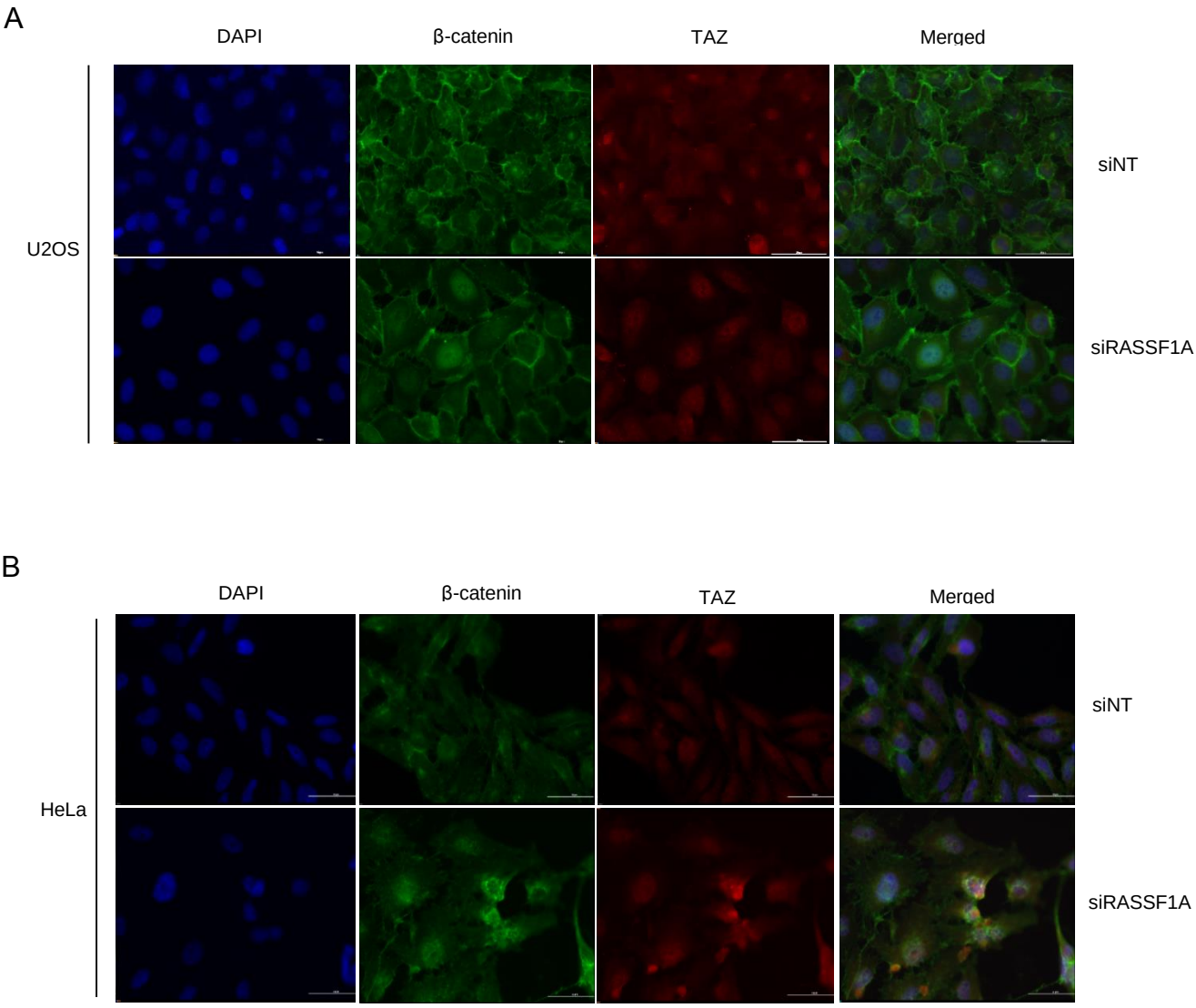


Figure 5.4. Loss of RASSF1A results in increased nuclear accumulation of both TAZ and β-catenin. A. U2OS cells were transfected with either non-targeting (siNT) or RASSF1A-targeting (siRASSF1A) siRNA. **A.** Immunofluorescence of β-cat and TAZ protein levels in the respective conditions 48 h post-transfection. **B.** Same as A, for HeLa cells.

5.5 RASSF1A regulates the downstream effector of Notch signalling, HES1

To uncover additional substrates that may be under RASSF1A tumour suppressive regulation, we performed an *in vitro* screen for RASSF1A binding partners in U2OS cells. The cells were transfected with a FLAG-RASSF1A construct and FLAG co-immunoprecipitations were carried out. The immunoprecipitates were subsequently subjected to mass spectrometry (MS) analysis to unravel the RASSF1A interactome (Supplementary Table 7.2).

One of the top hits of our screen was the stem cell differentiation repressor HES1, an established downstream target of the Notch signalling pathway (Artavanis-Tsakonas, Rand et al. 1999, Ohtsuka, Ishibashi et al. 1999, Kageyama, Ohtsuka et al. 2007). HES1 is expressed in an oscillatory fashion in various cell lines, including ESCs (Hirata, Yoshiura et al. 2002, Kobayashi, Mizuno et al. 2009) and is a member of the basic helix-loop-helix (bHLH) transcriptional repressors that regulate growth and differentiation during embryogenesis (reviewed by Ranganathan, Weaver et al. 2011). HES1 has been also linked with increased tumourigenesis and self-renewal of cancer stem cells (Camargo, Gokhale et al. 2007, Gao, Zhang et al. 2014). Interestingly, HES1 is stabilised by YAP1 during expansion of undifferentiated intestinal progenitor cells and YAP1 has emerged as an upstream regulator of Notch signalling (Camargo, Gokhale et al. 2007, Yimlamai, Christodoulou et al. 2014).

We inducibly overexpressed RASSF1A in U2OS Tet-On cells and western blotting of the nuclear and cytoplasmic fractions revealed that RASSF1A

overexpression was sufficient to reduce HES1 nuclear accumulation, whereas cytoplasmic HES1 levels remained unaffected (Figure 5.5). Based on the above reports, we reasoned that RASSF1A-mediated restriction of HES1 nuclear levels may inhibit dedifferentiation processes crucial for the progression of oncogenesis (Gabbert, Wagner et al. 1985, Ben-Porath, Thomson et al. 2008).

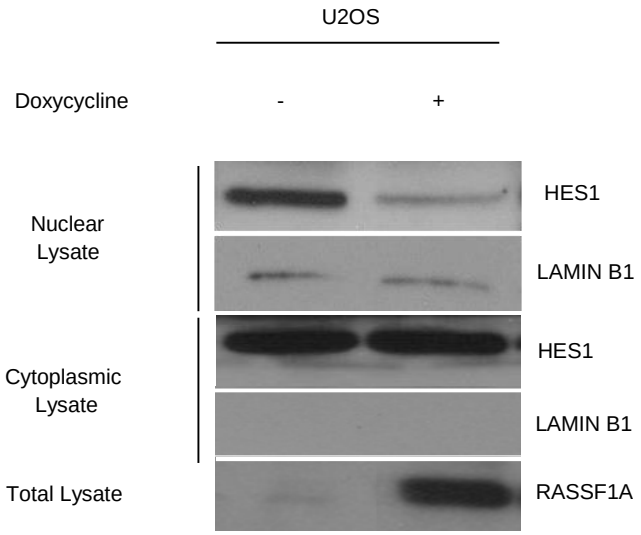


Figure 5.5. RASSF1A overexpression decreases endogenous HES1 levels. U2OS cells Tet-On inducibly expressing FLAG-RASSF1A were treated with doxycycline at a concentration of 0.5 µg/mL for 24 h. The cells were fractionated in order to acquire the nuclear and cytoplasmic extracts, which were subsequently western blotted and probed with the mentioned antibodies.

5.6 RASSF1A loss increases stem cell markers in cancer cells

Numerous reports have suggested that tumours often display elevated expression of “stemness” genes. These tumours account for poor clinical outcome due to increased resistance to therapy (Gabbert, Wagner et al. 1985, Hochedlinger, Yamada et al. 2005, Ben-Porath, Thomson et al. 2008, Chen, Shi et al. 2008, Viswanathan, Powers et al. 2009, Kumar, Liu et al. 2012, Leis, Eguiara et al. 2012). Our data showed that RASSF1A limited the nuclear activity of such a “stemness” factor (HES1; Figure 5.5), therefore we attempted to determine whether disruption of RASSF1A signalling, which is a common event in tumourigenesis, plays a role in the generation of a stem cell-like phenotype in cancer.

Thus, we downregulated RASSF1A via RNAi in U2OS and HeLa cells and conducted quantitative PCR for stem cell markers. siRASSF1A-transfected cells displayed significantly higher levels of HES1 mRNA compared to Control (siNT) (Figure 5.6A). This, along with our previous data (Figure 5.5), strongly indicated that RASSF1A negatively regulates the tumourigenic activity of the Notch effector HES1. Interestingly, silencing of RASSF1A also led to a significant increase in NANOG mRNA levels in both cell lines (Figure 5.6B).

We next sought to determine if other stem cell markers, in particular those of the core stem cell factor network (OCT4, SOX2) exhibited a similar regulation pattern in response to RASSF1A loss. Western blotting of U2OS cell lysates from the two conditions (siRASSF1A and siNT) revealed that in the absence of RASSF1A, NANOG, OCT4 and HES1 were substantially increased (Figure 5.7A). This observation was also verified in HeLa cells

(Figure 5.7B). In addition, immunofluorescence showed a clear upregulation in NANOG and SOX2 levels in siRASSF1A-transfected HeLa cells compared to siNT controls (Figure 5.7C).

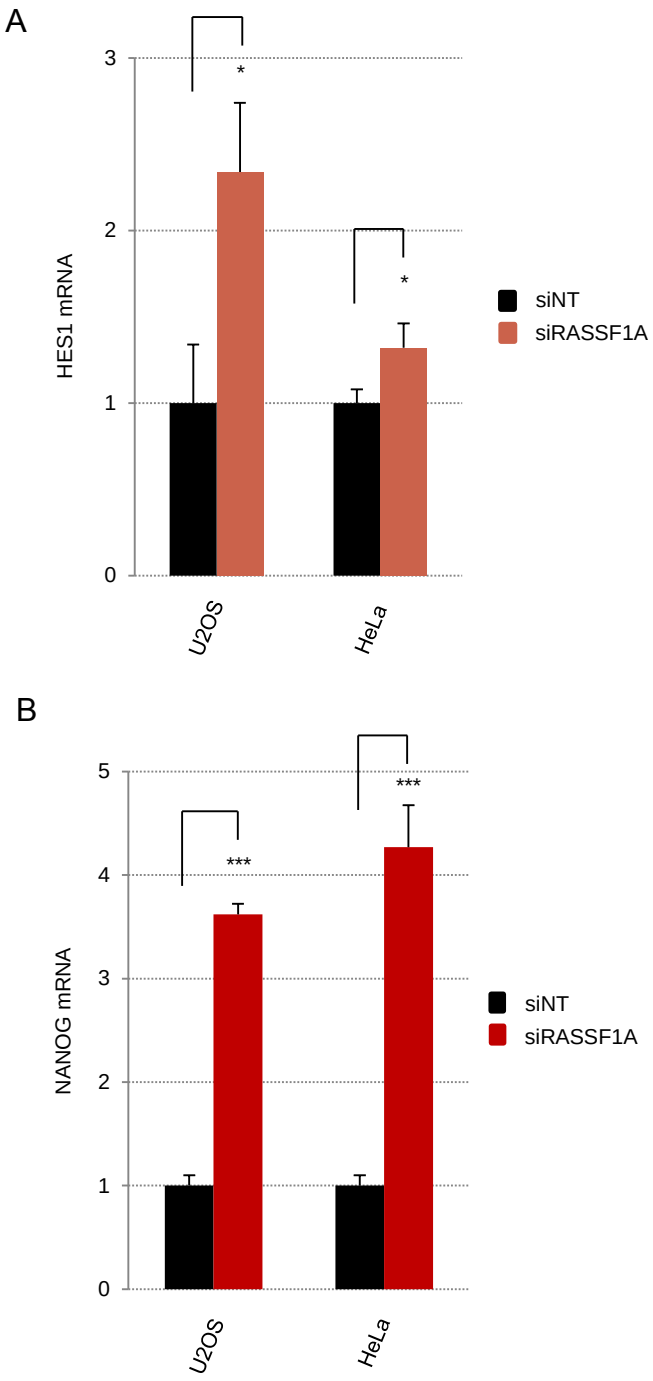


Figure 5.6. RASSF1A silencing increases endogenous HES1 and NANOG mRNA levels in cancer cells. U2OS and HeLa cells were transfected with either non-targeting (siNT) or RASSF1A-targeting (siRASSF1A) siRNA. **A.** qRT-PCR of HES1 mRNA levels from U2OS and HeLa cells 48 h post-transfection. P = 0.011 for siNT versus siRASSF1A in U2OS; P = 0.028 for siNT versus siRASSF1A in HeLa (Student's t test). **B.** qRT-PCR of NANOG mRNA levels in U2OS and HeLa cells 48 h post transfection. P < 0.001 for siNT versus siRASSF1A for both U2OS and HeLa cells (Student's t test).

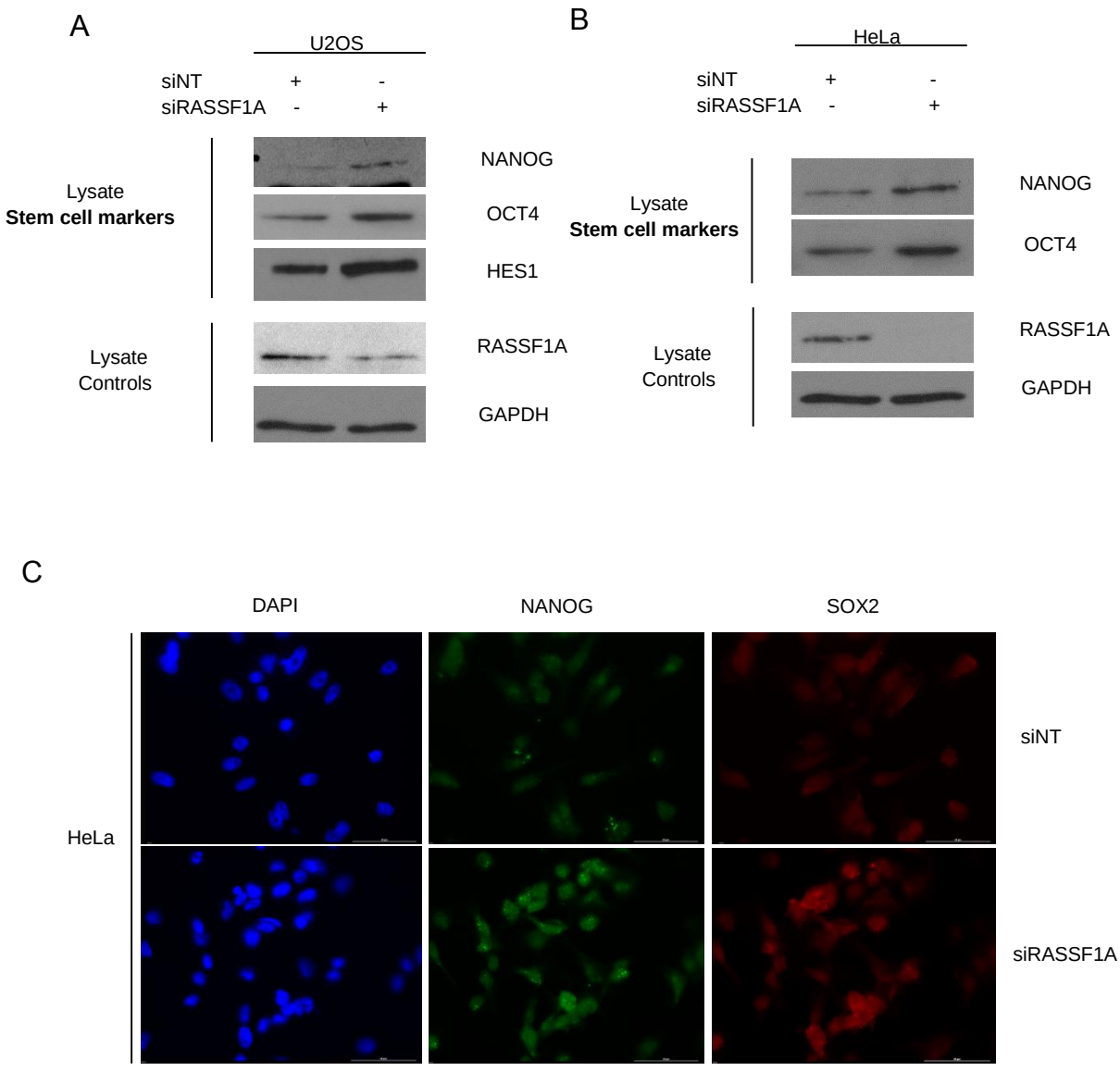


Figure 5.7. RASSF1A silencing upregulates the core stem cell marker protein levels in cancer cells. U2OS and HeLa cells were transfected with either non-targeting (siNT) or RASSF1A-targeting (siRASSF1A) siRNA. **A.** Western blot of U2OS cell lysates probed with the stated antibodies against stem cell marker and control proteins. **B.** Western blot of HeLa cell lysates probed with the stated antibodies. **C.** Immunofluorescence in HeLa cells for NANOG and SOX2 protein levels in response to siNT and siRASSF1A.

5.7 RASSF1A limits stem cell marker expression in cancer cells

Since RASSF1A loss was found to cause an increase in stem cell marker expression in cancer cells (Figures 5.6 and 5.7), we speculated that elevated RASSF1A expression should reverse the phenotype. Therefore, we inducibly overexpressed RASSF1A in U2OS Tet-On cells using increasing amounts of doxycycline (0-1 µg/mL). Western blotting of the cell lysates demonstrated that incremental expression of RASSF1A was indeed sufficient to restrict endogenous NANOG protein levels accordingly (Figure 5.8A).

To confirm that, we used the MDA-MB-231 breast cancer cell line, in which RASSF1A expression is epigenetically lost. MDA-MB-231 cells were transfected with either empty vector (pCDNA) or FLAG-RASSF1A and subsequent quantitative PCR showed a significant reduction of endogenous NANOG transcript levels upon RASSF1A overexpression (Figure 5.8B). This was in line with our observation in U2OS cells (Figure 5.8A). Notably, re-introduction of RASSF1A limited stem cell marker levels not only in cells in which RASSF1A expression has been lost (MDA-MB-231), but also in cells retaining a minimum expression level of RASSF1A, such as U2OS cells.

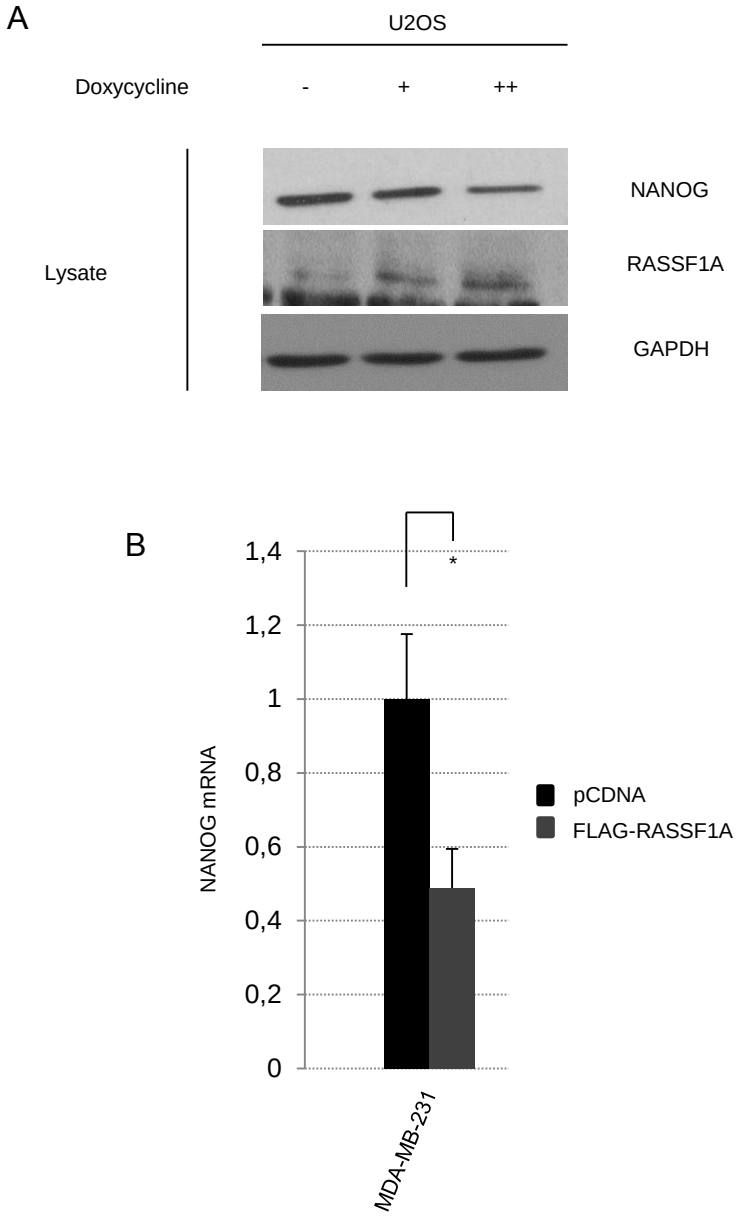


Figure 5.8. RASSF1A overexpression restricts stem cell marker expression in cancer cells. A. Increasing amounts of doxycycline (0-0.5-1 µg/mL) were used for 24 h to stimulate RASSF1A expression in Tet-On U2OS cells indubibly expressing FLAG-tagged RASSF1A. Western blotting of the cell lysates with the indicated antibodies. **B.** Breast cancer MDA-MB-231 (invasive ductal carcinoma) cells were transfected with either empty (pCDNA) or FLAG-RASSF1A vector. qRT-PCR of NANOG mRNA 48 h post-transfection. P = 0.014 for pCDNA versus FLAG-RASSF1A (Student's t test).

5.8 The RASSF1C isoform of RASSF1A has opposite effects on cancer stem cell generation

Promoter hypermethylation of the tumour suppressor RASSF1A has been identified as one of the most frequent epigenetic events across a wide spectrum of human cancers such as lung, breast, kidney, gastric, bladder, neuroblastoma, medulloblastoma and gliomas (Agathanggelou, Cooper et al. 2005). Contrary to RASSF1A, the expression of another isoform of the RASSF1 gene, RASSF1C, is not affected by promoter methylation or other epigenetic modifications, and hence, this isoform is present in the majority of cancers. Furthermore, due to its involvement in cellular proliferation, migration, β-catenin stabilisation and inhibition of apoptosis, RASSF1C appears to function more like an oncogene (Dammann, Li et al. 2000, Lerman and Minna 2000, Vos, Ellis et al. 2000, Dammann, Takahashi et al. 2001, Dreijerink, Braga et al. 2001, Liu, Yoon et al. 2002, Tommasi, Dammann et al. 2005, van der Weyden, Tachibana et al. 2005, Amaar, Minera et al. 2006, Estrabaud, Lassot et al. 2007, Reeves, Baldwin et al. 2010). The opposite functions exhibited by the two isoforms and recent reports providing a role for RASSF1C in stem cell self-renewal (Reeves, Baldwin et al. 2012, Reeves, Firek et al. 2014), intrigued us to investigate the effect of RASSF1C signalling on cancer stem cell generation.

To exclude the possibility of RASSF1A affecting RASSF1C activity, we used MDA-MB-231 breast cancer cells, which as mentioned above have lost RASSF1A expression. Cells were transfected either with a pCDNA empty vector or a FLAG-RASSF1C construct and subsequent immunofluorescence demonstrated clearly upregulated NANOG levels upon RASSF1C

overexpression (Figure 5.9). Controls for the expression of the FLAG-RASSF1C construct versus pCDNA are provided in Figure 5.10 (lysates).

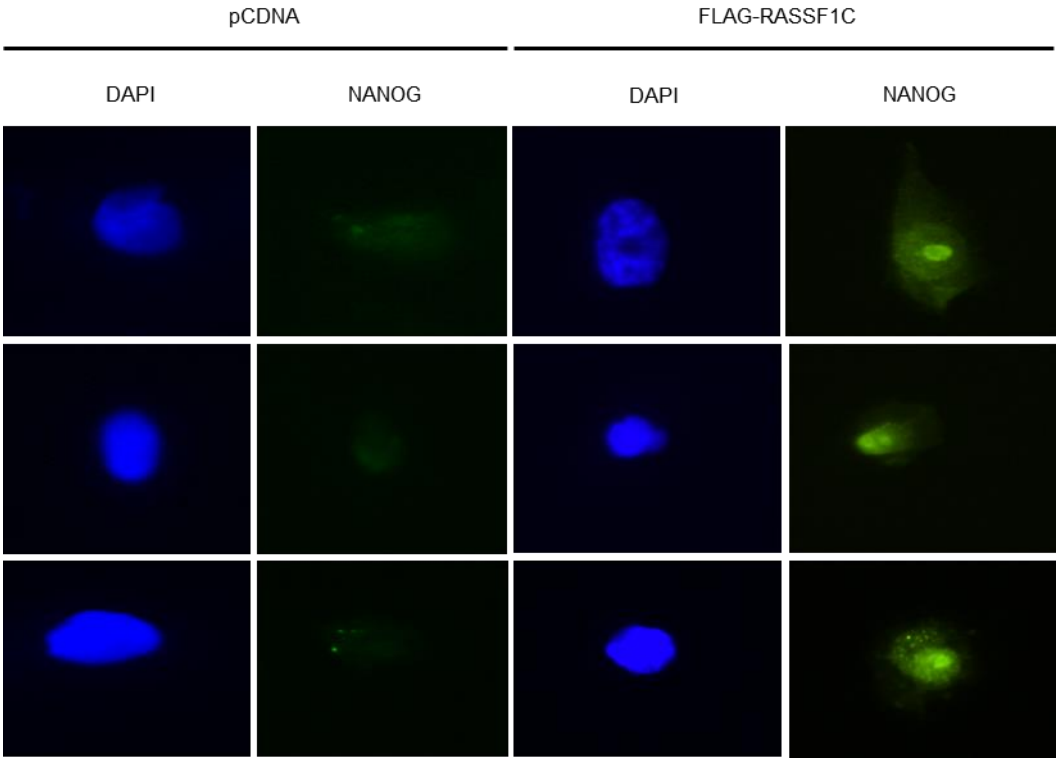


Figure 5.9. RASSF1C overexpression increases stem cell markers in cancer cells. MDA-MB-231 cells transfected either with empty (pCDNA) or FLAG-RASSF1C-expressing vector. Immunofluorescence of NANOG protein levels 48 h post-transfection.

We, next, aimed to assess the impact of RASSF1C signalling on TAZ transcriptional complexes. TAZ co-immmunoprecipitations from the same pool of cells as in Figure 5.9 showed that RASSF1C stablilised TAZ-TEAD1 complexes, whereas TAZ-p73 interaction was substantially limited (Figure 5.10). This observation was in line with the data stemming from RASSF1A loss in cancer cells (Figures 3.1, 3.3 and 5.2), implying that RASSF1C activity may mimic RASSF1A loss. This can also be inferred from the activation of EMT markers, such as c-MYC, displayed both upon RASSF1C

overexpression (Figure 5.10) and RASSF1A loss (Thaler, Schmidt et al. 2012). Surprisingly, however, RASSF1C did not appear to affect the association of TAZ with β-catenin (Figure 5.10), despite the clear stabilisation of the complex observed in the absence of RASSF1A (Figure 5.2).

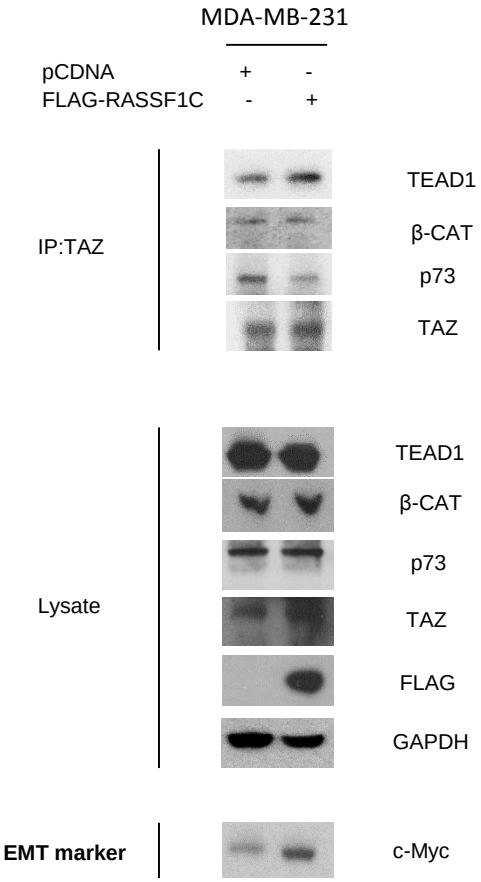


Figure 5.10. RASSF1C promotes TAZ-TEAD1 complexes at the expense of TAZ-p73 in MDA-MB-231 cells. MDA-MB-231 cells were transfected with either empty (pCDNA) or FLAG-RASSF1C expressing vector. TAZ immunoprecipitates and cell lysates were western blotted with the mentioned antibodies 48 h post-transfection.

5.9 RASSF1C functions in a paracrine manner

Del Re et al. (2010) suggested that RASSF1A silencing was accompanied by both cell-autonomous and autocrine/paracrine effects. More specifically, they demonstrated that lack of RASSF1A signalling in cardiac fibroblasts led to the secretion of TNF-α, which stimulated the growth of cardiomyocytes in a paracrine fashion. RASSF1A signalling, therefore, was considered to be a key regulator of cardiac growth. Based on the results described above, we set out to investigate whether the observed paracrine effects were also RASSF1C-mediated.

We, therefore, made use of pCDNA and FLAG-RASSF1C-transfected MDA-MB-231 cells used in Figures 5.9 and 5.10 and 48 h post transfection the cell growth medium from each condition was removed, centrifuged, carefully filtered and transferred onto cells belonging to the same or different cell lines. 24 h later the recipient cells were lysed and a quantitative PCR was performed to assess the expression levels of stem cell markers. Our data demonstrated that U2OS (Figure 5.11A), HeLa (Figure 5.11B), MDA-MB-231 (Figure 5.11C) and MCF7 (Figure 5.11D) cells which had received the medium of FLAG-RASSF1C-transfected MDA-MB-231 cells expressed OCT4 and/or NANOG at significantly higher levels in comparison to controls. Hence, we reasoned that RASSF1C signalling, was indeed followed by paracrine effects towards the generation of cancer stem cells.

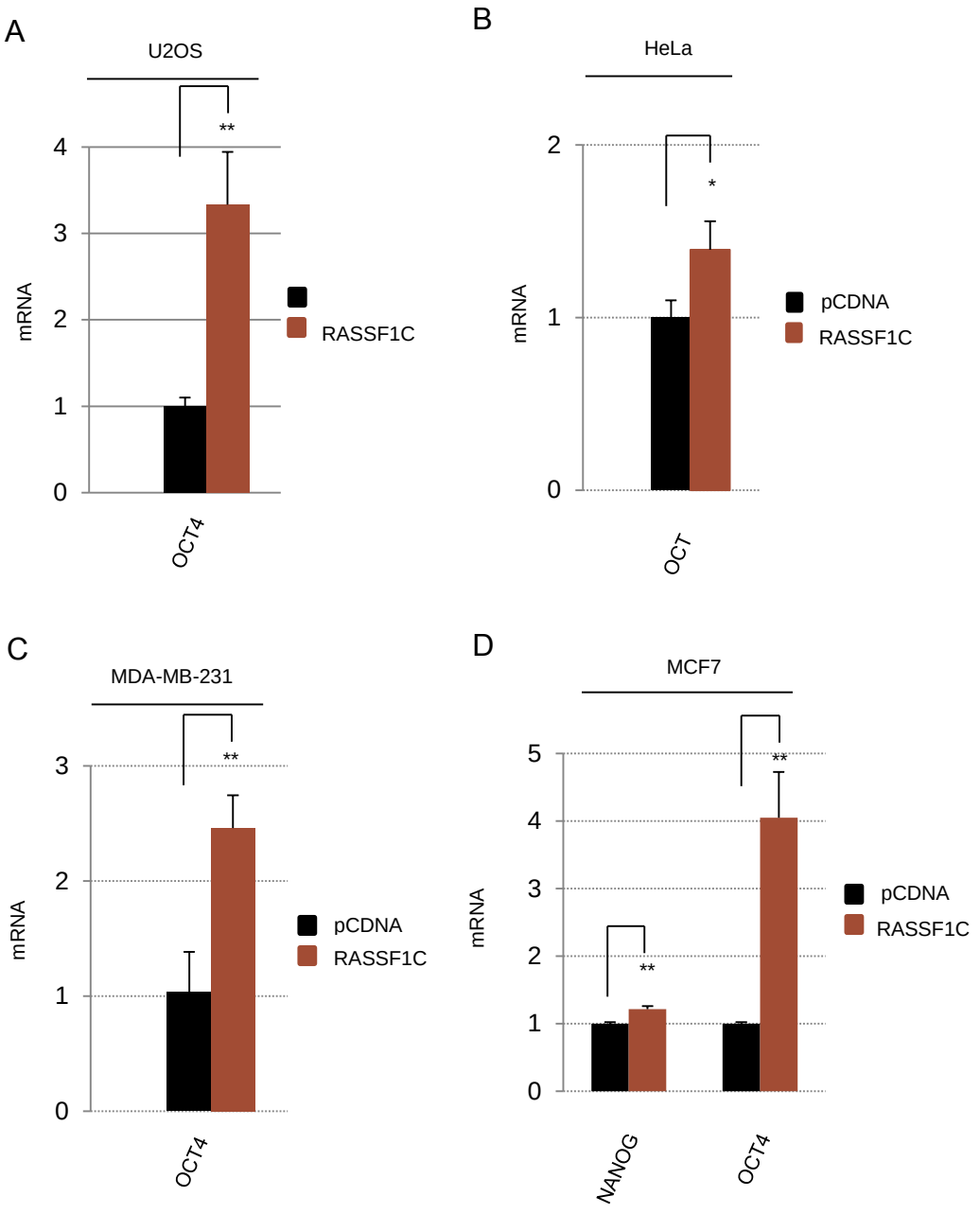


Figure 5.11. RASSF1C expression in MDA-MB-231 cells is accompanied by paracrine effects. MDA-MB-231 cells were either transfected with empty (pCDNA) or FLAG-RASSF1C (RASSF1C) expressing vector. 48 h later the medium into which the cells from both conditions (pCDNA and FLAG-RASSF1C) were growing was centrifuged and the supernatant was syringe-filtered to discard leftover cells and debris and transferred onto U2OS, HeLa, MDA-MB-231 and MCF7 cells, whose medium had been removed. 24 h later the recipient cells were harvested and qRT-PCR was performed for differences in stem cell marker mRNA levels between the two conditions in each cell line. **A.** qRT-PCR for OCT4 mRNA levels in U2OS cells. P = 0.003 for pCDNA against RASSF1C. **B.** Same as A in HeLa cells. P = 0.024 for pCDNA against RASSF1C. **C.** Same as A in MDA-MB-231 cells. P = 0.005 for pCDNA against RASSF1C. **D.** qRT-PCR for NANOG and OCT4 mRNA levels in MCF7 (breast cancer) cells. P = 0.002 for NANOG (pCDNA against RASSF1C); P = 0.0014 for OCT4 (pCDNA against RASSF1C). Statistics were derived using Student's t test.

5.10 Discussion

In this chapter, we explored the TAZ response to RASSF1A signalling and based on our observations (Figures 5.1 and 5.2) we suggest that TAZ and its paralog protein, YAP (Chapter 3), respond similarly, as illustrated by their common transcription factor binding pattern. This implies that YAP1 and TAZ may functionally complement each other, at least in response to RASSF1A signalling, whereas their functions may be separate in other contexts (Morin-Kensicki, Boone et al. 2006, Hossain, Ali et al. 2007, Zhang, Liu et al. 2009).

In Chapter 4, we provided evidence that Rassf1a loss in ESCs results in Yap1, Tead2 and β-catenin coming in a complex together, essential for stimulating Oct4 transcription, which in turn upregulates Nanog and Sox2 expression (Figures 4.18 and 4.21) and destabilises Yap1-p73 differentiation-promoting complexes (Figure 4.17). In this chapter, we demonstrated that in response to the same stimulus (lack of RASSF1A), TAZ also forms stable nuclear complexes with both TEAD1 and β-catenin and displays limited association with p73 (Figures 5.1-5.4), therefore we postulate that YAP/TAZ-dependent gene transcription could duly be responsible for the upregulation of stem cell markers upon RASSF1A loss in cancer cells (Figures 5.5-5.7). Further investigation is required to clarify whether YAP/TAZ-TEAD1 and YAP/TAZ-β-catenin are separate complexes or, like in ESCs, part of the same complex.

One point of note is that in ESCs and iPSCs Tead2 is the only member of the TEA domain family of transcription factors which can mediate proliferation and self-renewal in association with Yap1 (Figures 4.19A and C and Supp

Figure 7.5B). The important role of Tead2 and not Tead1 in this context can be underlined by the fact that Tead2 is the only gene of the family to be expressed in early development (Kaneko, Cullinan et al. 1997). However, this does not apply in cancer cells, where TEAD1 plays a pivotal role. Previous work in the lab has attributed this difference to the observation that in cancer cells YAP1-TEAD1 and YAP1-TEAD2 complexes regulate the transcription of different sets of target genes. Proliferation-controlling genes are transcribed solely by YAP1-TEAD1 complexes (Figures 3.5B, 3.6 and data not shown).

As mentioned before, our data are in keeping with a report demonstrating that combined targeted methylation of *RASSF1A* and *HIC1* plays an important role in the tumourigenic transformation of mesenchymal stem cells (MSCs), leading to elevated expression of stem cell markers, amongst other phenotypes (Teng, Hou et al. 2011). The present study extends this observation by suggesting that RASSF1A loss alone, through YAP/TAZ-dependent transcription, is sufficient to establish a stem-like phenotype in cancer cells.

HES1, the downstream effector of the Notch signalling pathway, has been shown to facilitate SC self-renewal and tumourigenesis, depending on the context (Camargo, Gokhale et al. 2007, Ranganathan, Weaver et al. 2011, Gao, Zhang et al. 2014). HES1 was found to associate with RASSF1A in an *in vitro* screen (Supp Table 7.2), which led us to explore the nature of this interaction. Interestingly, only nuclear HES1 levels appeared to be limited by RASSF1A, whereas the cytoplasmic pool remained unaffected (Figure 5.5). The presence of RNF4, a SUMO-targeted ubiquitin E3 ligase, however, in the RASSF1A interactome (Supp Table 7.2), whose homolog in Drosophila (Dgrn)

is known to mediate proteasome-dependent degradation of HES family members, provides a potential explanation for HES1 decrease (Barry, Abed et al. 2011). Moreover, the cytoplasmic pool remained unaffected likely because RNF4 is located exclusively in the nucleus of cells in which HES proteins are active (Barry, Abed et al. 2011). On the contrary, in the absence of RASSF1A, HES1 protein and mRNA levels increase (Figures 5.6A and 5.7), which correlates with the increased core stem cell marker levels (NANOG, OCT4, SOX2). The RASSF1A-dependent regulation of HES1 provided for the first time a link between RASSF1A signalling and the Notch pathway, which holds key roles in both embryogenesis and tumourigenesis, thus establishing an additional connection between RASSF1A loss and cancer stem cell generation.

Despite the frequent methylation of the *RASSF1A* promoter in cancer, the RASSF1C isoform is maintained and is increasingly implicated in tumour progression and metastasis of various cancer types (Vos, Ellis et al. 2000, Amaar, Minera et al. 2006, Reeves, Baldwin et al. 2010). Given the recent involvement of RASSF1C in the regulation of SC self-renewal genes (Reeves, Baldwin et al. 2012, Reeves, Firek et al. 2014), we queried whether RASSF1C was able to contribute to the emergence of cancer stem cell phenotypes. Our work demonstrated that RASSF1C expression in cancer cells lacking endogenous RASSF1A indeed increased stem cell marker expression (Figure 5.9), most likely due to stabilisation of YAP/TAZ-TEAD1 complexes at the expense of YAP/TAZ-p73 (Figure 5.10). Surprisingly, unlike in the absence of RASSF1A, TAZ-β-catenin complexes did not seem to be influenced by RASSF1C overexpression (Figure 5.10). Although YAP/TAZ-

TEAD1 complexes have been shown to be sufficient for driving proliferation in cancer (Zhao, Ye et al. 2008, Chan, Lim et al. 2009) and may, therefore, also be adequate for augmenting stem cell marker expression, further investigation is required to reveal how RASSF1C signals affect downstream targets, including YAP/TAZ transcriptional complexes.

We also tested whether RASSF1C was able to exert its functions in a paracrine fashion. Our data demonstrated that growth medium derived from RASSF1C-expressing cells contained factors which triggered stem cell marker expression in the recipient cells (Figure 5.11), verifying that RASSF1C employs a paracrine mechanism of action, in parallel to its cell-autonomous functions. Taken together, this body of evidence implied that the tumourigenic phenotypes stemming from RASSF1A loss might actually be RASSF1C-driven. RASSF1A stops proliferation and prevents dedifferentiation of cancer cells (Figures 3.1, 5.1, 5.5 and 5.8), implying that it might act to inactivate RASSF1C. Indeed, work by others in the lab has shown that RASSF1A activation inhibits RASSF1C oncogenic activity. However, further research is required in order to fully elucidate the role of RASSF1C in cancer.

The data in this Chapter highlighted the link RASSF1A signalling introduces between pluripotency and tumourigenesis. By shedding light on the key downstream players of RASSF1A signalling, YAP (Chapter 3) and TAZ, and revealing the interplay of RASSF1A with the Notch signalling pathway, we demonstrated that in the absence of RASSF1A, cancer cells acquire stem-like traits via similar mechanisms to those ESCs use to maintain their undifferentiated state.

Chapter 6

Discussion

The data presented in this thesis provide an insight into the role of RASSF1A in tumourigenesis and stem cell pluripotency. Although these biological processes are not inherently linked, we provide evidence that RASSF1A exerts combined regulation of their key characteristics. We show that by acting through a single pathway, the Hippo pathway, RASSF1A functions both as a tumour suppressor and cell fate determinant. This adds to the body of evidence connecting tumourigenesis and embryonic development.

In Chapter 3, we attempted to elucidate the molecular mechanism by which RASSF1A suppresses tumourigenesis by identifying factors synergising with it. One such factor was the YAP1 transcriptional partner RUNX2, whose loss, together with loss of RASSF1A, resulted in increased tumourigenesis through the enhancement of YAP1-TEAD1 complexes at the expense of YAP-p73.

These findings challenged us to investigate the role of RASSF1A in stem cells in Chapter 4, where we showed that Rassf1a may limit reprogramming efficiency and restrict pluripotency by activating differentiation circuits. Rassf1a promotes the formation of Yap1-p73 complexes, allowing the transcription of lineage-specific genes. Upon Rassf1a loss, Yap1-Tead2-β-catenin complexes are required to maintain pluripotency, via *Oct4* transcription.

Subsequently, in Chapter 5, we demonstrated that RASSF1A loss may cause tumourigenesis through upregulation of the core stem cell marker

network in cancer cells. RASSF1A loss deregulates the Hippo pathway by affecting YAP and its paralog, TAZ. Furthermore, cancer stem cell generation was achieved by overexpression of the RASSF1C isoform, a known onco-protein. The schematic in Figure 6.1 summarises the major points covered in Chapters 3,4 and 5 with regards to the RASSF1A regulatory effects in cancer and development.

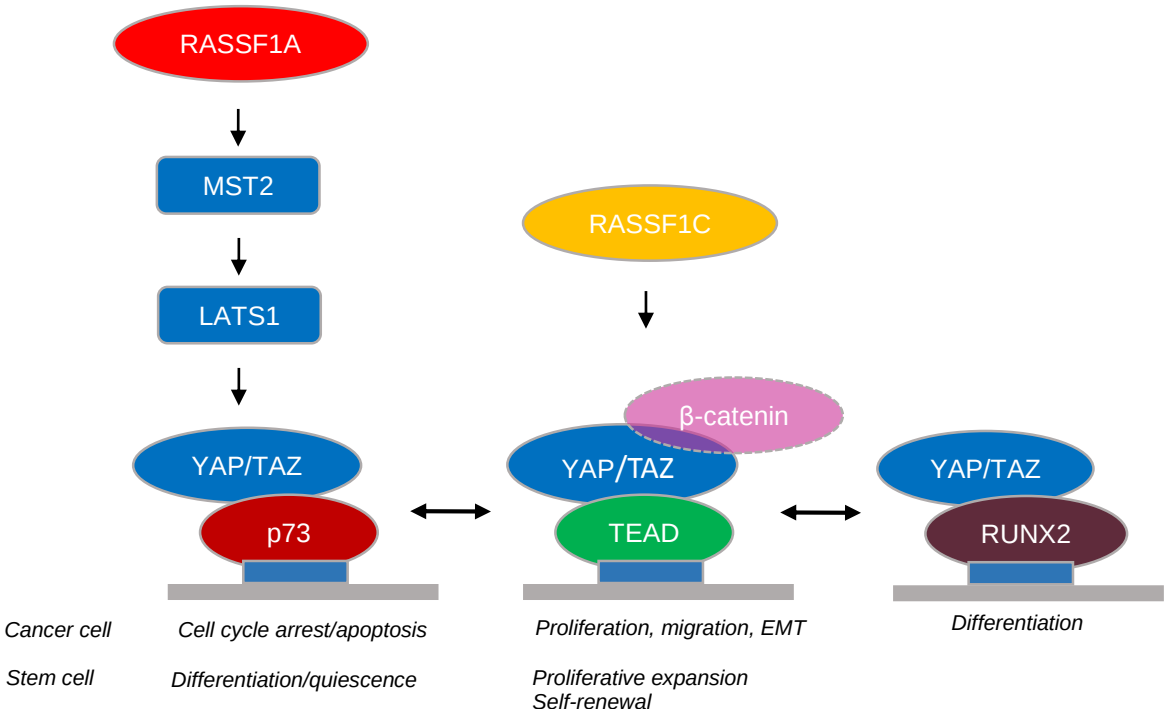


Figure 6.1. Model of RASSF1A/RASSF1C effects on YAP transcription factor partners. In cancer cells: RASSF1A prevents the formation of proliferative YAP/TAZ-TEAD1 complexes and promotes YAP/TAZ-p73-mediated cell cycle arrest and apoptosis. Genetic loss of RASSF1A results in elevation of YAP/TAZ-TEAD1 proliferative transcription at the expense of YAP/TAZ-p73 and YAP/TAZ-RUNX2. RASSF1C promotes YAP/TAZ-TEAD1 complex formation. In stem cells: RASSF1A prevents the formation of self-renewal-mediating YAP-TEAD2-β-catenin complexes and promotes YAP-p73-mediated differentiation. Loss of RASSF1A results in elevation of YAP-TEAD2-β-catenin complexes at the expense of YAP-p73. The role of RASSF1C in stem cells remains elusive. The same mechanism is responsible for the generation of cancer stem cells.

The siRNA and shRNA sequences targeting our main protein of interest, RASSF1A, were specifically designed against the 1α exon region encoding for the first 121 amino-acids, which are unique to RASSF1A and not contained in RASSF1C. Furthermore, silencing of RASSF1A in the cell lines used throughout this project does not affect other RASSF1 isoforms for the following reasons: RASSF1D and RASSF1E transcripts are expressed exclusively in cardiac and pancreatic cells respectively, while RASSF1F and RASSF1G expression is undetectable, therefore their biological function and their transcript sequences are classified as unknown (van der Weyden and Adams 2007). Knockdowns of RASSF1A were assessed either via quantitative PCR using specific pairs of primers targeting the 1α exon region (Table 2.1) or immunoblotting using an antibody against the C1/DAG domain of the protein (clone 3F3, sc-58470, Table 2.4), which is only encountered in the RASSF1A isoform.

Knockdown of RASSF1A in Chapters 3 and 5 of the thesis was validated via immunoblotting, as this was considered sufficient to derive the required information. Furthermore, quantitative PCR was not an established technique in our laboratory when part of those experiments was performed. However, as experiments in Chapter 4 required information regarding mRNA levels of RASSF1A and other factors, qRT-PCR was implemented on a routine basis.

In this thesis it was demonstrated that RASSF1A promotes stem cell differentiation. Due to this property, RASSF1A may also limit the stem-like characteristics cancer cells acquire, potentially rendering them more responsive to radio-chemotherapy. Several tumour suppressors have been charged with differentiation-promoting properties (Pomerantz and Blau 2013)

e.g. p53, whose activation was found to cause spontaneous differentiation of both human (Qin, Yu et al. 2007) and mouse (Lin, Chao et al. 2005) stem cells.

In Chapter 4, work in ESCs and the pre-implantation mouse embryo revealed that Rassf1a loss increased stem cell markers, leading to accelerated proliferation of ESCs in culture, but to no obvious developmental defects in the mouse embryo. Consistently, *Rassf1a -/-* mice appear to develop normally and be fertile, however, they are prone to spontaneous tumour formation (Tommasi, Dammann et al. 2005, van der Weyden, Tachibana et al. 2005). Interestingly, depletion of p53 also enhances pluripotency and improves iPSC generation efficiency and *p53 -/-* mice appear to be viable and fertile (Zhao, Yin et al. 2008, Hong, Takahashi et al. 2009, Kawamura, Suzuki et al. 2009, Marion, Strati et al. 2009). However, as both *Rassf1a* and *p53 -/-* mice are susceptible to spontaneous tumourigenesis (Donehower, Harvey et al. 1992, Tommasi, Dammann et al. 2005, van der Weyden, Tachibana et al. 2005), it can be inferred that loss of these fate determinants in the beginning of embryogenesis potentially predisposes mice to developing tumours at a later stage, through the upregulatiion of stem cell marker genes. This is further supported by the fact that *Rassf1a* and *p53* double knockout mice are remarkably tumour prone and develop malignancies significantly faster than single-mutant littermates (Tommasi, Besaratinia et al. 2011).

As *Rassf1a -/-* MEFs display increased reprogramming efficiency upon transfection with the “Yamanaka cocktail” of transcription factors, it would be interesting to explore whether loss of Rassf1a may replace any of these

transcription factors (Sox2, Klf4, Oct4, c-Myc) in the reprogramming process. Moreover, it would be challenging to investigate if *Rassf1a -/-* MEFs can spontaneously generate iPSCs without the use of the “Yamanaka cocktail”, in the presence of LIF or upon other stimuli. Of note, it has been shown that RASSF1A stabilises p53 in cancer cells (Song, Song et al. 2008). Given that p53 can affect stem cell pluripotency (Lin, Chao et al. 2005, Qin, Yu et al. 2007), it would be interesting to examine the effect of its potential regulation by RASSF1A in stem cells and development.

Furthermore, work in Chapter 4 revealed that RASSF1A expression not only abrogates iPSC induction from MEFs, but also affects the morphology of the resulting iPSC colonies. Given that compromised reprogramming efficiency is accompanied by decreased stem cell marker expression and activation of differentiation programmes, morphological changes in iPSC colonies might reflect this process. This would be in line with results obtained from LIF withdrawal assays. However, as this phenotype could also be the outcome of alternative functions of RASSF1A affecting cell-cell adhesion molecules, such as Rho GTPases Rac, Rho and CDC42, which act to stabilise cell-cell contacts (Parsons, Horwitz et al. 2010), these morphological differences need to be further explored.

In Chapter 5, it was shown that RASSF1A interacts with the differentiation repressor HES1 in the nucleus to decrease its endogenous levels. Camargo et al. (2007) demonstrated that HES1 and YAP1 have a common regulation pattern in intestinal stem cells. Therefore, it would be interesting to see whether in response to RASSF1A, YAP/TAZ and HES1 are able to form a transcriptional complex to regulate downstream gene expression. We predict

that RASSF1A loss would likely stabilise YAP/TAZ-HES1 complexes to inhibit differentiation processes. On the contrary, RASSF1A should limit the formation of these complexes. This regulation might be important in both stem cell fate determination and cancer stem cell generation. Furthermore, elucidating the mechanism underlying the common regulation pattern of YAP and HES1 would shed more light on the cross talk between the Hippo and Notch signalling pathways.

Our data in Chapter 5 revealed that the RASSF1C isoform of the *RASSF1* gene is involved in both cell-autonomous and paracrine effects regarding the upregulation of stem cell markers in cancer cells. Thus, it would be interesting to investigate the nature of the secreted signals, since this might provide insight into cancer stem cell generation. Immune signals, such as hepatocyte growth factor (HGF) and the cytokine stromal cell-derived factor 1 (SDF1) are secreted by cells to promote neoplastic transformation and cancer cell proliferation in the surrounding microenvironment (Bhowmick, Chytil et al. 2004, Orimo, Gupta et al. 2005). Furthermore, a number of reports have identified membrane vesicles named exosomes, which have the same topology as a cell and contain a wide variety of biologically active material. Exosomes are secreted by many cell types and upon fusion with the plasma membrane of the target cells, they release their biological content (Simons and Raposo 2009, Thery, Ostrowski et al. 2009). It has been shown that cancer cells can secrete exosomes functioning in an autocrine or paracrine fashion to promote immune suppression, angiogenesis and metastasis (Taylor and Gercel-Taylor 2011, Luga, Zhang et al. 2012, Peinado, Aleckovic et al. 2012). Therefore, it would be highly intriguing to investigate the

presence of these factors in the paracrine signals secreted by RASSF1C-expressing cells. Moreover, given that in the majority of cases RASSF1C activation recapitulates the phenotype of RASSF1A loss, it would be of interest to see whether these paracrine signals are also secreted by cells which have lost RASSF1A expression.

Furthermore, investigation is required to uncover the metastatic potential of RASSF1C-expressing tumours. We would predict that patients carrying promoter methylations only at the 1α locus, which encodes the RASSF1A isoform, would have worse prognosis and clinical outcome in comparison to patients carrying both 1α and 2γ promoter methylations. 2γ promoter methylations affect the expression of the RASSF1C isoform and are rare, however, they are usually encountered together with 1α promoter methylations, resulting in silencing of all isoforms of the *RASSF1* gene (Vos, Ellis et al. 2000, Dreijerink, Braga et al. 2001).

The role of RASSF1A and RASSF1C in cancer stem cell generation deserves to be more thoroughly investigated by employing techniques that allow the isolation of stem-like cells from tumours, e.g. FACS. The isolated cells should be subjected to stem cell culture, while simultaneously performing assays, such as mammosphere formation assays to further confirm the “stemness” tumours exhibit. In Chapter 5, cancer stem cells were identified via the expression of core stem cell markers, as a first approach to identifying cancer stem cells.

In this thesis, the role of RASSF1A in stem cell biology and embryonic development was thoroughly examined and a mechanism was provided for its

functions (Chapter 4). In Chapter 5, we demonstrate that RASSF1C regulates YAP/TAZ in a similar manner to RASSF1A loss. Taken together, these data imply an active role for RASSF1C in stem cell fate determination and embryonic development, which remains elusive. Additionally, work in the lab has shown that RASSF1A destabilises RASSF1C in cancer cells, hence it would be interesting to examine the impact of the interaction of the two isoforms on Oct4 expression.

Overally, our data demonstrate that in addition to being a prognostic biomarker for many tumour types (Kawai, Sakano et al. 2010, Buhmeida, Merdad et al. 2011, Wang, Wang et al. 2011, Xu, Shetty et al. 2012), RASSF1A may act as a stem cell marker, as its signalling through YAP regulates the core stem cell marker network, thereby determining stem cell and embryonic fate. Furthermore, by showing that RASSF1A exerts direct regulation of *Oct4* at the transcriptional level, we contribute to dissecting the mechanism upstream of the core stem cell marker network. Additionally, poorly understood areas of embryonic development, particularly embryonic fate determination through the Hippo pathway, can be better explained through the mechanism we provide. Currently, stem cells have limited applications in the clinic, partly due to the tumourigenic effects they exhibit on transplantation into animal models. RASSF1A can influence the tumourigenic potential of stem cells (Teng et al. 2011 and data in this thesis), which renders it a strong therapeutic candidate in overcoming these problems.

Lastly, it should be stressed that *RASSF1A* promoter methylation is already targeted in the clinic with the use of methyltransferase inhibitors, such as the DNMT inhibitor 5-aza-2'-deoxycytidine (Decitabine). YAP-TEAD is an

additional therapeutic target of interest and, indeed, pharmacological disruption of YAP-TEAD complexes using verteporfin is able to suppress the oncogenic activity of YAP (Liu-Chittenden, Huang et al. 2012). Data in this thesis (Chapter 5) have shown that TAZ may also elicit the effects of RASSF1A signalling. Preventing both TAZ and YAP from forming complexes with oncogenic factors such as TEAD and β-catenin might rescue completely the oncogenic effects of RASSF1A loss. As yet, there has been no known clinical agent targeting TAZ complexes. Additionally, as it is becoming clearer that in the absence of RASSF1A tumourigenesis is exacerbated due to the increase of stem cell markers, it is worth exploring whether direct targeting of pluripotency factors in the clinic can prevent tumourigenesis in cancers lacking RASSF1A. Furthermore, the data presented here render RASSF1C a potential clinical target of interest.

Chapter 7

Appendix

7.1 *Sleeping Beauty* mutagenesis screen

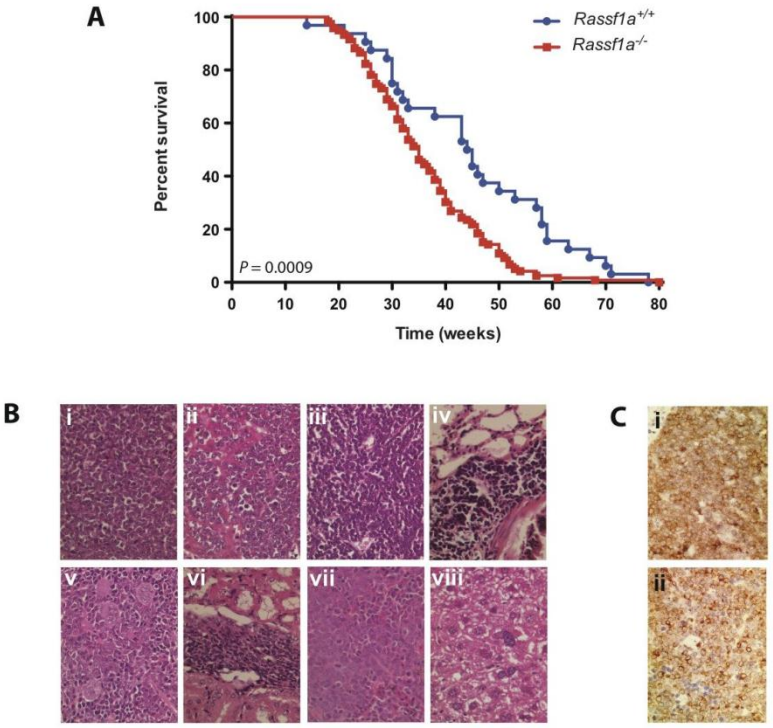


Figure 7.1. Loss of Rassf1a promotes tumourigenesis. These data were obtained from Dr Louise van der Weyden, David Adams Laboratory (Sanger Institute, Cambridge, UK). **A.** *Rassf1a* null mice show a decreased survival (due to tumour formation) compared to control mice ($P < 0.0009$) on a "jumping" background. **B.** Photomicrographs of formalin-fixed, hematoxylin and eosin-stained sections of a thymic lymphoma (i), that metastasised to the liver (ii), a splenic lymphoma (iii), that metastasised to the lung (iv), a leukemia that infiltrated the spleen (v), and kidney (vi), and a mouse that developed two independent tumours, specifically splenic lymphoma (vii) and hepatocellular carcinoma (viii). **C.** Photomicrographs of an immunohistochemically stained lung section infiltrated by a lymphoma of T-cell origin (i) and a spleen section (ii) infiltrated by myeloid leukemia (taken and adapted from van der Weyden and Papaspyropoulos et al., 2012).

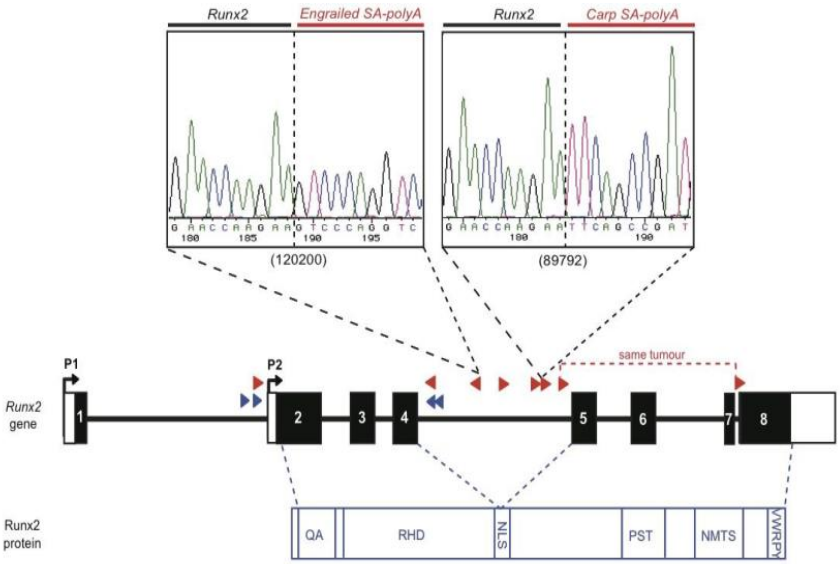


Figure 7.2. Insertions in the *Runx2* gene. These data were obtained from Dr Louise van der Weyden, David Adams Laboratory (Sanger Institute, Cambridge, UK). Seven *Rassf1a -/-* Sleeping Beauty mice that developed leukemia/lymphoma carried transposons, which had inserted into the *Runx2* gene (indicated by the red triangles; direction of triangle indicates orientation of the transposon). The blue triangles are *Rassf1a* +/+ Sleeping Beauty mice that developed leukemia/lymphoma and carried *Runx2* insertions, although these insertions did not constitute a statistically significant common insertion site (CIS) (taken and adapted from van der Weyden and Papaspyropoulos et al., 2012).

Table 7.1. The most statistically significant genes affected by transposon insertion in *Rassf1a -/- Sleeping Beauty* mice. These data were obtained from Dr Louise van der Weyden, David Adams Laboratory (Sanger Institute, Cambridge, UK).

CIS identification	Predicted affected gene	Other genes in CIS	Genomic location of CIS (chr:start-end)	Insertions (tumors)	P value
CIS12:100543835_75k	Foxn3	3300002A11Rik	12: 100477940-100609729	20 (16)	0.02848
CIS14:67677451_15k	Ppp2r2a	Bnip3l	14: 67657900-67692812	11 (X)	0.00026
CIS5:34769677_15k	Fam193a	Rnf4, Sh3bp2, Tnip2	5: 34753537-34781415	9 (X)	0.00261
CIS12:93020818_15k	Ston2	Sel1l	12: 93004760-93032497	9 (X)	0.01352
CIS3:104653212_15k	Capza1	Fam19a3, St7l, Mov10, Ppm1j, Rhoc, Wnt2b	3: 104639966-104662043	8 (X)	0.01081
CIS17:44818488_30k	Runx2	Supt3h	17: 44801068-44830102	8 (7)	0.03697
CIS4:97738853_15k	Nfia	-	4: 97727123-97749117	7 (X)	0.00078
CISX:39556669_15k	Stag2	Xiap	X: 39546415-39563993	7 (X)	0.01552
CIS16:4187397_15k	Crebbp	Adcy9, Trap1	16: 4175786-4197556	7 (X)	0.02029
CIS5:34056588_15k	Fgfr3	Fam53a, Letm1, Slbp, Tacc3, Tmem129	5: 34047785-34062457	7 (X)	0.02839

7.2 RASSF1 and RUNX2 expression in clinical samples

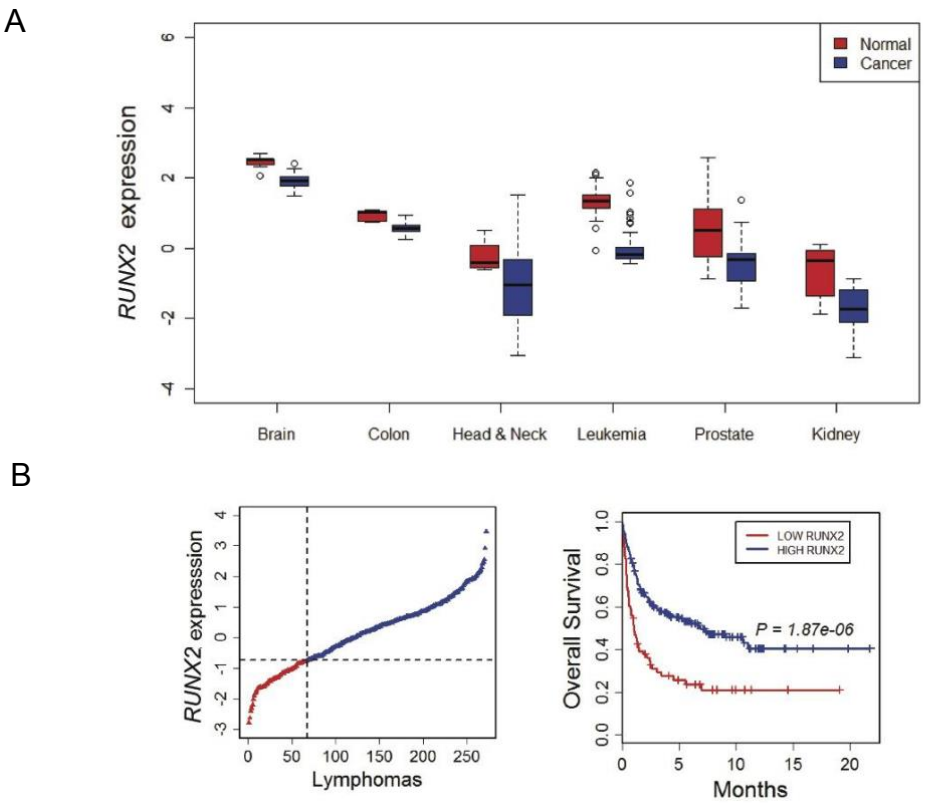


Figure 7.3. Analysis of RUNX2 and RASSF1 expression across different tumour types. These data were obtained from Dr George Poulogiannis (Harvard Medical School, Boston, Massachusetts, USA). **A.** Box plots indicating that RUNX2 expression is significantly lower in many tumor types compared with their corresponding normal tissues. From left to right: RUNX2 expression in normal brain (white matter, n=7) vs. brain tumor (astrocytoma, glioblastoma, oligodendroglioma, n=35), normal colon (n=5) vs. colorectal cancer (n=100), normal uvula (n=4) vs. head and neck squamous cell carcinoma (n=34), peripheral blood mononuclear cell (n=58) vs.B-cell acute lymphoblastic leukemia (n=114), prostate gland (n=21) vs. prostate carcinoma (n=30), normal kidney (n=10) vs. clear cell renal cell carcinoma (n=10). **B.** Left panel: ranked RUNX2 expression in a large data set of 272 lymphomas. Right panel: Kaplan–Meier survival curves comparing disease-free survival between lymphomas with the lowest (<25th percentile) versus highest (>25th percentile) RUNX2 expression (log-rank test, P = 1.87×10^{6}).

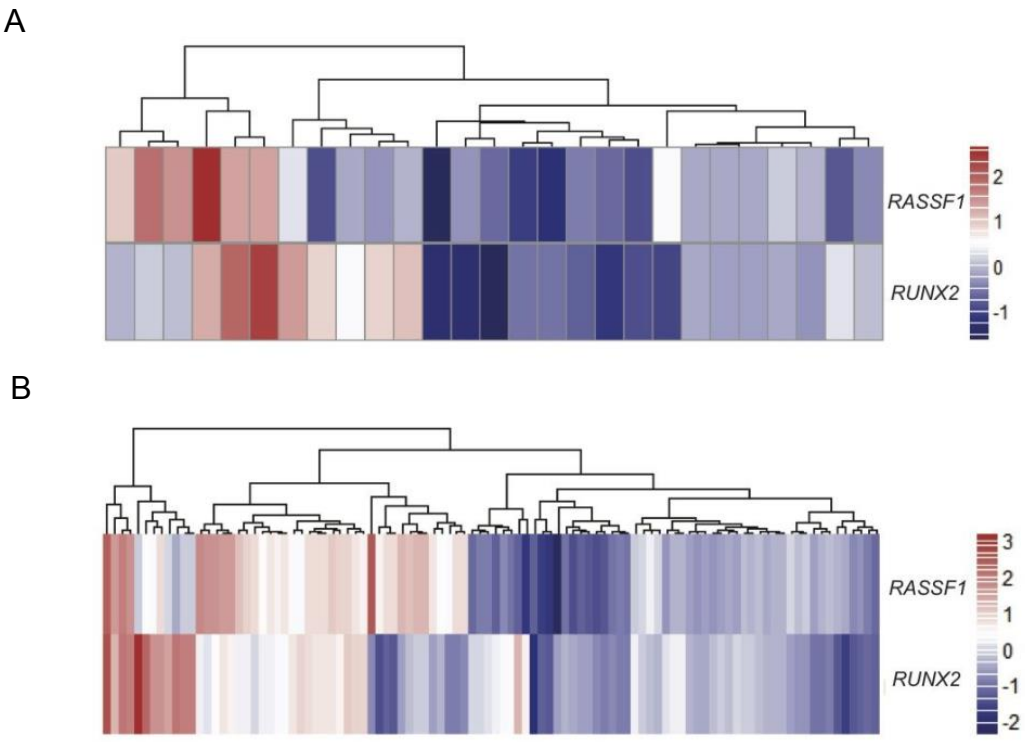


Figure 7.4. Microarray analysis of RUNX2 and RASSF1 expression in leukemias and colorectal cancers. These data were obtained from Dr George Poulogiannis (Harvard Medical School, Boston, Massachusetts, USA). **A.** Clustering and heatmap of RUNX2 and RASSF1 relative transcript levels in precursor T-cell lymphoblastic leukemias (n=27), of which 18 show concordant changes for these 2 transcripts. **B.** Clustering and heatmap of RUNX2 and RASSF1 relative transcript levels indicating a strong positive correlation (predominantly concordant downregulated expression) between RASSF1 and RUNX2 expression in colorectal adenocarcinomas (n=105). The colour bar indicates normalised expression levels with red signifying the magnitude of upregulation and blue of downregulation (taken and adapted from van der Weyden and Papaspyropoulos et al., 2012).

7.3 RASSF1A regulates stem cell fate in ESCs and iPSCs.

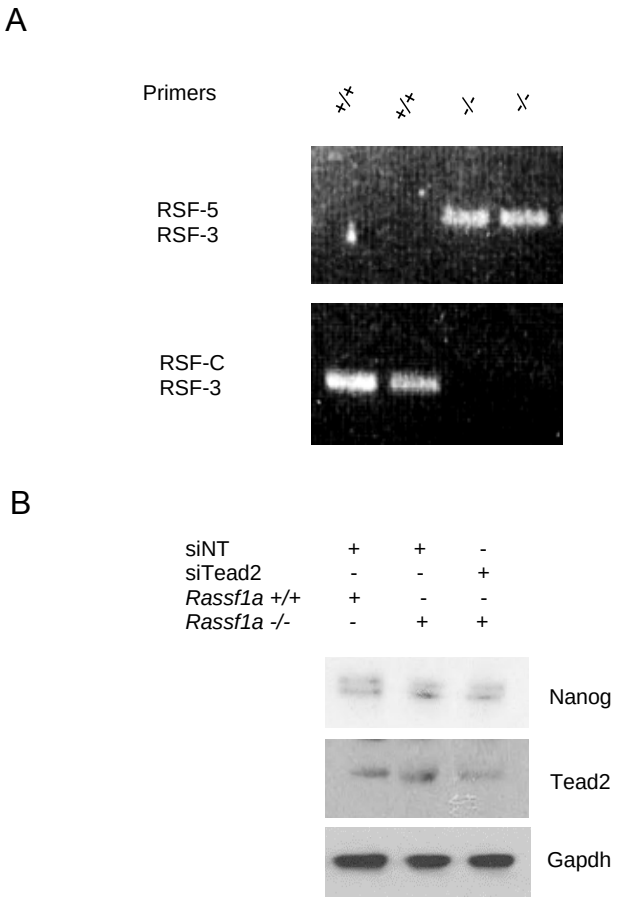


Figure 7.5. Tead2 KD reduces stem cell marker levels in *Rassf1a* -/- iPSCs. A. PCR from genomic DNA extracted from *Rassf1a* +/+ and -/- MEFs used in this project in order to validate the *Rassf1a* status. The primer pairs used (RSF-5/RSF-3 or RSF-C/RSF-3) and the expected product were first described by van der Weyden et al., 2005. **B.** *Rassf1a* +/+ and -/- iPSCs were transfected either with non-targeting (siNT) or Tead2-targeting (siTead2) siRNA. The cells were lysed and western blotted with the indicated antibodies.

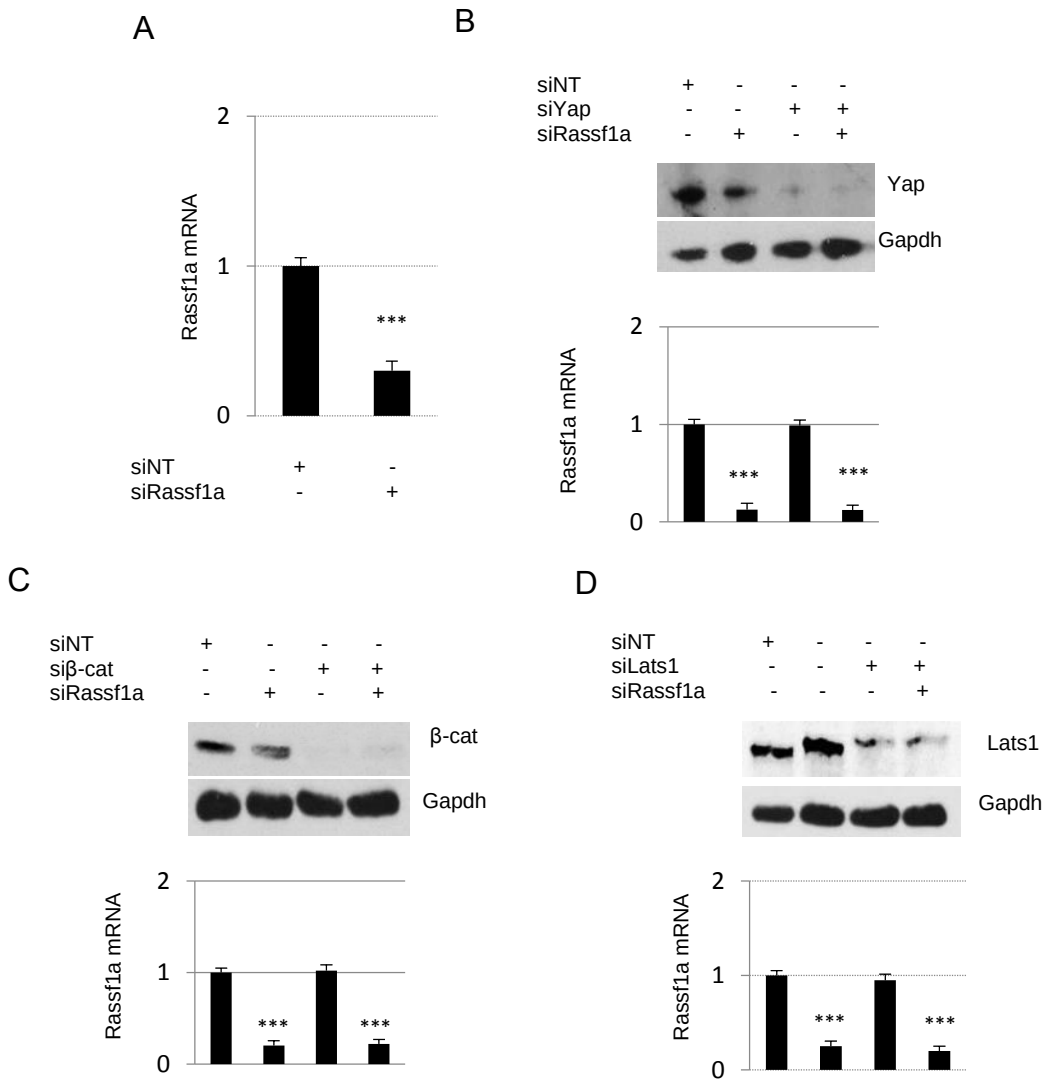


Figure 7.6. Experimental controls. A. qRT-PCR of Rassf1a mRNA to assess the KD from Figure 4.15. P < 0.001 (Student's t test). **B.** Western blot of the cell lysates probed with the indicated antibodies and qRT-PCR of Rassf1a mRNA to assess the KDs from Figure 4.18C. P < 0.001 for siNT vs siRassf1a (Student's t test). **C.** Western blot of the cell lysates probed with the indicated antibodies and qRT-PCR of Rassf1a mRNA to assess the KDs from Figure 4.19B. P < 0.001 for siNT vs siRassf1a (Student's t test). **D.** Western blot of the cell lysates probed with the indicated antibodies and qRT-PCR of Rassf1a mRNA to assess the KDs from Figure 4.22. P < 0.001 for siNT vs siRassf1a (Student's t test).

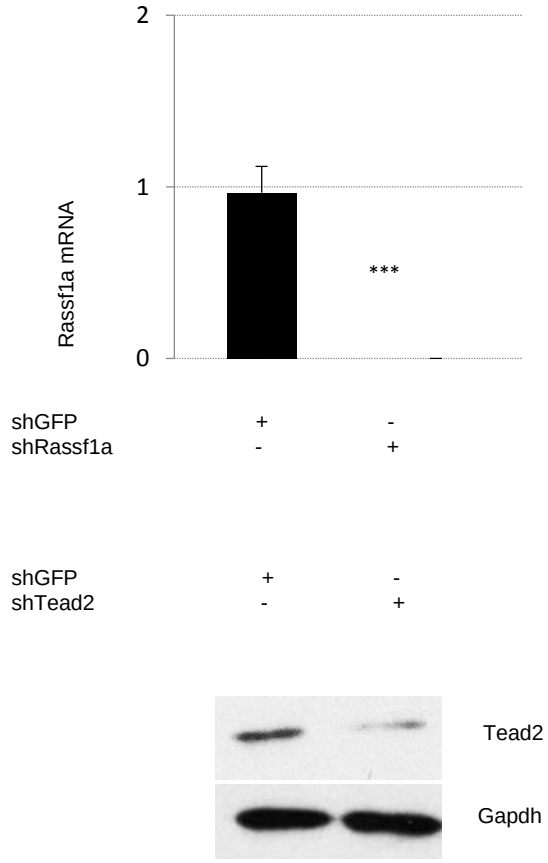


Figure 7.7. Controls for the generation of shRNA-expressing ESC lines. Top panel: qRT-PCR to validate the Rassf1a KD in stable shGFP against shRassf1a ESC lines. $P < 0.001$ for shGFP vs shRassf1a (Student's t test). Bottom panel: Western blot to validate the Tead2 KD in stable shGFP against shTead2 ESC lines.

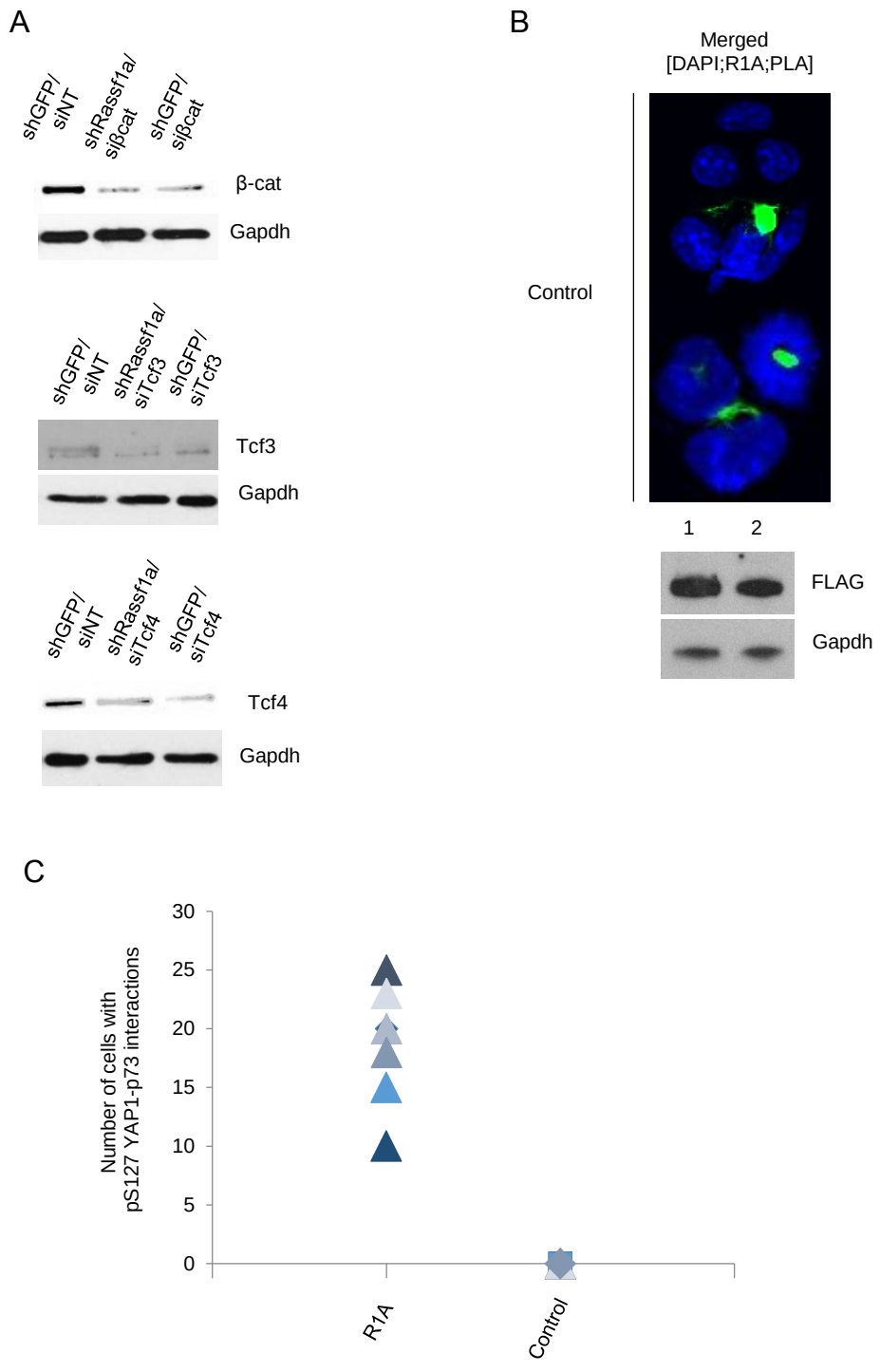


Figure 7.8. Additional experimental controls. A. Western blots of cell lysates to assess the knock down of the proteins targeted with the siRNAs indicated in Figure 4.21B. The lysates were probed with the indicated antibodies (right). **B.** Top panel: Negative control for the PLA experiment illustrated on Figure 4.24; ESCs were transfected with FLAG-YAP1 and zsGrRASSF1A (R1A) and subject to Proximity Ligation Assay (PLA) in presence of only one primary antibody (anti-FLAG). Immunofluorescence shows RASSF1A expression (green), however, red dots are missing (PLA). Bottom panel: Western blot of cell lysates for FLAG expression. 1,2: double loaded lysates from the same pool of ESCs of Figure 4.24. **C.** Graph illustrating the number of zsGrRASSF1A (R1A)-expressing ESCs containing pS127 YAP1-p73 complexes versus non-expressing (Control) ESCs, as assessed by PLA. Each triangle represents an independent experiment.

7.4 RASSF1A role in the mouse embryo

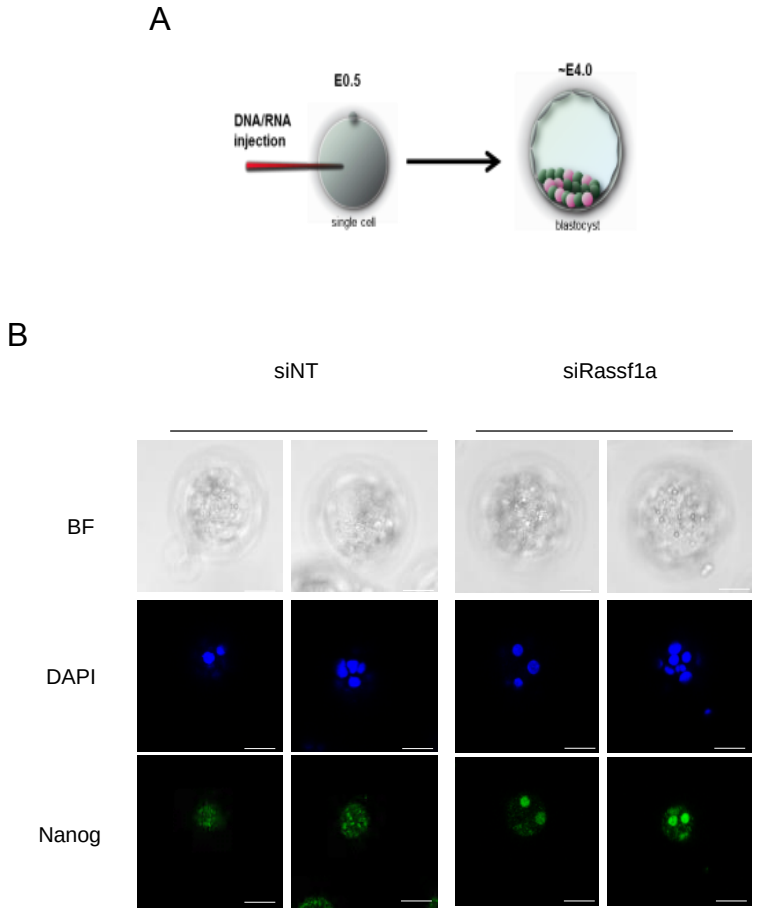


Figure 7.9. Rassf1a depletion increases stem cell marker protein expression in the mouse embryo. These data were obtained from C.Y. Leung, Magdalena Zernicka-Göetz lab (Gurdon Institute, Cambridge, UK). **A.** Schematic of the method by which knock-down (KD)/overexpression (OE) experiments were conducted in the mouse embryo. Blastomeres were microinjected with siRNAs/plasmid vectors at the single cell stage and allowed to grow to form blastocysts. **B.** Embryos were transfected with either non-targeting (siNT) or Rassf1a-targeting (siRassf1a) siRNA. Immunofluorescence for Nanog protein levels in cells from both conditions.

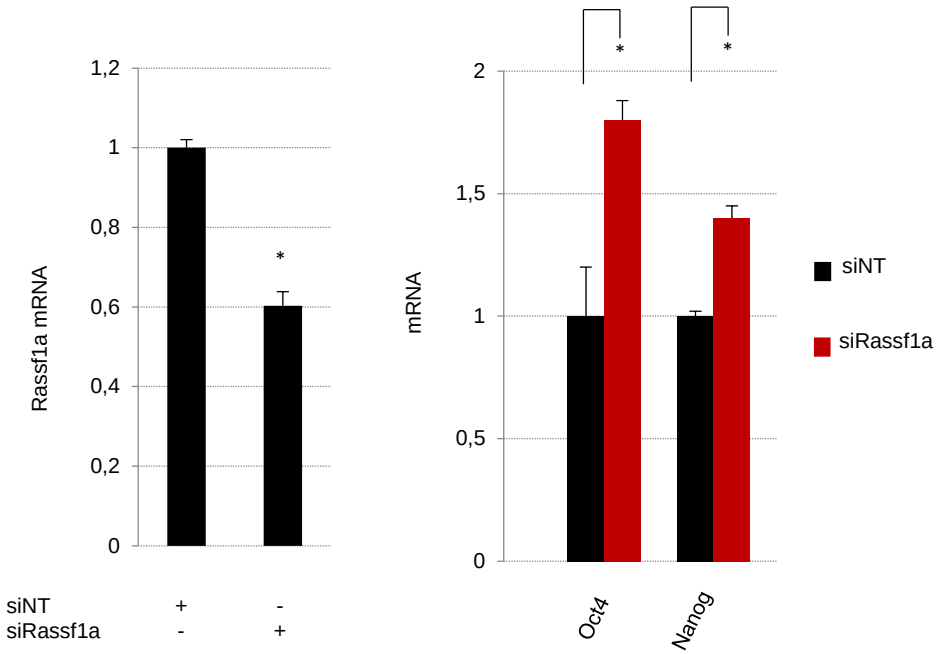


Figure 7.10. Rassf1a depletion increases stem cell marker transcript levels in the mouse embryo. These data were obtained from C.Y. Leung, Magdalena Zernicka-Göetz lab (Gurdon Institute, Cambridge, UK). Left panel: qRT-PCR of Rassf1a mRNA levels from embryos in B to assess the KD. P = 0.035 for siNT vs siRassf1a (Student's t test). Right panel: qRT-PCR of Oct4 and Nanog mRNA levels from cells in B. P < 0.05 for both Oct4 and Nanog (siNT vs siRassf1a, Student's t test).

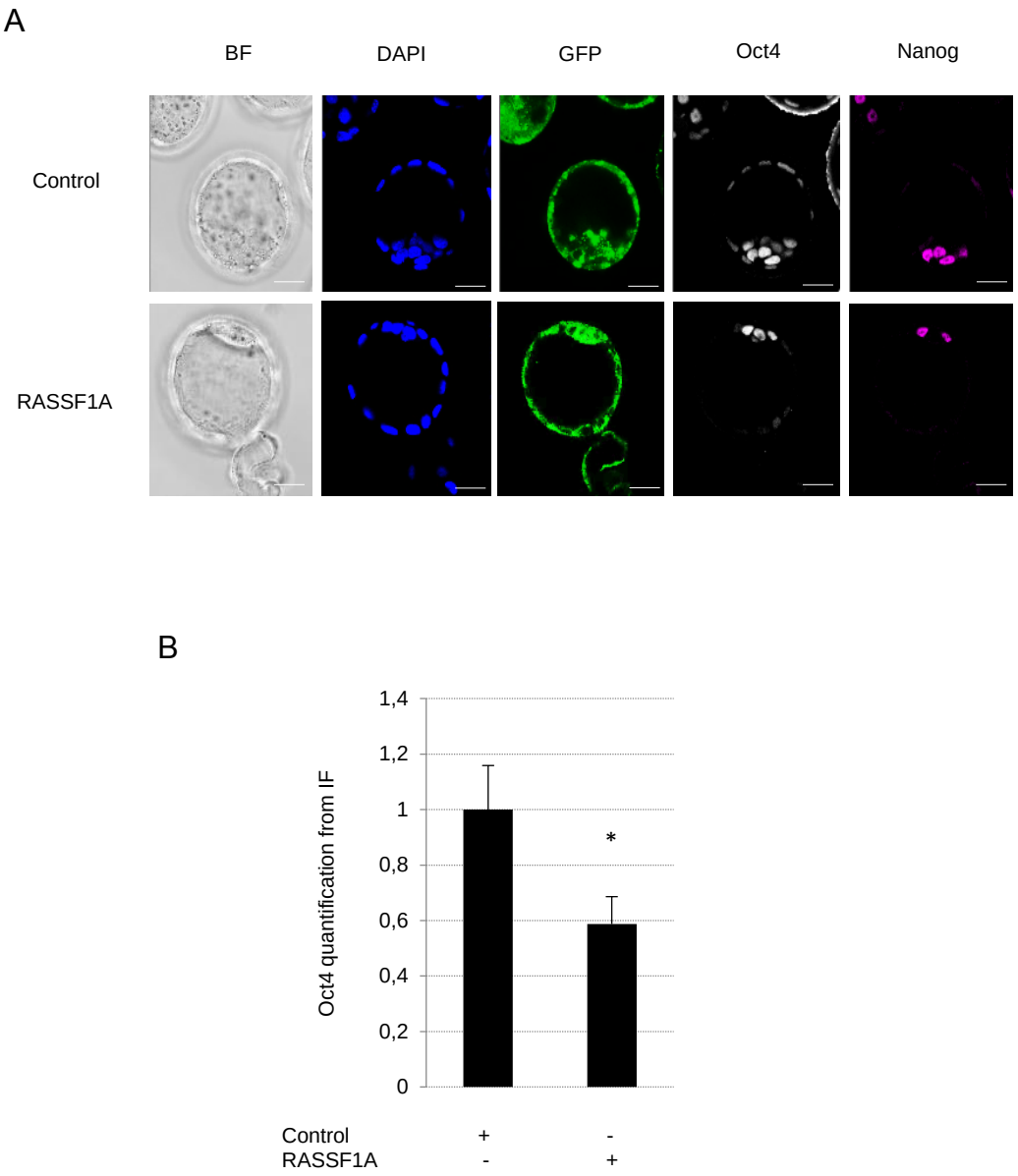


Figure 7.11. RASSF1A overexpression reduces stem cell markers. These data were obtained from C.Y. Leung, Magdalena Zernicka-Göetz lab (Gurdon Institute, Cambridge, UK). **A.** Embryos were transfected with 200 ng/µL of zsGrRASSF1A (RASSF1A) mRNA or zsGrCtrl (Control) at the 1/2-cell stage and allowed to grow until they formed blastocysts. Immunofluorescence of Oct4 and Nanog protein levels. **B.** Bar graph quantifying the Oct4 protein levels across the total number of embryos in the experiment expressing zsGrRASSF1A (RASSF1A, 200 ng/µL) versus zsGrCtrl empty vector (Control). P = 0.018 for Control versus RASSF1A (Student's t test).

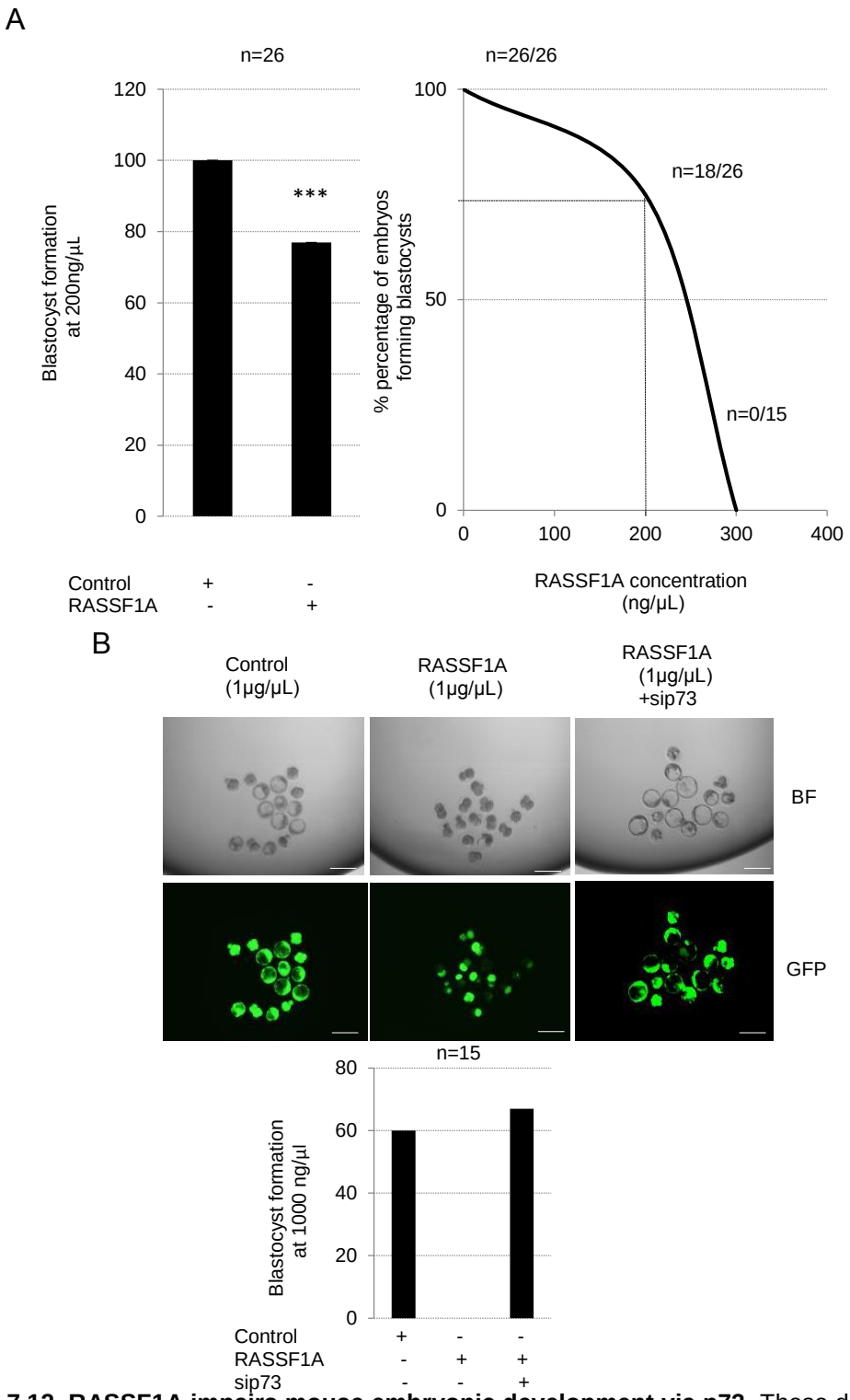


Figure 7.12. RASSF1A impairs mouse embryonic development via p73. These data were obtained from C.Y. Leung, Magdalena Zernicka-Göetz lab (Gurdon Institute, Cambridge, UK). **A.** Left panel: bar graph illustrating the number of RASSF1A mRNA-microinjected embryos (200 ng/µl) which were able to develop to the blastocyst level versus Control. $P < 0.001$ (n=26, Student's t test). Right panel: "kill curve" illustrating the different concentrations of Rassf1a mRNA microinjected into the embryos in proportion with viability (ability to form blastocysts). **B.** Top panel: 15 embryos were microinjected with either zsGrCtrl (Control) or zsGrRASSF1A (RASSF1A) mRNA at a lethal concentration (1µg/µL), along with p73-targeting (sip73) siRNA. Images demonstrating the viability status of the embryos in each condition. Bottom panel: bar graphs representing quantification of the percentage of embryos making it to blastocysts from each condition (n=15).

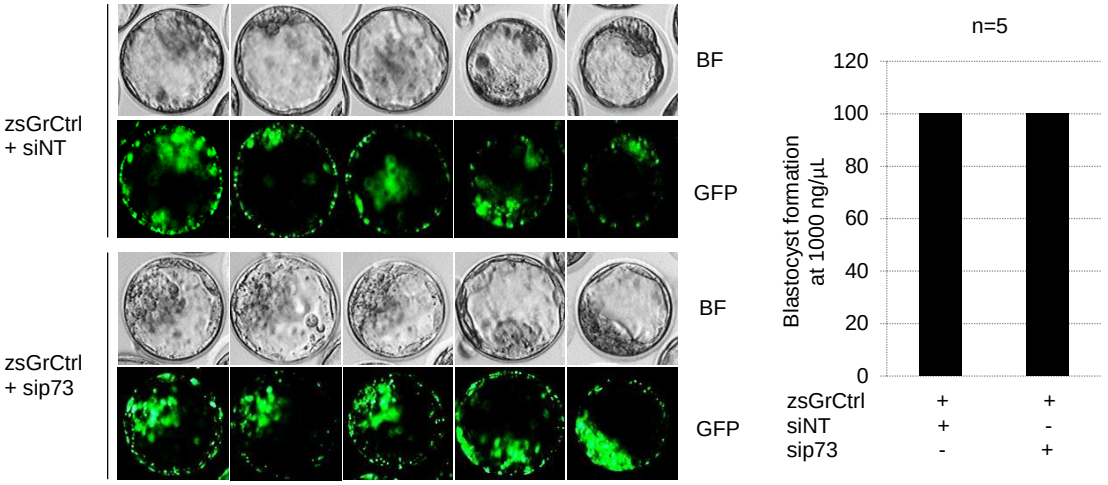


Figure 7.13. Knockdown of p73 alone does not cause a developmental defect. These data were obtained from C.Y. Leung, Magdalena Zernicka-Göetz lab (Gurdon Institute, Cambridge, UK). Left panel: 5 embryos were microinjected with zsGrCtrl mRNA (1 µg/µL), together with non-targeting siRNA (siNT) or p73-targeting siRNA (sip73). Images demonstrating the viability status of the embryos in each condition. Right panel: bar graphs representing quantification of the percentage of embryos surviving to the blastocyst stage from each condition (n=5).

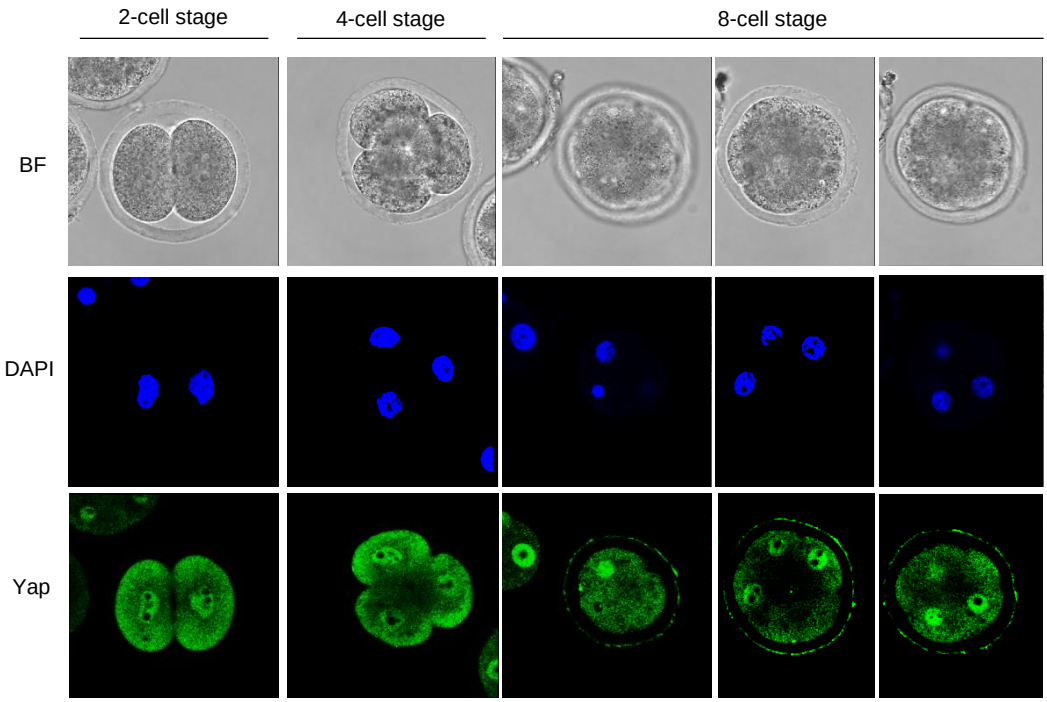


Figure 7.14. Yap1 nuclear localisation in the mouse embryo from 2-8-cell stage. These data were obtained from C.Y. Leung, Magdalena Zernicka-Göetz lab (Gurdon Institute, Cambridge, UK). Immunofluorescence of Yap1 protein in 2/4/8-cell stage embryos.

7.5 The role of RASSF1A in cancer stem cell generation

Table 7.2. RASSF1A interplay with the Notch signalling pathway. These data were obtained from Dr Eric O'Neill, University of Oxford, UK. *In vitro* screen for RASSF1A binding partners performed by mass spectrometry in human osteosarcoma U2OS cells. The list comprises a representative sample of RASSF1A binding partners. HES1 (highlighted in red) was of interest, as a well-known downstream effector of the Notch signalling pathway.

Protein Name	Mass
H1 histone family, member 3	22336
RuvB-like 2 (DNA helicase)	51125
Hes1 (Notch Signaling)	28143
alpha - tubulin	50126
RAN protein	25207
GDP-D-mannose-4,6 dehydratase	38667
CLTC protein (Clathrin)	187771
Histone H3.3	6896
Damage-specific DNA binding protein 1	126907
Histone H2B	13926
Emerin	28976
Lin7 homolog A	22702
Proteasome alpha 3 subunit, isoform 1	28433
VCAM-1	90886
Rab geranylgeranyl transferase	36827
Snurf/RNF4	35000

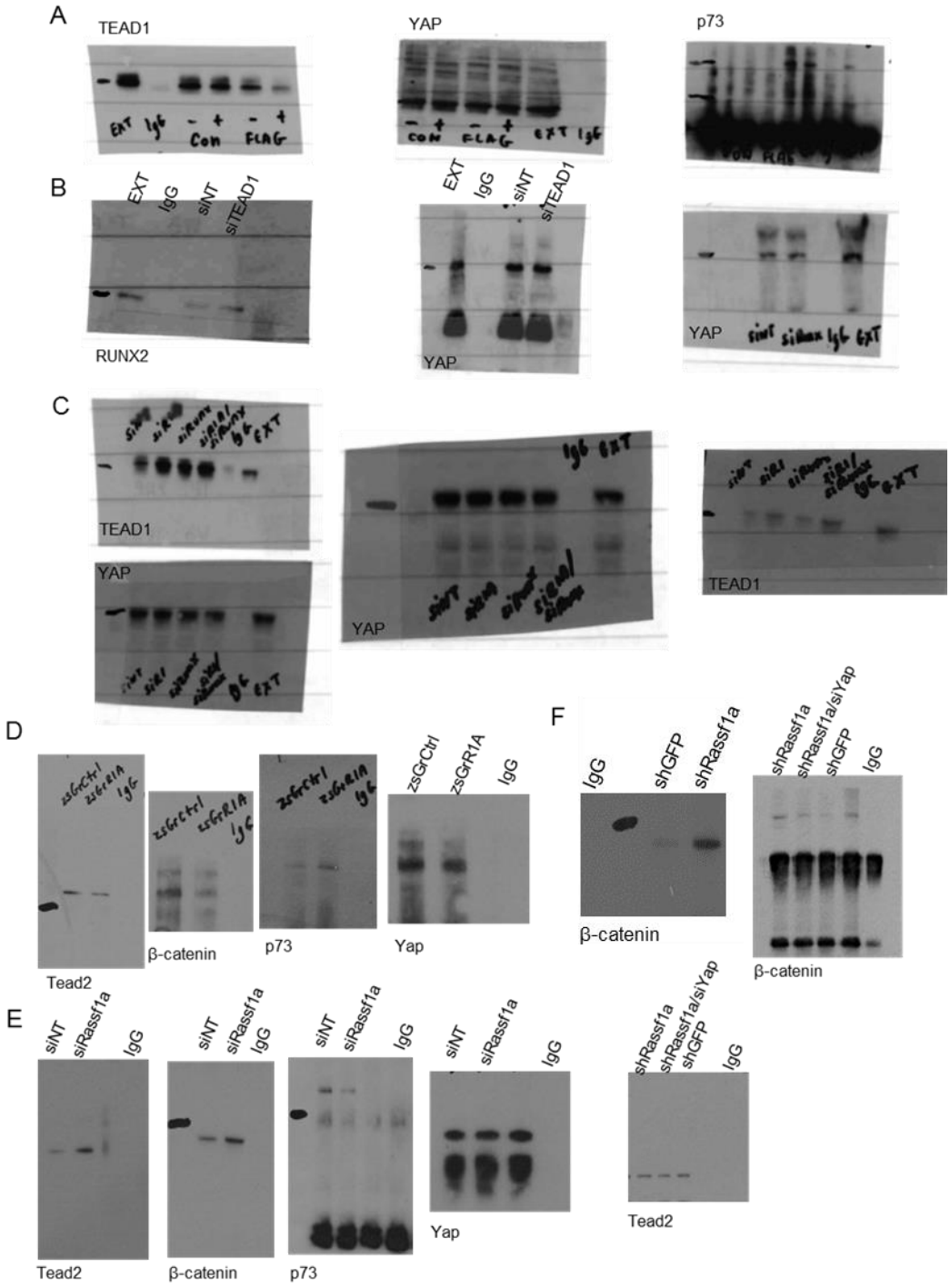


Figure 7.15. Raw experimental data from key experiments. Uncut blots from **A.** Figure 3.1, **B.** Figure 3.2, **C.** Figure 3.3, **D.** Figure 4.13, **E.** Figure 4.17 and **F.** Figure 4.18.

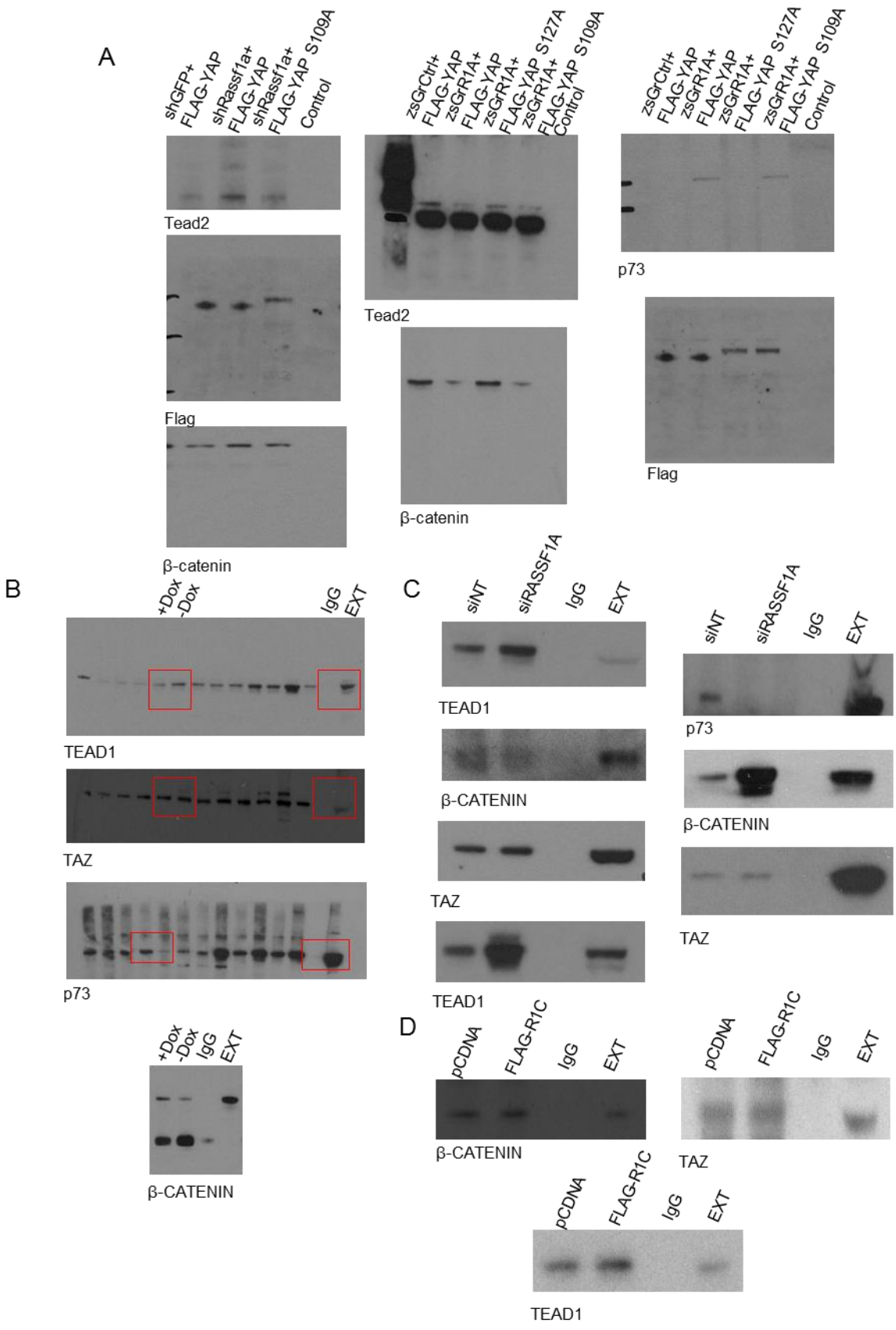


Figure 7.16. Additional raw experimental data from key experiments. Uncut blots from **A.** Figure 4.25, **B.** Figure 5.1, **C.** Figure 5.2 and **D.** Figure 5.10.

Chapter 8

References

Aberle, H., A. Bauer, J. Stappert, A. Kispert and R. Kemler (1997). "beta-catenin is a target for the ubiquitin-proteasome pathway." EMBO J **16**(13): 3797-3804.

Agathanggelou, A., W. N. Cooper and F. Latif (2005). "Role of the Ras-association domain family 1 tumor suppressor gene in human cancers." Cancer Res **65**(9): 3497-3508.

Agostini, M., P. Tucci, R. Killick, E. Candi, B. S. Sayan, P. Rivetti di Val Cervo, P. Nicotera, F. McKeon, R. A. Knight, T. W. Mak and G. Melino (2011). "Neuronal differentiation by TAp73 is mediated by microRNA-34a regulation of synaptic protein targets." Proc Natl Acad Sci U S A **108**(52): 21093-21098.

Ahmed-Choudhury, J., A. Agathanggelou, S. L. Fenton, C. Ricketts, G. J. Clark, E. R. Maher and F. Latif (2005). "Transcriptional regulation of cyclin A2 by RASSF1A through the enhanced binding of p120E4F to the cyclin A2 promoter." Cancer Res **65**(7): 2690-2697.

Akech, J., J. J. Wixted, K. Bedard, M. van der Deen, S. Hussain, T. A. Guise, A. J. van Wijnen, J. L. Stein, L. R. Languino, D. C. Altieri, J. Pratap, E. Keller, G. S. Stein and J. B. Lian (2010). "Runx2 association with progression of prostate cancer in patients: mechanisms mediating bone osteolysis and osteoblastic metastatic lesions." Oncogene **29**(6): 811-821.

Al-Ahmadie, H. A., G. Iyer, M. Janakiraman, O. Lin, A. Heguy, S. K. Tickoo, S. W. Fine, A. Gopalan, Y. B. Chen, A. Balar, J. Riches, B. Bochner, G. Dalbagni, D. F. Bajorin, V. E. Reuter, M. I. Milowsky and D. B. Solit (2011). "Somatic mutation of fibroblast growth factor receptor-3 (FGFR3) defines a distinct morphological subtype of high-grade urothelial carcinoma." J Pathol **224**(2): 270-279.

Al-Hajj, M., M. S. Wicha, A. Benito-Hernandez, S. J. Morrison and M. F. Clarke (2003). "Prospective identification of tumorigenic breast cancer cells." Proc Natl Acad Sci U S A **100**(7): 3983-3988.

Alarcon, C., A. I. Zaromytidou, Q. Xi, S. Gao, J. Yu, S. Fujisawa, A. Barlas, A. N. Miller, K. Manova-Todorova, M. J. Macias, G. Sapkota, D. Pan and J. Massague (2009). "Nuclear CDKs drive Smad transcriptional activation and turnover in BMP and TGF-beta pathways." Cell **139**(4): 757-769.

Amaar, Y. G., M. G. Minera, L. K. Hatran, D. D. Strong, S. Mohan and M. E. Reeves (2006). "Ras association domain family 1C protein stimulates human lung cancer cell proliferation." Am J Physiol Lung Cell Mol Physiol **291**(6): L1185-1190.

Artavanis-Tsakonas, S., M. D. Rand and R. J. Lake (1999). "Notch signaling: cell fate control and signal integration in development." Science **284**(5415): 770-776.

Aylon, Y., Y. Ofir-Rosenfeld, N. Yabuta, E. Lapi, H. Nojima, X. Lu and M. Oren (2010). "The Lats2 tumor suppressor augments p53-mediated apoptosis by promoting the nuclear proapoptotic function of ASPP1." Genes Dev **24**(21): 2420-2429.

Aylon, Y., A. Sarver, A. Tovy, E. Ainbinder and M. Oren (2014). "Lats2 is critical for the pluripotency and proper differentiation of stem cells." Cell Death Differ **21**(4): 624-633.
Azakie, A., S. B. Larkin, I. K. Farrance, G. Grenningloh and C. P. Ordahl (1996). "DTEF-1, a novel member of the transcription enhancer factor-1 (TEF-1) multigene family." J Biol Chem **271**(14): 8260-8265.
Azzolin, L., T. Panciera, S. Soligo, E. Enzo, S. Bicciato, S. Dupont, S. Bresolin, C. Frasson, G. Basso, V. Guzzardo, A. Fassina, M. Cordenonsi and S. Piccolo (2014). "YAP/TAZ Incorporation in the beta-Catenin Destruction Complex Orchestrates the Wnt Response." Cell.
Azzolin, L., F. Zanconato, S. Bresolin, M. Forcato, G. Basso, S. Bicciato, M. Cordenonsi and S. Piccolo (2012). "Role of TAZ as mediator of Wnt signaling." Cell **151**(7): 1443-1456.
Baksh, S., S. Tommasi, S. Fenton, V. C. Yu, L. M. Martins, G. P. Pfeifer, F. Latif, J. Downward and B. G. Neel (2005). "The tumor suppressor RASSF1A and MAP-1 link death receptor signaling to Bax conformational change and cell death." Mol Cell **18**(6): 637-650.
Balch, C., P. Yan, T. Craft, S. Young, D. G. Skalnik, T. H. Huang and K. P. Nephew (2005). "Antimitogenic and chemosensitizing effects of the methylation inhibitor zebularine in ovarian cancer." Mol Cancer Ther **4**(10): 1505-1514.
Banchereau, J. and R. M. Steinman (1998). "Dendritic cells and the control of immunity." Nature **392**(6673): 245-252.
Bar-Nur, O., H. A. Russ, S. Efrat and N. Benvenisty (2011). "Epigenetic memory and preferential lineage-specific differentiation in induced pluripotent stem cells derived from human pancreatic islet beta cells." Cell Stem Cell **9**(1): 17-23.
Barrandon, Y. and H. Green (1987). "Three clonal types of keratinocyte with different capacities for multiplication." Proc Natl Acad Sci U S A **84**(8): 2302-2306.
Barry, K. C., M. Abed, D. Kenyagin, T. R. Werwie, O. Boico, A. Orian and S. M. Parkhurst (2011). "The Drosophila STUbL protein Degringolade limits HES functions during embryogenesis." Development **138**(9): 1759-1769.
Bartucci, M., R. Dattilo, C. Moriconi, A. Pagliuca, M. Mottolese, G. Federici, A. D. Benedetto, M. Todaro, G. Stassi, F. Sperati, M. I. Amabile, E. Pilozzi, M. Patrizii, M. Biffoni, M. Maugeri-Sacca, S. Piccolo and R. De Maria (2014). "TAZ is required for metastatic activity and chemoresistance of breast cancer stem cells." Oncogene.
Basu, S., N. F. Totty, M. S. Irwin, M. Sudol and J. Downward (2003). "Akt phosphorylates the Yes-associated protein, YAP, to induce interaction with 14-3-3 and attenuation of p73-mediated apoptosis." Mol Cell **11**(1): 11-23.
Beaver, C. M., A. Ahmed and J. R. Masters (2014). "Clonogenicity: holoclones and meroclones contain stem cells." PLoS One **9**(2): e89834.
Beck, B. and C. Blanpain (2013). "Unravelling cancer stem cell potential." Nat Rev Cancer **13**(10): 727-738.
Behrens, J., J. P. von Kries, M. Kuhl, L. Bruhn, D. Wedlich, R. Grosschedl and W. Birchmeier (1996). "Functional interaction of beta-catenin with the transcription factor LEF-1." Nature **382**(6592): 638-642.
Ben-Porath, I., M. W. Thomson, V. J. Carey, R. Ge, G. W. Bell, A. Regev and R. A. Weinberg (2008). "An embryonic stem cell-like gene expression signature in poorly differentiated aggressive human tumors." Nat Genet **40**(5): 499-507.

Ben-Shushan, E., E. Pikarsky, A. Klar and Y. Bergman (1993). "Extinction of Oct-3/4 gene expression in embryonal carcinoma x fibroblast somatic cell hybrids is accompanied by changes in the methylation status, chromatin structure, and transcriptional activity of the Oct-3/4 upstream region." Mol Cell Biol **13**(2): 891-901.
Benhamouche, S., M. Curto, I. Saotome, A. B. Gladden, C. H. Liu, M. Giovannini and A. I. McClatchey (2010). "Nf2/Merlin controls progenitor homeostasis and tumorigenesis in the liver." Genes Dev **24**(16): 1718-1730.
Bennett, D. C. (1983). "Differentiation in mouse melanoma cells: initial reversibility and an on-off stochastic model." Cell **34**(2): 445-453.
Betschinger, J. and J. A. Knoblich (2004). "Dare to be different: asymmetric cell division in Drosophila, C. elegans and vertebrates." Curr Biol **14**(16): R674-685.
Beyrouthy, M. J., K. M. Garner, M. P. Hever, S. J. Freemantle, A. Eastman, E. Dmitrovsky and M. J. Spinella (2009). "High DNA methyltransferase 3B expression mediates 5-aza-deoxycytidine hypersensitivity in testicular germ cell tumors." Cancer Res **69**(24): 9360-9366.
Bhat, K. P., K. L. Salazar, V. Balasubramaniyan, K. Wani, L. Heathcock, F. Hollingsworth, J. D. James, J. Gumin, K. L. Diefes, S. H. Kim, A. Turski, Y. Azodi, Y. Yang, T. Doucette, H. Colman, E. P. Sulman, F. F. Lang, G. Rao, S. Copray, B. D. Vaillant and K. D. Aldape (2011). "The transcriptional coactivator TAZ regulates mesenchymal differentiation in malignant glioma." Genes Dev **25**(24): 2594-2609.
Bhowmick, N. A., A. Chytil, D. Plieth, A. E. Gorska, N. Dumont, S. Shappell, M. K. Washington, E. G. Neilson and H. L. Moses (2004). "TGF-beta signaling in fibroblasts modulates the oncogenic potential of adjacent epithelia." Science **303**(5659): 848-851.
Bjorklund, L. M., R. Sanchez-Pernaute, S. Chung, T. Andersson, I. Y. Chen, K. S. McNaught, A. L. Brownell, B. G. Jenkins, C. Wahlestedt, K. S. Kim and O. Isacson (2002). "Embryonic stem cells develop into functional dopaminergic neurons after transplantation in a Parkinson rat model." Proc Natl Acad Sci U S A **99**(4): 2344-2349.
Blyth, K., E. R. Cameron and J. C. Neil (2005). "The RUNX genes: gain or loss of function in cancer." Nat Rev Cancer **5**(5): 376-387.
Blyth, K., F. Vaillant, A. Jenkins, L. McDonald, M. A. Pringle, C. Huser, T. Stein, J. Neil and E. R. Cameron (2010). "Runx2 in normal tissues and cancer cells: A developing story." Blood Cells Mol Dis **45**(2): 117-123.
Boiko, A. D., O. V. Razorenova, M. van de Rijn, S. M. Swetter, D. L. Johnson, D. P. Ly, P. D. Butler, G. P. Yang, B. Joshua, M. J. Kaplan, M. T. Longaker and I. L. Weissman (2010). "Human melanoma-initiating cells express neural crest nerve growth factor receptor CD271." Nature **466**(7302): 133-137.
Boyer, L. A., T. I. Lee, M. F. Cole, S. E. Johnstone, S. S. Levine, J. P. Zucker, M. G. Guenther, R. M. Kumar, H. L. Murray, R. G. Jenner, D. K. Gifford, D. A. Melton, R. Jaenisch and R. A. Young (2005). "Core transcriptional regulatory circuitry in human embryonic stem cells." Cell **122**(6): 947-956.
Buhmeida, A., A. Merdad, J. Al-Maghrabi, F. Al-Thobaiti, M. Ata, A. Bugis, K. Syrjanen, A. Abuzenadah, A. Chaudhary, M. Gari, M. Al-Qahtani and A. Dallol (2011). "RASSF1A methylation is predictive of poor prognosis in female breast cancer in a background of overall low methylation frequency." Anticancer Res **31**(9): 2975-2981.

Burkert, U., T. von Ruden and E. F. Wagner (1991). "Early fetal hematopoietic development from in vitro differentiated embryonic stem cells." New Biol **3**(7): 698-708.
Busygina, V., M. C. Kottemann, K. L. Scott, S. E. Plon and A. E. Bale (2006). "Multiple endocrine neoplasia type 1 interacts with forkhead transcription factor CHES1 in DNA damage response." Cancer Res **66**(17): 8397-8403.
Buttitta, L. A. and B. A. Edgar (2007). "Mechanisms controlling cell cycle exit upon terminal differentiation." Curr Opin Cell Biol **19**(6): 697-704.
Byun, M. R., M. K. Sung, A. R. Kim, C. H. Lee, E. J. Jang, M. G. Jeong, M. Noh, E. S. Hwang and J. H. Hong (2014). "(-)-Epicatechin gallate (ECG) stimulates osteoblast differentiation via Runt-related transcription factor 2 (RUNX2) and transcriptional coactivator with PDZ-binding motif (TAZ)-mediated transcriptional activation." J Biol Chem **289**(14): 9926-9935.
Cai, J., N. Zhang, Y. Zheng, R. F. de Wilde, A. Maitra and D. Pan (2010). "The Hippo signaling pathway restricts the oncogenic potential of an intestinal regeneration program." Genes Dev **24**(21): 2383-2388.
Callus, B. A., A. M. Verhagen and D. L. Vaux (2006). "Association of mammalian sterile twenty kinases, Mst1 and Mst2, with hSalvador via C-terminal coiled-coil domains, leads to its stabilization and phosphorylation." FEBS J **273**(18): 4264-4276.
Camargo, F. D., S. Gokhale, J. B. Johnnidis, D. Fu, G. W. Bell, R. Jaenisch and T. R. Brummelkamp (2007). "YAP1 increases organ size and expands undifferentiated progenitor cells." Curr Biol **17**(23): 2054-2060.
Cao, X., S. L. Pfaff and F. H. Gage (2008). "YAP regulates neural progenitor cell number via the TEA domain transcription factor." Genes Dev **22**(23): 3320-3334.
Cartwright, P., C. McLean, A. Sheppard, D. Rivett, K. Jones and S. Dalton (2005). "LIF/STAT3 controls ES cell self-renewal and pluripotency by a Myc-dependent mechanism." Development **132**(5): 885-896.
Chambers, I., D. Colby, M. Robertson, J. Nichols, S. Lee, S. Tweedie and A. Smith (2003). "Functional expression cloning of Nanog, a pluripotency sustaining factor in embryonic stem cells." Cell **113**(5): 643-655.
Chambers, I., J. Silva, D. Colby, J. Nichols, B. Nijmeijer, M. Robertson, J. Vrana, K. Jones, L. Grotewold and A. Smith (2007). "Nanog safeguards pluripotency and mediates germline development." Nature **450**(7173): 1230-1234.
Chan, E. H., M. Nousiainen, R. B. Chalamalasetty, A. Schafer, E. A. Nigg and H. H. Sillje (2005). "The Ste20-like kinase Mst2 activates the human large tumor suppressor kinase Lats1." Oncogene **24**(12): 2076-2086.
Chan, S. W., C. J. Lim, Y. F. Chong, A. V. Pobbati, C. Huang and W. Hong (2011). "Hippo pathway-independent restriction of TAZ and YAP by angiomotin." J Biol Chem **286**(9): 7018-7026.
Chan, S. W., C. J. Lim, K. Guo, C. P. Ng, I. Lee, W. Hunziker, Q. Zeng and W. Hong (2008). "A role for TAZ in migration, invasion, and tumorigenesis of breast cancer cells." Cancer Res **68**(8): 2592-2598.
Chan, S. W., C. J. Lim, L. S. Loo, Y. F. Chong, C. Huang and W. Hong (2009). "TEADs mediate nuclear retention of TAZ to promote oncogenic transformation." J Biol Chem **284**(21): 14347-14358.

Chen, H. I. and M. Sudol (1995). "The WW domain of Yes-associated protein binds a proline-rich ligand that differs from the consensus established for Src homology 3-binding modules." Proc Natl Acad Sci U S A **92**(17): 7819-7823.
Chen, J., Y. Li, T. S. Yu, R. M. McKay, D. K. Burns, S. G. Kernie and L. F. Parada (2012). "A restricted cell population propagates glioblastoma growth after chemotherapy." Nature **488**(7412): 522-526.
Chen, L., S. W. Chan, X. Zhang, M. Walsh, C. J. Lim, W. Hong and H. Song (2010). "Structural basis of YAP recognition by TEAD4 in the hippo pathway." Genes Dev **24**(3): 290-300.
Chen, Y., L. Shi, L. Zhang, R. Li, J. Liang, W. Yu, L. Sun, X. Yang, Y. Wang, Y. Zhang and Y. Shang (2008). "The molecular mechanism governing the oncogenic potential of SOX2 in breast cancer." J Biol Chem **283**(26): 17969-17978.
Chen, Y. J., C. T. Liao, P. J. Chen, L. Y. Lee, Y. C. Li, I. H. Chen, H. M. Wang, J. T. Chang, L. J. Chen, T. C. Yen, C. Y. Tang and A. J. Cheng (2011). "Downregulation of Ches1 and other novel genes in oral cancer cells chronically exposed to areca nut extract." Head Neck **33**(2): 257-266.
Chen, Z., G. A. Friedrich and P. Soriano (1994). "Transcriptional enhancer factor 1 disruption by a retroviral gene trap leads to heart defects and embryonic lethality in mice." Genes Dev **8**(19): 2293-2301.
Chew, J. L., Y. H. Loh, W. Zhang, X. Chen, W. L. Tam, L. S. Yeap, P. Li, Y. S. Ang, B. Lim, P. Robson and H. H. Ng (2005). "Reciprocal transcriptional regulation of Pou5f1 and Sox2 via the Oct4/Sox2 complex in embryonic stem cells." Mol Cell Biol **25**(14): 6031-6046.
Chimge, N. O., S. K. Baniwal, J. Luo, S. Coetzee, O. Khalid, B. P. Berman, D. Tripathy, M. J. Ellis and B. Frenkel (2012). "Opposing effects of Runx2 and estradiol on breast cancer cell proliferation: in vitro identification of reciprocally regulated gene signature related to clinical letrozole responsiveness." Clin Cancer Res **18**(3): 901-911.
Chimge, N. O. and B. Frenkel (2013). "The RUNX family in breast cancer: relationships with estrogen signaling." Oncogene **32**(17): 2121-2130.
Chow, C., N. Wong, M. Pagano, S. W. Lun, K. I. Nakayama, K. Nakayama and K. W. Lo (2012). "Regulation of APC/CCdc20 activity by RASSF1A-APC/CCdc20 circuitry." Oncogene **31**(15): 1975-1987.
Clarke, M. F., J. E. Dick, P. B. Dirks, C. J. Eaves, C. H. Jamieson, D. L. Jones, J. Visvader, I. L. Weissman and G. M. Wahl (2006). "Cancer stem cells--perspectives on current status and future directions: AACR Workshop on cancer stem cells." Cancer Res **66**(19): 9339-9344.
Clarke, P. R., I. Hoffmann, G. Draetta and E. Karsenti (1993). "Dephosphorylation of cdc25-C by a type-2A protein phosphatase: specific regulation during the cell cycle in Xenopus egg extracts." Mol Biol Cell **4**(4): 397-411.
Clevers, H. (2005). "Stem cells, asymmetric division and cancer." Nat Genet **37**(10): 1027-1028.
Clevers, H. and R. Nusse (2012). "Wnt/beta-catenin signaling and disease." Cell **149**(6): 1192-1205.
Cockburn, K. and J. Rossant (2010). "Making the blastocyst: lessons from the mouse." J Clin Invest **120**(4): 995-1003.
Cordenonsi, M., F. Zanconato, L. Azzolin, M. Forcato, A. Rosato, C. Frasson, M. Inui, M. Montagner, A. R. Parenti, A. Poletti, M. G. Daidone, S. Dupont, G.

Basso, S. Bicciato and S. Piccolo (2011). "The Hippo transducer TAZ confers cancer stem cell-related traits on breast cancer cells." Cell **147**(4): 759-772.
Costanzo, A., P. Merlo, N. Pediconi, M. Fulco, V. Sartorelli, P. A. Cole, G. Fontemaggi, M. Fanciulli, L. Schiltz, G. Blandino, C. Balsano and M. Levrero (2002). "DNA damage-dependent acetylation of p73 dictates the selective activation of apoptotic target genes." Mol Cell **9**(1): 175-186.
Dallol, A., A. Agathanggelou, S. Tommasi, G. P. Pfeifer, E. R. Maher and F. Latif (2005). "Involvement of the RASSF1A tumor suppressor gene in controlling cell migration." Cancer Res **65**(17): 7653-7659.
Dammann, R., C. Li, J. H. Yoon, P. L. Chin, S. Bates and G. P. Pfeifer (2000). "Epigenetic inactivation of a RAS association domain family protein from the lung tumour suppressor locus 3p21.3." Nat Genet **25**(3): 315-319.
Dammann, R., U. Schagdarsurengin, C. Seidel, M. Strunnikova, M. Rastetter, K. Baier and G. P. Pfeifer (2005). "The tumor suppressor RASSF1A in human carcinogenesis: an update." Histol Histopathol **20**(2): 645-663.
Dammann, R., T. Takahashi and G. P. Pfeifer (2001). "The CpG island of the novel tumor suppressor gene RASSF1A is intensely methylated in primary small cell lung carcinomas." Oncogene **20**(27): 3563-3567.
De Laurenzi, V., G. Raschella, D. Barcaroli, M. Annicchiarico-Petruzzelli, M. Ranalli, M. V. Catani, B. Tanno, A. Costanzo, M. Levrero and G. Melino (2000). "Induction of neuronal differentiation by p73 in a neuroblastoma cell line." J Biol Chem **275**(20): 15226-15231.
de The, H. and Z. Chen (2010). "Acute promyelocytic leukaemia: novel insights into the mechanisms of cure." Nat Rev Cancer **10**(11): 775-783.
DeBerardinis, R. J., J. J. Lum, G. Hatzivassiliou and C. B. Thompson (2008). "The biology of cancer: metabolic reprogramming fuels cell growth and proliferation." Cell Metab **7**(1): 11-20.
Del Re, D. P., T. Matsuda, P. Zhai, S. Gao, G. J. Clark, L. Van Der Weyden and J. Sadoshima (2010). "Proapoptotic Rassf1A/Mst1 signaling in cardiac fibroblasts is protective against pressure overload in mice." J Clin Invest **120**(10): 3555-3567.
Depaepe, V., N. Suarez-Gonzalez, A. Dufour, L. Passante, J. A. Gorski, K. R. Jones, C. Ledent and P. Vanderhaeghen (2005). "Ephrin signalling controls brain size by regulating apoptosis of neural progenitors." Nature **435**(7046): 1244-1250.
Der, C. J., T. G. Krontiris and G. M. Cooper (1982). "Transforming genes of human bladder and lung carcinoma cell lines are homologous to the ras genes of Harvey and Kirsten sarcoma viruses." Proc Natl Acad Sci U S A **79**(11): 3637-3640.
DeVeale, B., I. Brokhman, P. Mohseni, T. Babak, C. Yoon, A. Lin, K. Onishi, A. Tomilin, L. Pevny, P. W. Zandstra, A. Nagy and D. van der Kooy (2013). "Oct4 is required ~E7.5 for proliferation in the primitive streak." PLoS Genet **9**(11): e1003957.
Dickey-Sims, C., A. J. Robertson, D. E. Rupp, J. J. McCarthy and J. A. Coffman (2005). "Runx-dependent expression of PKC is critical for cell survival in the sea urchin embryo." BMC Biol **3**: 18.
Doetschman, T. C., H. Eistetter, M. Katz, W. Schmidt and R. Kemler (1985). "The in vitro development of blastocyst-derived embryonic stem cell lines: formation of visceral yolk sac, blood islands and myocardium." J Embryol Exp Morphol **87**: 27-45.

Doi, A., I. H. Park, B. Wen, P. Murakami, M. J. Aryee, R. Irizarry, B. Herb, C. Ladd-Acosta, J. Rho, S. Loewer, J. Miller, T. Schlaeger, G. Q. Daley and A. P. Feinberg (2009). "Differential methylation of tissue- and cancer-specific CpG island shores distinguishes human induced pluripotent stem cells, embryonic stem cells and fibroblasts." Nat Genet **41**(12): 1350-1353.
Donehower, L. A., M. Harvey, B. L. Slagle, M. J. McArthur, C. A. Montgomery, Jr., J. S. Butel and A. Bradley (1992). "Mice deficient for p53 are developmentally normal but susceptible to spontaneous tumours." Nature **356**(6366): 215-221.
Dong, J., G. Feldmann, J. Huang, S. Wu, N. Zhang, S. A. Comerford, M. F. Gayyed, R. A. Anders, A. Maitra and D. Pan (2007). "Elucidation of a universal size-control mechanism in Drosophila and mammals." Cell **130**(6): 1120-1133.
Donninger, H., M. D. Vos and G. J. Clark (2007). "The RASSF1A tumor suppressor." J Cell Sci **120**(Pt 18): 3163-3172.
Dote, H., D. Cerna, W. E. Burgan, D. J. Carter, M. A. Cerra, M. G. Hollingshead, K. Camphausen and P. J. Tofilon (2005). "Enhancement of in vitro and in vivo tumor cell radiosensitivity by the DNA methylation inhibitor zebularine." Clin Cancer Res **11**(12): 4571-4579.
Dreijerink, K., E. Braga, I. Kuzmin, L. Geil, F. M. Duh, D. Angeloni, B. Zbar, M. I. Lerman, E. J. Stanbridge, J. D. Minna, A. Protopopov, J. Li, V. Kashuba, G. Klein and E. R. Zabarovsky (2001). "The candidate tumor suppressor gene, RASSF1A, from human chromosome 3p21.3 is involved in kidney tumorigenesis." Proc Natl Acad Sci U S A **98**(13): 7504-7509.
Driessens, G., B. Beck, A. Caauwe, B. D. Simons and C. Blanpain (2012). "Defining the mode of tumour growth by clonal analysis." Nature **488**(7412): 527-530.
Dupont, S., L. Morsut, M. Aragona, E. Enzo, S. Giulitti, M. Cordenonsi, F. Zanconato, J. Le Digabel, M. Forcato, S. Bicciato, N. Elvassore and S. Piccolo (2011). "Role of YAP/TAZ in mechanotransduction." Nature **474**(7350): 179-183.
Dupuy, A. J., K. Akagi, D. A. Largaespada, N. G. Copeland and N. A. Jenkins (2005). "Mammalian mutagenesis using a highly mobile somatic Sleeping Beauty transposon system." Nature **436**(7048): 221-226.
El-Kalla, M., C. Onyskiw and S. Baksh (2010). "Functional importance of RASSF1A microtubule localization and polymorphisms." Oncogene **29**(42): 5729-5740.
Esteller, M., P. G. Corn, S. B. Baylin and J. G. Herman (2001). "A gene hypermethylation profile of human cancer." Cancer Res **61**(8): 3225-3229.
Estrabaud, E., I. Lassot, G. Blot, E. Le Rouzic, V. Tanchou, E. Quemeneur, L. Daviet, F. Margottin-Goguet and R. Benarous (2007). "RASSF1C, an isoform of the tumor suppressor RASSF1A, promotes the accumulation of beta-catenin by interacting with betaTrCP." Cancer Res **67**(3): 1054-1061.
Evans, M. (2011). "Discovering pluripotency: 30 years of mouse embryonic stem cells." Nat Rev Mol Cell Biol **12**(10): 680-686.
Evans, M. J. and M. H. Kaufman (1981). "Establishment in culture of pluripotential cells from mouse embryos." Nature **292**(5819): 154-156.
Fairchild, P. J., F. A. Brook, R. L. Gardner, L. Graca, V. Strong, Y. Tone, M. Tone, K. F. Nolan and H. Waldmann (2000). "Directed differentiation of dendritic cells from mouse embryonic stem cells." Curr Biol **10**(23): 1515-1518.

Fan, R., N. G. Kim and B. M. Gumbiner (2013). "Regulation of Hippo pathway by mitogenic growth factors via phosphoinositide 3-kinase and phosphoinositide-dependent kinase-1." Proc Natl Acad Sci U S A **110**(7): 2569-2574.
Fendri, A., A. Masmoudi, A. Khabir, T. Sellami-Boudawara, J. Daoud, M. Frikha, A. Ghorbel, A. Gargouri and R. Mokdad-Gargouri (2009). "Inactivation of RASSF1A, RARbeta2 and DAP-kinase by promoter methylation correlates with lymph node metastasis in nasopharyngeal carcinoma." Cancer Biol Ther **8**(5): 444-451.
Fenton, S. L., A. Dallol, A. Agathanggelou, L. Hesson, J. Ahmed-Choudhury, S. Baksh, C. Sardet, R. Dammann, J. D. Minna, J. Downward, E. R. Maher and F. Latif (2004). "Identification of the E1A-regulated transcription factor p120 E4F as an interacting partner of the RASSF1A candidate tumor suppressor gene." Cancer Res **64**(1): 102-107.
Fillmore, C. M. and C. Kuperwasser (2008). "Human breast cancer cell lines contain stem-like cells that self-renew, give rise to phenotypically diverse progeny and survive chemotherapy." Breast Cancer Res **10**(2): R25.
Finlay, C. A., P. W. Hinds and A. J. Levine (1989). "The p53 proto-oncogene can act as a suppressor of transformation." Cell **57**(7): 1083-1093.
Foley, C. J., H. Freedman, S. L. Choo, C. Onyskiw, N. Y. Fu, V. C. Yu, J. Tuszynski, J. C. Pratt and S. Baksh (2008). "Dynamics of RASSF1A/MOAP-1 association with death receptors." Mol Cell Biol **28**(14): 4520-4535.
Foulds, C. E., M. L. Nelson, A. G. Blaszczak and B. J. Graves (2004). "Ras/mitogen-activated protein kinase signaling activates Ets-1 and Ets-2 by CBP/p300 recruitment." Mol Cell Biol **24**(24): 10954-10964.
Fuchs, E. (2007). "Scratching the surface of skin development." Nature **445**(7130): 834-842.
Gabbert, H., R. Wagner, R. Moll and C. D. Gerharz (1985). "Tumor dedifferentiation: an important step in tumor invasion." Clin Exp Metastasis **3**(4): 257-279.
Gao, F., Y. Zhang, S. Wang, Y. Liu, L. Zheng, J. Yang, W. Huang, Y. Ye, W. Luo and D. Xiao (2014). "Hes1 is involved in the self-renewal and tumourigenicity of stem-like cancer cells in colon cancer." Sci Rep **4**: 3963.
Garcia-Manero, G., H. M. Kantarjian, B. Sanchez-Gonzalez, H. Yang, G. Rosner, S. Verstovsek, M. Rytting, W. G. Wierda, F. Ravandi, C. Koller, L. Xiao, S. Faderl, Z. Estrov, J. Cortes, S. O'Brien, E. Estey, C. Bueso-Ramos, J. Fiorentino, E. Jabbour and J. P. Issa (2006). "Phase 1/2 study of the combination of 5-aza-2'-deoxycytidine with valproic acid in patients with leukemia." Blood **108**(10): 3271-3279.
Gergen, J. P. and B. A. Butler (1988). "Isolation of the Drosophila segmentation gene runt and analysis of its expression during embryogenesis." Genes Dev **2**(9): 1179-1193.
Gillotin, S. and X. Lu (2011). "The ASPP proteins complex and cooperate with p300 to modulate the transcriptional activity of p53." FEBS Lett **585**(12): 1778-1782.
Godin-Heymann, N., Y. Wang, E. Slee and X. Lu (2013). "Phosphorylation of ASPP2 by RAS/MAPK pathway is critical for its full pro-apoptotic function." PLoS One **8**(12): e82022.
Gordon, M. and S. Baksh (2011). "RASSF1A: Not a prototypical Ras effector." Small GTPases **2**(3): 148-157.

Gordon, M., M. El-Kalla, Y. Zhao, Y. Fiteih, J. Law, N. Volodko, A. Anwar-Mohamed, A. O. El-Kadi, L. Liu, J. Odenbach, A. Thiesen, C. Onyskiw, H. A. Ghazaleh, J. Park, S. B. Lee, V. C. Yu, C. Fernandez-Patron, R. T. Alexander, E. Wine and S. Baksh (2013). "The tumor suppressor gene, RASSF1A, is essential for protection against inflammation -induced injury." PLoS One **8**(10): e75483.
Greaves, M. and C. C. Maley (2012). "Clonal evolution in cancer." Nature **481**(7381): 306-313.
Grosse-Gehling, P., C. A. Fargeas, C. Dittfeld, Y. Garbe, M. R. Alison, D. Corbeil and L. A. Kunz-Schughart (2013). "CD133 as a biomarker for putative cancer stem cells in solid tumours: limitations, problems and challenges." J Pathol **229**(3): 355-378.
Guo, C., S. Tommasi, L. Liu, J. K. Yee, R. Dammann and G. P. Pfeifer (2007). "RASSF1A is part of a complex similar to the Drosophila Hippo/Salvador/Lats tumor-suppressor network." Curr Biol **17**(8): 700-705.
Guo, C., X. Zhang and G. P. Pfeifer (2011). "The tumor suppressor RASSF1A prevents dephosphorylation of the mammalian STE20-like kinases MST1 and MST2." J Biol Chem **286**(8): 6253-6261.
Gupta, P. B., C. M. Fillmore, G. Jiang, S. D. Shapira, K. Tao, C. Kuperwasser and E. S. Lander (2011). "Stochastic state transitions give rise to phenotypic equilibrium in populations of cancer cells." Cell **146**(4): 633-644.
Hamilton, G., K. S. Yee, S. Scrace and E. O'Neill (2009). "ATM regulates a RASSF1A-dependent DNA damage response." Curr Biol **19**(23): 2020-2025.
Hanahan, D. and R. A. Weinberg (2011). "Hallmarks of cancer: the next generation." Cell **144**(5): 646-674.
Harjes, E., S. Harjes, S. Wohlgemuth, K. H. Muller, E. Krieger, C. Herrmann and P. Bayer (2006). "GTP-Ras disrupts the intramolecular complex of C1 and RA domains of Nore1." Structure **14**(5): 881-888.
Harvey, K. F., C. M. Pfleger and I. K. Hariharan (2003). "The Drosophila Mst ortholog, hippo, restricts growth and cell proliferation and promotes apoptosis." Cell **114**(4): 457-467.
Harvey, K. F., X. Zhang and D. M. Thomas (2013). "The Hippo pathway and human cancer." Nat Rev Cancer **13**(4): 246-257.
Hattori, N., K. Nishino, Y. G. Ko, N. Hattori, J. Ohgane, S. Tanaka and K. Shiota (2004). "Epigenetic control of mouse Oct-4 gene expression in embryonic stem cells and trophoblast stem cells." J Biol Chem **279**(17): 17063-17069.
Hauf, S., E. Roitinger, B. Koch, C. M. Dittrich, K. Mechtler and J. M. Peters (2005). "Dissociation of cohesin from chromosome arms and loss of arm cohesion during early mitosis depends on phosphorylation of SA2." PLoS Biol **3**(3): e69.
Heallen, T., M. Zhang, J. Wang, M. Bonilla-Claudio, E. Klysik, R. L. Johnson and J. F. Martin (2011). "Hippo pathway inhibits Wnt signaling to restrain cardiomyocyte proliferation and heart size." Science **332**(6028): 458-461.
Hirata, H., S. Yoshiura, T. Ohtsuka, Y. Bessho, T. Harada, K. Yoshikawa and R. Kageyama (2002). "Oscillatory expression of the bHLH factor Hes1 regulated by a negative feedback loop." Science **298**(5594): 840-843.
Hochedlinger, K., Y. Yamada, C. Beard and R. Jaenisch (2005). "Ectopic expression of Oct-4 blocks progenitor-cell differentiation and causes dysplasia in epithelial tissues." Cell **121**(3): 465-477.

Honda, S., M. Haruta, W. Sugawara, F. Sasaki, M. Ohira, T. Matsunaga, H. Yamaoka, H. Horie, N. Ohnuma, A. Nakagawara, E. Hiyama, S. Todo and Y. Kaneko (2008). "The methylation status of RASSF1A promoter predicts responsiveness to chemotherapy and eventual cure in hepatoblastoma patients." Int J Cancer **123**(5): 1117-1125.
Hong, H., K. Takahashi, T. Ichisaka, T. Aoi, O. Kanagawa, M. Nakagawa, K. Okita and S. Yamanaka (2009). "Suppression of induced pluripotent stem cell generation by the p53-p21 pathway." Nature **460**(7259): 1132-1135.
Hong, J. H., E. S. Hwang, M. T. McManus, A. Amsterdam, Y. Tian, R. Kalmukova, E. Mueller, T. Benjamin, B. M. Spiegelman, P. A. Sharp, N. Hopkins and M. B. Yaffe (2005). "TAZ, a transcriptional modulator of mesenchymal stem cell differentiation." Science **309**(5737): 1074-1078.
Hong, J. H. and M. B. Yaffe (2006). "TAZ: a beta-catenin-like molecule that regulates mesenchymal stem cell differentiation." Cell Cycle **5**(2): 176-179.
Hong, W. and K. L. Guan (2012). "The YAP and TAZ transcription co-activators: key downstream effectors of the mammalian Hippo pathway." Semin Cell Dev Biol **23**(7): 785-793.
Hossain, Z., S. M. Ali, H. L. Ko, J. Xu, C. P. Ng, K. Guo, Z. Qi, S. Ponniah, W. Hong and W. Hunziker (2007). "Glomerulocystic kidney disease in mice with a targeted inactivation of Wwtr1." Proc Natl Acad Sci U S A **104**(5): 1631-1636.
Hu, L., G. Chen, H. Yu and X. Qiu (2010). "Clinicopathological significance of RASSF1A reduced expression and hypermethylation in hepatocellular carcinoma." Hepatol Int **4**(1): 423-432.
Huang, J., S. Wu, J. Barrera, K. Matthews and D. Pan (2005). "The Hippo signaling pathway coordinately regulates cell proliferation and apoptosis by inactivating Yorkie, the Drosophila Homolog of YAP." Cell **122**(3): 421-434.
Hulsken, J., W. Birchmeier and J. Behrens (1994). "E-cadherin and APC compete for the interaction with beta-catenin and the cytoskeleton." J Cell Biol **127**(6 Pt 2): 2061-2069.
Humbert, P. O., N. A. Grzeschik, A. M. Brumby, R. Galea, I. Elsum and H. E. Richardson (2008). "Control of tumourigenesis by the Scribble/Dlg/Lgl polarity module." Oncogene **27**(55): 6888-6907.
Hussein, S. M., N. N. Batada, S. Vuoristo, R. W. Ching, R. Autio, E. Narva, S. Ng, M. Sourour, R. Hamalainen, C. Olsson, K. Lundin, M. Mikkola, R. Trokovic, M. Peitz, O. Brustle, D. P. Bazett-Jones, K. Alitalo, R. Lahesmaa, A. Nagy and T. Otonkoski (2011). "Copy number variation and selection during reprogramming to pluripotency." Nature **471**(7336): 58-62.
Hwang, E., K. S. Ryu, K. Paakkonen, P. Guntert, H. K. Cheong, D. S. Lim, J. O. Lee, Y. H. Jeon and C. Cheong (2007). "Structural insight into dimeric interaction of the SARAH domains from Mst1 and RASSF family proteins in the apoptosis pathway." Proc Natl Acad Sci U S A **104**(22): 9236-9241.
Ikeda, M., A. Kawata, M. Nishikawa, Y. Tateishi, M. Yamaguchi, K. Nakagawa, S. Hirabayashi, Y. Bao, S. Hidaka, Y. Hirata and Y. Hata (2009). "Hippo pathway-dependent and -independent roles of RASSF6." Sci Signal **2**(90): ra59.
Imajo, M., K. Miyatake, A. Iimura, A. Miyamoto and E. Nishida (2012). "A molecular mechanism that links Hippo signalling to the inhibition of Wnt/beta-catenin signalling." EMBO J **31**(5): 1109-1122.
International Stem Cell, I., O. Adewumi, B. Aflatoonian, L. Ahrlund-Richter, M. Amit, P. W. Andrews, G. Beighton, P. A. Bello, N. Benvenisty, L. S. Berry, S.

Bevan, B. Blum, J. Brooking, K. G. Chen, A. B. Choo, G. A. Churchill, M. Corbel, I. Damjanov, J. S. Draper, P. Dvorak, K. Emanuelsson, R. A. Fleck, A. Ford, K. Gertow, M. Gertsenstein, P. J. Gokhale, R. S. Hamilton, A. Hampl, L. E. Healy, O. Hovatta, J. Hyllner, M. P. Imreh, J. Itskovitz-Eldor, J. Jackson, J. L. Johnson, M. Jones, K. Kee, B. L. King, B. B. Knowles, M. Lako, F. Lebrin, B. S. Mallon, D. Manning, Y. Mayshar, R. D. McKay, A. E. Michalska, M. Mikkola, M. Mileikovsky, S. L. Minger, H. D. Moore, C. L. Mummery, A. Nagy, N. Nakatsuji, C. M. O'Brien, S. K. Oh, C. Olsson, T. Otonkoski, K. Y. Park, R. Passier, H. Patel, M. Patel, R. Pedersen, M. F. Pera, M. S. Piekarczyk, R. A. Pera, B. E. Reubinoff, A. J. Robins, J. Rossant, P. Rugg-Gunn, T. C. Schulz, H. Semb, E. S. Sherrer, H. Siemen, G. N. Stacey, M. Stojkovic, H. Suemori, J. Szatkiewicz, T. Turetsky, T. Tuuri, S. van den Brink, K. Vintersten, S. Vuoristo, D. Ward, T. A. Weaver, L. A. Young and W. Zhang (2007). "Characterization of human embryonic stem cell lines by the International Stem Cell Initiative." Nat Biotechnol **25**(7): 803-816.

Jacquemin, P., J. J. Hwang, J. A. Martial, P. Dolle and I. Davidson (1996). "A novel family of developmentally regulated mammalian transcription factors containing the TEA/ATTS DNA binding domain." J Biol Chem **271**(36): 21775-21785.

Jaenisch, R. and R. Young (2008). "Stem cells, the molecular circuitry of pluripotency and nuclear reprogramming." Cell **132**(4): 567-582.

Jeong, H., S. Bae, S. Y. An, M. R. Byun, J. H. Hwang, M. B. Yaffe, J. H. Hong and E. S. Hwang (2010). "TAZ as a novel enhancer of MyoD-mediated myogenic differentiation." FASEB J **24**(9): 3310-3320.

Jiang, L., R. Rong, M. S. Sheikh and Y. Huang (2011). "Cullin-4A.DNA damage-binding protein 1 E3 ligase complex targets tumor suppressor RASSF1A for degradation during mitosis." J Biol Chem **286**(9): 6971-6978.

Jiang, L., R. Rong, M. S. Sheikh and Y. Huang (2014). "Mitotic arrest by tumor suppressor RASSF1A is regulated via CHK1 phosphorylation." Mol Cancer Res **12**(1): 119-129.

Jin, F., Y. Li, J. R. Dixon, S. Selvaraj, Z. Ye, A. Y. Lee, C. A. Yen, A. D. Schmitt, C. A. Espinoza and B. Ren (2013). "A high-resolution map of the three-dimensional chromatin interactome in human cells." Nature **503**(7475): 290-294.

Jones, P. A. and P. W. Laird (1999). "Cancer epigenetics comes of age." Nat Genet **21**(2): 163-167.

Justice, R. W., O. Zilian, D. F. Woods, M. Noll and P. J. Bryant (1995). "The Drosophila tumor suppressor gene warts encodes a homolog of human myotonic dystrophy kinase and is required for the control of cell shape and proliferation." Genes Dev **9**(5): 534-546.

Kageyama, R., T. Ohtsuka and T. Kobayashi (2007). "The Hes gene family: repressors and oscillators that orchestrate embryogenesis." Development **134**(7): 1243-1251.

Kajabova, V., B. Smolkova, I. Zmetakova, K. Sebova, T. Krivulcik, V. Bella, K. Kajo, K. Machalekova and I. Fridrichova (2013). "RASSF1A Promoter Methylation Levels Positively Correlate with Estrogen Receptor Expression in Breast Cancer Patients." Transl Oncol **6**(3): 297-304.

Kaneko, K. J., E. B. Cullinan, K. E. Latham and M. L. DePamphilis (1997). "Transcription factor mTEAD-2 is selectively expressed at the beginning of zygotic gene expression in the mouse." Development **124**(10): 1963-1973.

Karahoca, M. and R. L. Momparler (2013). "Pharmacokinetic and pharmacodynamic analysis of 5-aza-2'-deoxycytidine (decitabine) in the design of its dose-schedule for cancer therapy." Clin Epigenetics **5**(1): 3.
Kawai, Y., S. Sakano, Y. Suehiro, T. Okada, Y. Korenaga, T. Hara, K. Naito, H. Matsuyama and Y. Hinoda (2010). "Methylation level of the RASSF1A promoter is an independent prognostic factor for clear-cell renal cell carcinoma." Ann Oncol **21**(8): 1612-1617.
Kawamura, T., J. Suzuki, Y. V. Wang, S. Menendez, L. B. Morera, A. Raya, G. M. Wahl and J. C. Izpisua Belmonte (2009). "Linking the p53 tumour suppressor pathway to somatic cell reprogramming." Nature **460**(7259): 1140-1144.
Kelly, K. F., D. Y. Ng, G. Jayakumaran, G. A. Wood, H. Koide and B. W. Doble (2011). "beta-catenin enhances Oct-4 activity and reinforces pluripotency through a TCF-independent mechanism." Cell Stem Cell **8**(2): 214-227.
Keng, V. W., K. Yae, T. Hayakawa, S. Mizuno, Y. Uno, K. Yusa, C. Kokubu, T. Kinoshita, K. Akagi, N. A. Jenkins, N. G. Copeland, K. Horie and J. Takeda (2005). "Region-specific saturation germline mutagenesis in mice using the Sleeping Beauty transposon system." Nat Methods **2**(10): 763-769.
Kilbey, A., K. Blyth, S. Wotton, A. Terry, A. Jenkins, M. Bell, L. Hanlon, E. R. Cameron and J. C. Neil (2007). "Runx2 disruption promotes immortalization and confers resistance to oncogene-induced senescence in primary murine fibroblasts." Cancer Res **67**(23): 11263-11271.
Kim, J. S., Y. Chae, Y. S. Ha, I. Y. Kim, S. S. Byun, S. J. Yun and W. J. Kim (2012). "Ras association domain family 1A: a promising prognostic marker in recurrent nonmuscle invasive bladder cancer." Clin Genitourin Cancer **10**(2): 114-120.
Kim, K., A. Doi, B. Wen, K. Ng, R. Zhao, P. Cahan, J. Kim, M. J. Aryee, H. Ji, L. I. Ehrlich, A. Yabuuchi, A. Takeuchi, K. C. Cunniff, H. Hongguang, S. McKinney-Freeman, O. Naveiras, T. J. Yoon, R. A. Irizarry, N. Jung, J. Seita, J. Hanna, P. Murakami, R. Jaenisch, R. Weissleder, S. H. Orkin, I. L. Weissman, A. P. Feinberg and G. Q. Daley (2010). "Epigenetic memory in induced pluripotent stem cells." Nature **467**(7313): 285-290.
Kim, N. G., E. Koh, X. Chen and B. M. Gumbiner (2011). "E-cadherin mediates contact inhibition of proliferation through Hippo signaling-pathway components." Proc Natl Acad Sci U S A **108**(29): 11930-11935.
Kitagawa, D., H. Kajiho, T. Negishi, S. Ura, T. Watanabe, T. Wada, H. Ichijo, T. Katada and H. Nishina (2006). "Release of RASSF1C from the nucleus by Daxx degradation links DNA damage and SAPK/JNK activation." EMBO J **25**(14): 3286-3297.
Kobayashi, T., H. Mizuno, I. Imayoshi, C. Furusawa, K. Shirahige and R. Kageyama (2009). "The cyclic gene Hes1 contributes to diverse differentiation responses of embryonic stem cells." Genes Dev **23**(16): 1870-1875.
Koch, F., R. Fenouil, M. Gut, P. Cauchy, T. K. Albert, J. Zacarias-Cabeza, S. Spicuglia, A. L. de la Chapelle, M. Heidemann, C. Hintermair, D. Eick, I. Gut, P. Ferrier and J. C. Andrau (2011). "Transcription initiation platforms and GTF recruitment at tissue-specific enhancers and promoters." Nat Struct Mol Biol **18**(8): 956-963.
Komori, T., H. Yagi, S. Nomura, A. Yamaguchi, K. Sasaki, K. Deguchi, Y. Shimizu, R. T. Bronson, Y. H. Gao, M. Inada, M. Sato, R. Okamoto, Y. Kitamura, S. Yoshiki and T. Kishimoto (1997). "Targeted disruption of Cbfa1

results in a complete lack of bone formation owing to maturational arrest of osteoblasts." Cell **89**(5): 755-764.
Kompier, L. C., I. Lurkin, M. N. van der Aa, B. W. van Rhijn, T. H. van der Kwast and E. C. Zwarthoff (2010). "FGFR3, HRAS, KRAS, NRAS and PIK3CA mutations in bladder cancer and their potential as biomarkers for surveillance and therapy." PLoS One **5**(11): e13821.
Kreso, A. and J. E. Dick (2014). "Evolution of the cancer stem cell model." Cell Stem Cell **14**(3): 275-291.
Kumar, S. M., S. Liu, H. Lu, H. Zhang, P. J. Zhang, P. A. Gimotty, M. Guerra, W. Guo and X. Xu (2012). "Acquired cancer stem cell phenotypes through Oct4-mediated dedifferentiation." Oncogene **31**(47): 4898-4911.
Kuroda, T., M. Tada, H. Kubota, H. Kimura, S. Y. Hatano, H. Suemori, N. Nakatsuji and T. Tada (2005). "Octamer and Sox elements are required for transcriptional cis regulation of Nanog gene expression." Mol Cell Biol **25**(6): 2475-2485.
Lallemand, D., M. Curto, I. Saotome, M. Giovannini and A. I. McClatchey (2003). "NF2 deficiency promotes tumorigenesis and metastasis by destabilizing adherens junctions." Genes Dev **17**(9): 1090-1100.
Lane, D. P. and L. V. Crawford (1979). "T antigen is bound to a host protein in SV40-transformed cells." Nature **278**(5701): 261-263.
Lapi, E., S. Di Agostino, S. Donzelli, H. Gal, E. Domany, G. Rechavi, P. P. Pandolfi, D. Givol, S. Strano, X. Lu and G. Blandino (2008). "PML, YAP, and p73 are components of a proapoptotic autoregulatory feedback loop." Mol Cell **32**(6): 803-814.
Laurent, L. C., I. Ulitsky, I. Slavin, H. Tran, A. Schork, R. Morey, C. Lynch, J. V. Harness, S. Lee, M. J. Barrero, S. Ku, M. Martynova, R. Semechkin, V. Galat, J. Gottesfeld, J. C. Izpisua Belmonte, C. Murry, H. S. Keirstead, H. S. Park, U. Schmidt, A. L. Laslett, F. J. Muller, C. M. Nievergelt, R. Shamir and J. F. Loring (2011). "Dynamic changes in the copy number of pluripotency and cell proliferation genes in human ESCs and iPSCs during reprogramming and time in culture." Cell Stem Cell **8**(1): 106-118.
Lechler, T. and E. Fuchs (2005). "Asymmetric cell divisions promote stratification and differentiation of mammalian skin." Nature **437**(7056): 275-280.
Lee, J. H., T. S. Kim, T. H. Yang, B. K. Koo, S. P. Oh, K. P. Lee, H. J. Oh, S. H. Lee, Y. Y. Kong, J. M. Kim and D. S. Lim (2008). "A crucial role of WW45 in developing epithelial tissues in the mouse." EMBO J **27**(8): 1231-1242.
Lee, M. T., A. R. Bonneau, C. M. Takacs, A. A. Bazzini, K. R. DiVito, E. S. Fleming and A. J. Giraldez (2013). "Nanog, Pou5f1 and SoxB1 activate zygotic gene expression during the maternal-to-zygotic transition." Nature **503**(7476): 360-364.
Lei, Q. Y., H. Zhang, B. Zhao, Z. Y. Zha, F. Bai, X. H. Pei, S. Zhao, Y. Xiong and K. L. Guan (2008). "TAZ promotes cell proliferation and epithelial-mesenchymal transition and is inhibited by the hippo pathway." Mol Cell Biol **28**(7): 2426-2436.
Leis, O., A. Eguiara, E. Lopez-Arribillaga, M. J. Alberdi, S. Hernandez-Garcia, K. Elorriaga, A. Pandiella, R. Rezola and A. G. Martin (2012). "Sox2 expression in breast tumours and activation in breast cancer stem cells." Oncogene **31**(11): 1354-1365.

Lendahl, U., L. B. Zimmerman and R. D. McKay (1990). "CNS stem cells express a new class of intermediate filament protein." Cell **60**(4): 585-595.
Lerman, M. I. and J. D. Minna (2000). "The 630-kb lung cancer homozygous deletion region on human chromosome 3p21.3: identification and evaluation of the resident candidate tumor suppressor genes. The International Lung Cancer Chromosome 3p21.3 Tumor Suppressor Gene Consortium." Cancer Res **60**(21): 6116-6133.
Leung, C. Y. and M. Zernicka-Goetz (2013). "Angiomotin prevents pluripotent lineage differentiation in mouse embryos via Hippo pathway-dependent and -independent mechanisms." Nat Commun **4**: 2251.
Levanon, D., D. Bettoun, C. Harris-Cerruti, E. Woolf, V. Negreanu, R. Eilam, Y. Bernstein, D. Goldenberg, C. Xiao, M. Fliegauf, E. Kremer, F. Otto, O. Brenner, A. Lev-Tov and Y. Groner (2002). "The Runx3 transcription factor regulates development and survival of TrkC dorsal root ganglia neurons." EMBO J **21**(13): 3454-3463.
Levy, D., Y. Adamovich, N. Reuven and Y. Shaul (2008). "Yap1 phosphorylation by c-Abl is a critical step in selective activation of proapoptotic genes in response to DNA damage." Mol Cell **29**(3): 350-361.
Li, P., Y. Chen, K. K. Mak, C. K. Wong, C. C. Wang and P. Yuan (2013). "Functional role of Mst1/Mst2 in embryonic stem cell differentiation." PLoS One **8**(11): e79867.
Li, Q. L., K. Ito, C. Sakakura, H. Fukamachi, K. Inoue, X. Z. Chi, K. Y. Lee, S. Nomura, C. W. Lee, S. B. Han, H. M. Kim, W. J. Kim, H. Yamamoto, N. Yamashita, T. Yano, T. Ikeda, S. Itohara, J. Inazawa, T. Abe, A. Hagiwara, H. Yamagishi, A. Ooe, A. Kaneda, T. Sugimura, T. Ushijima, S. C. Bae and Y. Ito (2002). "Causal relationship between the loss of RUNX3 expression and gastric cancer." Cell **109**(1): 113-124.
Li, V. S. and H. Clevers (2013). "Intestinal regeneration: YAP-tumor suppressor and oncoprotein?" Curr Biol **23**(3): R110-112.
Li, V. S., S. S. Ng, P. J. Boersema, T. Y. Low, W. R. Karthaus, J. P. Gerlach, S. Mohammed, A. J. Heck, M. M. Maurice, T. Mahmoudi and H. Clevers (2012). "Wnt signaling through inhibition of beta-catenin degradation in an intact Axin1 complex." Cell **149**(6): 1245-1256.
Li, Y., M. A. Hibbs, A. L. Gard, N. A. Shylo and K. Yun (2012). "Genome-wide analysis of N1ICD/RBPJ targets in vivo reveals direct transcriptional regulation of Wnt, SHH, and hippo pathway effectors by Notch1." Stem Cells **30**(4): 741-752.
Li, Z., B. Zhao, P. Wang, F. Chen, Z. Dong, H. Yang, K. L. Guan and Y. Xu (2010). "Structural insights into the YAP and TEAD complex." Genes Dev **24**(3): 235-240.
Lian, I., J. Kim, H. Okazawa, J. Zhao, B. Zhao, J. Yu, A. Chinnaiyan, M. A. Israel, L. S. Goldstein, R. Abujarour, S. Ding and K. L. Guan (2010). "The role of YAP transcription coactivator in regulating stem cell self-renewal and differentiation." Genes Dev **24**(11): 1106-1118.
Lieberman-Aiden, E., N. L. van Berkum, L. Williams, M. Imakaev, T. Ragoczy, A. Telling, I. Amit, B. R. Lajoie, P. J. Sabo, M. O. Dorschner, R. Sandstrom, B. Bernstein, M. A. Bender, M. Groudine, A. Gnirke, J. Stamatoyannopoulos, L. A. Mirny, E. S. Lander and J. Dekker (2009). "Comprehensive mapping of long-range interactions reveals folding principles of the human genome." Science **326**(5950): 289-293.

Lin, T., C. Chao, S. Saito, S. J. Mazur, M. E. Murphy, E. Appella and Y. Xu (2005). "p53 induces differentiation of mouse embryonic stem cells by suppressing Nanog expression." Nat Cell Biol **7**(2): 165-171.
Liu-Chittenden, Y., B. Huang, J. S. Shim, Q. Chen, S. J. Lee, R. A. Anders, J. O. Liu and D. Pan (2012). "Genetic and pharmacological disruption of the TEAD-YAP complex suppresses the oncogenic activity of YAP." Genes Dev **26**(12): 1300-1305.
Liu, C. Y., X. Lv, T. Li, Y. Xu, X. Zhou, S. Zhao, Y. Xiong, Q. Y. Lei and K. L. Guan (2011). "PP1 cooperates with ASPP2 to dephosphorylate and activate TAZ." J Biol Chem **286**(7): 5558-5566.
Liu, C. Y., Z. Y. Zha, X. Zhou, H. Zhang, W. Huang, D. Zhao, T. Li, S. W. Chan, C. J. Lim, W. Hong, S. Zhao, Y. Xiong, Q. Y. Lei and K. L. Guan (2010). "The hippo tumor pathway promotes TAZ degradation by phosphorylating a phosphodegron and recruiting the SCF{beta}-TrCP E3 ligase." J Biol Chem **285**(48): 37159-37169.
Liu, L., C. Guo, R. Dammann, S. Tommasi and G. P. Pfeifer (2008). "RASSF1A interacts with and activates the mitotic kinase Aurora-A." Oncogene **27**(47): 6175-6186.
Liu, L., S. Tommasi, D. H. Lee, R. Dammann and G. P. Pfeifer (2003). "Control of microtubule stability by the RASSF1A tumor suppressor." Oncogene **22**(50): 8125-8136.
Liu, L., J. H. Yoon, R. Dammann and G. P. Pfeifer (2002). "Frequent hypermethylation of the RASSF1A gene in prostate cancer." Oncogene **21**(44): 6835-6840.
Liu, X., L. F. Sempere, H. Ouyang, V. A. Memoli, A. S. Andrew, Y. Luo, E. Demidenko, M. Korc, W. Shi, M. Preis, K. H. Dragnev, H. Li, J. Direnzo, M. Bak, S. J. Freemantle, S. Kauppinen and E. Dmitrovsky (2010). "MicroRNA-31 functions as an oncogenic microRNA in mouse and human lung cancer cells by repressing specific tumor suppressors." J Clin Invest **120**(4): 1298-1309.
Loh, Y. H., Q. Wu, J. L. Chew, V. B. Vega, W. Zhang, X. Chen, G. Bourque, J. George, B. Leong, J. Liu, K. Y. Wong, K. W. Sung, C. W. Lee, X. D. Zhao, K. P. Chiu, L. Lipovich, V. A. Kuznetsov, P. Robson, L. W. Stanton, C. L. Wei, Y. Ruan, B. Lim and H. H. Ng (2006). "The Oct4 and Nanog transcription network regulates pluripotency in mouse embryonic stem cells." Nat Genet **38**(4): 431-440.
Lu, M., H. Breyssens, V. Salter, S. Zhong, Y. Hu, C. Baer, I. Ratnayaka, A. Sullivan, N. R. Brown, J. Endicott, S. Knapp, B. M. Kessler, M. R. Middleton, C. Siebold, E. Y. Jones, E. V. Sviderskaya, J. Cebon, T. John, O. L. Caballero, C. R. Goding and X. Lu (2013). "Restoring p53 function in human melanoma cells by inhibiting MDM2 and cyclin B1/CDK1-phosphorylated nuclear iASPP." Cancer Cell **23**(5): 618-633.
Lu, R., Y. Qu, J. Ge, L. Zhang, Z. Su, S. C. Pflugfelder and D. Q. Li (2012). "Transcription factor TCF4 maintains the properties of human corneal epithelial stem cells." Stem Cells **30**(4): 753-761.
Luga, V., L. Zhang, A. M. Viloria-Petit, A. A. Ogunjimi, M. R. Inanlou, E. Chiu, M. Buchanan, A. N. Hosein, M. Basik and J. L. Wrana (2012). "Exosomes mediate stromal mobilization of autocrine Wnt-PCP signaling in breast cancer cell migration." Cell **151**(7): 1542-1556.

Macias, M. J., M. Hyvonen, E. Baraldi, J. Schultz, M. Sudol, M. Saraste and H. Oschkinat (1996). "Structure of the WW domain of a kinase-associated protein complexed with a proline-rich peptide." Nature **382**(6592): 646-649.
Magnifico, A., L. Albano, S. Campaner, D. Delia, F. Castiglioni, P. Gasparini, G. Sozzi, E. Fontanella, S. Menard and E. Tagliabue (2009). "Tumor-initiating cells of HER2-positive carcinoma cell lines express the highest oncoprotein levels and are sensitive to trastuzumab." Clin Cancer Res **15**(6): 2010-2021.
Mahoney, W. M., Jr., J. H. Hong, M. B. Yaffe and I. K. Farrance (2005). "The transcriptional co-activator TAZ interacts differentially with transcriptional enhancer factor-1 (TEF-1) family members." Biochem J **388**(Pt 1): 217-225.
Major, M. B., N. D. Camp, J. D. Berndt, X. Yi, S. J. Goldenberg, C. Hubbert, T. L. Biechele, A. C. Gingras, N. Zheng, M. J. Maccoss, S. Angers and R. T. Moon (2007). "Wilms tumor suppressor WTX negatively regulates WNT/beta-catenin signaling." Science **316**(5827): 1043-1046.
Marion, R. M., K. Strati, H. Li, M. Murga, R. Blanco, S. Ortega, O. Fernandez-Capetillo, M. Serrano and M. A. Blasco (2009). "A p53-mediated DNA damage response limits reprogramming to ensure iPS cell genomic integrity." Nature **460**(7259): 1149-1153.
Martin, J. W., M. Zielenska, G. S. Stein, A. J. van Wijnen and J. A. Squire (2011). "The Role of RUNX2 in Osteosarcoma Oncogenesis." Sarcoma **2011**: 282745.
Masui, S., Y. Nakatake, Y. Toyooka, D. Shimosato, R. Yagi, K. Takahashi, H. Okochi, A. Okuda, R. Matoba, A. A. Sharov, M. S. Ko and H. Niwa (2007). "Pluripotency governed by Sox2 via regulation of Oct3/4 expression in mouse embryonic stem cells." Nat Cell Biol **9**(6): 625-635.
Matallanas, D., D. Romano, K. Yee, K. Meissl, L. Kucerova, D. Piazzolla, M. Baccarini, J. K. Vass, W. Kolch and E. O'Neill (2007). "RASSF1A elicits apoptosis through an MST2 pathway directing proapoptotic transcription by the p73 tumor suppressor protein." Mol Cell **27**(6): 962-975.
Mates, L., M. K. Chuah, E. Belay, B. Jerchow, N. Manoj, A. Acosta-Sanchez, D. P. Grzela, A. Schmitt, K. Becker, J. Matrai, L. Ma, E. Samara-Kuko, C. Gysemans, D. Pryputniewicz, C. Miskey, B. Fletcher, T. VandenDriessche, Z. Ivics and Z. Izsvak (2009). "Molecular evolution of a novel hyperactive Sleeping Beauty transposase enables robust stable gene transfer in vertebrates." Nat Genet **41**(6): 753-761.
Matsui, Y., N. Nakano, D. Shao, S. Gao, W. Luo, C. Hong, P. Zhai, E. Holle, X. Yu, N. Yabuta, W. Tao, T. Wagner, H. Nojima and J. Sadoshima (2008). "Lats2 is a negative regulator of myocyte size in the heart." Circ Res **103**(11): 1309-1318.
Mauviel, A., F. Nallet-Staub and X. Varelas (2012). "Integrating developmental signals: a Hippo in the (path)way." Oncogene **31**(14): 1743-1756.
Mayshar, Y., U. Ben-David, N. Lavon, J. C. Biancotti, B. Yakir, A. T. Clark, K. Plath, W. E. Lowry and N. Benvenisty (2010). "Identification and classification of chromosomal aberrations in human induced pluripotent stem cells." Cell Stem Cell **7**(4): 521-531.
McClements, L., A. Yakkundi, A. Papaspyropoulos, H. Harrison, M. P. Ablett, P. V. Jithesh, H. D. McKeen, R. Bennett, C. Donley, A. Kissenpfennig, S. McIntosh, H. O. McCarthy, E. O'Neill, R. B. Clarke and T. Robson (2013). "Targeting treatment-resistant breast cancer stem cells with FKBPL and its

peptide derivative, AD-01, via the CD44 pathway." Clin Cancer Res **19**(14): 3881-3893.
Miura, K., Y. Okada, T. Aoi, A. Okada, K. Takahashi, K. Okita, M. Nakagawa, M. Koyanagi, K. Tanabe, M. Ohnuki, D. Ogawa, E. Ikeda, H. Okano and S. Yamanaka (2009). "Variation in the safety of induced pluripotent stem cell lines." Nat Biotechnol **27**(8): 743-745.
Mohrin, M., E. Bourke, D. Alexander, M. R. Warr, K. Barry-Holson, M. M. Le Beau, C. G. Morrison and E. Passegue (2010). "Hematopoietic stem cell quiescence promotes error-prone DNA repair and mutagenesis." Cell Stem Cell **7**(2): 174-185.
Molenaar, M., M. van de Wetering, M. Oosterwegel, J. Peterson-Maduro, S. Godsave, V. Korinek, J. Roose, O. Destree and H. Clevers (1996). "XTcf-3 transcription factor mediates beta-catenin-induced axis formation in Xenopus embryos." Cell **86**(3): 391-399.
Molkentin, J. D., Q. Lin, S. A. Duncan and E. N. Olson (1997). "Requirement of the transcription factor GATA4 for heart tube formation and ventral morphogenesis." Genes Dev **11**(8): 1061-1072.
Monk, M. and C. Holding (2001). "Human embryonic genes re-expressed in cancer cells." Oncogene **20**(56): 8085-8091.
Morin-Kensicki, E. M., B. N. Boone, M. Howell, J. R. Stonebraker, J. Teed, J. G. Alb, T. R. Magnuson, W. O'Neal and S. L. Milgram (2006). "Defects in yolk sac vasculogenesis, chorioallantoic fusion, and embryonic axis elongation in mice with targeted disruption of Yap65." Mol Cell Biol **26**(1): 77-87.
Morrison, H., L. S. Sherman, J. Legg, F. Banine, C. Isacke, C. A. Haipek, D. H. Gutmann, H. Ponta and P. Herrlich (2001). "The NF2 tumor suppressor gene product, merlin, mediates contact inhibition of growth through interactions with CD44." Genes Dev **15**(8): 968-980.
Morrison, S. J. and J. Kimble (2006). "Asymmetric and symmetric stem-cell divisions in development and cancer." Nature **441**(7097): 1068-1074.
Mullighan, C. G., J. Zhang, L. H. Kasper, S. Lerach, D. Payne-Turner, L. A. Phillips, S. L. Heatley, L. Holmfeldt, J. R. Collins-Underwood, J. Ma, K. H. Buetow, C. H. Pui, S. D. Baker, P. K. Brindle and J. R. Downing (2011). "CREBBP mutations in relapsed acute lymphoblastic leukaemia." Nature **471**(7337): 235-239.
Murry, C. E. and G. Keller (2008). "Differentiation of embryonic stem cells to clinically relevant populations: lessons from embryonic development." Cell **132**(4): 661-680.
Nakatake, Y., N. Fukui, Y. Iwamatsu, S. Masui, K. Takahashi, R. Yagi, K. Yagi, J. Miyazaki, R. Matoba, M. S. Ko and H. Niwa (2006). "Klf4 cooperates with Oct3/4 and Sox2 to activate the Lefty1 core promoter in embryonic stem cells." Mol Cell Biol **26**(20): 7772-7782.
Newton, A. C. (1995). "Protein kinase C. Seeing two domains." Curr Biol **5**(9): 973-976.
Nguyen, L. V., R. Vanner, P. Dirks and C. J. Eaves (2012). "Cancer stem cells: an evolving concept." Nat Rev Cancer **12**(2): 133-143.
Nichols, J., B. Zevnik, K. Anastassiadis, H. Niwa, D. Klewe-Nebenius, I. Chambers, H. Scholer and A. Smith (1998). "Formation of pluripotent stem cells in the mammalian embryo depends on the POU transcription factor Oct4." Cell **95**(3): 379-391.

Nishimoto, M., A. Fukushima, A. Okuda and M. Muramatsu (1999). "The gene for the embryonic stem cell coactivator UTF1 carries a regulatory element which selectively interacts with a complex composed of Oct-3/4 and Sox-2." Mol Cell Biol **19**(8): 5453-5465.
Nishioka, N., K. Inoue, K. Adachi, H. Kiyonari, M. Ota, A. Ralston, N. Yabuta, S. Hirahara, R. O. Stephenson, N. Ogonuki, R. Makita, H. Kurihara, E. M. Morin-Kensicki, H. Nojima, J. Rossant, K. Nakao, H. Niwa and H. Sasaki (2009). "The Hippo signaling pathway components Lats and Yap pattern Tead4 activity to distinguish mouse trophectoderm from inner cell mass." Dev Cell **16**(3): 398-410.
Niwa, H., J. Miyazaki and A. G. Smith (2000). "Quantitative expression of Oct-3/4 defines differentiation, dedifferentiation or self-renewal of ES cells." Nat Genet **24**(4): 372-376.
Noordermeer, J., J. Klingensmith, N. Perrimon and R. Nusse (1994). "dishevelled and armadillo act in the wingless signalling pathway in Drosophila." Nature **367**(6458): 80-83.
Nordhoff, V., K. Hubner, A. Bauer, I. Orlova, A. Malapetsa and H. R. Scholer (2001). "Comparative analysis of human, bovine, and murine Oct-4 upstream promoter sequences." Mamm Genome **12**(4): 309-317.
O'Neill, E., L. Rushworth, M. Baccarini and W. Kolch (2004). "Role of the kinase MST2 in suppression of apoptosis by the proto-oncogene product Raf-1." Science **306**(5705): 2267-2270.
Oh, H. J., K. K. Lee, S. J. Song, M. S. Jin, M. S. Song, J. H. Lee, C. R. Im, J. O. Lee, S. Yonehara and D. S. Lim (2006). "Role of the tumor suppressor RASSF1A in Mst1-mediated apoptosis." Cancer Res **66**(5): 2562-2569.
Ohtsuka, T., M. Ishibashi, G. Gradwohl, S. Nakanishi, F. Guillemot and R. Kageyama (1999). "Hes1 and Hes5 as notch effectors in mammalian neuronal differentiation." EMBO J **18**(8): 2196-2207.
Oka, T., V. Mazack and M. Sudol (2008). "Mst2 and Lats kinases regulate apoptotic function of Yes kinase-associated protein (YAP)." J Biol Chem **283**(41): 27534-27546.
Okazawa, H., K. Okamoto, F. Ishino, T. Ishino-Kaneko, S. Takeda, Y. Toyoda, M. Muramatsu and H. Hamada (1991). "The oct3 gene, a gene for an embryonic transcription factor, is controlled by a retinoic acid repressible enhancer." EMBO J **10**(10): 2997-3005.
Okuda, T., J. van Deursen, S. W. Hiebert, G. Grosveld and J. R. Downing (1996). "AML1, the target of multiple chromosomal translocations in human leukemia, is essential for normal fetal liver hematopoiesis." Cell **84**(2): 321-330.
Orimo, A., P. B. Gupta, D. C. Sgroi, F. Arenzana-Seisdedos, T. Delaunay, R. Naeem, V. J. Carey, A. L. Richardson and R. A. Weinberg (2005). "Stromal fibroblasts present in invasive human breast carcinomas promote tumor growth and angiogenesis through elevated SDF-1/CXCL12 secretion." Cell **121**(3): 335-348.
Ota, M. and H. Sasaki (2008). "Mammalian Tead proteins regulate cell proliferation and contact inhibition as transcriptional mediators of Hippo signaling." Development **135**(24): 4059-4069.
Otto, F., A. P. Thornell, T. Crompton, A. Denzel, K. C. Gilmour, I. R. Rosewell, G. W. Stamp, R. S. Beddington, S. Mundlos, B. R. Olsen, P. B. Selby and M. J. Owen (1997). "Cbfa1, a candidate gene for cleidocranial dysplasia syndrome,

is essential for osteoblast differentiation and bone development." Cell **89**(5): 765-771.
Overholtzer, M., J. Zhang, G. A. Smolen, B. Muir, W. Li, D. C. Sgroi, C. X. Deng, J. S. Brugge and D. A. Haber (2006). "Transforming properties of YAP, a candidate oncogene on the chromosome 11q22 amplicon." Proc Natl Acad Sci U S A **103**(33): 12405-12410.
Ovitt, C. E. and H. R. Scholer (1998). "The molecular biology of Oct-4 in the early mouse embryo." Mol Hum Reprod **4**(11): 1021-1031.
Owens, D. M. and F. M. Watt (2003). "Contribution of stem cells and differentiated cells to epidermal tumours." Nat Rev Cancer **3**(6): 444-451.
Page, M. (1989). "Changing patterns of cytokeratins and vimentin in the early chick embryo." Development **105**(1): 97-107.
Palakurthy, R. K., N. Wajapeyee, M. K. Santra, C. Gazin, L. Lin, S. Gobeil and M. R. Green (2009). "Epigenetic silencing of the RASSF1A tumor suppressor gene through HOXB3-mediated induction of DNMT3B expression." Mol Cell **36**(2): 219-230.
Palmieri, S. L., W. Peter, H. Hess and H. R. Scholer (1994). "Oct-4 transcription factor is differentially expressed in the mouse embryo during establishment of the first two extraembryonic cell lineages involved in implantation." Dev Biol **166**(1): 259-267.
Pan, D. (2010). "The hippo signaling pathway in development and cancer." Dev Cell **19**(4): 491-505.
Pan, G. J., Z. Y. Chang, H. R. Scholer and D. Pei (2002). "Stem cell pluripotency and transcription factor Oct4." Cell Res **12**(5-6): 321-329.
Parada, L. F., C. J. Tabin, C. Shih and R. A. Weinberg (1982). "Human EJ bladder carcinoma oncogene is homologue of Harvey sarcoma virus ras gene." Nature **297**(5866): 474-478.
Park, D., A. P. Xiang, F. F. Mao, L. Zhang, C. G. Di, X. M. Liu, Y. Shao, B. F. Ma, J. H. Lee, K. S. Ha, N. Walton and B. T. Lahn (2010). "Nestin is required for the proper self-renewal of neural stem cells." Stem Cells **28**(12): 2162-2171.
Park, I. H., R. Zhao, J. A. West, A. Yabuuchi, H. Huo, T. A. Ince, P. H. Lerou, M. W. Lensch and G. Q. Daley (2008). "Reprogramming of human somatic cells to pluripotency with defined factors." Nature **451**(7175): 141-146.
Parsons, J. T., A. R. Horwitz and M. A. Schwartz (2010). "Cell adhesion: integrating cytoskeletal dynamics and cellular tension." Nat Rev Mol Cell Biol **11**(9): 633-643.
Pauklin, S., R. A. Pedersen and L. Vallier (2011). "Mouse pluripotent stem cells at a glance." J Cell Sci **124**(Pt 22): 3727-3732.
Pearce, L. R., D. Komander and D. R. Alessi (2010). "The nuts and bolts of AGC protein kinases." Nat Rev Mol Cell Biol **11**(1): 9-22.
Peifer, M., P. D. McCrea, K. J. Green, E. Wieschaus and B. M. Gumbiner (1992). "The vertebrate adhesive junction proteins beta-catenin and plakoglobin and the Drosophila segment polarity gene armadillo form a multigene family with similar properties." J Cell Biol **118**(3): 681-691.
Peinado, H., M. Aleckovic, S. Lavotshkin, I. Matei, B. Costa-Silva, G. Moreno-Bueno, M. Hergueta-Redondo, C. Williams, G. Garcia-Santos, C. Ghajar, A. Nitadori-Hoshino, C. Hoffman, K. Badal, B. A. Garcia, M. K. Callahan, J. Yuan, V. R. Martins, J. Skog, R. N. Kaplan, M. S. Brady, J. D. Wolchok, P. B. Chapman, Y. Kang, J. Bromberg and D. Lyden (2012). "Melanoma exosomes

educate bone marrow progenitor cells toward a pro-metastatic phenotype through MET." Nat Med **18**(6): 883-891.
Pellegrini, G., O. Golisano, P. Paterna, A. Lambiase, S. Bonini, P. Rama and M. De Luca (1999). "Location and clonal analysis of stem cells and their differentiated progeny in the human ocular surface." J Cell Biol **145**(4): 769-782.
Pelosi, G., C. Fumagalli, M. Trubia, A. Sonzogni, N. Rekhtman, P. Maisonneuve, D. Galetta, L. Spaggiari, G. Veronesi, A. Scarpa, G. Malpeli and G. Viale (2010). "Dual role of RASSF1 as a tumor suppressor and an oncogene in neuroendocrine tumors of the lung." Anticancer Res **30**(10): 4269-4281.
Pereira, L., F. Yi and B. J. Merrill (2006). "Repression of Nanog gene transcription by Tcf3 limits embryonic stem cell self-renewal." Mol Cell Biol **26**(20): 7479-7491.
Phillips-Cremins, J. E., M. E. Sauria, A. Sanyal, T. I. Gerasimova, B. R. Lajoie, J. S. Bell, C. T. Ong, T. A. Hookway, C. Guo, Y. Sun, M. J. Bland, W. Wagstaff, S. Dalton, T. C. McDevitt, R. Sen, J. Dekker, J. Taylor and V. G. Corces (2013). "Architectural protein subclasses shape 3D organization of genomes during lineage commitment." Cell **153**(6): 1281-1295.
Piccirillo, S. G., B. A. Reynolds, N. Zanetti, G. Lamorte, E. Binda, G. Broggi, H. Brem, A. Olivi, F. Dimeco and A. L. Vescovi (2006). "Bone morphogenetic proteins inhibit the tumorigenic potential of human brain tumour-initiating cells." Nature **444**(7120): 761-765.
Polo, J. M., S. Liu, M. E. Figueroa, W. Kulalert, S. Eminli, K. Y. Tan, E. Apostolou, M. Stadtfeld, Y. Li, T. Shioda, S. Natesan, A. J. Wagers, A. Melnick, T. Evans and K. Hochedlinger (2010). "Cell type of origin influences the molecular and functional properties of mouse induced pluripotent stem cells." Nat Biotechnol **28**(8): 848-855.
Pomerantz, J. H. and H. M. Blau (2013). "Tumor suppressors: enhancers or suppressors of regeneration?" Development **140**(12): 2502-2512.
Praskova, M., A. Khoklatchev, S. Ortiz-Vega and J. Avruch (2004). "Regulation of the MST1 kinase by autophosphorylation, by the growth inhibitory proteins, RASSF1 and NORE1, and by Ras." Biochem J **381**(Pt 2): 453-462.
Praskova, M., F. Xia and J. Avruch (2008). "MOBKL1A/MOBKL1B phosphorylation by MST1 and MST2 inhibits cell proliferation." Curr Biol **18**(5): 311-321.
Puri, M. C. and A. Nagy (2012). "Concise review: Embryonic stem cells versus induced pluripotent stem cells: the game is on." Stem Cells **30**(1): 10-14.
Qin, H., K. Blaschke, G. Wei, Y. Ohi, L. Blouin, Z. Qi, J. Yu, R. F. Yeh, M. Hebrok and M. Ramalho-Santos (2012). "Transcriptional analysis of pluripotency reveals the Hippo pathway as a barrier to reprogramming." Hum Mol Genet **21**(9): 2054-2067.
Qin, H., T. Yu, T. Qing, Y. Liu, Y. Zhao, J. Cai, J. Li, Z. Song, X. Qu, P. Zhou, J. Wu, M. Ding and H. Deng (2007). "Regulation of apoptosis and differentiation by p53 in human embryonic stem cells." J Biol Chem **282**(8): 5842-5852.
Ranganathan, P., K. L. Weaver and A. J. Capobianco (2011). "Notch signalling in solid tumours: a little bit of everything but not all the time." Nat Rev Cancer **11**(5): 338-351.
Real, E., A. Kaiser, G. Raposo, A. Amara, A. Nardin, A. Trautmann and E. Donnadieu (2004). "Immature dendritic cells (DCs) use chemokines and intercellular adhesion molecule (ICAM)-1, but not DC-specific ICAM-3-grabbing

nonintegrin, to stimulate CD4+ T cells in the absence of exogenous antigen." J Immunol **173**(1): 50-60.
Reeves, M. E., M. L. Baldwin, R. Aragon, S. Baldwin, S. T. Chen, X. Li, S. Mohan and Y. G. Amaar (2012). "RASSF1C modulates the expression of a stem cell renewal gene, PIWIL1." BMC Res Notes **5**: 239.
Reeves, M. E., S. W. Baldwin, M. L. Baldwin, S. T. Chen, J. M. Moretz, R. J. Aragon, X. Li, D. D. Strong, S. Mohan and Y. G. Amaar (2010). "Ras-association domain family 1C protein promotes breast cancer cell migration and attenuates apoptosis." BMC Cancer **10**: 562.
Reeves, M. E., M. Firek, S. T. Chen and Y. G. Amaar (2014). "Evidence that RASSF1C Stimulation of Lung Cancer Cell Proliferation Depends on IGFBP-5 and PIWIL1 Expression Levels." PLoS One **9**(7): e101679.
Remue, E., K. Meerschaert, T. Oka, C. Boucherie, J. Vandekerckhove, M. Sudol and J. Gettemans (2010). "TAZ interacts with zonula occludens-1 and -2 proteins in a PDZ-1 dependent manner." FEBS Lett **584**(19): 4175-4180.
Ren, R., B. J. Mayer, P. Cicchetti and D. Baltimore (1993). "Identification of a ten-amino acid proline-rich SH3 binding site." Science **259**(5098): 1157-1161.
Richter, A. M., G. P. Pfeifer and R. H. Dammann (2009). "The RASSF proteins in cancer; from epigenetic silencing to functional characterization." Biochim Biophys Acta **1796**(2): 114-128.
Rius, C. and P. Aller (1992). "Vimentin expression as a late event in the in vitro differentiation of human promonocytic cells." J Cell Sci **101 (Pt 2)**: 395-401.
Rivera, M. N., W. J. Kim, J. Wells, D. R. Driscoll, B. W. Brannigan, M. Han, J. C. Kim, A. P. Feinberg, W. L. Gerald, S. O. Vargas, L. Chin, A. J. Iafrate, D. W. Bell and D. A. Haber (2007). "An X chromosome gene, WTX, is commonly inactivated in Wilms tumor." Science **315**(5812): 642-645.
Rocquain, J., V. Gelsi-Boyer, J. Adelaide, A. Murati, N. Carbuccia, N. Vey, D. Birnbaum, M. J. Mozziconacci and M. Chaffanet (2010). "Alteration of cohesin genes in myeloid diseases." Am J Hematol **85**(9): 717-719.
Rodda, D. J., J. L. Chew, L. H. Lim, Y. H. Loh, B. Wang, H. H. Ng and P. Robson (2005). "Transcriptional regulation of nanog by OCT4 and SOX2." J Biol Chem **280**(26): 24731-24737.
Rojas, A., S. De Val, A. B. Heidt, S. M. Xu, J. Bristow and B. L. Black (2005). "Gata4 expression in lateral mesoderm is downstream of BMP4 and is activated directly by Forkhead and GATA transcription factors through a distal enhancer element." Development **132**(15): 3405-3417.
Roman-Gomez, J., A. Jimenez-Velasco, J. A. Castillejo, X. Agirre, M. Barrios, G. Navarro, F. J. Molina, M. J. Calasanz, F. Prosper, A. Heiniger and A. Torres (2004). "Promoter hypermethylation of cancer-related genes: a strong independent prognostic factor in acute lymphoblastic leukemia." Blood **104**(8): 2492-2498.
Romano, D., D. Matallanas, G. Weitsman, C. Preisinger, T. Ng and W. Kolch (2010). "Proapoptotic kinase MST2 coordinates signaling crosstalk between RASSF1A, Raf-1, and Akt." Cancer Res **70**(3): 1195-1203.
Rong, R., W. Jin, J. Zhang, M. S. Sheikh and Y. Huang (2004). "Tumor suppressor RASSF1A is a microtubule-binding protein that stabilizes microtubules and induces G2/M arrest." Oncogene **23**(50): 8216-8230.
Rosenbluh, J., D. Nijhawan, A. G. Cox, X. Li, J. T. Neal, E. J. Schafer, T. I. Zack, X. Wang, A. Tsherniak, A. C. Schinzel, D. D. Shao, S. E. Schumacher, B. A. Weir, F. Vazquez, G. S. Cowley, D. E. Root, J. P. Mesirov, R. Beroukhim,

C. J. Kuo, W. Goessling and W. C. Hahn (2012). "beta-Catenin-driven cancers require a YAP1 transcriptional complex for survival and tumorigenesis." Cell **151**(7): 1457-1473.
Rouleau, G. A., P. Merel, M. Lutchman, M. Sanson, J. Zucman, C. Marineau, K. Hoang-Xuan, S. Demczuk, C. Desmaze, B. Plougastel and et al. (1993). "Alteration in a new gene encoding a putative membrane-organizing protein causes neuro-fibromatosis type 2." Nature **363**(6429): 515-521.
Rubinfeld, B., B. Souza, I. Albert, O. Muller, S. H. Chamberlain, F. R. Masiarz, S. Munemitsu and P. Polakis (1993). "Association of the APC gene product with beta-catenin." Science **262**(5140): 1731-1734.
Ruter, B., P. W. Wijermans and M. Lubbert (2006). "Superiority of prolonged low-dose azanucleoside administration? Results of 5-aza-2'-deoxycytidine retreatment in high-risk myelodysplasia patients." Cancer **106**(8): 1744-1750.
Sachlos, E., R. M. Risueno, S. Laronde, Z. Shapovalova, J. H. Lee, J. Russell, M. Malig, J. D. McNicol, A. Fiebig-Comyn, M. Graham, M. Levadoux-Martin, J. B. Lee, A. O. Giacomelli, J. A. Hassell, D. Fischer-Russell, M. R. Trus, R. Foley, B. Leber, A. Xenocostas, E. D. Brown, T. J. Collins and M. Bhatia (2012). "Identification of drugs including a dopamine receptor antagonist that selectively target cancer stem cells." Cell **149**(6): 1284-1297.
Saigusa, S., K. Tanaka, Y. Toiyama, T. Yokoe, Y. Okugawa, Y. Ioue, C. Miki and M. Kusunoki (2009). "Correlation of CD133, OCT4, and SOX2 in rectal cancer and their association with distant recurrence after chemoradiotherapy." Ann Surg Oncol **16**(12): 3488-3498.
Santos, E., S. R. Tronick, S. A. Aaronson, S. Pulciani and M. Barbacid (1982). "T24 human bladder carcinoma oncogene is an activated form of the normal human homologue of BALB- and Harvey-MSV transforming genes." Nature **298**(5872): 343-347.
Sanyal, A., B. R. Lajoie, G. Jain and J. Dekker (2012). "The long-range interaction landscape of gene promoters." Nature **489**(7414): 109-113.
Sato, M., E. Morii, T. Komori, H. Kawahata, M. Sugimoto, K. Terai, H. Shimizu, T. Yasui, H. Ogihara, N. Yasui, T. Ochi, Y. Kitamura, Y. Ito and S. Nomura (1998). "Transcriptional regulation of osteopontin gene in vivo by PEBP2alphaA/CBFA1 and ETS1 in the skeletal tissues." Oncogene **17**(12): 1517-1525.
Sato, N., L. Meijer, L. Skaltsounis, P. Greengard and A. H. Brivanlou (2004). "Maintenance of pluripotency in human and mouse embryonic stem cells through activation of Wnt signaling by a pharmacological GSK-3-specific inhibitor." Nat Med **10**(1): 55-63.
Savatier, P., H. Lapillonne, L. A. van Grunsven, B. B. Rudkin and J. Samarut (1996). "Withdrawal of differentiation inhibitory activity/leukemia inhibitory factor up-regulates D-type cyclins and cyclin-dependent kinase inhibitors in mouse embryonic stem cells." Oncogene **12**(2): 309-322.
Sawada, A., H. Kiyonari, K. Ukita, N. Nishioka, Y. Imuta and H. Sasaki (2008). "Redundant roles of Tead1 and Tead2 in notochord development and the regulation of cell proliferation and survival." Mol Cell Biol **28**(10): 3177-3189.
Schepers, A. G., H. J. Snippert, D. E. Stange, M. van den Born, J. H. van Es, M. van de Wetering and H. Clevers (2012). "Lineage tracing reveals Lgr5+ stem cell activity in mouse intestinal adenomas." Science **337**(6095): 730-735.
Schlegelmilch, K., M. Mohseni, O. Kirak, J. Pruszak, J. R. Rodriguez, D. Zhou, B. T. Kreger, V. Vasioukhin, J. Avruch, T. R. Brummelkamp and F. D. Camargo

(2011). "Yap1 acts downstream of alpha-catenin to control epidermal proliferation." Cell **144**(5): 782-795.
Schreiber, E., P. Matthias, M. M. Muller and W. Schaffner (1989). "Rapid detection of octamer binding proteins with 'mini-extracts', prepared from a small number of cells." Nucleic Acids Res **17**(15): 6419.
Schroeder, M. C. and G. Halder (2012). "Regulation of the Hippo pathway by cell architecture and mechanical signals." Semin Cell Dev Biol **23**(7): 803-811.
Sherwood, V., R. Manbodh, C. Sheppard and A. D. Chalmers (2008). "RASSF7 is a member of a new family of RAS association domain-containing proteins and is required for completing mitosis." Mol Biol Cell **19**(4): 1772-1782.
Sherwood, V., A. Recino, A. Jeffries, A. Ward and A. D. Chalmers (2010). "The N-terminal RASSF family: a new group of Ras-association-domain-containing proteins, with emerging links to cancer formation." Biochem J **425**(2): 303-311.
Shiojima, I. and K. Walsh (2006). "Regulation of cardiac growth and coronary angiogenesis by the Akt/PKB signaling pathway." Genes Dev **20**(24): 3347-3365.
Shivakumar, L., J. Minna, T. Sakamaki, R. Pestell and M. A. White (2002). "The RASSF1A tumor suppressor blocks cell cycle progression and inhibits cyclin D1 accumulation." Mol Cell Biol **22**(12): 4309-4318.
Simons, M. and G. Raposo (2009). "Exosomes--vesicular carriers for intercellular communication." Curr Opin Cell Biol **21**(4): 575-581.
Song, M. S., J. S. Chang, S. J. Song, T. H. Yang, H. Lee and D. S. Lim (2005). "The centrosomal protein RAS association domain family protein 1A (RASSF1A)-binding protein 1 regulates mitotic progression by recruiting RASSF1A to spindle poles." J Biol Chem **280**(5): 3920-3927.
Song, M. S., S. J. Song, N. G. Ayad, J. S. Chang, J. H. Lee, H. K. Hong, H. Lee, N. Choi, J. Kim, H. Kim, J. W. Kim, E. J. Choi, M. W. Kirschner and D. S. Lim (2004). "The tumour suppressor RASSF1A regulates mitosis by inhibiting the APC-Cdc20 complex." Nat Cell Biol **6**(2): 129-137.
Song, M. S., S. J. Song, S. J. Kim, K. Nakayama, K. I. Nakayama and D. S. Lim (2008). "Skp2 regulates the antiproliferative function of the tumor suppressor RASSF1A via ubiquitin-mediated degradation at the G1-S transition." Oncogene **27**(22): 3176-3185.
Song, M. S., S. J. Song, S. Y. Kim, H. J. Oh and D. S. Lim (2008). "The tumour suppressor RASSF1A promotes MDM2 self-ubiquitination by disrupting the MDM2-DAXX-HAUSP complex." EMBO J **27**(13): 1863-1874.
Song, S. J., S. J. Kim, M. S. Song and D. S. Lim (2009). "Aurora B-mediated phosphorylation of RASSF1A maintains proper cytokinesis by recruiting Syntaxin16 to the midzone and midbody." Cancer Res **69**(22): 8540-8544.
Song, S. J., M. S. Song, S. J. Kim, S. Y. Kim, S. H. Kwon, J. G. Kim, D. F. Calvisi, D. Kang and D. S. Lim (2009). "Aurora A regulates prometaphase progression by inhibiting the ability of RASSF1A to suppress APC-Cdc20 activity." Cancer Res **69**(6): 2314-2323.
Sotiropoulou, P. A., A. Candi, G. Mascre, S. De Clercq, K. K. Youssef, G. Lapouge, E. Dahl, C. Semeraro, G. Denecker, J. C. Marine and C. Blanpain (2010). "Bcl-2 and accelerated DNA repair mediates resistance of hair follicle bulge stem cells to DNA-damage-induced cell death." Nat Cell Biol **12**(6): 572-582.

Stanger, B. Z., A. J. Tanaka and D. A. Melton (2007). "Organ size is limited by the number of embryonic progenitor cells in the pancreas but not the liver." Nature **445**(7130): 886-891.
Strano, S., O. Monti, N. Pediconi, A. Baccarini, G. Fontemaggi, E. Lapi, F. Mantovani, A. Damalas, G. Citro, A. Sacchi, G. Del Sal, M. Levrero and G. Blandino (2005). "The transcriptional coactivator Yes-associated protein drives p73 gene-target specificity in response to DNA Damage." Mol Cell **18**(4): 447-459.
Strano, S., E. Munarriz, M. Rossi, L. Castagnoli, Y. Shaul, A. Sacchi, M. Oren, M. Sudol, G. Cesareni and G. Blandino (2001). "Physical interaction with Yes-associated protein enhances p73 transcriptional activity." J Biol Chem **276**(18): 15164-15173.
Su, L. K., B. Vogelstein and K. W. Kinzler (1993). "Association of the APC tumor suppressor protein with catenins." Science **262**(5140): 1734-1737.
Sudol, M. (1994). "Yes-associated protein (YAP65) is a proline-rich phosphoprotein that binds to the SH3 domain of the Yes proto-oncogene product." Oncogene **9**(8): 2145-2152.
Sudol, M., P. Bork, A. Einbond, K. Kastury, T. Druck, M. Negrini, K. Huebner and D. Lehman (1995). "Characterization of the mammalian YAP (Yes-associated protein) gene and its role in defining a novel protein module, the WW domain." J Biol Chem **270**(24): 14733-14741.
Sudol, M. and K. F. Harvey (2010). "Modularity in the Hippo signaling pathway." Trends Biochem Sci **35**(11): 627-633.
Sugioka, K., K. Mizumoto and H. Sawa (2011). "Wnt regulates spindle asymmetry to generate asymmetric nuclear beta-catenin in C. elegans." Cell **146**(6): 942-954.
Surani, M. A., K. Hayashi and P. Hajkova (2007). "Genetic and epigenetic regulators of pluripotency." Cell **128**(4): 747-762.
Takahashi, K., K. Tanabe, M. Ohnuki, M. Narita, T. Ichisaka, K. Tomoda and S. Yamanaka (2007). "Induction of pluripotent stem cells from adult human fibroblasts by defined factors." Cell **131**(5): 861-872.
Takahashi, K. and S. Yamanaka (2006). "Induction of pluripotent stem cells from mouse embryonic and adult fibroblast cultures by defined factors." Cell **126**(4): 663-676.
Tam, W. L., C. Y. Lim, J. Han, J. Zhang, Y. S. Ang, H. H. Ng, H. Yang and B. Lim (2008). "T-cell factor 3 regulates embryonic stem cell pluripotency and self-renewal by the transcriptional control of multiple lineage pathways." Stem Cells **26**(8): 2019-2031.
Tamm, C., N. Bower and C. Anneren (2011). "Regulation of mouse embryonic stem cell self-renewal by a Yes-YAP-TEAD2 signaling pathway downstream of LIF." J Cell Sci **124**(Pt 7): 1136-1144.
Tan, M. H., K. F. Au, D. E. Leong, K. Foygel, W. H. Wong and M. W. Yao (2013). "An Oct4-Sall4-Nanog network controls developmental progression in the pre-implantation mouse embryo." Mol Syst Biol **9**: 632.
Tapon, N., K. F. Harvey, D. W. Bell, D. C. Wahrer, T. A. Schiripo, D. Haber and I. K. Hariharan (2002). "salvador Promotes both cell cycle exit and apoptosis in Drosophila and is mutated in human cancer cell lines." Cell **110**(4): 467-478.
Taylor, D. D. and C. Gercel-Taylor (2011). "Exosomes/microvesicles: mediators of cancer-associated immunosuppressive microenvironments." Semin Immunopathol **33**(5): 441-454.

ten Berge, D., D. Kurek, T. Blauwkamp, W. Koole, A. Maas, E. Eroglu, R. K. Siu and R. Nusse (2011). "Embryonic stem cells require Wnt proteins to prevent differentiation to epiblast stem cells." Nat Cell Biol **13**(9): 1070-1075.
Teng, I. W., P. C. Hou, K. D. Lee, P. Y. Chu, K. T. Yeh, V. X. Jin, M. J. Tseng, S. J. Tsai, Y. S. Chang, C. S. Wu, H. S. Sun, K. D. Tsai, L. B. Jeng, K. P. Nephew, T. H. Huang, S. H. Hsiao and Y. W. Leu (2011). "Targeted methylation of two tumor suppressor genes is sufficient to transform mesenchymal stem cells into cancer stem/initiating cells." Cancer Res **71**(13): 4653-4663.
Thaler, S., M. Schmidt, A. Schad and J. P. Sleeman (2012). "RASSF1A inhibits estrogen receptor alpha expression and estrogen-independent signalling: implications for breast cancer development." Oncogene **31**(47): 4912-4922.
Thery, C., M. Ostrowski and E. Segura (2009). "Membrane vesicles as conveyors of immune responses." Nat Rev Immunol **9**(8): 581-593.
Thirunavukkarasu, K., M. Mahajan, K. W. McLarren, S. Stifani and G. Karsenty (1998). "Two domains unique to osteoblast-specific transcription factor Osf2/Cbfa1 contribute to its transactivation function and its inability to heterodimerize with Cbfbeta." Mol Cell Biol **18**(7): 4197-4208.
Tokuzawa, Y., E. Kaiho, M. Maruyama, K. Takahashi, K. Mitsui, M. Maeda, H. Niwa and S. Yamanaka (2003). "Fbx15 is a novel target of Oct3/4 but is dispensable for embryonic stem cell self-renewal and mouse development." Mol Cell Biol **23**(8): 2699-2708.
Tommasi, S., A. Besaratinia, S. P. Wilczynski and G. P. Pfeifer (2011). "Loss of Rassf1a enhances p53-mediated tumor predisposition and accelerates progression to aneuploidy." Oncogene **30**(6): 690-700.
Tommasi, S., R. Dammann, Z. Zhang, Y. Wang, L. Liu, W. M. Tsark, S. P. Wilczynski, J. Li, M. You and G. P. Pfeifer (2005). "Tumor susceptibility of Rassf1a knockout mice." Cancer Res **65**(1): 92-98.
Tommasi, S., R. Pinto, D. Petriella, B. Pilato, R. Lacalamita, D. Santini, F. Zito, G. Colucci, A. Paradiso and N. Silvestris (2011). "Oncosuppressor methylation: a possible key role in colon metastatic progression." J Cell Physiol **226**(7): 1934-1939.
Trigiante, G. and X. Lu (2006). "ASPP [corrected] and cancer." Nat Rev Cancer **6**(3): 217-226.
Trofatter, J. A., M. M. MacCollin, J. L. Rutter, J. R. Murrell, M. P. Duyao, D. M. Parry, R. Eldridge, N. Kley, A. G. Menon, K. Pulaski and et al. (1993). "A novel moesin-, ezrin-, radixin-like gene is a candidate for the neurofibromatosis 2 tumor suppressor." Cell **75**(4): 826.
van de Wetering, M., R. Cavallo, D. Dooijes, M. van Beest, J. van Es, J. Loureiro, A. Ypma, D. Hursh, T. Jones, A. Bejsovec, M. Peifer, M. Mortin and H. Clevers (1997). "Armadillo coactivates transcription driven by the product of the Drosophila segment polarity gene dTCF." Cell **88**(6): 789-799.
van der Weyden, L. and D. J. Adams (2007). "The Ras-association domain family (RASSF) members and their role in human tumourigenesis." Biochim Biophys Acta **1776**(1): 58-85.
van der Weyden, L., M. J. Arends, O. M. Dovey, H. L. Harrison, G. Lefebvre, N. Conte, F. V. Gergely, A. Bradley and D. J. Adams (2008). "Loss of Rassf1a cooperates with Apc(Min) to accelerate intestinal tumourigenesis." Oncogene **27**(32): 4503-4508.
van der Weyden, L., A. Papaspyropoulos, G. Poulogiannis, A. G. Rust, M. Rashid, D. J. Adams, M. J. Arends and E. O'Neill (2012). "Loss of RASSF1A

synergizes with deregulated RUNX2 signaling in tumorigenesis." Cancer Res **72**(15): 3817-3827.
van der Weyden, L., K. K. Tachibana, M. A. Gonzalez, D. J. Adams, B. L. Ng, R. Petty, A. R. Venkitaraman, M. J. Arends and A. Bradley (2005). "The RASSF1A isoform of RASSF1 promotes microtubule stability and suppresses tumorigenesis." Mol Cell Biol **25**(18): 8356-8367.
Varelas, X., B. W. Miller, R. Sopko, S. Song, A. Gregorieff, F. A. Fellouse, R. Sakuma, T. Pawson, W. Hunziker, H. McNeill, J. L. Wrana and L. Attisano (2010). "The Hippo pathway regulates Wnt/beta-catenin signaling." Dev Cell **18**(4): 579-591.
Varelas, X., R. Sakuma, P. Samavarchi-Tehrani, R. Peerani, B. M. Rao, J. Dembowy, M. B. Yaffe, P. W. Zandstra and J. L. Wrana (2008). "TAZ controls Smad nucleocytoplasmic shuttling and regulates human embryonic stem-cell self-renewal." Nat Cell Biol **10**(7): 837-848.
Varelas, X., P. Samavarchi-Tehrani, M. Narimatsu, A. Weiss, K. Cockburn, B. G. Larsen, J. Rossant and J. L. Wrana (2010). "The Crumbs complex couples cell density sensing to Hippo-dependent control of the TGF-beta-SMAD pathway." Dev Cell **19**(6): 831-844.
Vassilev, A., K. J. Kaneko, H. Shu, Y. Zhao and M. L. DePamphilis (2001). "TEAD/TEF transcription factors utilize the activation domain of YAP65, a Src/Yes-associated protein localized in the cytoplasm." Genes Dev **15**(10): 1229-1241.
Verma, S. K., T. S. Ganesan and P. J. Parker (2008). "The tumour suppressor RASSF1A is a novel substrate of PKC." FEBS Lett **582**(15): 2270-2276.
Vichalkovski, A., E. Gresko, H. Cornils, A. Hergovich, D. Schmitz and B. A. Hemmings (2008). "NDR kinase is activated by RASSF1A/MST1 in response to Fas receptor stimulation and promotes apoptosis." Curr Biol **18**(23): 1889-1895.
Vigneron, A. M., R. L. Ludwig and K. H. Vousden (2010). "Cytoplasmic ASPP1 inhibits apoptosis through the control of YAP." Genes Dev **24**(21): 2430-2439.
Vigneron, A. M. and K. H. Vousden (2012). "An indirect role for ASPP1 in limiting p53-dependent p21 expression and cellular senescence." EMBO J **31**(2): 471-480.
Villa-Diaz, L. G., A. M. Ross, J. Lahann and P. H. Krebsbach (2013). "Concise review: The evolution of human pluripotent stem cell culture: from feeder cells to synthetic coatings." Stem Cells **31**(1): 1-7.
Viswanathan, S. R., J. T. Powers, W. Einhorn, Y. Hoshida, T. L. Ng, S. Toffanin, M. O'Sullivan, J. Lu, L. A. Phillips, V. L. Lockhart, S. P. Shah, P. S. Tanwar, C. H. Mermel, R. Beroukhim, M. Azam, J. Teixeira, M. Meyerson, T. P. Hughes, J. M. Llovet, J. Radich, C. G. Mullighan, T. R. Golub, P. H. Sorensen and G. Q. Daley (2009). "Lin28 promotes transformation and is associated with advanced human malignancies." Nat Genet **41**(7): 843-848.
Volodko, N., M. Gordon, M. Salla, H. A. Ghazaleh and S. Baksh (2014). "RASSF tumor suppressor gene family: Biological functions and regulation." FEBS Lett.
von Gise, A., Z. Lin, K. Schlegelmilch, L. B. Honor, G. M. Pan, J. N. Buck, Q. Ma, T. Ishiwata, B. Zhou, F. D. Camargo and W. T. Pu (2012). "YAP1, the nuclear target of Hippo signaling, stimulates heart growth through cardiomyocyte proliferation but not hypertrophy." Proc Natl Acad Sci U S A **109**(7): 2394-2399.

Vos, M. D., C. A. Ellis, A. Bell, M. J. Birrer and G. J. Clark (2000). "Ras uses the novel tumor suppressor RASSF1 as an effector to mediate apoptosis." J Biol Chem **275**(46): 35669-35672.
Wallmen, B., M. Schrempp and A. Hecht (2012). "Intrinsic properties of Tcf1 and Tcf4 splice variants determine cell-type-specific Wnt/beta-catenin target gene expression." Nucleic Acids Res **40**(19): 9455-9469.
Wang, F., H. Wang, H. Wu, H. Qiu, C. Zeng, L. Sun and B. Liu (2013). "TEAD1 controls C2C12 cell proliferation and differentiation and regulates three novel target genes." Cell Signal **25**(3): 674-681.
Wang, J., B. Wang, X. Chen and J. Bi (2011). "The prognostic value of RASSF1A promoter hypermethylation in non-small cell lung carcinoma: a systematic review and meta-analysis." Carcinogenesis **32**(3): 411-416.
Wang, Q. T., K. Piotrowska, M. A. Ciemerych, L. Milenkovic, M. P. Scott, R. W. Davis and M. Zernicka-Goetz (2004). "A genome-wide study of gene activity reveals developmental signaling pathways in the preimplantation mouse embryo." Dev Cell **6**(1): 133-144.
Warburg, O. (1956). "On respiratory impairment in cancer cells." Science **124**(3215): 269-270.
Warburg, O. (1956). "On the origin of cancer cells." Science **123**(3191): 309-314.
Warburg, O. (1925). "Uber den stoffwechsel der carcinomzelle." Klin. Wochenschr. 1925;4:534-536.
Webb, C., A. Upadhyay, F. Giuntini, I. Eggleston, M. Furutani-Seiki, R. Ishima and S. Bagby (2011). "Structural features and ligand binding properties of tandem WW domains from YAP and TAZ, nuclear effectors of the Hippo pathway." Biochemistry **50**(16): 3300-3309.
Whang, Y. M., Y. H. Kim, J. S. Kim and Y. D. Yoo (2005). "RASSF1A suppresses the c-Jun-NH2-kinase pathway and inhibits cell cycle progression." Cancer Res **65**(9): 3682-3690.
Winnier, G., M. Blessing, P. A. Labosky and B. L. Hogan (1995). "Bone morphogenetic protein-4 is required for mesoderm formation and patterning in the mouse." Genes Dev **9**(17): 2105-2116.
Winzler, C., P. Rovere, M. Rescigno, F. Granucci, G. Penna, L. Adorini, V. S. Zimmermann, J. Davoust and P. Ricciardi-Castagnoli (1997). "Maturation stages of mouse dendritic cells in growth factor-dependent long-term cultures." J Exp Med **185**(2): 317-328.
Woltjen, K., I. P. Michael, P. Mohseni, R. Desai, M. Mileikovsky, R. Hamalainen, R. Cowling, W. Wang, P. Liu, M. Gertsenstein, K. Kaji, H. K. Sung and A. Nagy (2009). "piggyBac transposition reprograms fibroblasts to induced pluripotent stem cells." Nature **458**(7239): 766-770.
Xin, M., Y. Kim, L. B. Sutherland, X. Qi, J. McAnally, R. J. Schwartz, J. A. Richardson, R. Bassel-Duby and E. N. Olson (2011). "Regulation of insulin-like growth factor signaling by Yap governs cardiomyocyte proliferation and embryonic heart size." Sci Signal **4**(196): ra70.
Xu, J., P. B. Shetty, W. Feng, C. Chenault, R. C. Bast, Jr., J. P. Issa, S. G. Hilsenbeck and Y. Yu (2012). "Methylation of HIN-1, RASSF1A, RIL and CDH13 in breast cancer is associated with clinical characteristics, but only RASSF1A methylation is associated with outcome." BMC Cancer **12**: 243.

Xu, M. Z., T. J. Yao, N. P. Lee, I. O. Ng, Y. T. Chan, L. Zender, S. W. Lowe, R. T. Poon and J. M. Luk (2009). "Yes-associated protein is an independent prognostic marker in hepatocellular carcinoma." Cancer **115**(19): 4576-4585.
Yagi, R., L. F. Chen, K. Shigesada, Y. Murakami and Y. Ito (1999). "A WW domain-containing yes-associated protein (YAP) is a novel transcriptional co-activator." EMBO J **18**(9): 2551-2562.
Yee, K. S., L. Grochola, G. Hamilton, A. Grawenda, E. E. Bond, H. Taubert, P. Wurl, G. L. Bond and E. O'Neill (2012). "A RASSF1A polymorphism restricts p53/p73 activation and associates with poor survival and accelerated age of onset of soft tissue sarcoma." Cancer Res **72**(9): 2206-2217.
Yeom, Y. I., G. Fuhrmann, C. E. Ovitt, A. Brehm, K. Ohbo, M. Gross, K. Hubner and H. R. Scholer (1996). "Germline regulatory element of Oct-4 specific for the totipotent cycle of embryonal cells." Development **122**(3): 881-894.
Yi, F., L. Pereira, J. A. Hoffman, B. R. Shy, C. M. Yuen, D. R. Liu and B. J. Merrill (2011). "Opposing effects of Tcf3 and Tcf1 control Wnt stimulation of embryonic stem cell self-renewal." Nat Cell Biol **13**(7): 762-770.
Yi, F., L. Pereira and B. J. Merrill (2008). "Tcf3 functions as a steady-state limiter of transcriptional programs of mouse embryonic stem cell self-renewal." Stem Cells **26**(8): 1951-1960.
Yimlamai, D., C. Christodoulou, G. G. Galli, K. Yanger, B. Pepe-Mooney, B. Gurung, K. Shrestha, P. Cahan, B. Z. Stanger and F. D. Camargo (2014). "Hippo pathway activity influences liver cell fate." Cell **157**(6): 1324-1338.
Ying, Q. L., J. Wray, J. Nichols, L. Batlle-Morera, B. Doble, J. Woodgett, P. Cohen and A. Smith (2008). "The ground state of embryonic stem cell self-renewal." Nature **453**(7194): 519-523.
Yu, F. X., B. Zhao, N. Panupinthu, J. L. Jewell, I. Lian, L. H. Wang, J. Zhao, H. Yuan, K. Tumaneng, H. Li, X. D. Fu, G. B. Mills and K. L. Guan (2012). "Regulation of the Hippo-YAP pathway by G-protein-coupled receptor signaling." Cell **150**(4): 780-791.
Yuan, H., N. Corbi, C. Basilico and L. Dailey (1995). "Developmental-specific activity of the FGF-4 enhancer requires the synergistic action of Sox2 and Oct-3." Genes Dev **9**(21): 2635-2645.
Yuan, M., V. Tomlinson, R. Lara, D. Holliday, C. Chelala, T. Harada, R. Gangeswaran, C. Manson-Bishop, P. Smith, S. A. Danovi, O. Pardo, T. Crook, C. A. Mein, N. R. Lemoine, L. J. Jones and S. Basu (2008). "Yes-associated protein (YAP) functions as a tumor suppressor in breast." Cell Death Differ **15**(11): 1752-1759.
Zaidi, S. K., A. J. Sullivan, R. Medina, Y. Ito, A. J. van Wijnen, J. L. Stein, J. B. Lian and G. S. Stein (2004). "Tyrosine phosphorylation controls Runx2-mediated subnuclear targeting of YAP to repress transcription." EMBO J **23**(4): 790-799.
Zender, L., M. S. Spector, W. Xue, P. Flemming, C. Cordon-Cardo, J. Silke, S. T. Fan, J. M. Luk, M. Wigler, G. J. Hannon, D. Mu, R. Lucito, S. Powers and S. W. Lowe (2006). "Identification and validation of oncogenes in liver cancer using an integrative oncogenomic approach." Cell **125**(7): 1253-1267.
Zhang, H., C. Y. Liu, Z. Y. Zha, B. Zhao, J. Yao, S. Zhao, Y. Xiong, Q. Y. Lei and K. L. Guan (2009). "TEAD transcription factors mediate the function of TAZ in cell growth and epithelial-mesenchymal transition." J Biol Chem **284**(20): 13355-13362.

Zhang, H., H. A. Pasolli and E. Fuchs (2011). "Yes-associated protein (YAP) transcriptional coactivator functions in balancing growth and differentiation in skin." Proc Natl Acad Sci U S A **108**(6): 2270-2275.
Zhang, N., H. Bai, K. K. David, J. Dong, Y. Zheng, J. Cai, M. Giovannini, P. Liu, R. A. Anders and D. Pan (2010). "The Merlin/NF2 tumor suppressor functions through the YAP oncoprotein to regulate tissue homeostasis in mammals." Dev Cell **19**(1): 27-38.
Zhang, X., J. George, S. Deb, J. L. Degoutin, E. A. Takano, S. B. Fox, A. S. group, D. D. Bowtell and K. F. Harvey (2011). "The Hippo pathway transcriptional co-activator, YAP, is an ovarian cancer oncogene." Oncogene **30**(25): 2810-2822.
Zhang, X., B. Han, J. Huang, B. Zheng, Q. Geng, F. Aziz and Q. Dong (2010). "Prognostic significance of OCT4 expression in adenocarcinoma of the lung." Jpn J Clin Oncol **40**(10): 961-966.
Zhao, B., L. Li, Q. Lu, L. H. Wang, C. Y. Liu, Q. Lei and K. L. Guan (2011). "Angiomotin is a novel Hippo pathway component that inhibits YAP oncoprotein." Genes Dev **25**(1): 51-63.
Zhao, B., L. Li, K. Tumaneng, C. Y. Wang and K. L. Guan (2010). "A coordinated phosphorylation by Lats and CK1 regulates YAP stability through SCF(beta-TRCP)." Genes Dev **24**(1): 72-85.
Zhao, B., X. Wei, W. Li, R. S. Udan, Q. Yang, J. Kim, J. Xie, T. Ikenoue, J. Yu, L. Li, P. Zheng, K. Ye, A. Chinnaiyan, G. Halder, Z. C. Lai and K. L. Guan (2007). "Inactivation of YAP oncoprotein by the Hippo pathway is involved in cell contact inhibition and tissue growth control." Genes Dev **21**(21): 2747-2761.
Zhao, B., X. Ye, J. Yu, L. Li, W. Li, S. Li, J. Yu, J. D. Lin, C. Y. Wang, A. M. Chinnaiyan, Z. C. Lai and K. L. Guan (2008). "TEAD mediates YAP-dependent gene induction and growth control." Genes Dev **22**(14): 1962-1971.
Zhao, Y., X. Yin, H. Qin, F. Zhu, H. Liu, W. Yang, Q. Zhang, C. Xiang, P. Hou, Z. Song, Y. Liu, J. Yong, P. Zhang, J. Cai, M. Liu, H. Li, Y. Li, X. Qu, K. Cui, W. Zhang, T. Xiang, Y. Wu, Y. Zhao, C. Liu, C. Yu, K. Yuan, J. Lou, M. Ding and H. Deng (2008). "Two supporting factors greatly improve the efficiency of human iPSC generation." Cell Stem Cell **3**(5): 475-479.
Zhou, D., Y. Zhang, H. Wu, E. Barry, Y. Yin, E. Lawrence, D. Dawson, J. E. Willis, S. D. Markowitz, F. D. Camargo and J. Avruch (2011). "Mst1 and Mst2 protein kinases restrain intestinal stem cell proliferation and colonic tumorigenesis by inhibition of Yes-associated protein (Yap) overabundance." Proc Natl Acad Sci U S A **108**(49): E1312-1320.
Zhou, X., T. T. Li, X. Feng, E. Hsiang, Y. Xiong, K. L. Guan and Q. Y. Lei (2012). "Targeted polyubiquitylation of RASSF1C by the Mule and SCFbeta-TrCP ligases in response to DNA damage." Biochem J **441**(1): 227-236.
Zhou, Z., Y. Hao, N. Liu, L. Raptis, M. S. Tsao and X. Yang (2011). "TAZ is a novel oncogene in non-small cell lung cancer." Oncogene **30**(18): 2181-2186.
Zhu, A. J. and F. M. Watt (1999). "beta-catenin signalling modulates proliferative potential of human epidermal keratinocytes independently of intercellular adhesion." Development **126**(10): 2285-2298.